ENGINEERING RESEARCH INSTITUTE
THE UNIVERSITY OF MICHIGAN
ANN ARBOR

SMALL-SIGNAL THEORY OF ELECTRON-WAVE INTERACTION IN CROSSED ELECTRIC AND MAGNETIC FIELDS

Technical Report No. 22
Electron Tube Laboratory
Department of Electrical Engineering

by

George E. Dombrowski

Approved by: J. E. Rowe

ERI Project 2275-2

CONTRACT NO. DA-36-039 sc-56714
SIGNAL CORPS, DEPARTMENT OF THE ARMY
DEPARTMENT OF THE ARMY PROJECT NO. 3-30-06-032
SIGNAL CORPS PROJECT NO. 1143A
PLACED BY THE U. S. ARMY SIGNAL CORPS
ENGINEERING LABORATORIES
FORT MONMOUTH, NEW JERSEY

October, 1957

engn
UHR1048

ACKNOWLEDGMENT

The author wishes to express his appreciation to Professor William G. Dow, the chairman of his doctoral committee, and also to Professor Gunnar Hok for the many stimulating discussions and guidance which have led to a more mature understanding of the subject matter of this dissertation and related topics.

This report has also been submitted as a dissertation in partial fulfillment of the requirements for the degree of Doctor of Philosophy in The University of Michigan, 1958.

TABLE OF CONTENTS

TABLE OF CONTENTS (Continued)

LIST OF TABLES

LIST OF FIGURES

LIST OF SYMBOLS

A, A_n	Coefficients used in representations of the r-f potential function
$\vec{a}$	General vector
a_k	Coefficient in Taylor series
a	(Subscript) denotes lower edge of electron stream
B, B_n	Coefficients used in representations of the r-f potential function
$\vec{B}$	Magnetic flux density vector
$B_{d\text{-}c}$	Steady magnetic flux density (scalar)
b	Electron stream velocity synchronism parameter
b_k	Coefficient of Taylor series
b	(Subscript) denotes upper edge of electron stream
b	(Subscript) denotes backward space harmonic
B_m	Susceptance parameter of equivalent electric network
C, C', C_n	Coefficients used in representations of the r-f potential function
C	(Also with subscripts) capacitance parameter of equivalent electric network
c	Velocity of light <u>in vacuo</u>
c	(Subscript) denotes convection current
D, D', D_n	Coefficients used in representations of the r-f potential function
$\vec{D}$	(Also with subscripts) electric flux density vector and components
D_i	Interaction parameter (gain parameter)
d-c	(Subscript) denotes steady (unperturbed) quantity
d	(Subscript) denotes anode plane

E, E_n	Coefficients used in representations of the r-f potential function
$\vec{E}$	(Also with subscripts) electric field intensity vector and components
e	Absolute magnitude of the electronic charge
e	Base of Naperian logarithms
e	(Subscript) denotes evaluation along electron trajectory
F, F_n	Coefficients used in representations of the r-f potential function
$\vec{F}$	(Also with subscripts) force vector
f	Generalized physical quantity
f	General function
G	Geometric function defined in Eq. 8.62
g	General function
H	Geometric function defined in Eq. 8.32
h	Width (along x direction) of electron stream
h	General function
Im	"The imaginary part of," the imaginary axis
I_{beam}	D-c beam current magnitude
$\vec{i}$	Current vector
i	(Subscript) denotes induced quantity
J_o	Bessel function, first kind, zero order
$\vec{j}$	Current density vector
j	$\sqrt{-1}$
K	(Also with subscripts) r-f impedance parameter
K_o	Bessel function, second kind, zero order
k	Amplitude coefficients of displacement waves
k	(Subscript) denotes surface of electrode k

k	(Subscript) index of summation
L	Inductance parameter of equivalent electric network
l	Amplitude coefficient of displacement waves
$[M]$	Matrix defined in Eq. 8.24
$\|M\|$	Determinant of [M]
m	Amplitude coefficient of "pure space-charge waves"
m	(Subscript) denotes mth space harmonic
N	The number of terms in a summation; the number of waves in a class
n, n'	(Subscript) index identifying individual waves in a class or in an interaction region
o	(Subscript) denotes unperturbed component
P, P_n	Coefficient used in representations of the r-f potential function
P	(Also with subscripts) power
P, Q, R	Points and regions in space
p, p_n	Normalized perturbation of propagation constant
q	Quantity of electric charge
Re	"The real part of," the real axis
$\vec{r}$	Position coordinate vector
r	Normalized stream thickness parameter; "space-charge parameter"
S	General scalar
S	Surface of an electrode
s_u	Velocity spread parameter
s	(Subscript) denotes sole plane
t	Time coordinate
U	Velocity potential
u	(Also with subscripts) electron velocity
$\bar{u}_o$	Average d-c velocity of the stream

v	(Without subscripts) electric potential
v	(With subscripts) r-f wave velocity
V	(Also with subscripts) magnitudes of electric potentials
X	Series reactance parameter of equivalent electric network
X, x Y, y Z, z	Coordinate axes; (also with subscripts) space coordinates
$\bar{y}$	Mean y coordinate of electron stream
α	Stream thickness parameter of MacFarlane and Hay
α	Attenuation constant
β	Phase constant
Γ	Complex propagation constant
Δ	Determinants
$\delta\vec{r}$, δz	Perturbations of space coordinates of particles
δ	Kronecker delta
ϵ_o	Dielectric permittivity (dielectric constant) of free space
ϵ	"Error" measure
ζ	Function described in Eq. 4.28
η	Ratio of absolute charge to mass of electron
θ	Electrical angle
κ	Normalized mean-d-c stream velocity difference from cold circuit phase velocity
ℓ	Normalized perturbation of propagation constant
μ	Real component of ℓ
ν	Imaginary component of ℓ
ξ	Variable defined by Eq. 3.39
ρ	Volume space-charge density

σ	Surface charge density
τ	Linear charge density
ϕ	Electric potential function
χ	Variable defined by Eq. 4.14 and Eq. 4.15
ψ	Coupling function, theory of induced charge
Ω	Complex frequency experienced on electron trajectory
ω	Signal frequency
ω_c	Cyclotron frequency
+	(Subscript) denotes faster cyclotron wave (singularity $\xi = +1$)
-	(Subscript) denotes slower cyclotron wave (singularity $\xi = -1$)

ABSTRACT

A theory is developed for small perturbations of a thin electron stream through crossed electric-and-magnetic fields. The stream is assumed to have the d-c characteristics of rectilinear Brillouin flow, and the theory accounts for the velocity gradient of such a beam and also for the r-f space-charge effects. Waves propagated by the stream-circuit combination describe interaction of both synchronous and "cyclotron" types.

Conditions at the ends of the transmission medium formed by the stream and electrode structure are treated as combined electromagnetic and hydrodynamic boundary-value problems characterized by continuity requirements at all points in the cross-sections of entrance and exit. It is shown that a reasonably accurate solution of such a boundary value problem can be obtained with the relatively few waves obtained from the perturbation theory.

The theory makes the customary small-signal approximations and arrives at a differential equation describing the perturbations which is equivalent to that of MacFarlane and Hay (1950). Solutions of this differential equation are expressed as power series expansions in the neighborhoods corresponding to synchronous and cyclotron interactions.

The important parameters governing the propagation of quasi-synchronous waves are: (a) an interaction parameter, D_i, similar to the gain parameter, C, of traveling-wave tube theory; (b) a stream-thickness parameter, r; (c) the location of the stream relative to the electrodes; and (d) the mean velocity of the stream relative to the circuit phase velocity. The propagation constants of the quasi-synchronous waves are presented in a form normalized to D_i for several values of the other parameters.

Wave solutions are also found in the neighborhood of cyclotron resonance between the stream and wave, assuming that the wave is not synchronous with any circuit space harmonic. The two waves of this type do not exhibit growth or decay for thin streams at frequencies of order of the cyclotron frequency or less.

An additional "phantom" wave solution is presented, in which all strata of the beam are in precise synchronism with the wave. The transverse displacements of the electrons within the stream are arbitrary, but all field and velocity components are zero, as well as the surface ripple and the longitudinal displacement. The stream as perturbed by this "wave" cannot

be distinguished externally from the unperturbed state. This solution is thus a mathematical device useful in the boundary-value problem.

The entrance and exit boundary-value problems are idealized by treating the input to the interaction space as an ideal gap and by assuming that there is no reflection at the exit from the interaction region. The problem of matching fields and kinetic quantities at all points on the entrance cross-section is solved approximately, using only one or two terms in the power series solutions of the differential equation for the stream perturbations. It is shown that the approximate solution so obtained is correct to the first order. Numerical calculations are presented which show that this theory predicts a gain of the forward-wave magnetron amplifier greater than that predicted by the simple theory (Pierce, 1950), which does not account for the r-f space-charge or the d-c velocity gradient in the stream. It is also found that the start-oscillation current of the M-Carcinotron may be much less than that calculated from the simple theory.

PART I

INTRODUCTION

CHAPTER I

STATEMENT OF THE PROBLEM AND DISCUSSION OF PREVIOUS THEORY

1.1 Statement of the Problem

In the magnetron oscillator[1-4*] and the "M-Carcinotron,"**[5] an electron stream is made to interact with the fields of a high-frequency delay line in the presence of d-c electric and magnetic fields which are mutually perpendicular and are also perpendicular to the direction of the general motion of the electrons. Similar devices have been made into amplifiers of high-frequency signals,[6] but have not been brought to the same degree of perfection as the oscillator.

Although the operation of these devices is understood qualitatively, attempts to analyze the interaction between the stream and circuit in crossed fields in detail have not been completely successful. For example, it has been observed that the magnitude of d-c beam current necessary for the initiation of oscillations in the M-Carcinotron is often much smaller than that predicted by simple theory.*** Also, parasitic oscillations and other spurious oscillations are observed to occur in the M-Carcinotron,[7] as well as a complication of the interaction attributed to the "rising sun effect" which also occurs in magnetron oscillators.**** No quantitative description yet exists for these phenomena. Although many factors affect the development of useful oscillators and amplifiers of the

---

*Raised numerals refer to correspondingly numbered entries in the References at the end of the text.

**"Carcinotron" is trademark registered by the Compagnie General Telegraphie sans Fils.

***This comparison is made graphically in Fig. 3 of Ref. 5.

****Ref. 1, pp. 203-205.

magnetron type, not the least of which is the technology of materials and fabrication, it is nonetheless true that a suitable theoretical understanding of the interaction process in crossed fields would materially advance the state of perfection of these devices.

The purpose of the research leading to this disseration was to obtain a small-perturbation theory for the interaction in crossed-field devices. A more accurate determination of the criteria for oscillation in the M-Carcinotron is one of the objectives of such a theory, although the analysis is to be more general than this. A small-signal amplifier theory is also desired. Such a small-signal theory embracing both the Carcinotron and the amplifier, useful in itself, would also be a starting-point for large-signal calculations.

1.2 Previous Theory in Relation to the Present Problem

The theory of the traveling-wave magnetron was at first developed primarily for large-signal conditions.* This is a rather striking feature of crossed-field interaction theory, in comparison with the history of such devices as the traveling-wave tube.[10-12] There are some cogent reasons for this difference:

(1) The magnetron was first known as an oscillator only. In all self-excited oscillators, the oscillation level is determined by some non-linear element in either the energy conversion mechanism or in a feedback system. The magnetron oscillator is, therefore, always operated in a non-linear fashion; the interaction proceeds at signal levels large enough so that the non-

*See, for example, pp. 265-274 and pp. 288-338 of Ref. 2; see also Refs. 7 and 8. One of the few small-signal analyses, that of Ref. 9, was apparently not given much credence (cf. Ref. 2, p. 253).

linearity of the electronic behavior is pronounced.

(2) Qualitative analysis of the traveling-wave magnetron interaction discloses the important phenomenon known as "phase-focussing,"* which contributes greatly to the efficiency of all such devices. This phenomenon is attributed to the non-linear behavior of the electron stream. The interaction must therefore proceed at high level to obtain the benefits of phase-focussing, even in traveling-wave magnetron devices such as amplifiers, which need not obey the self-excited oscillator requirement of item (1).

As an example of a quantitative analysis of large-signal crossed field interaction, the work of Hartree may be cited.** Hartree and his co-workers computed numerically, by trial and error, the electron trajectories in an oscillating magnetron of a particular design, operating under particular conditions of applied fields and high-frequency load. From such a computation, the performance of the oscillator can be evaluated for the particular design and the particular operating conditions. A separate calculation is required, however, for each change of one of the design parameters or of one of the operating conditions. The computation process, being one of trial and error, requires an accurate estimate of the solution beforehand and also requires machine calculation to arrive at reasonably accurate results.

On the other hand, useful results concerning the behavior of the magnetron oscillator have been obtained by making rather rough approxi-

---

*Ref. 1, p. 192.
**A detailed description of this work is given in Ref. 2, pp. 265-274. The original reports, Refs. 7 and 8, are not generally available.

mations concerning the behavior of the electron stream.[13-15] Thus, while the Hartree method is extreme in that many individual electron trajectories are calculated, the method of using crude approximations concerning the aggregate stream behavior is another extreme.

Consideration of the possible use of the magnetron[6,16-19] as an amplifier and the advent of the M-Carcinotron, or backward-wave magnetron, have indicated the desirability of an adequate small-signal interaction theory. In these devices such linear interaction may be presumed to occur under certain operating conditions, although high-level operation is generally more desirable. Even at high level, however, some portions of the electron stream may undergo low-level interaction. A small-signal theory would thus be useful as a starting point for such a device.

In the discussion of the traveling-wave crossed-field interaction it should be recognized that this type of interaction has much in common with the conventional traveling-wave tube interaction. In spite of the complexities of the forces and the motions involved, the principle of continuous interaction between a stream and a slow electromagnetic wave is a fundamentally important element common to both devices. This common characteristic makes possible a unified treatment of the conventional and crossed-fields types of traveling-wave interaction with regard to many of their properties.[20]

The common features noted above are important because advances in the science of the one type often can be translated to the other. Thus, for example, delay lines used in magnetrons have been introduced into the traveling-wave tube technology* and vice-versa.** In regard to the prob-

*The interdigital line described in Ref. 21 was first used in magnetron oscillators as described in Refs. 22 and 23.
**Ref. 6. Traveling-wave tube type helices were used in these early magnetron amplifiers.

lem at hand, the idea of a small-signal theory for crossed-field devices received considerable impetus from the success of a small-signal theory of the traveling-wave tube. This theory, due to Pierce[10,11] is a departure from previous theories, such as that of Kompfner.[12] In the Pierce theory, the complex nature of the electric fields and motion is considered to be composed of a number of wave-like perturbations. The nature of each perturbational wave is analyzed, and the theory is made complete by determining which combination of the perturbations is present in the device. The perturbation technique thus described is a powerful tool; it has application to the analysis of crossed-field interaction as well.

Pierce applied his technique to a simple model of the traveling wave magnetron interaction.* He discovered the possibility of wave perturbations which gain in amplitude with distance in a forward-wave circuit, but did not pursue the analysis much further. Harman, in his book on electron motion,[22] carries on the analysis to the extent of combining a number of wave perturbations to satisfy a simplified set of input conditions. He thereby obtains an expression for the gain and bandwidth of such an amplifier.

Further interest was aroused when workers in France reported the realization of an oscillator of the magnetron type operating on a backward-wave space harmonic of the delay line;[4,5] they named their invention the "M-Carcinotron." It was noted that, in both the conventional and the magnetron types of traveling-wave devices, changing the proper parameter adapts Pierce's theory to backward-wave interaction. Theoretical criteria are thereby obtained for the initiation of oscillations in backward-wave devices. Although the theoretical predictions are accurately verified by experiment,[23,24] a complete theoretical explanation of crossed-field

*Ref. 11, Chapter XV.

backward-wave interaction does not appear to be given by the simple theory based on Pierce's model.

The disparity between the extension of the simple Pierce theory and experiment may be laid to the oversimplified treatment of the electron stream. The simple theory represents the stream as an infinitely thin sheet, and furthermore neglects the effects of the forces exerted by the electrons themselves on each other (space-charge forces). Various analyses have been made which avoid these oversimplifications. A particularly valuable work in this respect is that of MacFarlane and Hay,[25] in which account is taken of the finite size of the stream, its corresponding velocity and space charge density characteristics (assumed to be those of the "Brillouin type," described in Sec. 3.1) and also the space charge forces between the various parts of the stream. MacFarlane and Hay present some calculations of gain of the growing perturbations of such a stream in the presence of a slow-wave circuit, although their principal interest was in the possibility of obtaining gain without any slow-wave circuit. They did not combine their wave solutions in the manner necessary to evaluate the performance of an actual device. To some extent, the present dissertation is a more approximate treatment of the situation considered by MacFarlane and Hay with the addition of the solution of the longitudinal boundary value problem (Part V) for the determining the combination of waves on the system.

More recently, Gould published an analysis of the interaction of the M-Carcinotron.[26] He chose, however, a mathematical model somewhat simpler than that of MacFarlane and Hay. In this model, the electron stream bears a resemblance to the streams thought to exist in practical devices, i.e., those in which the space charge density is much lower than in the Brillouin stream. Such a stream has a rather complicated motion; Gould neg-

lects these complications and assumes that the electrons of the stream move in simple rectilinear trajectories as in the sheet beam and the Brillouin stream. This approach has an advantage over the simple sheet beam model in that space-charge forces and stream thickness effects can be taken into account. Gould finds three wave solutions and is therefore unable to solve the longitudinal boundary problem in the exact (field-theoretical) sense. His approximate solution, however, is in better agreement with experiment in regard to the start-oscillation criteria, thus the sheet beam results.[27] The present dissertation attempts to solve the longitudinal boundary value problem more exactly, using more than three wave perturbational solutions.

CHAPTER II

THE METHOD OF ANALYSIS

2.1 The Principal Assumptions

It seems desirable to collect all restrictions on the analysis in one place for reference purposes. Discussion of the assumptions and arguments relating to their justification are presented as the assumptions are introduced in the text. The principal assumptions are:

(1) The electron stream is assumed to have as a homogeneous, isotropic fluid. The discrete nature of the electron and its Coulomb field are ignored (Secs. 3.7 and 3.8).

(2) Non-relativistic (Newtonian) mechanics is assumed to be sufficiently accurate for the purposes of analysis (Sec. 3.4).

(3) All wave disturbances in the interaction region propagate with phase velocities small in comparison with the velocity of light in vacuo, so that the fields are accurately given as derived from a scalar potential (Sec. 3.4).

(4) The unperturbed stream has the characteristics of Brillouin flow (Sec. 3.1).

(5) Signals are small enough so that linear perturbation theory is applicable (Sec. 3.3).

(6) The electron stream is synchronous with the fields of only one of the space-harmonics of the circuit. In periodic structures with essentially monovelocity

streams, the phase velocities of all space harmonics save one are very much different from the electron velocities (Sec. 6.3.2).

(7) Various assumptions are made regarding the thickness of the stream in relation to the signal and cyclotron frequencies. The stream is assumed to be very thin, but still of finite thickness, if the signal frequency is large in comparison with the cyclotron frequency. The stream may be rather thick if the signal frequency is much lower than the cyclotron frequency.

(8) The steady (d-c) fields applied are uniform in space as well as time (Sec. 3.1).

The assumption (4) regarding the d-c stream is perhaps the most critical one in the sense that the other assumptions can be justified by building actual devices in which the conditions are satisfied within an arbitrary degree of accuracy. The nature of the d-c stream, however, is not so easily measured or controlled as the other parameters of the device.

Other assumptions are made, but not listed above, concerning matters of convenience in computation. They are not essential to the soundness of the treatment, but no improvement in the accuracy of the results would be obtained by using a more rigorous method of computation.

2.2 Plan of the Analysis

The small-signal analysis of interaction in crossed electric and magnetic fields consists of the two main tasks of determining the natures of the waves capable of propagating on the stream-circuit medium and of

determining the amplitudes of the waves which are excited at the ends of, or discontinuities in, such a medium.

2.2.1 The Determination of the Wave Characteristics

The first task of the analysis, that of calculation of the propagation constants, field and stream configurations accompanying all significant waves on the system, is accomplished in Parts II, III, and IV of this dissertation.

Part II deals with the determination of the behavior of the stream under the influence of an arbitrary circuit excitation, i.e., without regard as to the source of the circuit potential. In Chapter III, the laws of electron dynamics are applied to form a differential equation which governs the transverse behavior, or profiles, of the various stream and field quantities in the three regions which comprise the interaction space. This is an involved equation; Chapter IV is devoted to evaluating the solutions of it by approximate methods in the various regions of the complex ξ-plane (ξ being a variable expressing both the propagation constant of the wave and the space coordinate). Chapter V considers the matching of the fields at the interfaces between the electrode planes and the three regions of the interaction space; this is the transverse boundary value problem. The result of Part II of the analysis is the determination of the relationships between all field and stream quantities in the interaction space and the wave of potential on the anode plane.

Part III is the converse of Part II: assuming the stream to be perturbed in an arbitrary fashion, the wave of potential generated in the circuit is calculated from induced charge theory and the circuit characteristics. The result is the "induction" equation, or the "circuit equation."

Part IV combines the results of Parts II and III to form a self-consistent system. This self-consistency requirement leads to the determination of the propagation constants of characteristic waves, i.e., waves that are capable of freely propagating on the stream-circuit medium. Wave solutions which are found are:

(1) Quasi-synchronous waves, both with a slow wave circuit (Chapter IX) and without any slow wave circuit, as in a "drift" region (Sec. 8.7).

(2) Cyclotron waves, which are assumed to have negligible interaction with the circuit (Chapter X).

(3) "Non-interacting" waves, which is an omnibus classification for electromagnetic waves which are present even without the stream and which do not interact with the stream (Chapter XI), and

(4) Synchronous "trivial" solutions, which in aggregate constitute a "phantom" solution.

2.2.2 The Longitudinal Boundary Value Problem

The second part of the theoretical problem is the determination of the combination of the waves found above that meet the boundary requirements at discontinuities in the uniform stream circuit medium which is the interaction space. In Chapter XIII the longitudinal boundary value problem thus defined is formulated for the special case of an unmodulated stream entering the interaction space, which is terminated at its downstream end in a reflectionless manner.

An approximate solution to the longitudinal boundary problem in this special case is presented in Chapter XIV. Calculations based on this

solution are presented in Chapter XV for forward-wave interaction and in Chapter XVI for backward-wave interaction.

PART II

STREAM PERTURBATIONS PRODUCED BY THE FIELDS

CHAPTER III

DIFFERENTIAL EQUATIONS FOR PERTURBATIONS IN THE INTERACTION SPACE

3.1 The Static System

The stage on which all high-frequency interaction phenomena are to take place is defined with reference to Fig. 3.1. The interaction space is the region confined by the parallel planes $y = y_s$ (the "sole" surface) and $y = y_d$ (the anode surface). The assumption of a planar configuration considerably simplifies the analysis of both the static and the dynamic characteristics of the interaction. Furthermore, in actual systems the interaction space is usually the space between concentric cylinders (or a portion of such a space), the radius of curvature of the cylinders being much larger than the radial extent of the space. Thus, many cylindrical configurations may be analyzed as planar ones with little error.

The interaction space is immersed in a steady, uniform magnetic field which is directed along the x-axis. The density of the d-c magnetic flux is*

$$\vec{B} = B_{d\text{-}c}\hat{x} \text{ weber/meter}^2 \quad . \tag{3.1}$$

At the planar boundaries of the interaction space are electrodes to which are applied suitable d-c electric potentials, thereby establishing a d-c electric field. The "sole"--or, more usually, the anode--may serve to guide an electromagnetic wave of high frequency. In such

*MKS, rationalized units are used throughout this dissertation.

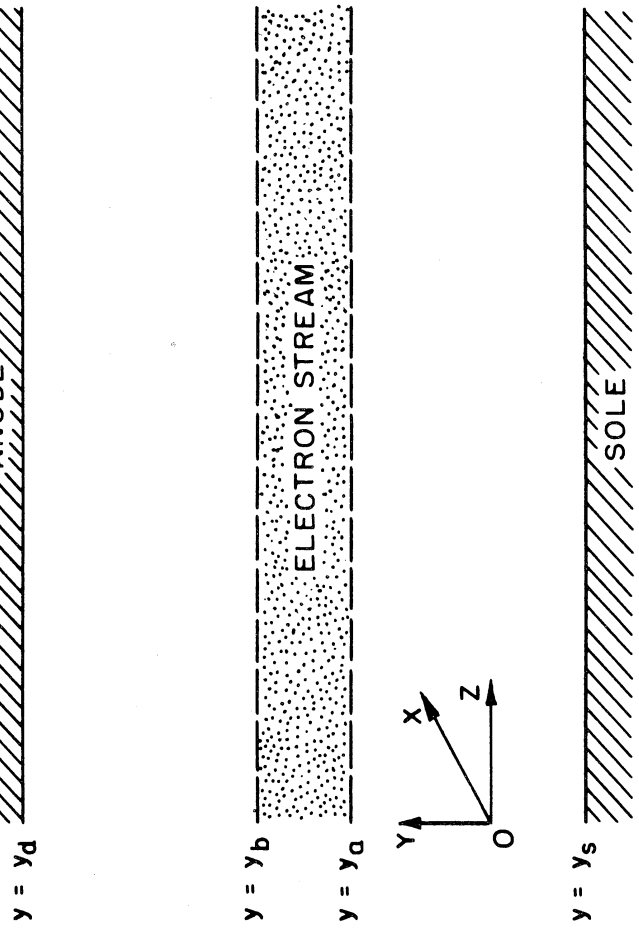

FIG. 3.1 COORDINATE SYSTEM USED IN THE ANALYSIS.

cases the electrode surfaces may not be the smooth planes of Fig. 3.1; the d-c electric field may then vary spatially because of the electrode geometry. This spatially non-uniform d-c electric field exerts a force on the moving electrons which varies rapidly with time. Because of the inertia of the electrons, however, the motion resulting from the time-varying component of the force experienced by the electrons is generally quite small. Such motion may be appreciable if the force on individual electrons varies periodically at approximately the cyclotron frequency, although this condition rarely obtains in practice. It is therefore assumed that the effect of the non-uniformity of the d-c electric field arising from irregularities of electrode shape is negligible; the electron stream is considered to be essentially that stream which would exist if the actual electrodes were plane surfaces.

The assumptions concerning the nature of the steady electron flow between the parallel planes are much more difficult to justify than the assumptions made above. In the first place, only the "beam" type of stream is considered, i.e., one in which the gross motion of the stream is rectilinear in the z direction and in which all of the electrons have nearly the same velocity. This is the type of stream employed in the Carcinotron,[1] for example.

The description given above is not sufficiently precise for the present analysis because even small differences of the characteristics of different parts of the stream are expected to have important effects. The exact stream behavior is quite complex, however. Neither theoretical[28-30] nor experimental[31-33] attack on the problem has yet produced any detailed description of the motion. The calculation of interaction phenomena with such a complex d-c stream, even if it were precisely known, would be a formidable problem defying analysis.

As in many other physical problems, it becomes necessary to make some judicious idealizations leading to a mathematical model conducive to analysis while yet retaining the essential physical characteristics of interest. Thus, Gould chose, in his analysis[26] of the M-type oscillator, to recognize the fact that the average space-charge density of the streams of useful tubes is quite small. His mathematical model is realistic in that the space-charge density is small, but it neglects the transverse (y directed) quasi-trochoidal motion of the electrons of the actual d-c stream.

The idealization made in the present dissertation follows a different course. It is recognized that one of the possible theoretical solutions of the static beam problem is the so-called Brillouin-flow[34] situation, in which there is no transverse motion of the electrons. If the electron stream originates from a unipotential source and if the electrons do not exchange energy, then this type of stream is further characterized by uniform d-c space-charge density and linear y-dependence of the z-component of velocity (the only d-c velocity component). Thus, referring to Fig. 3.1, the stream is mathematically defined by

$$\rho_o = -\frac{\omega_c^2 \epsilon_o}{\eta} , \quad y_a \leq y \leq y_b , \tag{3.2}$$

$$u_{zo} = \omega_c y , \tag{3.3}$$

$$u_{xo} = u_{yo} = 0 . \tag{3.4}$$

Equation 3.3 implies that the plane y = 0 is at cathode potential.

The use of the Brillouin-flow model is justified because it is mathematically convenient and because it is in principle physically realizable. Furthermore, it is thought to be a desideratum of high-power devices, since the current in a Brillouin stream is the highest

attainable under specified conditions of magnetic field and stream cross-sectional area.

It is shown in Appendix I that the stream of Eqs. 3.2-3.4 can be made to have any desired position in relation to the electrode system. Thus, the d-c potential of the anode electrode (relative to the emitter) must be

$$V_{o\ anode} = \frac{\omega_c^2\, y_b}{\eta} \left(y_d - 1/2\ y_b\right) , \tag{3.5}$$

while the d-c potential of the "sole" electrode (on the lower-velocity side of the stream) must be

$$V_{o\ sole} = \frac{\omega_c^2\, y_a}{\eta} \left(y_s - 1/2\ y_a\right) . \tag{3.6}$$

3.2 General Nature of the Perturbations

Let f represent any of the physical quantities associated with conditions in the interaction space, e.g., electric field, electron velocity, or charge density. Then f can be resolved into two components: an unperturbed value, f_o, and a perturbational component, $\tilde{f}$. Thus,

$$f = f_o + \tilde{f} . \tag{3.7}$$

This can always be done, regardless of the nature of the perturbations. In keeping with Pierce's method of small-signal analysis, however, it is assumed that the perturbation, $\tilde{f}$, is the linear sum of a number of waves; thus

$$f = \mathrm{Re} \sum_{n=1}^{N} \sqrt{2}\, f_n \exp\left(j\omega t - \Gamma_n z\right) , \tag{3.8}$$

where $\sqrt{2}\, f_n$ is the complex amplitude of the nth wave. This nth wave, which has the propagation factor Γ_n, has an rms magnitude equal to the absolute value $|f_n|$. The system of notation used is summarized in Table

3.1. In addition, Table 3.2 lists some of the more important variables of the analysis which f may be taken to represent.

TABLE 3.1. NOTATION USED TO DESCRIBE PERTURBED PHYSICAL QUANTITIES

Symbol	Description of Symbol	Quantity Represented
f	Plain	Total (actual) quantity
f_o	Zero subscript	Unperturbed component (d-c)
$\tilde{f}$	Tilde	Total perturbation (a-c, or r-f) component
f_n	Nonzero subscript	Rms (complex) value of nth wave

TABLE 3.2. PHYSICAL QUANTITIES REPRESENTED BY THE SYMBOL f

Symbol	Quantity
v	Electric potential
$\vec{E}$ $(\bar{E}_y, E_z)$	Electric field strength (components)
$\vec{u}$ (u_y, u_z)	Electron velocity (components)
$\vec{\delta r}$ (δ_y, δ_z)	Electron displacement from unperturbed position (components)
ρ	Space-charge density

The conditions necessary for the validity of the representation of Eq. 3.8 are developed below. It should be noted that there is assumed to be no x-variation of any quantity; y-variations are implicit in the y-dependence of the rms magnitudes f_n. Also, the only time variation is at the rate corresponding to the single frequency ω.

3.3 Perturbations of the Electron Motion

In view of the representation of physical quantities as functions of the space coordinates and time rather than related to individual particles, it is convenient to express the total time derivatives of motion in terms of the partial derivatives of space and time. Hence,

$$\left.\frac{df}{dt}\right|_e = \frac{\partial f}{\partial t} + u_z \frac{\partial f}{\partial z} + u_y \frac{\partial f}{\partial y} \quad . \tag{3.9}$$

Again, this is perfectly general, it being understood that the quantities f, u_z, and u_y are the total quantities and that $\left.\frac{df}{dt}\right|_e$ represents the time derivative along a trajectory.

The resolution of each quantity f as in Eqs. 3.7 and 3.8 leads to

$$\begin{aligned}\left.\frac{df}{dt}\right|_e = & \frac{\partial f_o}{\partial t} + u_{zo} \frac{\partial f_o}{\partial z} + u_{yo} \frac{\partial f_o}{\partial y} \\ & + \frac{\partial \tilde{f}}{\partial t} + u_{zo} \frac{\partial \tilde{f}}{\partial z} + u_{yo} \frac{\partial \tilde{f}}{\partial y} + \tilde{u}_z \frac{\partial f_o}{\partial z} + \tilde{u}_y \frac{\partial f_o}{\partial y} \\ & + \tilde{u}_z \frac{\partial \tilde{f}}{\partial z} + \tilde{u}_y \frac{\partial \tilde{f}}{\partial y} \quad ,\end{aligned} \tag{3.10}$$

where terms on the right side have been grouped as products of unperturbed quantities, products of unperturbed quantities and perturbations, and products of perturbation componente on separate lines, respectively. There is no change with time of any characteristic of the unperturbed beam:

$$\frac{\partial f_o}{\partial t} = 0 \quad . \tag{3.11}$$

Because, in addition, the stream is longitudinally uniform in the unperturbed state,

$$\frac{\partial f_o}{\partial z} = 0 \quad . \tag{3.12}$$

Finally, the unperturbed Brillouin stream has no transverse, or y, com-

ponent of motion. Consequently, Eq. 3.10 becomes

$$\left.\frac{df}{dt}\right|_e = \frac{\partial \tilde{f}}{\partial t} + u_{zo}\frac{\partial \tilde{f}}{\partial z} + \tilde{u}_y\frac{\partial f_o}{\partial y} + \tilde{u}_z\frac{\partial \tilde{f}}{\partial z} + \tilde{u}_y\frac{\partial \tilde{f}}{\partial y} \quad , \qquad (3.13)$$

in which there are no d-c terms.

The only kinematic variable for which the d-c, or unperturbed, portion has variation with y is the velocity—specifically, the z-component of the velocity. Using Eq. 3.3, the partial derivative expansion for the time derivative of u_z along a trajectory is shown to be

$$\left.\frac{du_z}{dt}\right|_e = \frac{\partial \tilde{u}_z}{\partial t} + u_{zo}\frac{\partial \tilde{u}_z}{\partial z} + \omega_c\tilde{u}_y + \tilde{u}_z\frac{\partial \tilde{u}_z}{\partial z} + \tilde{u}_y\frac{\partial u_y}{\partial y} \quad . \qquad (3.14)$$

If f is taken to represent the other kinetic variables, then

$$\left.\frac{df}{dt}\right|_e = \frac{\partial \tilde{f}}{\partial t} + u_{zo}\frac{\partial \tilde{f}}{\partial z} + \tilde{u}_z\frac{\partial \tilde{f}}{\partial z} + \tilde{u}_y\frac{\partial \tilde{f}}{\partial y} \quad . \qquad (3.15)$$

The essence of the linear perturbation theory is that the products of perturbations must be negligible; Eq. 3.8 cannot otherwise be written. Thus, Eq. 3.14 becomes in this linearizing process the linear sum of waves having rms magnitudes

$$\left(\left.\frac{du_z}{dt}\right|_e\right)_n = \left(j\omega - u_{zo}\,\Gamma_n\right)u_{zn} + \omega_c\,u_{yn} = \Omega_n\,u_{zn} + \omega_c\,u_{yn} \quad , \qquad (3.16)$$

in which the operator form is the result of performing the differentiations on the terms of Eq. 3.8. Equation 3.16 also serves to define Ω_n, a time-differentiation operator along a trajectory. Ω_n may be interpreted as the complex frequency of the forces and other phenomena experienced by the electrons which have the unperturbed velocity u_{zo}. Using the same linearizing process on Eq. 3.15 leads to

$$\left(\left.\frac{df}{dt}\right|_e\right)_n = (j\omega - u_{zo}\Gamma_n)\, f_n = \Omega_n f_n \quad . \qquad (3.17)$$

The nonlinear terms dropped in transition from Eqs. 3.14 and 3.15 to Eqs. 3.16 and 3.17 are truly negligible only if their effect is small in comparison with subsequently manipulated combinations of the linear terms, and not merely if the nonlinear terms happen to be small in comparison with the linear terms considered individually. As an illustration of this principle, consider Eqs. 3.15 and 3.17 when $\Omega_n = 0$. Then the linear portion is zero and the omission of the nonlinear terms is not warranted.

3.4 Perturbations of the Force Field Within the Electron Stream

Fundamentally, the forces acting on the electrons of the stream can be obtained from the electric and magnetic fields through the Lorentz force equation

$$\vec{F} = -e\vec{E} - e(\vec{u} \times \vec{B}) \quad , \qquad (3.18)$$

where -e is the electronic charge. This becomes somewhat simplified in that certain of the field and force components do not appear in the present instance.

Some worthwhile further simplification can be made. First, the ratio of the magnetic force of an electromagnetic wave on a charged particle to the electric force of the wave is equal to the ratio of the particle velocity to the velocity of light.* The perturbation of the magnetic field may therefore be omitted from the force equation in the vast majority of cases, since the electron energy in most crossed-field devices rarely exceeds a thousand electron-volts, corresponding to ve-

*Ref. 35, p. 328.

locities less than 1/16 th the velocity of light. The second simplification arises from the fact that, for waves which are propagated with phase velocities small in comparison with the velocity of light, the electric field is represented with sufficient accuracy as derived from a scalar electric potential.[36]

The notation of Sec. 3.2 is slightly modified in describing the electric potential as a space-time function in the interaction region. The electric potential is the sum of an unperturbed value and a number of wave-like perturbations:

$$v(y,z,t) = V \phi_o + \mathrm{Re} \sum_{n=1}^{N} \sqrt{2}\, V_n \phi_n \exp (j\omega - \Gamma_n z) \quad . \qquad (3.19)$$

The difference here is that the complex amplitude of the nth wave, $\sqrt{2}\, V_n \phi_n$, contains a y-dependent portion, ϕ_n, and the factor V_n which does not vary spatially. The convenience of this notation becomes apparent when V_n can be identified with potential on a propagating anode or sole structure, if there is such a structure. The electric field components of the nth wave have rms values

$$E_{zn} = \Gamma_n \phi_n V_n \qquad (3.20)$$

and

$$E_{yn} = - V_n \frac{\partial \phi_n}{\partial y} \quad . \qquad (3.21)$$

With the above representation, the two components of the Lorentz force equation become

$$F_{zn} = - e \Gamma_n V_n \phi_n + e B_{d\text{-}c} u_{yn} \qquad (3.22)$$

and

$$F_{yn} = e V_n \frac{d\phi_n}{dy} - e B_{d\text{-}c} u_{zn} . \qquad (3.23)$$

3.5 The Newtonian Equations of the Electron Motion

Assuming the validity of non-relativistic mechanics, the forces of Sec. 3.4 are equated to the time rate of change of electron momenta obtained from Sec. 3.3. The following equations are obtained for the velocity components:

$$u_{zn} = \frac{-\eta V_n \Gamma_n \phi_n}{\Omega_n} \tag{3.24}$$

and

$$u_{yn} = \frac{\eta V_n \frac{d\phi_n}{dy}}{\Omega_n} + \frac{\eta \omega_c \Gamma_n V_n \phi_n}{\Omega_n^2} \quad , \tag{3.25}$$

Since the velocity is the total time derivative (along a trajectory) of the electron space coordinate, and the a-c velocity is the total time derivative of the electron displacement from its unperturbed orbit, the a-c velocity and displacement components are related by

$$u_{zn} = \left(\frac{d\delta z}{dt}\bigg|_e\right)_n = \Omega_n \delta z_n \tag{3.26}$$

and

$$u_{yn} = \left(\frac{d\delta y}{dt}\bigg|_e\right)_n = \Omega_n \delta y_n \quad , \tag{3.27}$$

which are obtained from Eq. 3.17 by letting f represent the displacement components δz and δy, respectively. The positional displacement components are therefore

$$\delta z_n = \frac{u_{zn}}{\Omega_n} = \frac{-\eta V_n \Gamma_n \phi_n}{\Omega_n^2} \tag{3.28}$$

and

$$\delta y_n = \frac{u_{yn}}{\Omega_n} = \frac{\eta V_n \frac{d\phi_n}{dy}}{\Omega_n^2} + \frac{\eta V_n \omega_c \Gamma_n \phi_n}{\Omega_n^3} \quad . \tag{3.29}$$

The equations for the velocity and displacement components completely describe the electron motion in terms of the electric space potential. This potential is determined partly by the excitation of the interaction space by the electrode system and partly by the presence of electric charge in the region. The application of the law of conservation of charge and either Coulomb's law or Poisson's law will serve to complete the description of the potential function.

3.6 The Law of Conservation of Charge

The law of conservation of charge is usually stated as

$$\frac{\partial \rho}{\partial t} + \nabla \cdot (\rho \vec{u}) = 0 \quad , \tag{3.30}$$

which is also called the equation of continuity of charge. A form of this equation which is particularly suited for the perturbation theory is obtained by letting the general symbol, f, of Sec. 3.2 correspond to the charge density. Thus,

$$\left.\frac{d\rho}{dt}\right|_e = \frac{\partial \tilde{\rho}}{\partial t} + u_{zo} \frac{\partial \tilde{\rho}}{\partial z} \quad . \tag{3.31}$$

Then, if the divergence of the product $\rho\vec{u}$ is expanded according to the identity

$$\nabla \cdot (S\vec{a}) \equiv \vec{a} \cdot \nabla S + S \nabla \cdot \vec{a} \tag{3.32}$$

and nonlinear terms are discarded,

$$0 = \frac{\partial \tilde{\rho}}{\partial t} + u_{zo} \frac{\partial \tilde{\rho}}{\partial z} + \rho_o \nabla \cdot \tilde{u} \quad . \tag{3.33}$$

The first two terms on the right of Eq. 3.33 are recognized as the right side of Eq. 3.31; hence

$$\Omega_n \rho_n = - \rho_o \nabla \cdot \vec{u}_n \quad , \tag{3.34}$$

which is the simple form desired.

In the present case, the indicated operations on the velocity lead to the result that the rms value of the charge perturbation of the nth wave can be expressed as

$$\rho_n = -\eta \rho_o V_n \left\{ \frac{\frac{d^2\phi_n}{dy^2} + \Gamma_n^2 \phi_n}{\Omega_n^2} + \frac{2\omega_c \Gamma_n \frac{d\phi_n}{dy}}{\Omega_n^3} + \frac{2\omega_c^2 n^2 \phi_n}{\Omega_n^4} \right\} . \quad (3.35)$$

3.7 Coulomb's Law

To calculate the contribution of the charge carried by the electrons to the potential at a point in space, one could in principle determine the Coulomb potential arising from the influence of each electron in the entire stream. The sum of these contributions would then be the "space-charge" effect on the potential at the point. Such an approach is hardly practical considering the large number of electrons, their complex distribution, and the long-range nature of the Coulomb field. A more tractable mathematical method is used in the present analysis; it is described in Sec. 3.8.

Certain poorly understood phenomena--the fact of anode current in a non-oscillating cut-off magnetron,[37] and various matters pertaining to noise--have been observed in crossed-field devices. It is generally believed that the explanation of such phenomena must account for the individuality of the electrons;* this aspect of the electron stream is often referred to as the "discrete electron-to-electron interaction."[38]

3.8 Poisson's Law

The microscopically discrete nature of the electron stream is ignored, in the application of Poisson's law, in favor of a representation of the stream as a charge-bearing fluid having the same macroscopic

*Ref. 2, p. 222.

properties. Thus, a macroscopically small volume element of the stream containing N electrons is represented as though the N electrons were "smeared out," or "blurred," into a homogeneous, isotropic fluid having a total charge of -Ne units in the volume element, where -e is the electronic charge. Since the discrete nature of the electrons is disregarded in this approach, no results can be expected concerning the phenomena discussed in Sec. 3.7. Nevertheless, the "charged fluid" treatment may be expected to yield accurate results concerning energy interchange and other aspects which make crossed-field devices useful.

Poisson's equation is

$$\nabla^2 V = -\frac{\rho}{\epsilon_o} , \tag{3.36}$$

which takes the perturbational form, for the nth wave,

$$V_n \left[\frac{d^2\phi_n}{dy^2} + \Gamma_n^2 \phi_n\right] = -\frac{\rho_n}{\epsilon_o} . \tag{3.37}$$

3.9 The Differential Equation Governing the Transverse Variation of the Electric Potential Function Within the Electron Stream

The equations of motion and of charge continuity together with Poisson's equation combine to define completely the electric potential by means of a second-order differential equation. Thus, by eliminating both V_n and ρ_n from Eqs. 3.35 and 3.37, and again making use of Eq. 3.2 describing the static stream, the following differential equation is obtained:

$$\left(1 + \frac{\Omega_n^2}{\omega_c^2}\right)\frac{d^2\phi_n}{dy^2} + \frac{2\,\omega_c \Gamma_n}{\Omega_n}\frac{d\phi_n}{dy} + \Gamma_n^2\left(1 + \frac{\Omega_n^2}{\omega_c^2} + \frac{2\,\omega_c^2}{\Gamma_n^2}\right)\phi_n = 0 . \tag{3.38}$$

Equation 3.38 suggests the normalization of Ω_n to the cyclotron frequency; the actual normalization is made with respect to $j\omega_c$:

$$\xi_n = \frac{\Omega_n}{j\omega_c} = \frac{j\omega - u_{zo}\Gamma_n}{j\omega_c} = \frac{\omega}{\omega_c} + j\frac{\Gamma u_{zo}}{\omega_c} \quad . \qquad (3.39)$$

The static Brillouin stream has the velocity given by Eq. 3.3; hence the new variable can also be written in the useful form

$$\xi_n = \frac{\omega}{\omega_c} + j\Gamma_n y \quad . \qquad (3.40)$$

Since ξ_n is a function of y, the independent variable can also be chosen as ξ_n; the differential equation then takes the form

$$\xi^2(1-\xi^2)\frac{d^2\phi_n}{d\xi^2} - 2\xi\frac{d\phi_n}{d\xi} + [2 + \xi^2(\xi^2-1)]\,\phi_n = 0 \quad . \qquad (3.41)$$

3.10 The Differential Equation Governing the Transverse Variation of the Electric Potential Function Outside the Electron Stream

Outside the stream, where there are no charges, Poisson's law degenerates into the Laplace equation. Thus, Eq. 3.37 with ρ_n equal to zero yields

$$\frac{d^2\phi_n}{dy^2} + \Gamma_n^2\phi_n = 0 \quad . \qquad (3.42)$$

CHAPTER IV

SOLUTIONS OF THE POTENTIAL DIFFERENTIAL EQUATIONS

4.1 Solutions of the Differential Equation Governing the Electric Potential Outside the Stream

The perturbational form of the Laplace equation, which applies outside the stream for slow waves, has been shown to be

$$\frac{d^2\phi_n}{dy^2} + \Gamma_n^2\phi_n = 0 \quad . \tag{4.1}$$

The two solutions of this differential equation can be written

$$\phi_n = C_1 \exp j\Gamma_n y + C_2 \exp (-j\Gamma_n y) \tag{4.2}$$

or

$$\phi_n = C_3 \sinh j\Gamma_n y + C_4 \cosh j\Gamma_n y \tag{4.3}$$

or

$$\phi_n = C_5 \sin \Gamma_n y + C_6 \cos \Gamma_n y \quad , \tag{4.4}$$

where the six coefficients, the C's, are arbitrary.

4.2 Discussion of the Differential Equation Governing the Electric Potential Within the Stream

4.2.1 Relation to the Differential Equation of MacFarlane and Hay

The differential equation satisfied by the potential function within the electron stream has been shown to be

$$\xi^2(1-\xi^2)\frac{d^2\phi}{d\xi^2} - 2\xi\frac{d\phi}{d\xi} + [\xi^2(\xi^2-1)+2]\phi = 0 \; . \tag{4.5}$$

The substitution

$$U = \frac{\phi}{\xi} \tag{4.6}$$

transforms this differential equation into

$$\frac{d^2U}{d\xi^2} + \frac{2\xi}{\xi^2-1}\frac{dU}{d\xi} - U = 0 \quad , \tag{4.7}$$

which was originally derived by MacFarlane and Hay.[25] The function U is proportional to a velocity potential for the wave; since the perturbational motion is very nearly irrotational, the velocity perturbation is accurately represented as derived from a scalar velocity potential. MacFarlane and Hay used numerical techniques to solve the differential equation; their results have apparently not been published.

The form of the differential equation involving the electric potential, Eq. 4.5, will be used in preference to that involving the velocity potential in the present analysis, since expressions are needed for the electric potential for the purpose of matching electric fields at discontinuities.

4.2.2 Mathematical Discussion of the Potential Differential Equation

The differential equation, Eq. 4.5, which is satisfied by the potential function within the stream, is a linear, homogeneous equation of the second order having variable coefficients. As is the case with all but the simplest second order differential equations, there is no general method by which an exact solution can be obtained. Recourse is usually had to a number of mathematical techniques,[39,40] the success and accuracy of which depend on the particular nature of the differential equation. Two such techniques are applied in the present analysis, viz., the representation of the solutions as power series of the independent variable and the representation of the solutions as those solutions of a slightly different differential equation which admits of an exact solution. In the latter case, the two differential equations are asymp-

totically identical as one of the parameters of either equation approaches some limiting value.

4.2.3 The Power Series Solutions of the Differential Equation

The representation of the solution of the differential equation as a power series[39]—or, equivalently, the method of "integration in series"[40]—can be applied. However, since the differential equation has singularities, more than one series is required to describe the solution for the entire range of the independent variable. In Fig. 4.1, two regions of the ξ-plane are shown, in which the following functional representations are adequate:

$$\text{in region P:} \qquad \phi = C_1 g_1 + K_2 h_1 \ , \tag{4.8}$$

$$\text{in region Q:} \qquad \phi = C_2 g_2 + K_2 h_2 \ . \tag{4.9}$$

On the intersection of P and Q, the two representations above of the solutions of the differential equation must be related to each other. Because the differential equation is a linear one, the relationship must be a linear one. Thus, for example, the first solution, g_1, of Eq. 4.8 is expressible as a linear combination of the two functions g_2 and h_2 of Eq. 4.9. This property is readily seen in the three different representations of the solution of the Laplace equation in Sec. 4.1.

The choice of the value of ξ about which the power series expansion is to be made depends on the mathematical nature of the differential equation and also on the physical phenomena which are described. Thus, an expansion about $\xi = 0$ is made in Sec. 4.3 because this condition corresponds to the propagation of a quasi-synchronous wave and it is expected that strong electron interaction will occur with such a wave. Mathematically, the expansion about the origin of the ξ-plane is convenient, and the series representations are convergent everywhere inside

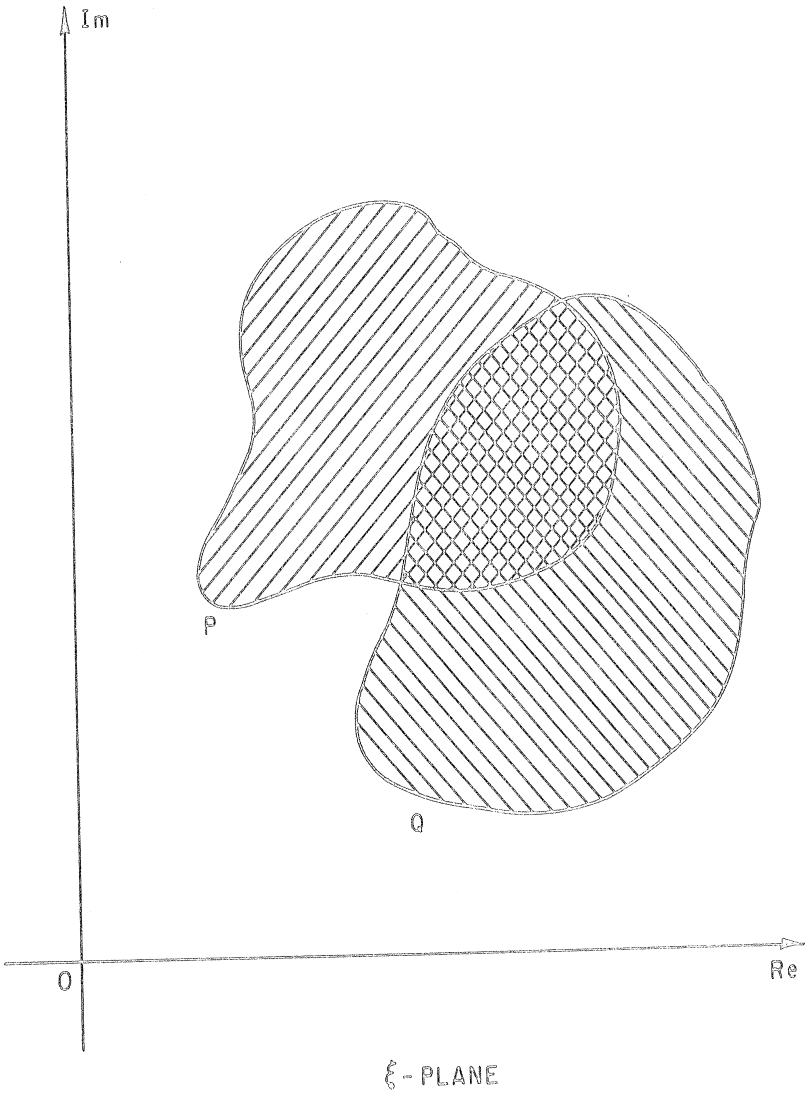

FIG. 4.1 GENERAL REGIONS OF THE ξ-PLANE.

the unit circle[41] as shown in Fig. 4.2.

Representations near the singularities $\xi = +1$ and $\xi = -1$ are desired because the occurrence of plasma waves in other devices suggests that waves with propagation constants governed in a similar way by the average (d-c) space-charge density may propagate here also. Mathematically, a separate expansion in series about each singularity is easiest; the series so obtained are convergent in the regions shaded in Fig. 4.3.

4.3 Representation of the Solutions Within the Stream by Power Series near Synchronism

The Taylor series $\sum_{k=0}^{\infty} a_k \xi^k$ is substituted for the potential function, ϕ, in the differential equation, Eq. 4.5. When the indicated differentiations are performed, the following algebraic equation is obtained:

$$\sum_{k=0}^{\infty} [k(k-1)a_k - 2k\, a_k + 2a_k]\xi^{k-2} - \sum_{k=0}^{\infty} [k(k-1)+1]a_k \xi^k + \sum_{k=0}^{\infty} a_k \xi^{k+2} = 0 \,. \tag{4.10}$$

By changing the indices of summation, this can be written as

$$\sum_{k=-2}^{\infty} \left\{k(k+1)a_{k+2} - [k(k-1)+1]a_k + a_{k-2}\right\} \xi^k = 0 \,, \tag{4.11}$$

where the a_k are all zero for negative k. The recurrence relation

$$k(k+1)a_{k+2} - [k(k-1)+1]a_k + a_{k-2} = 0 \tag{4.12}$$

is a relation among either even-indexed coefficients or among odd-indexed coefficients. Equation 4.12 therefore determines all the coefficients in terms of two arbitrary coefficients, one for k even and one for k odd. The series representation for the y-dependence of the potential function is accordingly

$$\begin{aligned} \phi = {} & C\xi \left(1 + \frac{\xi^2}{2} + \frac{5}{24}\,\xi^4 + \frac{31}{240}\,\xi^6 + \cdots\right) \\ & + D\xi^2 \left(1 + \frac{\xi^2}{2} + \frac{11}{40}\,\xi^4 + \cdots \qquad\right) , \end{aligned} \tag{4.13}$$

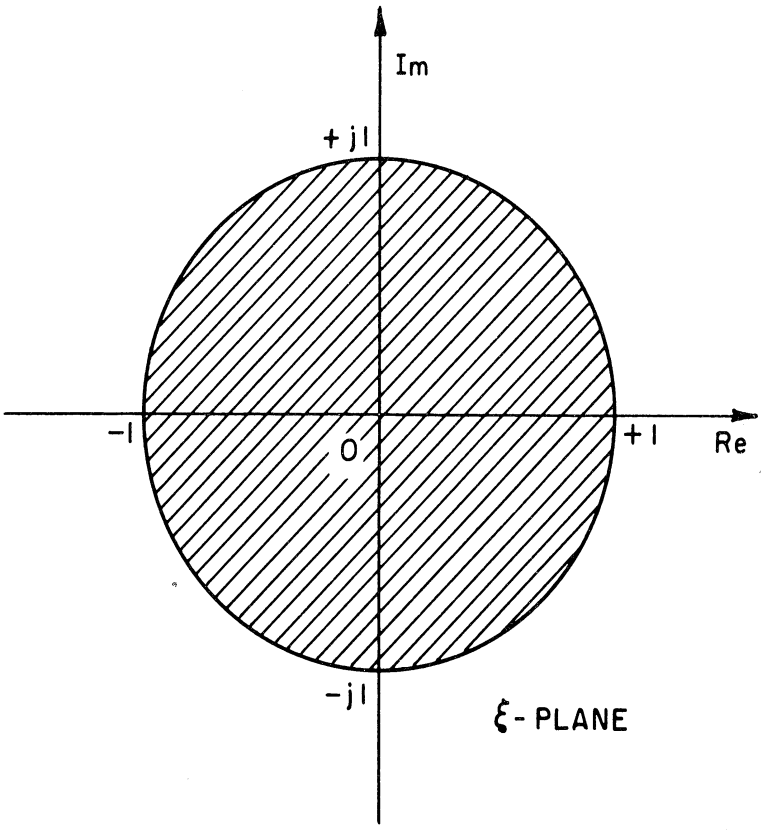

FIG. 4.2

THE REGION OF CONVERGENCE
OF THE QUASI-SYNCHRONOUS EXPANSION

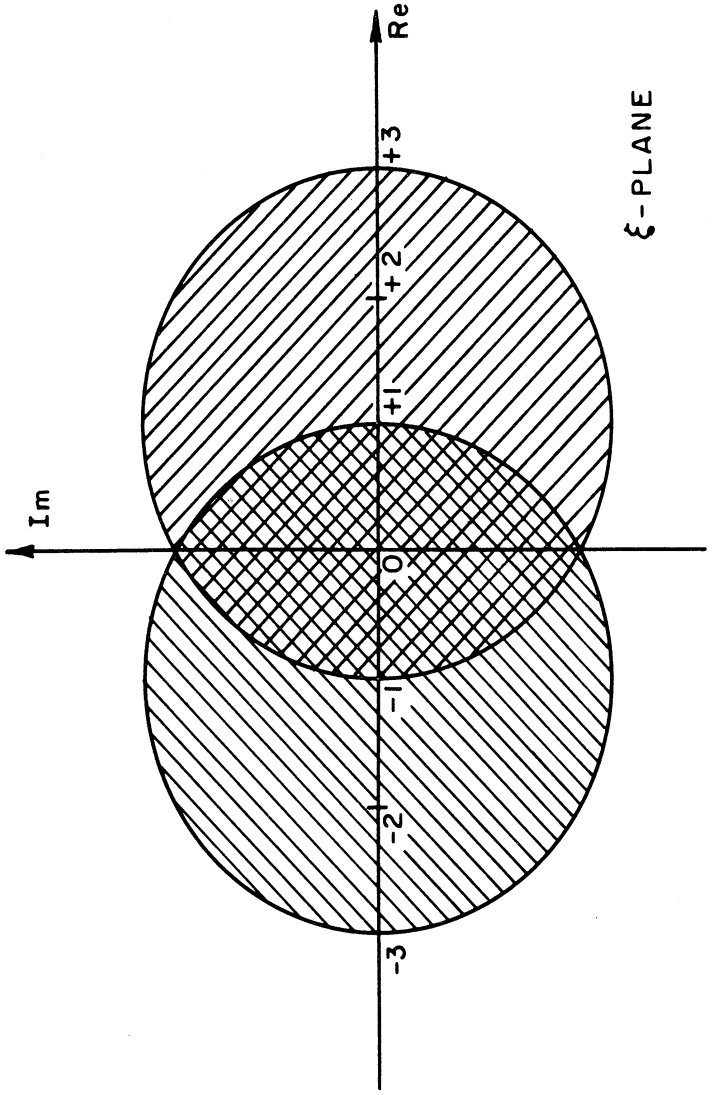

FIG. 4.3 THE REGIONS OF CONVERGENCE OF THE EXPANSIONS ABOUT THE SINGULARITIES OF THE DIFFERENTIAL EQUATION.

where C and D are the arbitrary constants. This is the same result obtained by Brewer[43] and also by Hok.[44]

4.4 Representations of the Solutions Within the Stream by Power Series near the Singularities

The expansion of the differential equation about the singularities is facilitated by transforming the independent variable by letting

$$\xi = 1 - \chi \tag{4.14}$$

for the expansion about the singularity $\xi = +1$, and

$$\xi = -(1 - \chi) \tag{4.15}$$

for the singularity $\xi = -1$. The treatment of the two singularities is combined through the use of the more compact notation

$$\xi = \pm (1 - \chi) \quad . \tag{4.16}$$

It will be observed that the differential equation, Eq. 4.5, is invariant to a transformation of the independent variable from ξ to $-\xi$. Therefore, the differential equation in terms of the new variables assumes the same form for either singularity; this is

$$(2\chi-5\chi^2+4\chi^3-\chi^4)\frac{d^2\phi}{d\chi^2} + (2-2\chi)\frac{d\phi}{d\chi} + (2-2\chi+5\chi^2-4\chi^3+\chi^4)\phi = 0 \quad . \tag{4.17}$$

Use of a Taylor series of powers of χ to represent the potential function in the same manner as in Sec. 4.3 leads to

$$0 = 2(k+1)^2 a_{k+1} - (5k+2)(k-1)a_k + [4(k-1)(k-2)-2]a_{k-1} - [(k-2)(k-3)-5]a_{k-2} - 4a_{k-3} - a_{k-4} \tag{4.18}$$

as a recurrence relation. Since this relation interrelates the even and odd coefficients, the Taylor series contains only one arbitrary coefficient. The calculation of the coefficients is in Appendix II. The single representation thus defined is

$$\phi = C'\left(1 - \chi + \frac{\chi^2}{4} - \frac{2}{9}\chi^3 - .001735\,\chi^4 - .019512\,\chi^5 + \ldots\right) . \tag{4.19}$$

The singular nature of the differential equation infers a second solution which is singular at $\chi = 0$ and is not obtainable from a Taylor series expansion. The method used here to find a second solution is motivated by comparison of the differential equation, Eq. 4.17, with the following transformed form of Bessel's equation:[45]

$$\frac{d^2y}{dx^2} - \frac{1}{x}\frac{dy}{dx} + \frac{y}{x} = 0 . \tag{4.20}$$

The two equations are asymptotically identical in the limit $\chi \to 0$. The first solution of this transformed form of Bessel's equation is quite similar to the exact series solution, Eq. 4.19, of the actual differential equation:

$$y = J_0\,(2\sqrt{x}) = 1 - x + \frac{x^2}{4} - \frac{x^3}{36} + \ldots - \ldots + (j)^{2n}\frac{x^n}{(n!)} + \ldots . \tag{4.21}$$

The second solution of Eq. 4.20 is the Bessel function of the second kind of zero order having the argument $2\sqrt{x}$:[46]

$$K_0\,(2\sqrt{x}) = J_0\,(2\sqrt{x})\,\ln 2\sqrt{x} + 4x - \frac{3}{8}x + \ldots . \tag{4.22}$$

The second solution of the exact (actual) differential equation is constructed from the first solution in a way suggested by the relationship between the two solutions of Eq. 4.20. Using $S_1(\chi)$ as an abbreviation for the first solution, Eq. 4.19, the second solution is written as

$$S_2(\chi) = S_1 \ln 2\sqrt{\chi} + \sum_{k=1}^{\infty} b_k \chi^k . \tag{4.23}$$

The determination of the coefficients b_k proceeds along previous lines.

The result of this calculation, presented in Appendix III, is that the second solution can be represented as

$$\phi = D'\left[\left(1-\chi+\frac{\chi^2}{4}-\frac{2}{9}\chi^3-.001735\,\chi^4-.019512\,\chi^5+\ldots\right)\ln 2\sqrt{\chi}+\frac{\chi}{4}-\frac{5}{16}\chi^2+\ldots\right] . \tag{4.24}$$

For the purposes of further analysis, where the functions will be represented by only a few terms of the series, the solution for the y-dependence of the potential function is preferably written in the form

$$\phi = C\left(1-\chi+\frac{\chi^2}{4}-\frac{2}{9}\chi^3+\ldots\right)$$

$$+ D\left[\left(1-\chi+\frac{\chi^2}{4}-\frac{2}{9}\chi^3+\ldots\right)\ln\chi+\frac{\chi}{2}-\frac{5}{8}\chi^2+\ldots\right] , \tag{4.25}$$

which is identical to the results of Eqs. 4.19 and 4.24 when

$$D = \frac{1}{2}D' \tag{4.26}$$

and

$$C = C' + D'\ln 2 . \tag{4.27}$$

An aspect of the methodology used above should be made clear. The comparison of the actual differential equation with the transformed Bessel equation was made to show the motivation; it has nothing to do with the accuracy of the solution to the actual differential equation. The solution expressed by the series of Eq. 4.25 can be made as accurate as desired by taking a sufficient number of terms. On the other hand, if the link between two differential equations, as discussed in Sec. 4.2.2, is not close, there may be considerable error in replacing the actual differential equation by a similar one. Such a situation is described below.

4.5 Solutions of the Differential Equation Within the Stream in the Region Outside the Unit Circle of the ξ-Plane

For the purpose of this part of the analysis, the form of the differential equation used by MacFarlane and Hay, Eq. 4.7, will be used. It is further simplified by reduction to its mathematically normal form through the substitution

$$U = \frac{\zeta}{\sqrt{\xi^2-1}} \quad . \tag{4.28}$$

Thus, the differential equation satisfied by ζ has the normal form

$$\frac{d^2\zeta}{d\xi^2} - \left(1 - \frac{1}{(\xi^2-1)^2}\right)\zeta = 0 \quad . \tag{4.29}$$

For values of $|\xi|$ somewhat larger than unity Eq. 4.29 suggests an approximately exponential solution, since it approaches asymptotically, for $\xi \to \infty$, the form

$$\frac{d^2\zeta}{d\xi^2} - \zeta = 0 \quad . \tag{4.30}$$

which has exponentials as exact solutions. Of course, a similar approximation could be made in connection with the MacFarlane-Hay equation itself; Gould has done this. The exponential approximation to Eq. 4.29 is much more accurate, however. If the quantity

$$\epsilon = \frac{1}{\zeta}\frac{d^2\zeta}{d\xi^2} - \left[1 - \frac{1}{(\xi^2-1)^2}\right] = \frac{1}{(\xi^2-1)^2} \tag{4.31}$$

is taken as a measure of the error involved in the approximation, then this "error" is less than 10% in the region $|\xi| > 2.04$. Using a similar measure of error of the approximation of the solution of the MacFarlane-Hay equation by exponentials, it is found that to have an "error" less than 10% for all arguments of ξ the value of ξ must lie in either the region $|\xi| > 20$ or the region $|\xi| < 1/20$.

Solutions for the velocity potential outside the unit circle are therefore approximately

$$U = \frac{C'e^{\xi}}{\sqrt{\xi^2-1}} + \frac{D'e^{-\xi}}{\sqrt{\xi^2-1}} \quad ; \tag{4.32}$$

for the electric potential,

$$\phi = \frac{C\,\xi e^{\xi}}{\sqrt{\xi^2-1}} + \frac{D\,\xi e^{-\xi}}{\sqrt{\xi^2-1}} \quad . \tag{4.33}$$

4.6 Summary

Consideration of the various regions of the ξ-plane has led to solutions of the differential equation in those regions. In Fig. 4.4 are shown the regions of convergence of the solutions expanded about the origin and the singularities and also the region in which the solution of Eq. 4.33 is in "error" by less than 10%. Although it would appear that a complete covering of the ξ-plane has been achieved, the situation regarding the practical matter of the accuracy of the truncated series used in the subsequent analysis—the degree of convergence, in other words—is not quite as satisfactory.

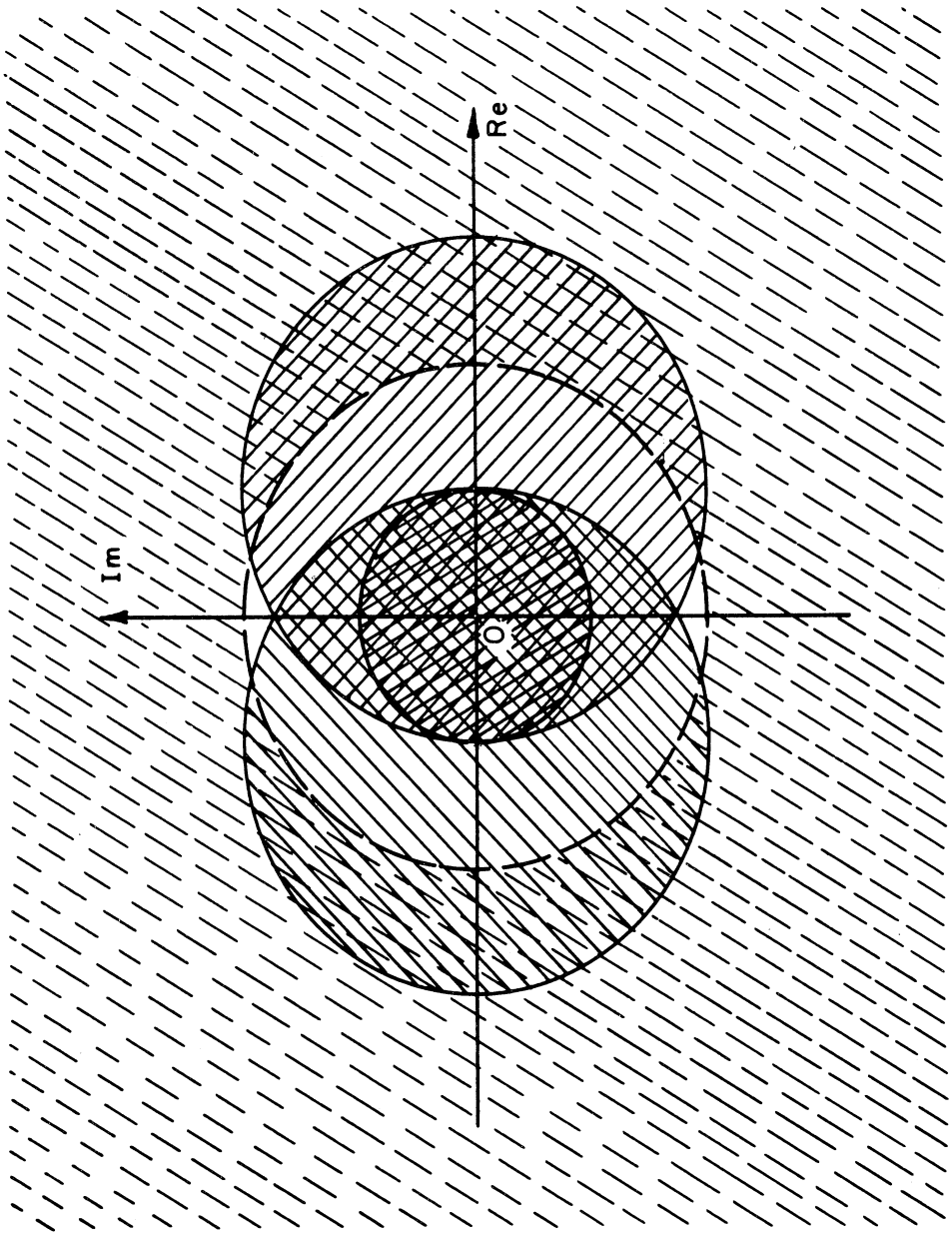

FIG. 4.4 REGIONS OF THE ξ-PLANE IN WHICH ACCURATE SOLUTIONS OF THE DIFFERENTIAL EQUATION CAN BE OBTAINED.

CHAPTER V

THE TRANSVERSE BOUNDARY-VALUE PROBLEM

5.1 General

The system of differential equations governing a quantity in a region and the relations governing the behavior of the quantity and its derivatives at the surfaces bounding the region determine the boundary-value problem. It is found convenient to treat relations at the bounding surfaces in two parts: those relating to the planes y = constant, parallel to the direction of wave propagation, and those relating to the planes z = constant, perpendicular to the general direction of propagation. The former are designated transverse boundary relations; the latter are designated longitudinal boundary relations.

The reason for this division is that the transverse boundary system—the differential equations and the transverse boundary relations—determine the nature of the waves which the system can propagate. This is the objective of the present chapter. The longitudinal boundary system determines the extent to which each of the waves is present on the system; it is treated in Chapter XIII.

5.2 The Transverse Boundary Relations

5.2.1 Conditions at the Edge of the Electron Stream

Both the electric potential and its derivatives normal and tangential to the bounding surface of the electron stream are continuous at such a surface; this is true of electron beams in general. A difficulty arises in this instance because of the fact that the surface of the stream is not a simple surface such as a plane. The surface of the

electron stream is perturbed in a wavelike manner; for the nth wave, the perturbation is the real part of

$$(\delta y)_n \exp (j\omega t - \Gamma_n z) \quad , \tag{5.1}$$

which is the displacement from their unperturbed positions of those electrons which would define the edge of the unperturbed beam. This is so because, as Gabor has shown,[47] the velocity perturbation is very nearly irrotational and no crossings of flight-lines, or "electron collisions," occur. The general shape of the stream surface at an instant of time is shown in Fig. 5.1, in which the "ripple" is greatly exaggerated for the purpose of illustration. The analysis developed below requires that the actual perturbation be much smaller than the spatial period of the wave. Under this condition, the local perturbation of the electric field at a point such as Q is essentially the same as though the stream boundary were still planar, but translated to R; the approximation corresponds to Fig. 5.2. The field perturbation is considered to have only a transverse component, which can be determined by integrating the divergence equation

$$Ey(Q) - Ey(P) = \int_P^Q \frac{\partial Ey}{\partial y}\, dy = \int_P^R \frac{\rho}{\epsilon_o}\, dy \quad . \tag{5.2}$$

Since the beam surface displacement, $\overline{PR}$, has the wave nature given by Eq. 5.1, the perturbation of the electric field caused by the surface ripple is also a wave:

$$[Ey(Q) - Ey(P)]_n = \int_{y=y_b}^{y=y_b+(\delta y)_n \exp(j\omega t - \Gamma_n z)} \left[\frac{\rho_o}{\epsilon_o} + \frac{\rho_n}{\epsilon_n} \exp (j\omega t - \Gamma_n z)\right] dy$$

$$\approx \frac{\rho_o}{\epsilon_o} (\delta y)_n \exp (j\omega t - \Gamma_n z) \quad . \tag{5.3}$$

It is noted that the contribution of the r-f perturbational space-charge

FIG. 5.1 A PORTION OF THE UPPER EDGE OF THE ELECTRON FLUID.

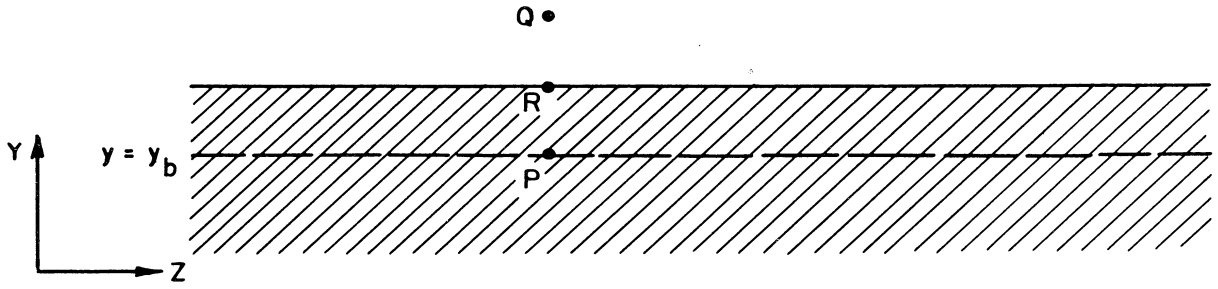

FIG. 5.2 THE SMALL SIGNAL APPROXIMATE SHAPE OF A SMALL PORTION OF THE UPPER EDGE OF THE FLUID. (THE SCALE OF DIMENSIONS HAS BEEN GREATLY EXPANDED FROM THAT OF FIG. 5.1.)

density, ρ_n, to the integral of Eq. 5.2 is by virtue of the small-signal assumptions negligible. Its effect is to introduce nonlinear (harmonic) terms.

The result of the above analysis can be conveniently considered as the replacement of the amount of charge lying between the perturbed and unperturbed boundaries by an equal amount of charge similarly distributed on the unperturbed surface as in Fig. 5.3. Such a surface charge, Re $\sqrt{2}$ $\sigma_n \exp(j\omega t - \Gamma_n z)$, introduces a surface discontinuity in the transverse electric field obtainable from the surface-divergence relation

$$E_y(Q) - E_y(P) = \int_P^Q \nabla_s \cdot E\,dy = \frac{\sigma_s}{\epsilon_o} \exp(j\omega t - \Gamma_n z)$$

$$= \int_{y=b}^{y=b+(\delta y)_n} \frac{\rho}{\epsilon_o} \exp(j\omega t - \Gamma_n z)\,dy \quad . \tag{5.4}$$

Again, there is no discontinuity in the longitudinal electric field.

It is convenient to express the effect of the beam surface ripple in terms of the effect on the potential function and its transverse derivative. In consequence of Eqs. 3.20 and 3.21,

$$V_n \phi_n (y = y_{b+}) = V_n \phi_n (y = y_{b-}) \quad , \tag{5.5}$$

$$V_n \left.\frac{d\phi_n}{dy}\right|_{y=y_{b+}} - V_n \left.\frac{d\phi_n}{dy}\right|_{y=y_{b-}} = -\frac{\rho_o}{\epsilon_o} (\delta y)_n \Big|_{y=y_{b-}} \quad , \tag{5.6}$$

where by $y = y_{b-}$ is understood the interior of the stream at its upper surface; by $y = y_{b+}$, the exterior region of the stream at its upper surface.

Conditions at the lower edge of the stream are expressed similarly, except that in this case an outward displacement of the stream edge corresponds to downward, or negative, electron displacement. Thus,

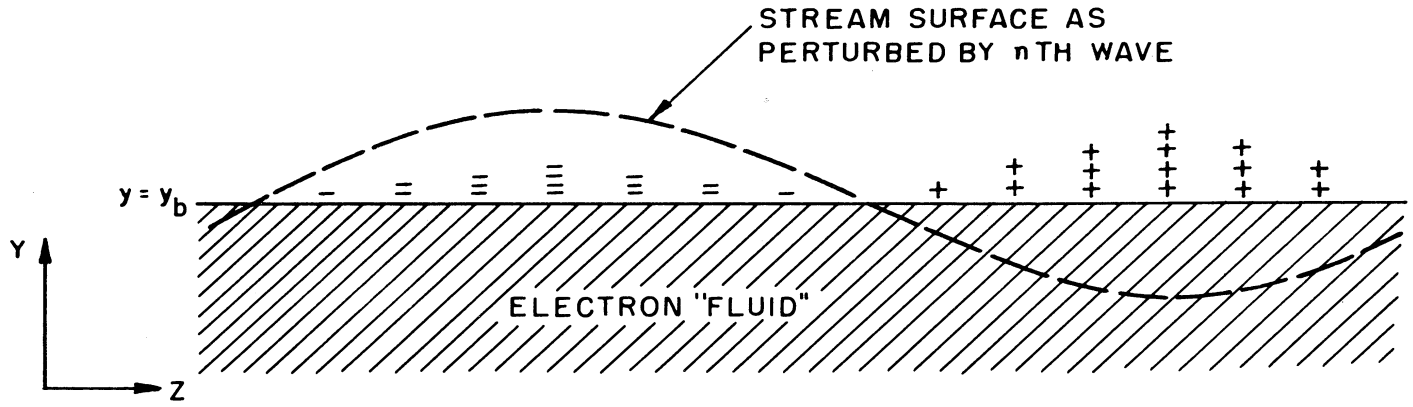

FIG. 5.3 THE REPRESENTATION OF THE DISTORTED EDGE OF THE STREAM BY A SURFACE CHARGE OF VARYING DENSITY, LYING ON A PLANE SURFACE (THE UNPERTURBED SURFACE).

$$V_n \phi_n (y = y_{a+}) = V_n \phi_n (y = y_{a-}) \quad , \tag{5.7}$$

$$V_n \left.\frac{d\phi_n}{dy}\right|_{y=y_{a+}} - V_n \left.\frac{d\phi_n}{dy}\right|_{y=y_{a-}} = + \frac{\rho_o}{\epsilon_o} (\delta y)_n \Big|_{y=y_{a+}} \quad . \tag{5.8}$$

The general concept of accounting for the perturbed surface of a stream in terms of an equivalent surface charge distributed on a coordinate surface is due to W. Hahn;[48] it is often called, for short, the "Hahn procedure." Hahn first derived its validity by considering the equivalence relation in terms of the magnetic field generated by the convection current arising from the motion of the charge lying between the rippled and the unperturbed surfaces. Inasmuch as the magnetic field is not considered in the present analysis, the derivation given above seems more appropriate and consistent.

Utilizing Eq. 3.29, the relation derived in Chapter III for the stream ripple, Eq. 5.6 can be written

$$V_n \left.\frac{d\phi_n}{dy}\right|_{y=y_{b+}} = V_n \left.\frac{d\phi_n}{dy}\right|_{y=y_{b-}} \left[1 + \frac{\omega_c^2}{\Omega_n^2}\right] + V_n \phi_n \Gamma_n \frac{\omega_c^3}{\Omega_n^3} \quad , \tag{5.9}$$

in which the independent variable, y, is implicit in Ω_n and the potential function, ϕ_n. A similar equation can be written at the lower edge of the stream:

$$V_n \left.\frac{d\phi_n}{dy}\right|_{y=y_{a-}} = V_n \left.\frac{d\phi_n}{dy}\right|_{y=y_{a+}} \left[1 + \frac{\omega_c^2}{\Omega_n^2}\right] + V_n \phi_n \Gamma_n \frac{\omega_c^3}{\Omega_n^3} \quad . \tag{5.10}$$

The two equations have the same mathematical form; they relate the potential gradient outside the stream (left side) to the conditions immediately inside the stream (right side).

5.2.2 Conditions at the Sole

The sole electrode is assumed to be a smooth, perfectly conducting electrode. Consequently, at the sole the tangential (longitudinal) component of electric field must be zero. Since the longitudinal field is proportional to the potential (Eq. 3.20) and since Γ_n is different from zero,

$$\phi_n\ (y = y_s) = 0 \qquad \text{[at the sole]} \ . \tag{5.11}$$

5.2.3 Conditions at the Anode

If the anode electrode is smooth and perfectly conducting as well as the sole, the potential at the anode is also zero:

$$\phi_n\ (y = y_d) = 0 \qquad \text{[smooth anode]} \ . \tag{5.12}$$

The component of potential gradient normal to the anode (and the sole also) can be related to the current in the structure comprising the electrode. The potential gradient is therefore related to the circuit properties of the electrode structures which bound the interaction space. For smooth, perfectly conducting electrodes, the currents produce no effect on the interaction and can be ignored. In the case in which the anode is part of a slow-wave structure, however, the circuit properties enter into the analysis in an important way.

The accounting for the circuit properties of the anode can be done in two ways:

(a) The relation between the potential and potential gradient at the anode plane can be determined by a study of the circuit. This relation, together with the foregoing boundary conditions, form a set of relations which can be solved to find the eigenvalues and eigenfunctions of the boundary-value problem.

(b) The boundary requirement regarding the potential gradient normal to the anode can be ignored for the time being. The role of the circuit can be introduced by calculating the induction effects on the circuit produced by the charges in the interaction space. This is done in Chapter VI; the relationship there derived, together with the boundary relations obtained in this chapter, form a set of relations which can be solved for the eigenvalues and eigenfunctions.

The second of the methods outlined above is the one used in the present dissertation. Thus, the potential function is normalized to unity at the anode:

$$\phi_n \, (y = y_d) \;=\; 1 \qquad \text{[slow-wave anode structure]} \;, \tag{5.13}$$

and the transverse component of potential gradient is ignored for the present.

5.3 Summary

Equations 5.5, 5.7, 5.9, 5.10, 5.11, and either 5.12 or 5.13 are six boundary relations. It has been shown in Chapter IV that the differential equations for the potential function, ϕ, in each of the three regions of the interaction space, each have two solutions; there are therefore six solutions which represent the potential function in these three regions. These solutions are represented as

$$\phi \;=\; A\, g_1 + B\, g_2 \;, \qquad y_b \le y \le y_d \;, \tag{5.14}$$

$$\phi \;=\; C\, g_3 + D\, g_4 \;, \qquad y_a \le y \le y_b \;, \tag{5.15}$$

and

$$\phi \;=\; E\, g_5 + F\, g_6 \;, \qquad y_s \le y \le y_a \;. \tag{5.16}$$

The six boundary relations are therefore sufficient to determine the six coefficients A-F in terms of Γ_n. The result is that the behavior of the

stream in the presence of a wave in the interaction region is completely determined if V_n and Γ_n are specified. Such a determination is the equivalent of Pierce's "ballistic equation"* in the one-dimensional traveling-wave tube theory.

*Ref. 11, Eq. 2.22.

PART III

INDUCTION THEORY

CHAPTER VI

EFFECT OF THE STREAM ON THE CIRCUIT— THE "CIRCUIT EQUATION"

6.1 Introduction

The task of this chapter is the complement of the foregoing ballistic theory. A relationship is sought between the "forcing current" arising from the presence of a modulated electron stream in the interaction region and wave propagation on a slow-wave structure (the anode). A preliminary discussion of propagation in the absence of an electron stream will serve to define the properties of the propagating structure itself and also to set forth the assumptions to be made regarding it.

6.2 The Cold Circuit

Figure 6.1 is a schematic representation of the periodic type of slow-wave structure used in devices of the magnetron type[1,2] and also in many tubes of the conventional traveling-wave, or "O" type.[21,43] The upper (wave guide) portion of the figure symbolizes the function of the propagation of energy along the structure; the lower portion indicates the function of establishing an electric field in the interaction region which lies just below the electrodes. The excitation of the electrodes is provided by connection to different parts of the wave guide, as shown symbolically in the figure.

In practice, of course, the two functions cannot be so easily associated with the different portions of the physical structure. Thus, in Fig. 6.2, which shows a slow-wave structure used in an actual device, the vane electrodes, F, serve both to establish an electric field in the

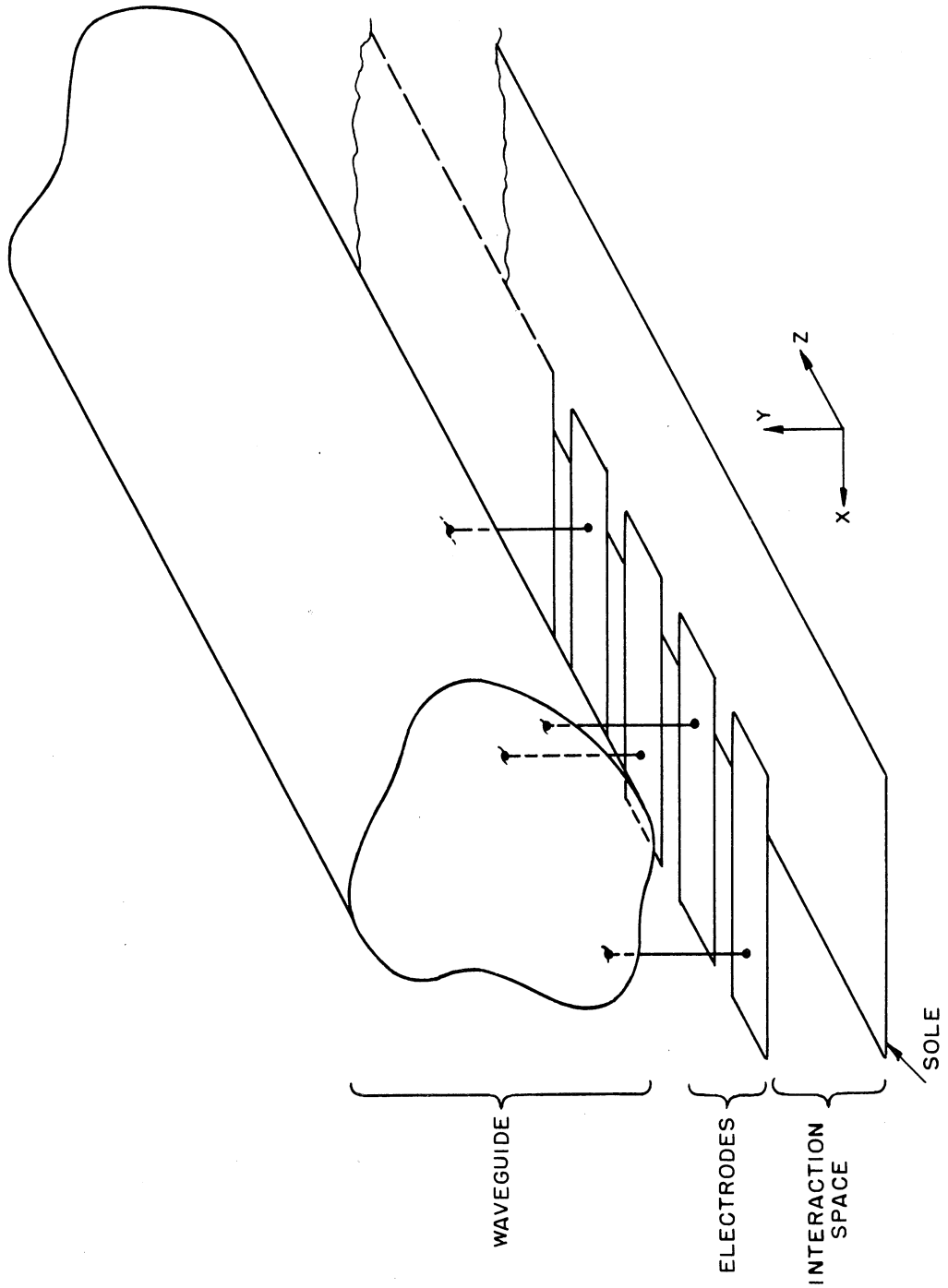

FIG. 6.1 A SCHEMATIC REPRESENTATION OF A DELAY LINE EMPLOYED IN TRANSVERSE-FIELD TUBES.

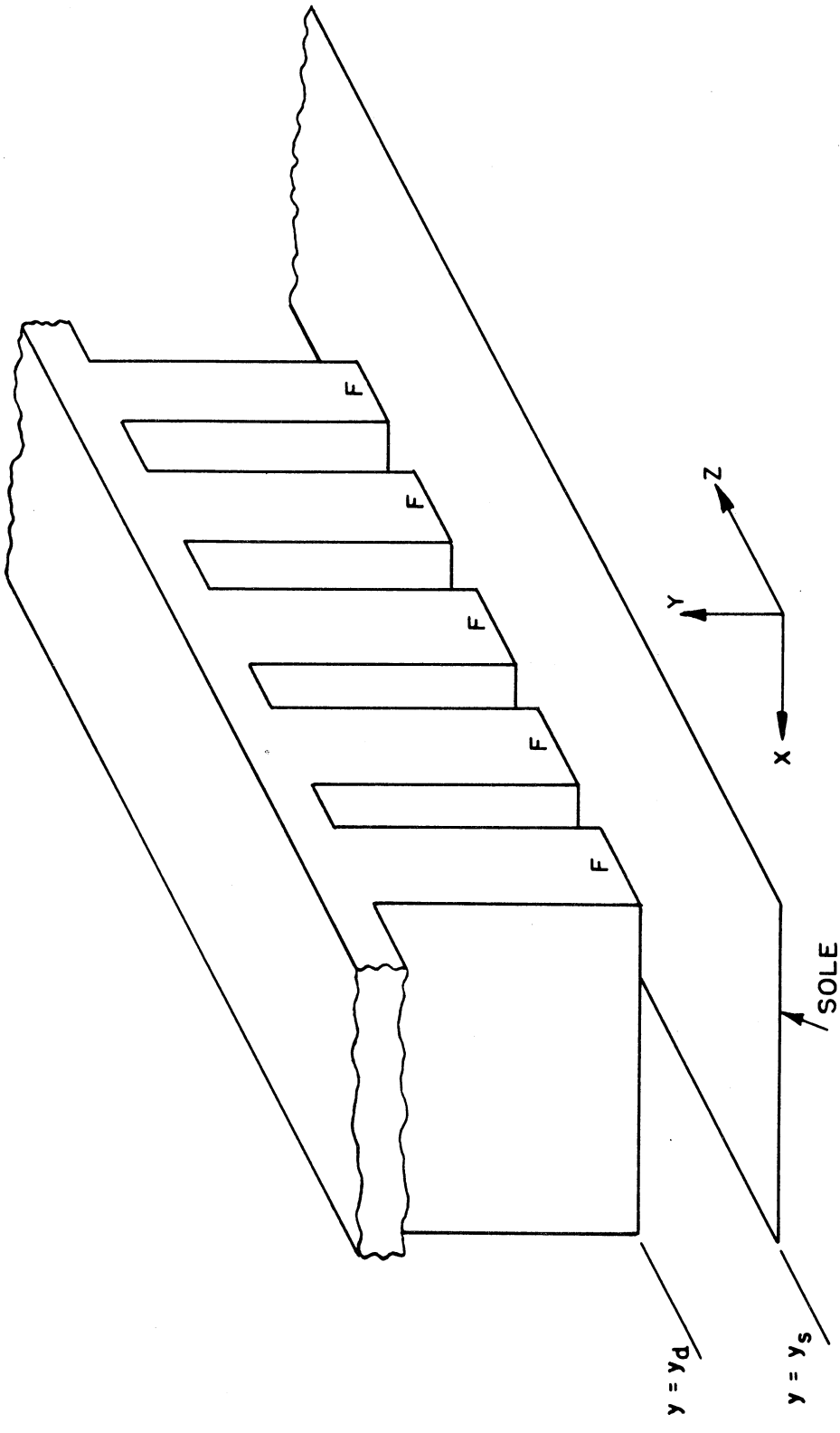

FIG. 6.2 A VANE-TYPE DELAY LINE

interaction region and to propagate electromagnetic energy in the longitudinal z-direction. Figure 6.3 illustrates yet another structure suitable for use in magnetron-type devices.[21] In this case, the finger-like elements, F, serve to establish the electric interaction field; energy propagation is guided principally by the pair of wires S,S', although the fingers do incidentally affect the propagation.

The slow-wave structure in general has several modes by which the energy transmission function can be accomplished. These modes are characterized by particular values of the velocity of propagation of energy (ordinarily the group velocity*) and by frequency ranges for which propagation can occur. These quantities are summarized in the Brillouin diagram,[50,51] a plot of frequency and phase constant, as shown in Fig. 6.4.

The phase velocity is given by

$$v_{ph} = \frac{\omega}{\beta} \quad . \tag{6.1}$$

The group velocity is

$$v_g = \frac{d\omega}{d\beta} \quad ; \tag{6.2}$$

it is the slope of the ω-β characteristic for each mode. In practice, the slow-wave structure is designed so that propagation in only one mode can occur within the useful frequency range; multi-mode energy propagation leads to undesirable multi-mode electronic behavior.

The electrode configuration which serves to establish a suitable electric field in the interaction region in general produces a complicated spatial variation of the field. Since the electrodes are alike and are situated periodically in space, the fields are spatially periodic. Fourier analysis of the field configuration indicates that for each mode of propagation, the field in the interaction region is describable as the

*Ref. 35, pp. 330-340.

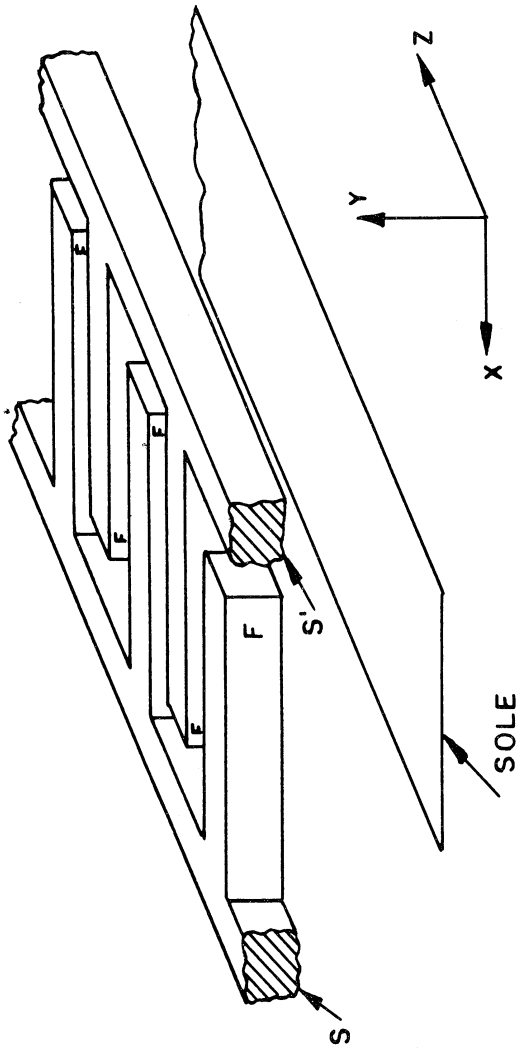

FIG. 6.3 AN INTERDIGITAL DELAY LINE.

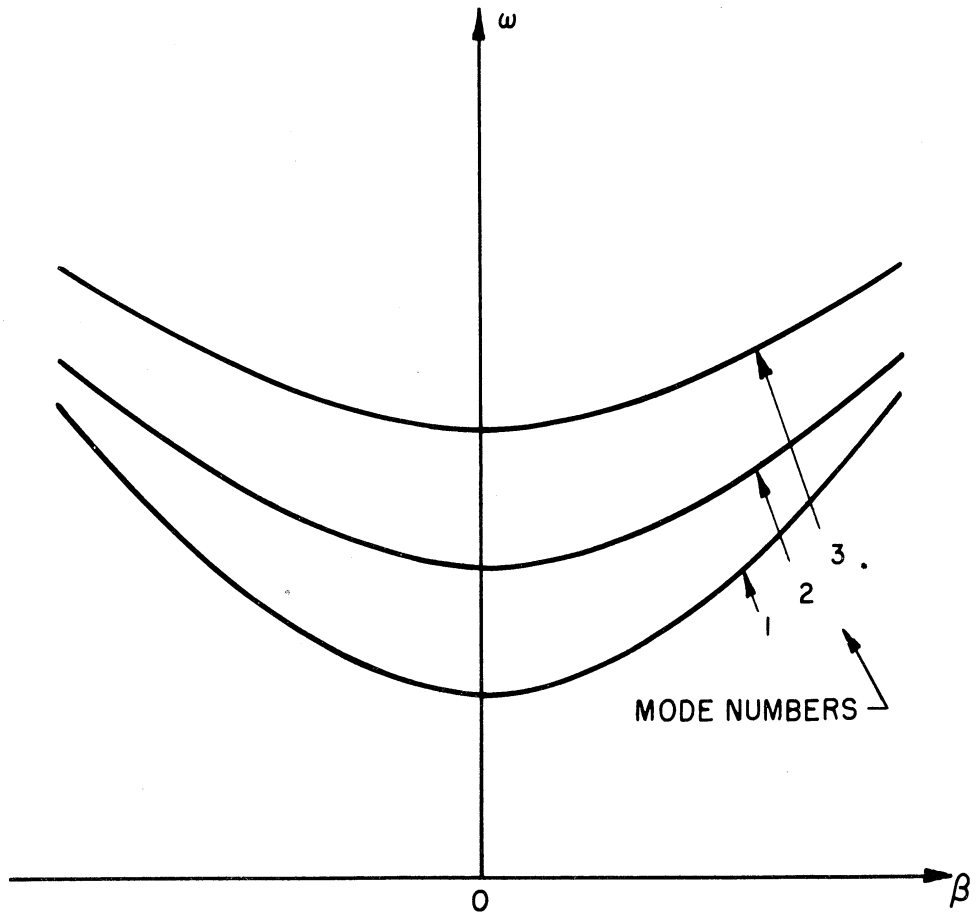

FIG. 6.4 BRILLOUIN DIAGRAM FOR A UNIFORM TRANSMISSION LINE.

sum of components having spatial periods equal to the electrode system period and submultiples thereof. These components are the so-called "space-harmonics" or "Hartree-harmonics"* of the total field. They have representations in the Brillouin diagram as shown in Fig. 6.5; the diagram extends infinitely in a regular fashion because of the periodicity of the structure.

For the purpose of analysis of interaction in which the stream velocity is very nearly equal to the phase velocity of only one of the space-harmonics, the actual slow-wave structure may be considered to have the properties of that distributed-constant, aperiodic equivalent circuit of Fig. 6.6 which is appropriate to the space harmonic with which the interaction occurs. The equivalence is restricted to the sense that:

(a) The propagation constant of the circuit is the same as that of the space harmonic, and

(b) If the potential wave on the equivalent circuit is equal to that of the space-harmonic component of the wave on the anode plane, $y = y_d$, of the actual structure, then the power transmitted by the equivalent circuit is equal to the power flow (all field components) of the actual structure.

Obviously, the equivalence does not extend to such other quantities as energy density and group velocity. Nevertheless, the properties of the slow-wave structure which are pertinent to the interaction are those listed above. Whether energy is propagated as fields associated with other space-harmonics or in regions inaccessible to the stream is of little importance. If such circuits as in Fig. 6.6 could be realized, they would produce the same interaction with the stream as does the actual structure, assuming that there is negligible interaction between the stream and the other space-harmonic field components.

*Ref. 2, p. 32.

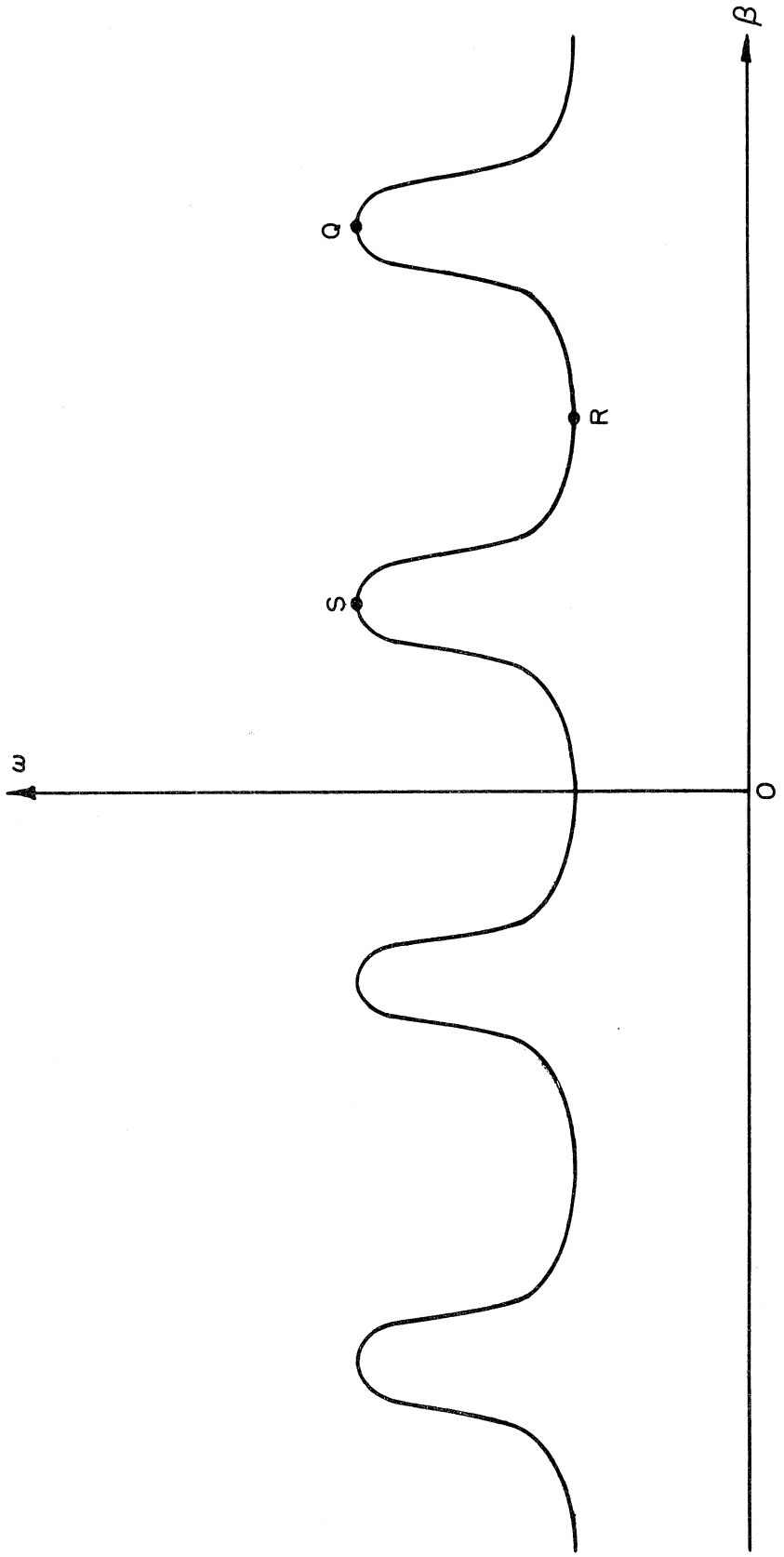

FIG. 6.5 BRILLOUIN DIAGRAM FOR A PERIODICALLY LOADED DELAY LINE HAVING ONLY ONE MODE OF PROPAGATION.

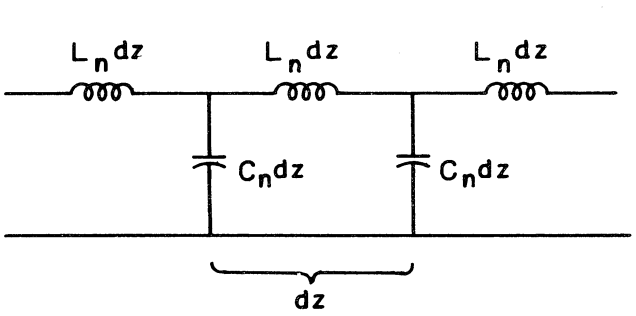

a. FORWARD WAVES

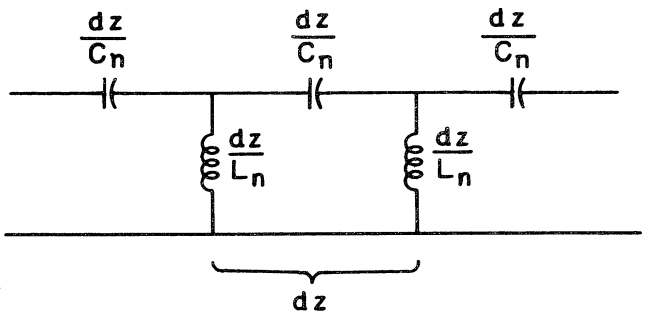

b. BACKWARD WAVES

FIG. 6.6 EQUIVALENT APERIODIC DISTRIBUTED CONSTANT REPRESENTATION OF A PERIODICALLY LOADED LINE FOR PURPOSES OF ANALYSIS OF INTERACTION WITH ONLY ONE SPACE HARMONIC.

In view of Eq. 6.2 for the group velocity and in view of the Brillouin diagram, it is evident that the space harmonics fall into two categories:

(1) Those space harmonics for which β has the same algebraic sign as the group velocity, v_g, as exemplified by the branch RQ in Fig. 6.5. The equivalent network is shown in the left half of Fig. 6.6. Such space harmonics are called forward waves[20,23] because for positive values of β (i.e., for waves with which electrons moving in the positive z-direction can interact synchronously), the energy flow (group velocity) is also in the positive z-direction. The equivalence conditions are

$$\Gamma_m = j\omega \sqrt{L_{fm}\, C_{fm}} \quad , \tag{6.3}$$

$$P_{fm} = \frac{V_{fm}\, V_{fm}^*}{K_{fm}} \quad , \tag{6.4}$$

$$K_{fm} = \sqrt{\frac{L_{fm}}{C_{fm}}} \quad . \tag{6.5}$$

(2) Those space harmonics for which β has the opposite sign from the group velocity, as on the branch RS of Fig. 6.5. The equivalent network is that shown in the right half of Fig. 6.6. Such space harmonics are called "backward space harmonics"[20,23] because for positive values of β, the energy flow is in the negative z-direction, or "backwards." The equivalence relations for the backward space harmonics are

$$\Gamma_m = j/\omega \sqrt{L_{bm}\, C_{bm}} \quad , \tag{6.6}$$

$$P_{bm} = \frac{V_{bm}\, V_{bm}^*}{K_{bm}} \quad , \tag{6.7}$$

$$K_{bm} = \sqrt{\frac{L_{bm}}{C_{bm}}} \quad . \tag{6.8}$$

It may be noted that the equivalent circuit of Fig. 6.6b, corresponding to a backward wave, is not realizable physically because both the series capacitance and shunt inductance elements required would be infinite for network sections of infinitesimal length. The equivalent circuit is then only an abstraction useful for the visualization of the delay line properties. The equivalent circuit for forward waves, Fig. 6.6a, is a realizable one.

For the sake of simplicity, the losses of the circuit have been ignored and the propagation constant has been assumed to have only the imaginary component, β. The losses of an actual circuit are usually Joulean heat losses; they can be taken into account by inserting resistance elements into the series sections of the equivalent circuit. These are usually sufficiently small that the reactive part of the characteristic impedance that results from their presence is negligibly small in comparison with the real part.* The effect of losses on the propagation constant, however, is often not negligible. The present analysis avoids this complication, however, in considering only circuits which have negligible loss in this sense. Extension of the analysis to circuits of appreciable loss can be made in the straightforward manner of Pierce's analysis.

6.3 Induced-Current Calculation

When a modulated stream is present, its effect on the circuit can be determined from consideration of the currents induced in the equivalent network, by virtue of the linear nature of the network characteristics.

---

*Ref. 11, art. 7.1.

6.3.1 Induced-Charge Theorems

Several important and well-known theorems can be demonstrated from quasi-stationary electrodynamics.[53] They are therefore valid when the space dimensions are small in comparison with the free-space wavelength, as in the present situation. These theorems are stated below without proof.

(1) Charges distributed in a region induce charges on the electrodes defining that region; the induced charge depends only on the distribution of the charge within the region.

(2) If in a region confined by electrodes ψ_k is a scalar "coupling" function defined by

$$\nabla^2 \psi_k = 0 \tag{6.9}$$

$$\psi_k = \begin{cases} 1 \text{ on } S_k, \text{ the surface of the kth electrode} \\ 0 \text{ on all other electrode surfaces and at infinity,} \end{cases} \tag{6.10}$$

then the total charge induced on the kth electrode by the charge in the region is

$$q_k = -\int_{\text{volume}} \rho \, \psi_k \, d\tau \quad , \tag{6.11}$$

the integral extending over the volume of the region confined by the electrodes.

The function ψ_k clearly describes the potential in the region in the absence of space charge when unit potential is applied to the kth electrode, all other electrodes having zero potential and with zero potential at infinity.

(3) If the electric field is considered to be composed of a divergence-free component (the "circuit field") and a space-charge dependent component (the "space-charge field"):

$$\nabla \cdot \vec{E}_1 = 0 \quad , \tag{6.12}$$

$$\nabla \cdot \vec{E}_2 = \frac{\rho}{\epsilon_o} \quad , \tag{6.13}$$

$\vec{E}_2$ being normal to all electrode surfaces, then

(a) the electric flux component at S_k [as in (2)]

$$\vec{D}_{2k} = \epsilon_o \vec{E}_{2k}$$

equals the surface-charge density induced on the kth electrode by the presence of the space charge;

(b) the element of energy transfer

$$\vec{j}_c \cdot \vec{E}_1 \, d\tau \tag{6.15}$$

represents energy transferred, by electron interaction with the electric field, from the volume element $d\tau$ to the circuit:

(c) the element of energy transfer

$$\vec{j}_c \cdot \vec{E}_2 \, d\tau \tag{6.16}$$

represents energy transfer to the space charge. It appears as kinetic energy of the electrons.

6.3.2 Application of the Induced-Current Theorems

The foregoing concepts relating to the induction of charge are applied to the configuration of Fig. 3.1, taking note of the wave nature of the perturbations.

The actual propagating structure at the anode is replaced by an "impedance wall" (analogous to the "admittance wall"[54,55] used in analyses of similar types) having the circuit properties of one of the space harmonic equivalent circuits of Fig. 6.6, because significant interaction is assumed to take place between the electron stream and the field of only the one space harmonic represented by the equivalent circuit. The

impedance of this line is made to account for all the energy transmitted by the total field; thus

$$K = \frac{P_{TOT}}{V_m V_m^*} = \sqrt{\frac{L_w}{C_w}} \quad . \tag{6.17}$$

This impedance wall is a plane situated at the anode level, $y = y_d$. It has the additional property that no electric flux penetrates its upper surface. Thus, the charge induced in the impedance wall is equal to the flux entering it from the interaction space below it. Both the space-charge-induced electric flux and the self-induced electric flux terminate at the wall. The space-charge-induced flux is by far the smaller of the two in the usual case where the perturbation of the electron stream is small.

To determine the charge induced in the impedance wall by the electron stream, it is necessary to know the coupling function. Use is made of the fact that this coupling function is also the space-charge-free potential function described in the second theorem of Sec. 6.3.1. Since the space-charge-density perturbation is, in the linear perturbation theory of Sec. 3.2, composed of a number of waves typified by

$$\text{Re } [\sqrt{2}\, \rho_n \exp (j\omega t - \Gamma_n z)] \quad , \tag{6.18}$$

it follows at once from the linear differential equations that describe the circuit that there will be induced in the anode impedance wall a wave of surface-charge density of the same frequency and z-dependence:

$$\sigma_i = \text{Re } [\sqrt{2}\, \sigma_{i_n} \exp (j\omega t - \Gamma_k z)] \quad . \tag{6.19}$$

Since the perturbations are of a wave nature, a scalar coupling function for each wave of space charge in the stream is defined with reference to Fig. 6.7. To paraphrase the second theorem concerning induced charge:

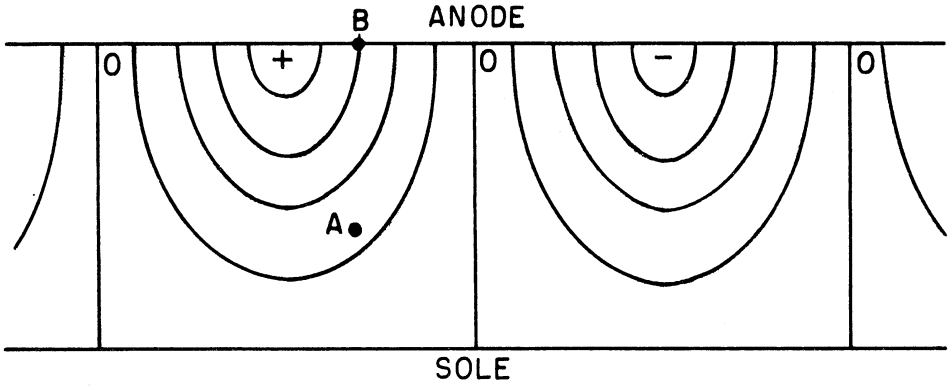

a. EQUIPOTENTIALS OF THE "CIRCUIT FIELD". (NO SPACE CHARGE)

$$\psi = \frac{\text{POTENTIAL AT A}}{\text{POTENTIAL AT B}}$$

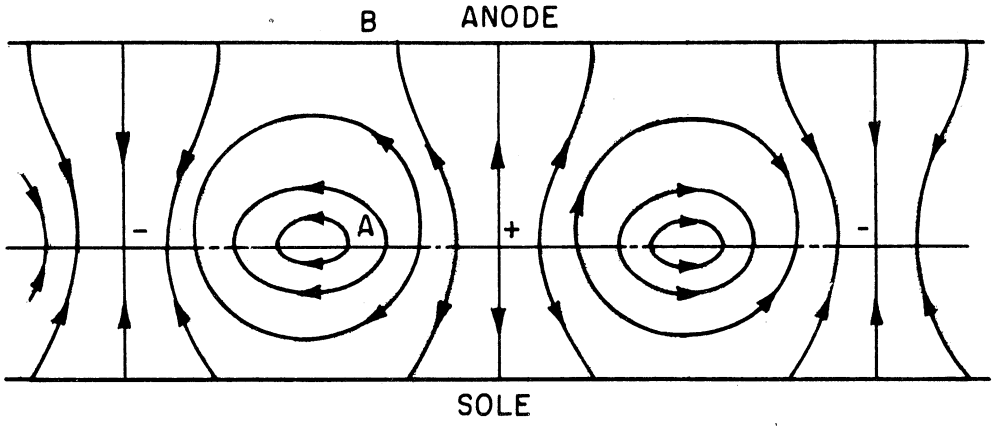

b. FLUX OF A WAVE OF SPACE CHARGE ON PLANE THROUGH A. (NO CIRCUIT.)

$$\psi = \frac{\text{SURFACE CHARGE DENSITY AT B (INDUCED)}}{\text{SURFACE CHARGE DENSITY AT A}}$$

FIG. 6.7 ILLUSTRATION OF THE INDUCED CHARGE THEOREM RELATING TO THE COUPLING FUNCTION, ψ.

provided that the circuit field of Fig. 6.7a has the same propagation constant, Γ_n, as the space charge of Fig. 6.7b, then the electric field (potential) decreases with distance from the anode (source) at the same rate that the electric "space-charge" component of field decreases with distance from the sheet of charge. The coupling function for the nth wave, considering the anode plane (wall) as the kth electrode, is $\psi_{n\ \text{anode}}$, or simply ψ_n, since the anode wall is the only electrode for which the induced current is sought. This coupling function is evidently the ratio of rms potentials

$$\psi_n(y) = \frac{\phi_n(y)}{\phi_n(y_d)} \quad \text{, [no space charge present]} \quad . \qquad (6.20)$$

It may be noted that in Fig. 6.7b the induced electric flux is shown as though the anode were an equipotential surface, whereas in fact the anode is not such a surface. The correctness of the representation is seen, however, from the fact that the flux shown is not the total flux, but only the space-charge-dependent component, D_2, as defined in the third theorem of Sec. 6.3.1. This component is normal to all electrode surfaces; having no components tangential to any electrodes, the space-charge flux pattern is independent of the electrical nature of the electrode boundary surface.

The comparison used in Fig. 6.7 to determine the charge coupling function may be thought of as an experimental way, in principle, avoiding the measurement of the ratio of induced charge to space charge by measuring instead the potential in the region between the electrodes. The latter measurement is a much more practical one.

For the planar configuration of Fig. 3.1, the coupling function is relatively easily evaluated theoretically. The calculation, using the representation of Eq. 4.3 for the charge-free potential function, yields

the result

$$\psi_n(y) = \frac{\sinh j\,\Gamma_n(y-y_s)}{\sinh j\,\Gamma_n(y-y_d)} \quad . \tag{6.21}$$

The coupling function of the transverse coordinate, for various values of the electrical wave angle between sole and anode as the parameter $\Gamma_n(y_d-y_s)$, is shown graphically in Fig. 6.8.

It may be noted that when Γ_n is large, i.e., when the wavelength is small, other things equal, the space charge induces little charge on the anode. This is readily appreciated from Fig. 6.7b, in which some of the electric flux emanating from the (positive) space charge terminates not on the anode, but on the nearby negative space charge. When the wavelength is small a larger fraction of the total space-charge electric flux is confined to the stream, resulting in the reduction in coupling to the external electrode systems (sole as well as anode).

6.3.3 Calculation of the Induced Anode-Wall Charge

The use of the coupling function, ψ_n, for the nth wave in accordance with the application of the second induced charge theorem calls for the evaluation of

$$\sigma_{i_n} = -\int_{y_s}^{y_d} \rho_n(y)\,\psi_n(y)\,dy \quad . \tag{6.22}$$

The indicated integration is simplified by the use of the Hahn approach of Sec. 5.2.1, in which the actual electron stream is replaced by its equivalent, viz.,

(1) a body of density-modulated space charge lying between the two planes, $y = y_a$ and $y = y_b$, which define the unperturbed stream;

(2) a surface charge distributed on the plane $y = y_a$, accounting for the distortion of the lower surface of the actual stream; and

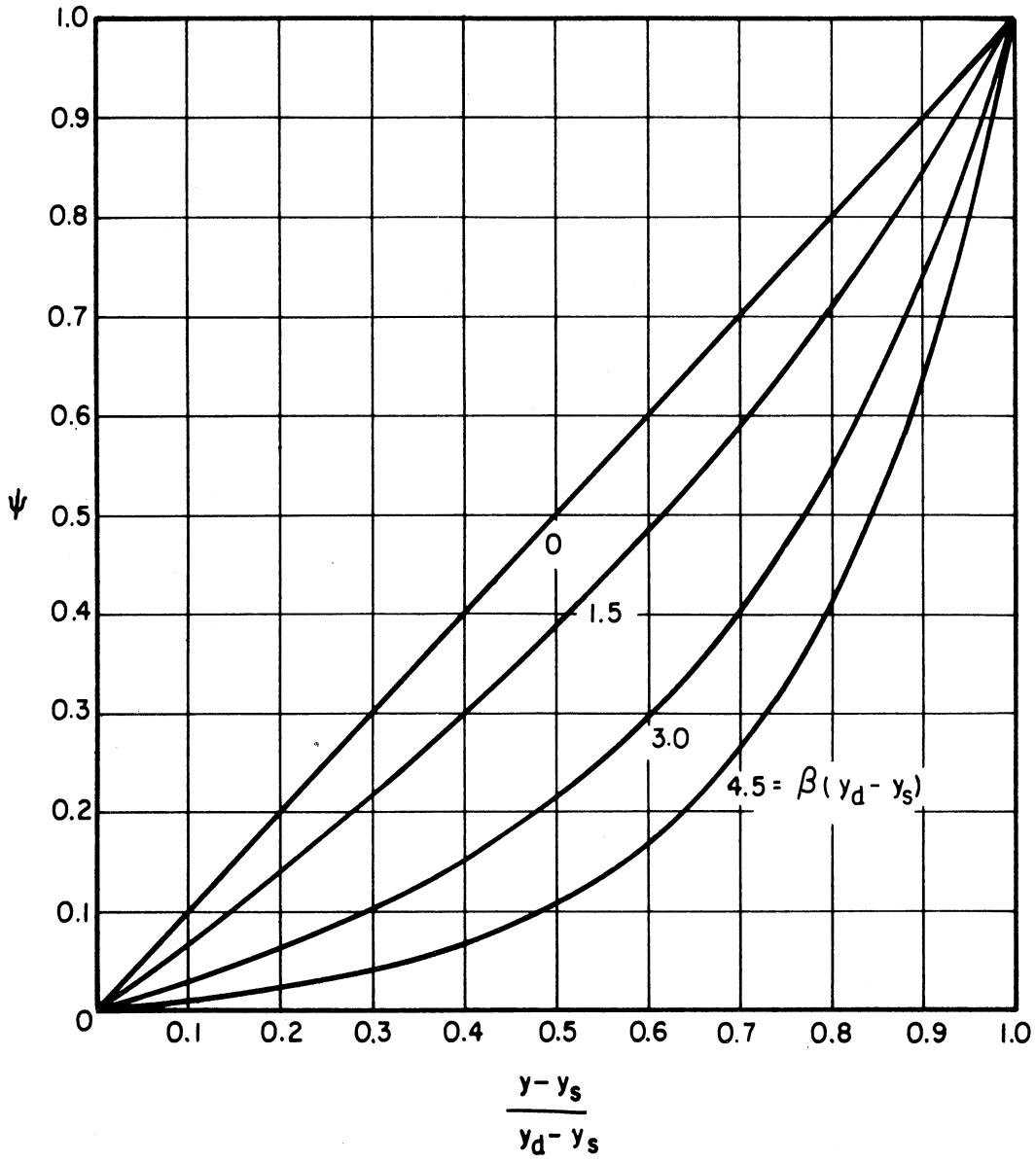

FIG. 6.8 THE DEPENDENCE OF THE COUPLING FUNCTION, ψ_n, ON THE TRANSVERSE COORDINATE.

(3) a surface charge distributed on the plane $y = y_b$, accounting for the distortion (perturbation) of the upper surface of the actual stream.

Each of these charges makes a contribution to the integral of Eq. 6.22; the first of these is

$$[\tau_{i(1)}]_n = - h \int_{y_a}^{y_b} \rho_n(y)\, \psi_n(y)\, dy \quad , \tag{6.23}$$

in which is introduced h, the depth along the magnetic field (the x-direction) of the electron stream. (It has been assumed that there are no variations in the x-direction.) The other two contributions to the induced charge integrals are, respectively,

$$[\tau_{i(2)}]_n = - h\, \sigma_n(y_a)\, \psi_n(y_a) = \rho_o h\, \psi_n(y_a)(\delta y)_n\Big|_{y_a} \tag{6.24}$$

and

$$[\tau_{i(3)}]_n = - h\, \sigma_n(y_b)\, \psi_n(y_b) = -\rho_o h\, \psi_n(y_b)(\delta y)_n\Big|_{y_b} \tag{6.25}$$

The combination of the three contributions to the induced charge can be conveniently written

$$(\tau_i)_n = - \rho_o h\, [\psi_n(\delta y)_n]_{y_a}^{y_b} - h \int_{y_a}^{y_b} \rho_n\, \psi\, dy \quad , \tag{6.26}$$

where the first term on the right has the usual meaning of the integral calculus.

6.4 Derivation of the Circuit Equation

Use of the divergence theorem as applied to the impedance wall,

$$\frac{\partial \tau}{\partial t} = - \frac{\partial i}{\partial z} \quad , \tag{6.27}$$

gives, in the perturbational form for the rms values of the nth wave,

$$j\omega(\tau_i)_n = \Gamma(i_i)_n \quad . \tag{6.28}$$

This induced current summarizes the effect of the space charge on the circuit. The flow of this induced current in the impedance wall of characteristic impedance K excites on the impedance wall a potential wave having the same propagation constant, Γ_n, as the wave of space charge. Along with this wave is a wave of self-induced charge; use of the divergence theorem indicates that a self-induced current, i_s, also flows in the impedance wall.

The induced anode potential wave is calculated using the transmission line equations which apply to the impedance wall:

$$\frac{\partial v}{\partial z} = - i X_m \quad , \tag{6.29}$$

$$\frac{\partial i}{\partial z} = - v B_m + \frac{\partial i_i}{\partial z} \quad . \tag{6.30}$$

The effect of the electron stream appears in the second term on the right side of Eq. 6.30. This equation is rewritten with the aid of the divergence theorem, Eq. 6.27; the resulting form of Eq. 6.30 is

$$\frac{\partial i}{\partial z} = - v B_m - j\omega \tau_i \quad . \tag{6.31}$$

Differentiation with respect to z of Eq. 6.29 and subsequent combination with Eq. 6.31 serve to eliminate the current i. Thus,

$$\frac{\partial^2 v}{\partial z^2} - B_m X_m v - j\omega X_m \tau_i = 0 \quad . \tag{6.32}$$

This equation is now specialized to apply to the nth wave in the linear perturbation theory. Differentiation twice with respect to z is equivalent, in the operator notation, to multiplication by Γ_n^2. Furthermore, the product $B_m X_m$ can be replaced by

$$B_m X_m = \Gamma_m^2 \quad , \tag{6.33}$$

the propagation constant, Γ_m, being a more fundamental property of the

circuit. The result of these manipulations is

$$(\Gamma_n^2 - \Gamma_m^2)\, V_n = j\omega\, X_m\, (\tau_i)_n \quad . \tag{6.34}$$

It is also desirable to eliminate the series reactance element, X_m, from this equation; X_m can be expressed in terms of Γ_m and K_m. It is necessary, however, to distinguish between the two types of space harmonics—backward waves and forward waves—since the series reactances are different in the two cases. In the case of a forward space harmonic, X_m can be written

$$X_m = j\omega\, L_m = j\omega \sqrt{L_m\, C_m}\, \sqrt{\frac{L_m}{C_m}} = \Gamma_m\, K_m \quad . \tag{6.35}$$

The form taken by Eq. 6.34 for forward-wave circuits is therefore

$$(\Gamma_n^2 - \Gamma_m^2)\, V_n = j\omega\, \Gamma_m\, K_m\, (\tau_i)_n \quad , \qquad \text{[forward wave]} \; . \tag{6.36}$$

In the case of backward space harmonics, X_m can be written

$$X_m = \frac{1}{j\omega\, C_m} = \frac{1}{j\omega \sqrt{L_m\, C_m}}\, \sqrt{\frac{L_m}{C_m}} = -\, K_m\, \Gamma_m \quad , \qquad \text{[backward wave]} \; . \tag{6.37}$$

The form of Eq. 6.34 in this case is

$$(\Gamma_n^2 - \Gamma_m^2)\, V_n = -\, j\omega\, \Gamma_m\, K_m\, (\tau_i)_n \quad , \qquad \text{[backward wave]} \; . \tag{6.38}$$

The two cases are combined for the sake of convenience in the form

$$(\Gamma_n^2 - \Gamma_m^2)\, V_n = \pm\, j\omega\, \Gamma_m\, K_m\, (\tau_i)_n \quad , \tag{6.39}$$

where the upper, positive sign applies if the circuit space harmonic is a forward-wave harmonic, and the lower, negative sign applies in the case of backward-wave interaction.

Using the expression Eq. 6.26 for the rms magnitude of the induced circuit charge, the above equation becomes

$$(\Gamma_n^2 - \Gamma_m^2)\, V_n = \mp j\omega \Gamma_m K_m h \left\{ [\rho_o \psi_n (\delta y)_n]_{y_a}^{y_b} + \int_{y_a}^{y_b} \rho_n \psi_n \, dy \right\} . \tag{6.40}$$

This is the "induction," or "circuit" equation; it relates the voltage wave on the circuit to the space charge in the interaction space which excites the circuit.

PART IV

GUIDED-WAVE SOLUTIONS

CHAPTER VII

THE SELF-CONSISTENT COMBINATION OF THE BALLISTIC EQUATION AND THE INDUCTION EQUATION—THE DISPERSION EQUATIONS

7.1 The Self-Consistency Requirement and the Dispersion Relations

The induction equation developed in Chapter VI determines the amplitude of the potential wave on the anode caused by the stream modulation which is thought to arise from unspecified causes. The ballistic equation, on the other hand, determines the stream modulation produced by the circuit potential which in the ballistic theory is imagined to arise from an unspecified cause.

When it is demanded that the circuit potential in both instances be the actual potential of a wave propagating on the system and that the stream modulation be the actual stream modulation, the complementary calculations of the induction and ballistic theory yield a pair of simultaneous relations which must be satisfied. These equations are partial differential equations in operator form. Furthermore, the amplitudes of the physical quantities involved may be eliminated from these relations by virtue of the linearizing process used in the ballistic theory and by virtue of the linearity of the circuit.

This self-consistency requirement then leads to an equation which must be satisfied by the propagation constant of the actual guided wave (a "freely propagating" wave); the relations so obtained describe the dispersion properties of the propagating system, for they relate the propagation constant, Γ, to the frequency, ω. In a system as complex as that of a circuit and an electron stream in crossed electric and magnetic fields, the dispersion relation is quite complex. It is possible to have

several waves—as many as five in which appreciable interaction occurs—of different propagation constants.

The term "guided wave" is used to denote the combination of wave solutions in the three regions of the interaction space which satisfy the boundary conditions at the interfaces between the regions and at the electrode surfaces.

7.2 General Discussion of the Dispersion Equations

Because, as shown in Chapter IV, it is not possible to express the potential function as a single pair of functions valid for the entire ξ-plane, it is not possible to write a single dispersion relation yielding all the guided waves capable of existing on the system. Thus, while a dispersion equation could be obtained in the region shown in Fig. 4.2, it could not be relied on to yield accurate predictions of wave solutions corresponding to the unshaded region of that figure.

The problem is attacked by writing dispersion relations for each of the regions for which potential solutions were obtained in Chapter IV. Since each of these regions of the ξ-plane yields wave solutions in which the interaction has a different physical interpretation, the self-consistent solutions for the different regions are treated separately in the remaining chapters of this Part.

CHAPTER VIII

THE DISPERSION EQUATION FOR QUASI-SYNCHRONOUS WAVES

8.1 Significance of Quasi-Synchronous Waves

Two conditions are involved in the conception of a quasi-synchronous wave:

(1) The wave is to have a propagation constant such that the perturbational forces on any one electron vary only slowly. This condition leads to strong interaction, since there is opportunity for continual, nearly unidirectional energy interchange between each electron and the fields.

Mathematically, this requirement is stated as

$$|\dot{\xi}_n| = \left|\frac{\omega}{\omega_c} + j\,\Gamma_n y\right| \ll 1 \quad , \tag{8.1}$$

which means that everywhere in the electron stream the complex frequency of the force experienced by an individual electron is

$$|\Omega_n| \ll \omega_c \quad . \tag{8.2}$$

This requirement assures the rapid convergence of the power series representation, Eq. 4.13, for the potential function and indeed makes possible an accurate representation using only the first few terms of the series.

(2) If the anode is part of a slow-wave structure, then the quasi-synchronous wave is to have a propagation constant nearly equal to that of one of the space harmonics of the "cold," or unperturbed, circuit. Thus,

$$\Gamma_n \approx \Gamma_o \quad . \tag{8.3}$$

When this requirement is met, strong interaction will occur because a relatively small stream modulation will cause large induction effects (cf. the induction equation, Eq. 6.36).

If no slow-wave structure is present—as in the case of a smooth, perfectly conducting plane anode electrode (drift section)—this second requirement is meaningless and is disregarded.

These two requirements predicate approximate equality between the d-c electron velocity and the phase velocities of the actual waves and of the cold circuit wave. Hence, in the definitions

$$\Gamma_n \equiv j \frac{\omega}{\bar{u}_o} (1 + p_n) \tag{8.4}$$

and

$$\bar{u} \equiv v_o (1 + \kappa) \quad , \tag{8.5}$$

where $\bar{u}_o = \omega_c \frac{(y_b+y_a)}{2}$ is the average d-c velocity of the stream,

v_o is the phase velocity of the cold circuit space harmonic,

p_n is the normalized perturbation of the propagation constant, and

κ is the excess velocity of the stream normalized to the cold circuit phase velocity,

both $|p_n|$ and $|\kappa|$ are quantities much smaller than unity.

8.2 Special Notation Used in Part IV

In Chapters VIII, IX, and X the large amount of detailed calculation would be extremely difficult to follow without some simplification in the notation. This simplification takes the form of the omission of the subscript n, which denotes the particular wave under discussion. In these chapters it will be assumed that unless specifically stated otherwise

the discussion relates to only one of these waves and not to any group of them. Thus, for example, by the propagation constant Γ is meant the propagation constant, Γ_n, of the nth wave. Table 8.1 lists the variables whose subscripts are omitted in this manner.

TABLE 8.1. SPECIAL NOTATION USED IN THE DERIVATION OF THE DISPERSION EQUATION

Wave Quantity of nth Wave	Abbreviated Notation	Defined in Section
Γ_n	Γ	3.2
ϕ_n	ϕ	3.4
ξ_n	ξ	3.9
p_n	p	8.1
ℓ_n	ℓ	8.8
A_n	A	5.2
B_n	B	
C_n	C	
D_n	D	
E_n	E	

8.3 The Potential Function Representations

The most useful expressions for the potential function outside the electron stream are obtained from Eqs. 4.2 and 4.3 in the regions between the stream and the circuit and between the stream and the sole, respectively. In the former case (anode side of the stream)

$$\phi(y) = A \exp(j\Gamma y) + B \exp(-j\Gamma y) , \qquad (8.6)$$

and in particular at the anode, $y = y_d$,

$$\phi(y_d) = A \exp(j\Gamma y_d) + B \exp(-j\Gamma y_d) = 0 \quad \text{(drift tube anode)} , \qquad (8.7)$$

$$\phi(y_d) = A \exp(j\Gamma y_d) + B \exp(-j\Gamma y_d) = 1 \quad \text{(slow-wave anode)} . \quad (8.8)$$

On the sole side of the stream, since the potential at the sole must be zero (Eq. 5.11), the potential function may be represented by the single function

$$\phi(y) = E \sinh j\Gamma_n(y-y_s), \quad y_s \leq y \leq y_a , \quad (8.9)$$

the coefficient F of Eq. 5.16 being zero.

The potential function inside the stream is approximated by the following truncated series obtained from Eq. 4.13:

$$\phi(y) = C\xi\left(1 + \frac{1}{2}\xi^2 + \frac{5}{24}\xi^4\right) + D\xi^2\left(1 + \frac{1}{2}\xi^2\right) . \quad (8.10)$$

8.4 Requirements on the Potential Function at the Stream Boundaries

The requirement of continuity of potential across the surface $y = y_b$ is, according to Eq. 5.5,

$$A \exp(j\Gamma y_b) + B \exp(-j\Gamma y_b) = C\left(\xi_b + \frac{1}{2}\xi_b^3 + \frac{5}{24}\xi_b^5\right) + D\left(\xi_b^2 + \frac{1}{2}\xi_b^4\right) . \quad (8.11)$$

Here and in the presentation below the symbols ξ_b and ξ_a are understood to mean

$$\xi_b \equiv \xi_n(y=y_b) = \frac{\omega}{\omega_c} + j\Gamma_n y_b , \quad (8.12)$$

and

$$\xi_a \equiv \xi_n(y=y_a) = \frac{\omega}{\omega_c} + j\Gamma_n y_a . \quad (8.13)$$

Similarly, the continuity of potential requirement at the plane $y = y_a$ is, according to Eq. 5.7,

$$E \sinh j\Gamma(y_a-y_s) = C\left(\xi_a + \frac{1}{2}\xi_a^3 + \frac{5}{24}\xi_a^5\right) + D\left(\xi_a^2 + \frac{1}{2}\xi_a^4\right) . \quad (8.14)$$

8.5 Requirements on the Transverse Gradient of the Potential Function at the Stream Boundaries

Equation 5.6 indicates the need for the performance of some preliminary operations, as follows:

$$\left.\frac{d\phi}{dy}\right|_{y_{b+}} = j\Gamma\left[A \exp\left(j\Gamma y_b\right) - B \exp\left(-j\Gamma y_b\right)\right] \tag{8.15}$$

and

$$\left.\frac{d\phi}{dy}\right|_{y_{b-}} = \left.\frac{d\phi}{d\xi}\right|_{y_{b-}} \frac{d\xi}{dy} = j \left.\frac{d\phi}{d\xi}\right|_{\xi_b}$$

$$= j\Gamma\left[C\left(1 + \frac{3}{2}\xi_b^2 + \frac{25}{24}\xi_b^4\right) + D\left(2\xi_b + 2\xi_b^3\right)\right]. \tag{8.16}$$

Using the definition of ξ, Eq. 3.39,

$$\frac{\omega_c}{\Omega} = \frac{1}{j\xi} \quad , \tag{8.17}$$

the right hand side of Eq. 5.9 becomes

$$\left.\frac{d\phi}{dy}\right|_{y_{b-}} = \left[1 + \left(\frac{\omega_c}{\Omega}\right)^2\right] + \Gamma\phi\left(\frac{\omega_c}{\Omega}\right)^3 = j\Gamma\left[\left.\frac{d\phi}{dy}\right|_{y_{b-}}\left(1 - \frac{1}{\xi_b^2}\right) + \frac{\phi}{\xi_b^3}\right]. \tag{8.18}$$

On using Eq. 8.15 and Eq. 8.18, the boundary requirement at $y = y_b$ regarding the transverse potential gradient becomes

$$A \exp\left(j\Gamma y_b\right) - B \exp\left(-j\Gamma y_b\right) = \left.\frac{d\phi}{d\xi}\right|_{\xi_b}\left(1 - \frac{1}{\xi_b^2}\right) + \frac{\phi(y_{b-})}{\xi_b^3} \quad . \tag{8.19}$$

Evaluation of ϕ and its derivative (Eqs. 8.10 and 8.16) further leads to

$$A \exp\left(j\Gamma y_b\right) - B \exp\left(-j\Gamma y_b\right) = C\left(\frac{2}{3}\xi_b^2\right) + D\left(-\frac{1}{\xi_b} + \frac{1}{2}\xi_b\right), \tag{8.20}$$

in which powers of ξ_b greater than 2 have been discarded. It may be noted that the lowest power of ξ_b is that of the simple pole, $1/\xi_b$, in the term

multiplied by D. Some exact cancellation of terms in the manipulation leading to Eq. 8.20 prevents the appearance of poles in the portion multiplied by C; this fact has a profound influence on the results of the analysis.

Arguing from the identity of form noted between Eqs. 5.9 and 5.10, an expression similar to Eq. 8.20 can immediately be written concerning the lower edge of the stream, $y = y_a$:

$$E \cosh j\Gamma(y_a - y_s) = C\left(\frac{2}{3}\,\xi_a^2\right) + D\left(-\frac{1}{\xi_a} + \frac{1}{2}\,\xi_a\right) \qquad (8.21)$$

8.6 The Ballistic Equation

Equations 8.7 or 8.8, 8.11, 8.14, 8.20 and 8.21—five equations in the five unknown coefficients A, B, C, D, and E—can be solved. There is then sufficient information to calculate all stream and field quantities in terms of Γ and the rms wave magnitude, V. This set of equations is thus the counterpart of the ballistic equation of Pierce; it can be conveniently represented in the matrix forms

$$[M] \times \begin{bmatrix} A \\ B \\ C \\ D \\ E \end{bmatrix} = \begin{bmatrix} 0 \\ 0 \\ 0 \\ 0 \\ 0 \end{bmatrix} \quad \text{(drift-tube anode)} \qquad (8.22)$$

$$[M] \times \begin{bmatrix} A \\ B \\ C \\ D \\ E \end{bmatrix} = \begin{bmatrix} 1 \\ 0 \\ 0 \\ 0 \\ 0 \end{bmatrix} \quad \text{(slow-wave anode)} \ , \qquad (8.23)$$

in which [M] is the matrix of Eq. 8.24, on the following page.

$$
[M] = \begin{bmatrix}
\exp(j\Gamma y_d) & \exp(-j\Gamma y_d) & 0 & 0 & 0 \\
\exp(j\Gamma y_b) & -\exp(-j\Gamma y_b) & -\frac{2}{3}\xi_b^2 & \frac{1}{\xi_b} - \frac{1}{2}\xi_b & 0 \\
\exp(j\Gamma y_b) & \exp(-j\Gamma y_b) & -\xi_b - \frac{1}{2}\xi_b^3 & -\xi_b^2 & 0 \\
0 & 0 & -\frac{2}{3}\xi_a^2 & \frac{1}{\xi_a} - \frac{1}{2}\xi_a & \cosh j\Gamma(y_a - y_s) \\
0 & 0 & -\xi_a - \frac{1}{2}\xi_a^3 & -\xi_a^2 & \sinh j\Gamma(y_a - y_s)
\end{bmatrix}
\tag{8.24}
$$

8.7 Smooth, Perfectly Conducting Anode—Drift-Tube Waves

The case of Eq. 8.22 is unique in that the ballistic equation alone, without the use of the induction equation, leads to a dispersion equation. The reason for this is that the properties of the "circuit" are completely stated in the requirement that the r-f potential be zero at the anode, i.e., there simply is no slow-wave circuit. Thus, the ballistic equation yields the propagation constants as well as the values of the coefficients A-E.

Since the matrix on the right side of Eq. 8.22 is in this case zero, the solutions of Eq. 8.22 are of two types:

either

(1) $A = B = C = D = E = 0$, with Γ arbitrary. This is the "trivial" solution in the mathematical sense. This solution has physical significance for certain values of Γ, however. The discussion of such a situation is deferred to Chapter XII.

or

(2) the determinant, $|M|$, of the matrix [M] is zero. In this case, the coefficients A-E are generally different from zero. The propagation constant, Γ, then must have only certain values, which may be called the "characteristic values" or "eigenvalues" of the transverse boundary value problem.

Only the second possibility, that of the nontrivial solution will be considered in this chapter. The dispersion equation is therefore

$$|M| = 0 \quad . \tag{8.25}$$

The relation between Γ and the frequency, ω, the interaction space geometry and the stream parameters is obtained by evaluating the determinant, $|M|$, and equating the result to zero.

Since the determinant contains ξ_a and ξ_b in two of its columns, the evaluation of $|M|$ leads to terms involving products of ξ_a and ξ_b of the type

$$\xi_a^r \, \xi_b^s \quad , \tag{8.26}$$

in which r and s are integers. Because of the truncation of the series expression for the potential function, ϕ, the dispersion equation lacks terms of the type in Eq. 8.26 for which r + s is large. The lowest value of r + s which is missing from the expansion of $|M|$ is 3; the expansion is therefore accurate through terms for which r + s is as high as 2. Although some terms having values of r + s greater than 2 occur in the expansion, it is useless to retain them, because of the terms left out by the truncation of the series. Since $|\xi| \ll 1$ everywhere in the stream, the omission of higher order values of r + s does not lead to significant error.

The expansion of the determinant by minors thus results in terms of the type Eq. 8.26 in which r + s takes on the values 0, 1, and 2. This expansion is resolved into groups containing terms of like values of r + s; thus

$$|M| = \Delta_0 + \Delta_1 + \Delta_2 \quad . \tag{8.27}$$

In detail, evaluation of Δ_0, Δ_1, and Δ_2 lead to the following:

$$\Delta_0 = -2\left[\cosh j\Gamma(y_d-y_b) \sinh j\Gamma(y_a-y_s) \frac{\xi_b}{\xi_a} + \sinh j\Gamma(y_d-y_b) \cosh j\Gamma(y_a-y_s) \frac{\xi_a}{\xi_b}\right] , \tag{8.28}$$

$$\Delta_1 = -\frac{4}{3} \sinh j\Gamma(y_d-y_b) \sinh j\Gamma(y_a-y_s) \left(\frac{\xi_a^2}{\xi_b} - \frac{\xi_b^2}{\xi_a}\right) , \tag{8.29}$$

$$\Delta_2 = -\left[\cosh j\Gamma(y_d-y_b) \sinh j\Gamma(y_a-y_s) \left(\xi_a\xi_b - \frac{\xi_b^3}{\xi_a}\right) + \sinh j\Gamma(y_d-y_b) \cosh j\Gamma(y_a-y_s) \left(\xi_a\xi_b - \frac{\xi_a^3}{\xi_b}\right)\right] . \tag{8.30}$$

The expression of the determinant, Eq. 8.25, in terms of Eqs. 8.28-8.30 is cumbersome. Since it is assumed that $|\xi| \ll 1$, a valid method of successive approximations is to equate to zero Δ_o, $\Delta_o + \Delta_1$, and $\Delta_o + \Delta_1 + \Delta_2$. The first of these approximations yields

$$\xi_b^2 + H\,\xi_a^2 = 0 \quad , \tag{8.31}$$

where

$$H \equiv \tanh j\Gamma(y_d - y_b) \Big/ \tanh j\Gamma(y_a - y_s) \quad , \tag{8.32}$$

or

$$H = \tanh \theta_b \,/\, \tanh \theta_a \quad , \tag{8.33}$$

which define θ_b and θ_a, the electrical distances, measured in terms of the propagation constant, Γ, from the stream to the anode and from the stream to the sole, respectively.

Now, ξ_a and ξ_b are related to the propagation constant and the space coordinates through Eq. 3.39. This can also be written, in the case of $y = y_b$, for instance,

$$\xi_b = \frac{\omega}{\omega_c}\left[1 - \frac{\Gamma}{j\,\frac{\omega}{\bar{u}_o}}\,\frac{u_{zo}(y_b)}{\bar{u}_o}\right] . \tag{8.34}$$

Then use is made of the definitions

$$u_{zo}(y_b) = \bar{u}_o\,(1 + s_u) \tag{8.35}$$

and

$$u_{zo}(y_a) = \bar{u}_o\,(1 - s_u) \tag{8.36}$$

which define the fractional "velocity spread" of the stream, $2\,s_u$. These definitions are used together with Eq. 8.4, which defines the normalized perturbation of the propagation constant, to transform Eq. 8.34 into

$$\xi_b = \frac{\omega}{\omega_c}\,(-p - s_u) \quad . \tag{8.37}$$

Similarly, at $y = y_a$,

$$\xi_a = \frac{\omega}{\omega_c}(-p + s_u) \quad . \tag{8.38}$$

In arriving at these expressions, the products of p and s_u, each of which is small in comparison with one, have been dismissed as negligible. This would not be justified if p and s_u were equal, but hindsight shows that p is complex, while s_u is a purely real quantity.

Substitution of the above forms for ξ_a and ξ_b into Eq. 8.31 leads to the following quadratic relation for the incremental propagation constants:

$$p^2 + 2 s_u \left(\frac{1 - H}{1 + H}\right) p + s_u^2 = 0 \quad . \tag{8.39}$$

The solution of this equation is

$$p \equiv p_r + jp_i = s_u \left(\frac{H - 1}{H + 1} \pm j \frac{2\sqrt{H}}{H+1}\right) \quad . \tag{8.40}$$

The two solutions are indicative of two waves, one of which grows with distance as

$$\exp \frac{\omega}{u_o} \frac{2\sqrt{H}}{H+1} z \quad , \tag{8.41}$$

and the other decays with distance at an equal rate. The real and imaginary components of p are functions of the stream-to-electrode spacings through the function H defined in Eq. 8.32; this dependence is shown in Fig. 8.1.

The phenomenon thus described in which disturbances may grow or decline along a stream in crossed electric and magnetic fields without the need for a slow-wave structure was studied previously by MacFarlane and Hay. They accounted for rather thick streams—their α, equal to the quantity s_u of the present theory, ranges up to unity—but considered only the case where both electrodes were infinitely remote from the stream

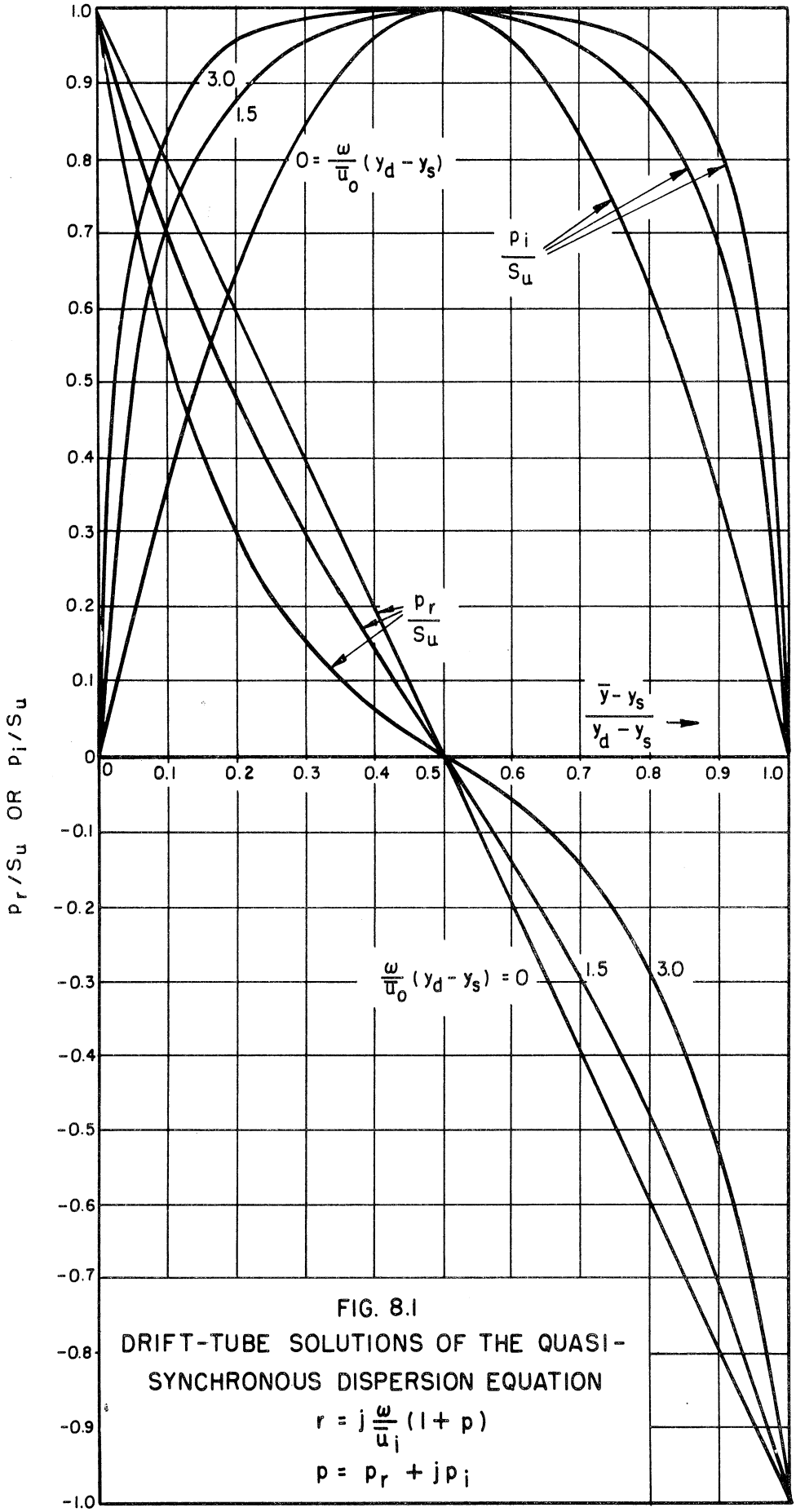

FIG. 8.1
DRIFT-TUBE SOLUTIONS OF THE QUASI-SYNCHRONOUS DISPERSION EQUATION

$$r = j\frac{\omega}{\bar{u}_i}(1 + p)$$

$$p = p_r + jp_i$$

(requiring infinite d-c electrode potentials!). Some of their results are shown in Fig. 8.2, which is a plot of the exponential gain rate vs the ratio of signal frequency to cyclotron frequency. The present theory shows good agreement with that of MacFarlane and Hay in the linear portions of the curves. The discrepancy arises from two causes:

(1) neglect of the products $p \cdot s_u$ in obtaining Eqs. 8.37 and 8.38;

(2) omission of the higher order components such as Δ_1 and Δ_2 from the dispersion relation. Accounting for only this source of error, as shown in Fig. 8.2, does much to remove the discrepancy.

It is sufficient for the present purpose to note that for thin streams the approximations of the present theory are amply justified. Furthermore, the present theory extends that of MacFarlane and Hay to account for the presence of the electrode system. The effect of the electrodes is in all cases to inhibit the gain/decay of the waves.

8.8 Dispersion Equation for Quasi-Synchronous Waves in the Presence of a Slow-Wave Circuit

8.8.1 Ballistic Properties

When the anode is an impedance sheet which propagates a slow wave, the potential function is normalized to unity at the anode; the right side of Eq. 8.23 therefore contains unity as one of its elements. This equation is solved for the coefficients A-E. In particular, knowledge of C and D makes possible the calculation of all stream quantities. These two coefficients are

$$C = \frac{1}{\xi_a} \frac{1}{\cosh j\,(y_d - y_b)} \left[\frac{1}{\frac{\xi_b}{\xi_a} + H \frac{\xi_a}{\xi_b}}\right] \tag{8.42}$$

and

$$D = - C \left\{ \xi_a^2 \left[\cosh j\,(y_a - y_s) - \frac{2}{3}\,\xi_a + \xi_a^2 \cosh j\,(y_a - y_s)\right]\right\} . \tag{8.43}$$

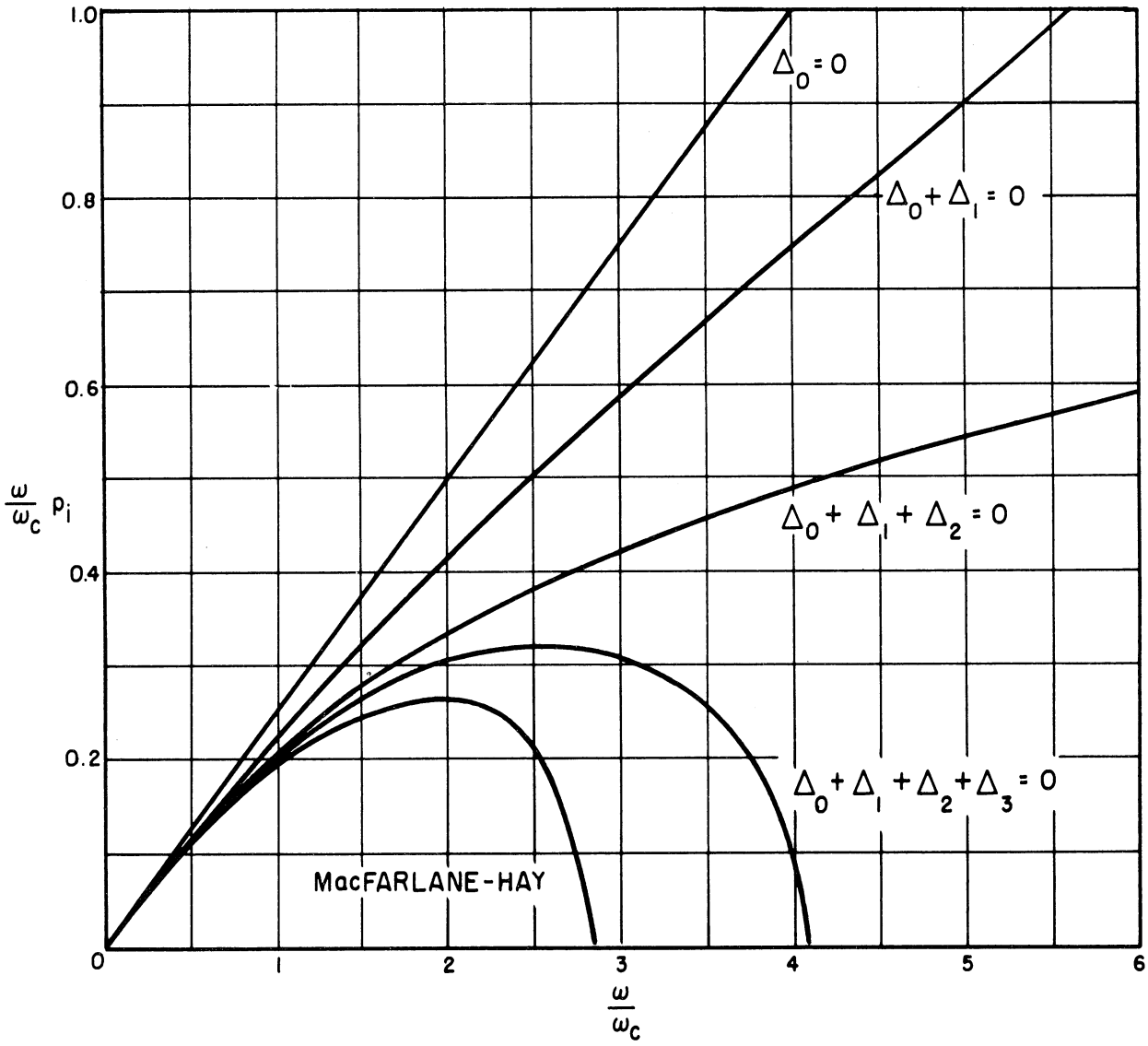

FIG. 8.2 COMPARISON OF DRIFT-TUBE WAVE CALCULATIONS WITH RESULTS PUBLISHED BY MacFARLANE & HAY.

($s_u = a = 1/4$)

It is noted that, except for very small sole-to-stream spacings,

$$|D| \ll |C| \tag{8.44}$$

and that the potential function within the stream can therefore be written in the approximate form

$$\phi \approx C\xi , \qquad y_a \leq y \leq y_b \ . \tag{8.45}$$

The stream quantities which enter into the induction equation, Eq. 6.40 will be evaluated next. Attention will first be given to calculation of the equivalent charge on the surface of the unperturbed stream (the Hahn equivalent surface charge). Using at $y = y_b$ the representation of Eq. 8.10 for the potential in the y-displacement perturbation relation, Eq. 3.29, it is found that (after rearrangement)

$$\sigma_b\psi_b = \rho_o(\delta y)_{y_b}\ \psi(y_b) = j\Gamma\psi_b\epsilon_o V\left(\frac{D}{\xi_b} + C + \frac{3}{2}D\ \xi_b + \frac{5}{6}C\ \xi_b^2\right) . \tag{8.46}$$

The quantities σ_b and ψ are discussed in Chapter VI.

With the use of Eq. 8.43, D is eliminated from the above expression to give

$$\sigma_b\psi_b = j\Gamma\psi_b\epsilon_o VC\left[-\frac{\xi_a^2}{\xi_b}\coth j\ (y_a-y_s) + \frac{2}{3}\frac{\xi_a^2}{\xi_b} + 1 + \frac{5}{6}\xi_b^2\right] . \tag{8.47}$$

A similar expression is found for the lower edge, $y = y_a$, of the stream. On combining the two expressions, the negative of the induced anode charge arising from the fact that the edges of the stream is rippled is found to be

$$-\tau_{ripple} = [\rho_o\delta y\psi]_{y_a}^{y_b} = j\Gamma_o VC\left\{\psi_b - \psi_a - \xi_a^2\coth j\Gamma(y_a-y_s)\left[\frac{\psi_b}{\xi_b} - \frac{\psi_a}{\xi_a}\right]\right.$$
$$\left. + \frac{5}{6}(\xi_b^2\psi_b - \xi_a^2\psi_a) + \frac{2}{3}\xi_a^2\left[\frac{\psi_b}{\xi_b} - \frac{\psi_a}{\xi_a}\right]\right\} . \tag{8.48}$$

It is again convenient to group the terms of this equation according to

the degree to which ξ_a and ξ_b appear. Thus,

$$-\tau_{ripple} = -\sum_k \tau_{ripple,k} = -\sum_k A_k \xi_b^r \xi_a^s , \qquad r+s = k . \tag{8.49}$$

The largest of these components—the "zero-order" component, $-\tau_{ripple,0}$—is

$$-\tau_{ripple,0} = j\Gamma\epsilon_o VC \left[\psi_b - \psi_a + j\Gamma(y_b-y_a)\,\psi_a \coth j\Gamma(y_a-y_s)\,\frac{\xi_a}{\xi_b}\right] . \tag{8.50}$$

The other components are obtained similarly.

Further simplification is made through the use of the following approximate relations valid for a thin stream:

$$\psi_b - \psi_a \approx \left.\frac{d\psi}{dy}\right|_{\overline{y}} (y_b-y_a) \equiv \overline{\frac{d\psi}{dy}}\,\Delta y , \tag{8.51}$$

and

$$\frac{d\psi}{dy} \approx \left.\frac{d\psi}{dy}\right|_{y=y_a} = j\Gamma\,\psi_a \coth j\Gamma(y_a-y_s) . \tag{8.52}$$

Hence,

$$-\tau_{ripple,0} \approx j\Gamma\epsilon_o VC\,\overline{\frac{d\psi}{dy}}\,\Delta y \left(1 + \frac{\xi_a}{\xi_b}\right) . \tag{8.53}$$

The remaining component of the induced anode charge arises from the r-f space charge within the unperturbed stream edges, $y = y_a$ and $y = y_b$. The density of this charge is calculated using Poisson's Law, Eq. 3.37, again using Eq. 8.10 for the potential. The result is

$$\rho = 2\Gamma^2\epsilon_o V\left(C\xi + \frac{3}{2}\,d\xi^2\right) . \tag{8.54}$$

Once again, Eq. 8.43 is used to eliminate D, and the terms are suitably grouped. The integration over the cross section of the stream is performed, using the linear approximation for ψ and the fact that ξ is the linear function of y given by Eq. 3.40. The result is that there is no

zero-order term; the largest term arising from Eq. 8.54 is the first-order term

$$-\tau_{\rho,1} = \left(\int_{y_a}^{y_b} \rho\psi dy\right)_1 = 2\Gamma^2\epsilon_o VC \int_{y_a}^{y_b} \xi\psi dy = j2\Gamma\epsilon_o VC \overline{\frac{d\psi}{dy}}\, \xi(\bar{y})\Delta y \ . \quad (8.55)$$

The fact that Eq. 8.50 is the only zero-order term means that the "ripple," or distortion of the stream boundaries, is the predominant mechanism by which the stream affects the circuit in quasi-synchronous operation. In the event that $\xi_a = -\xi_b$, however, the zero-order term is zero; the first-order terms arising from the "ripple" and the bulk space charge effects would then be taken into account.

The conclusion that the stream ripple is the predominant factor in the interaction is restricted to the quasi-synchronous waves. The situation is quite different in the case of cyclotron waves, as shown in Chapter X.

8.8.2 The Combination of the Ballistic and Induction Equations—The Dispersion Equation

The induction equation, Eq. 6.43, will now be put into a more useful form by using the definitions Eqs. 8.4 and 8.5. Equation 6.40 then becomes

$$(p - \kappa)V = \pm j \frac{\omega K h \tau}{2\Gamma_o} \ , \quad (8.56)$$

because, for quasi-synchronous waves,

$$\Gamma \approx \Gamma_o \approx j\frac{\omega}{u_o} \ . \quad (8.57)$$

When the zero-order expression for the induced charge, Eq. 8.53, is substituted in the above equation, and C is evaluated as in Eq. 8.42, the dispersion equation takes the following form:

$$p - \kappa = \mp\left\{\frac{2\omega\,\epsilon_o\,Kh\,s_u\,\bar{\psi}}{(1+H)\cosh j\Gamma_o(y_d-y_b)}\right\}\frac{p(1+H)}{(p+s_u)^2 + H(p-s_u)^2} \quad , \qquad (8.58)$$

where the ξ's are eliminated through Eqs. 8.37 and 8.38.

The quantity in the braces of Eq. 8.58, a dimensionless ratio, summarizes the properties of the circuit and the stream and the position of the stream in relation to the circuit; its square root is appropriately called an "interaction parameter" or, by comparison with small signal traveling-wave amplifier theory, a "gain parameter." This interaction parameter will be labeled, in keeping with the convention apparent in the literature, D_i; the subscript i has been added in the present usage in order to avoid confusion with the coefficient D used above. Thus, the interaction parameter, D_i, is defined by

$$D_i^2 = 2\omega\,\epsilon_o\,Kh\,s_u\,\frac{\bar{\psi}}{\cosh j\Gamma_o(y_d-y_b)}\,\frac{1}{1+H} \quad . \qquad (8.59)$$

D_i as defined above is positive and real for a lossless circuit. An equivalent expression which makes use of the properties of the d-c Brillouin stream is

$$D_i^2 = \frac{\omega}{\omega_c}\,\frac{K\,I_{beam}}{2\,V_{beam}}\,G^2 \quad . \qquad (8.60)$$

Here,

$$V_{beam} \equiv \frac{\bar{u}_o^2}{2\eta} \quad , \qquad (8.61)$$

is the voltage equivalent of the mean d-c electron velocity, and the definition

$$G^2(\bar{y},y_d,y_s) \equiv -\frac{1}{2}\,\frac{\sinh j2\Gamma_o(\bar{y}-y_s)}{\sinh^2[j\Gamma_o(y_d-y_s)]} \qquad (8.62)$$

is introduced to describe the variation of the interaction parameter with the location of the stream relative to the electrodes. It should be noted

that the characteristic impedance, K, is defined in Eq. 6.20 in terms of the potential at the anode. This departure from conventional traveling-wave tube practice is taken because the anode seems to be the logical reference plane and also so that all geometrical variations of the interaction parameter may be conveniently grouped into the single function, G. Figure 8.3 shows the nature of the function G for several values of the radian sole-to-anode distance, $j\Gamma_o(y_d-y_s)$, as a parameter. It is apparent that the behavior of the function G accounts for the fact that, for large values of $|\Gamma_o|$, the fields decay rapidly with distance of the stream from the anode surface.

The dispersion equation, Eq. 8.60, may be compared with the "sheet beam" result of Pierce in the limiting case of zero beam thickness ($s_u \to 0$) of the present analysis. In that limit, Eq. 8.60 becomes

$$p(p-\kappa) = -D_i^2 \quad , \tag{8.63}$$

which is the same as Pierce's equation 15.24, except for differences of notation.

It is useful to normalize the variables of the dispersion relation in terms of the interaction parameter, D_i, thereby eliminating the interaction parameter from the dispersion equation. Thus,

(1) let

$$\ell = \mu - j\nu = p/D_i \tag{8.64}$$

represent the normalized increment of the propagation constant. This equation, together with Eq. 8.4, shows that the propagation constant is

$$\Gamma = j\frac{\omega}{u_o}(1+\mu D_i - j\nu D_i) = \nu D_i \beta_e + (1+\mu D_i)\beta_e \quad . \tag{8.65}$$

Thus, a positive value of μ, the real component of ℓ, indicates

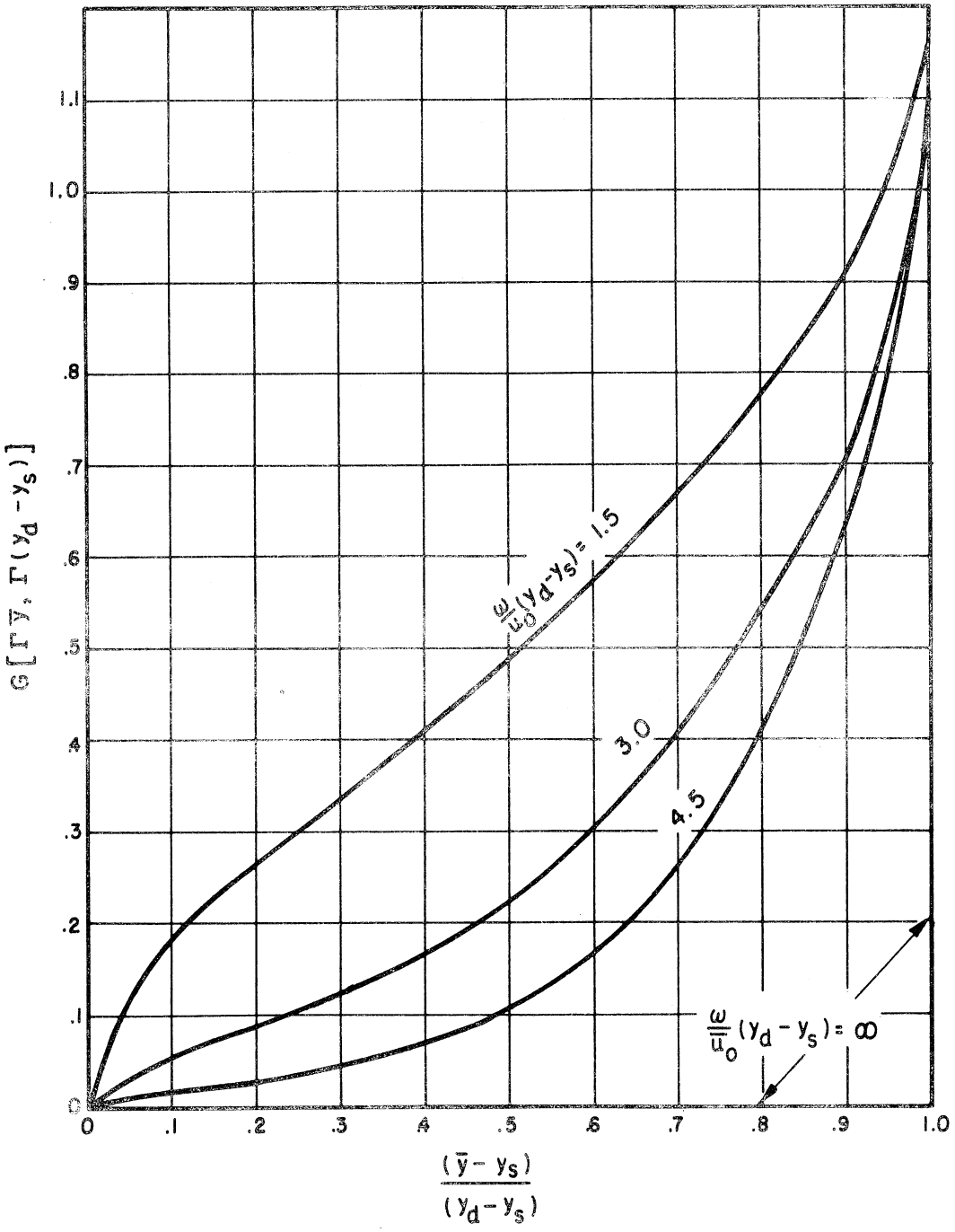

FIG. 8.3 THE FUNCTION G, WHICH DESCRIBES THE DEPENDENCE OF THE INTERACTION PARAMETER, D_i, ON THE STREAM LOCATION RELATIVE TO SOLE AND ANODE.

an increase in phase constant relative to $\beta_e \equiv \omega/\bar{u}_o$ or, equivalently, a wave having a lower phase velocity than the mean d-c electron velocity. A positive value of ν, the imaginary component of ℓ, indicates growth of the wave in the positive z-direction; a negative value of ν indicates decay.

(2) let

$$b \equiv \kappa/D_i \quad . \tag{8.66}$$

The quantity b, an "injection velocity parameter," measures the mean d-c electron stream velocity relative to the phase velocity of the "cold" circuit; thus

$$\bar{u}_o = v_o (1 + b D_i) \quad . \tag{8.67}$$

(3) let

$$r^2 \equiv s_u/D_i \quad . \tag{8.68}$$

The parameter r is a normalized measure of the "velocity spread" or "beam thickness" parameter, s_u, in terms of the interaction parameter, D_i, of the circuit. It is therefore a measure of the importance of the "space-charge" effects relative to the "circuit effects."

Use of these three definitions in Eq. 8.60 leads to the following dispersion equation for quasi-synchronous waves:

$$(\ell - b)\left(\ell^2 + 2r\,\frac{1-H}{1+H}\,\ell + r^2\right) \pm \ell = 0 \quad , \tag{8.69}$$

where the positive sign refers to forward-wave interaction ($K > 0$), and the negative sign refers to backward-wave interaction ($K < 0$).

In the form of Eq. 8.69, the dispersion relation is readily seen to be a cubic equation. Attention is given in the next chapter to the determination of the three roots of Eq. 8.69 as functions of the three parameters b, r, and H.

CHAPTER IX

SOLUTIONS OF THE QUASI-SYNCHRONOUS DISPERSION EQUATION

9.1 Discussion of the Dispersion Equation

The compact form of the dispersion equation for waves which are nearly synchronous with both the electron stream and the "cold" circuit space harmonic was derived in the preceding chapter; it is

$$(\ell - b)\left[\ell^2 - 2\frac{(H - 1)}{1 + H} r \ell + r^2\right] \pm \ell = 0. \qquad (9.1)$$

In this chapter the solutions of the dispersion equation are obtained and the interpretations of them are discussed.

Three factors enter into the dispersion relation in an important way:

(1) The type of circuit space harmonic with which interaction takes place. The plus sign corresponds to forward-wave interaction; the negative sign, to backward-wave interaction. The solutions for the two cases are radically different in the neighborhood of "synchronism," i.e., for small values of b.

(2) The beam thickness, which is expressed by the parameter, r. This parameter may be described loosely as a "space-charge parameter." More specifically, it is an index of the amount of space charge in the interaction region and is also an index of the d-c velocity "spread" of the beam. These two aspects of streams in general cause different phenomena, but they are intimately connected in the Brillouin stream of present interest. Thus, behavior of the r-f waves (i.e., the roots of the dispersion equation) which arises because of the factor r cannot be attributed solely to the amount of space charge or to the velocity spread. Both

aspects enter into r, and a more detailed analysis of the perturbation equations would be required to determine which of the two is the more important aspect.

(3) The location of the stream relative to the electrodes, expressed by the ratio $(H - 1)/(H + 1)$. This quantity is equal to the normalized real component, $\frac{p_r}{s_u}$, of the drift-tube wave value of $\frac{p}{s_u}$ in Eq. 8.40; Fig. 8.1 shows the variation with stream location.

Although the interaction parameter, D_i, is itself a function of the stream location, the factor considered here is an additional complication which depends on the beam thickness parameter, r, in Eq. 8.67. The meaning of this combination of beam thickness and beam location will become apparent in the course of interpretation of the solutions in the sections below.

The two cases of item (1) are treated separately below. Also, the following conditions are extremes for which the dispersion equation assumes simple forms, thus justifying consideration as special cases:

(1) $r = 0$, corresponding to an infinitesimally thin stream carrying an infinitesimal beam current. This condition corresponds to the limit of zero surface-charge density in Pierce's sheet-beam theory. It is therefore of particular interest because it facilitates the comparison of the two theories.

(2) $H = 0$, corresponding to $\bar{y} = y_d$, i.e., the stream grazing the anode surface.

(3) $H = 1$, corresponding to $\bar{y} = \frac{y_d + y_s}{2}$, i.e., the stream being located midway between the sole and the anode.

The case $H \to \infty$, corresponding to $\bar{y} \to y_s$, i.e., the stream adjacent to the sole, cannot be considered here because the approximations made in equa-

tions of the type Eq. 8.52 are not justified in this case. It would appear, in view of Eqs. 8.42 and 8.43, that the field configuration and the resulting wave propagation would be quite different in this case as compared with items (2) and (3) above. This case would not be of much practical interest, however, since the fields at the sole are relatively weak. Since the fields are entirely transverse, possible use may arise from peculiar noise properties of the device. This matter is beyond the scope of the present analysis.

Hindsight shows that when $|b|$ becomes very large the solutions of Eq. 8.69 are the same as the solutions of

$$(\ell - b)\left[\ell^2 + 2\,\frac{1 - H}{1 + H}\,r\,\ell + r^2\right] = 0, \quad [|b| \to \infty] \quad . \tag{9.2}$$

These assymptotic solutions are

$$\ell = b, \quad [|b| \to \infty] \tag{9.3}$$

and

$$\ell = \left(\frac{H - 1}{H + 1} \pm j\,\frac{2\sqrt{H}}{H + 1}\right) r, \quad [|b| \to \infty] \quad . \tag{9.4}$$

It is readily seen that the omitted term, $\pm\ell$, in Eq. 8.69 has negligible magnitude in comparison with the terms which are retained.

The first of these solutions corresponds to

$$\Gamma = j\,\frac{\omega}{u_o}\,(1 + bD_i) = j\,\frac{\omega}{u_o}(1 + \kappa) \approx j\,\frac{\omega}{v_o}\;; \tag{9.5}$$

it thus represents the wave propagated on the circuit in the absence of the stream. In the charts of the wave solutions presented below, this assymptote is labelled the "unperturbed circuit wave." The second and third assymptotes, those of Eq. 9.4, correspond to the drift-tube waves discussed in Sec. 8.7. These assymptotes are labelled "drift-tube limit"

on the charts below; in general, both real and imaginary components of these assymptotes exist.

9.2 Forward-wave Interaction

9.2.1 Infinitesimal Beam Thickness—r = 0

In this case, the dispersion equation, Eq. 8.69, becomes

$$(\ell - b)\ell^2 + \ell = 0 \tag{9.6}$$

and the dependence on the stream location parameter, H, does not appear. Thus, the solutions obtained from Eq. 9.6 apply equally well to any stream locations with the exception of the case where the stream is extremely close to the sole.

One of the roots of Eq. 9.6 is obviously

$$\ell = 0 \ . \tag{9.7}$$

Upon division of Eq. 9.6 by ℓ, the equation for the remaining roots takes the quadratic form

$$\ell^2 - b\ell + 1 = 0 \ . \tag{9.8}$$

The solution of this quadratic equation yields

$$\ell = \frac{b}{2} \pm \sqrt{\left(\frac{b}{2}\right)^2 - 1} = \frac{b}{2} \pm j\sqrt{1 - \left(\frac{b}{2}\right)^2} \ . \tag{9.9}$$

Figure 9.1 is a chart of the real component, μ, and the imaginary component, ν, of the solutions, Eqs. 9.7 and 9.9, of the dispersion equation.

Near "synchronism" ($|b| < 2$), the three solutions describe the following waves (cf. Eqs. 8.4 and 8.64):

(1) One wave, $\ell_1 = \mu_1 - \nu_1$, obtained from Eq. 9.9, propagates with

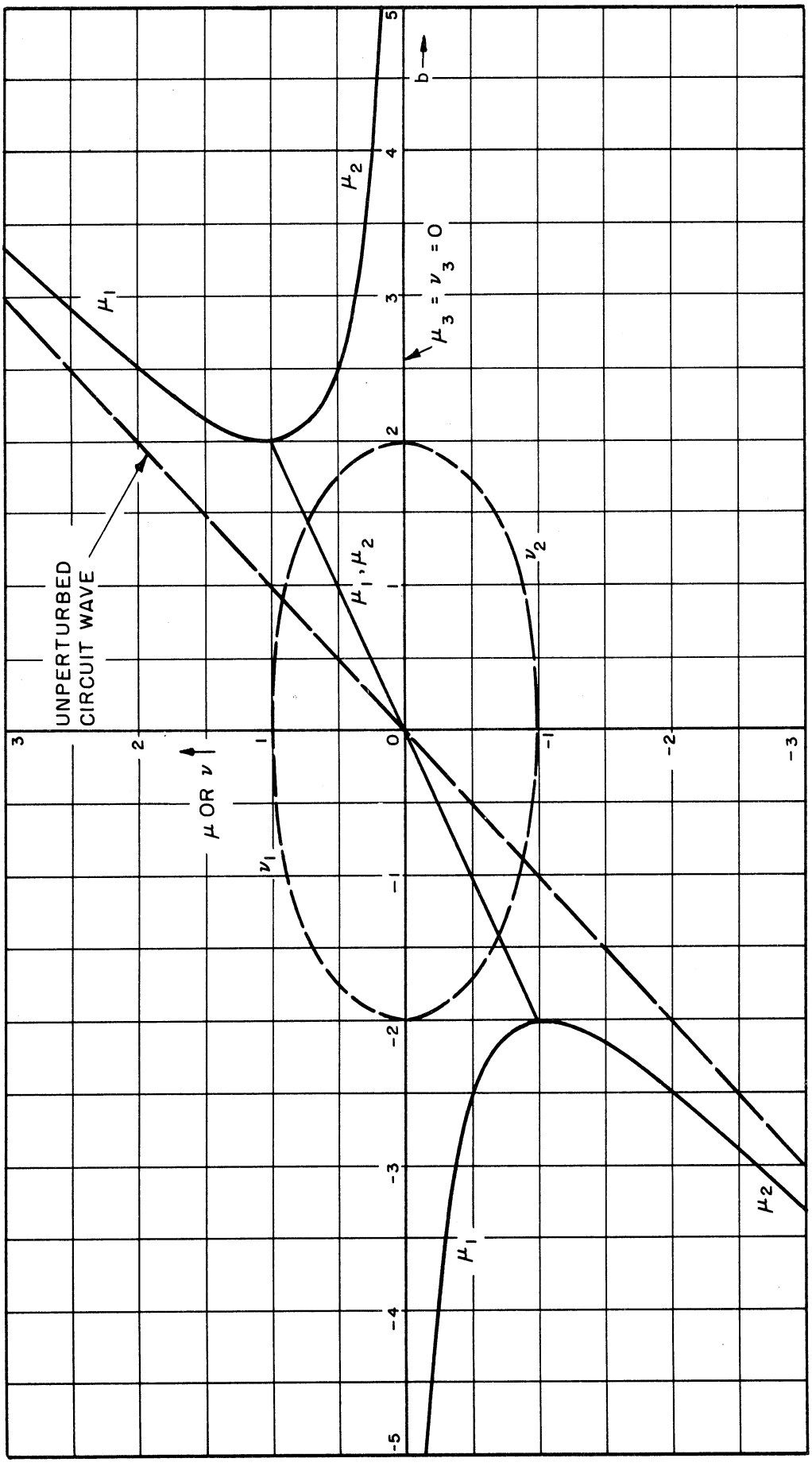

FIG. 9.1 SOLUTIONS OF THE QUASI-SYNCHRONOUS DISPERSION EQUATION: FORWARD-WAVE INTERACTION; $r = 0$. $\Gamma = j\frac{\omega}{u_0}(1 + \mu - j\nu)$

a phase velocity which is the average of the cold circuit phase velocity and the mean d-c stream velocity (line AB in Fig. 9.1) and which grows exponentially in the positive z-direction (the upper half-ellipse).

(2) One wave, $\ell_2 = \mu_2 - j\nu_2$, also obtained from Eq. 9.9, which propagates with the same phase velocity as in item (1), but which decays in the positive z-direction (the lower half-ellipse in Fig. 9.1).

(3) One wave, $\ell_3 = 0$, obtained from Eq. 9.7. This solution is represented by the horizontal axis of Fig. 9.1. This wave is always synchronous with the mean d-c electron velocity.

Farther from "synchronism" ($|b| > 2$), there is no growth or decay in any of the three wave solutions. The phase-velocity behavior of these waves is described by the hyperbolic branches (waves 1 and 2) and by the horizontal axis (wave 3) in Fig. 9.1. There appears to be little interaction of interest under such circumstances.

The above solution is precisely the same as obtained by Pierce and Muller, who used a sheet-beam model.

9.2.2 Finite Beam Thickness—r > 0

When r appears in Eq. 9.1, it carries with it the factor $p_r/s_u = (H - 1)/(H + 1)$; thus, for forward-wave interaction,

$$(\ell - b)\left[\ell^2 - 2\, r\, \frac{H - 1}{H + 1}\, \ell + r^2\right] + \ell = 0 \quad . \tag{9.10}$$

The effect of the stream thickness, contained in r, therefore depends on the stream location, expressed by the function H. The midplane of the interaction space, defined by

$$y = y_c = \frac{y_s + y_d}{2} \quad , \tag{9.11}$$

is shown in Fig. 8.1 to be a plane of symmetry for the factor $\frac{(H - 1)}{(H + 1)}$.

Hence there appears in the dispersion equation a symmetry which facilitates the calculation of the roots. It is found that if the mean position of the stream is $\bar{y} = y_c + d$, and if the roots of the dispersion equation are

$$\ell(\bar{y}, b, r) = \ell(y_c + d, b, r) \qquad (9.12)$$

then the roots of the dispersion equation when $\bar{y} = y_c - d$ are given by

$$\ell(y_c - d, b, r) = -\ell(y_c + d, -b, r) \quad . \qquad (9.13)$$

This can be verified by direct substitution in Eq. 9.10.

Inspection of Fig. 8.1 shows that for common values (say, 3) of the radian width, $-j\Gamma(y_d - y_s)$, the factor $p_r/s_u = (H - 1)/(H + 1)$ is small if the stream is close to the midplane of the interaction space. The special case $\bar{y} = y_c$, or H = 1 and $[(H - 1)/(H + 1)] = 0$, is thus important because it approximates many practical situations. The special case in which the stream is adjacent to the anode, H = 0, is considered also, along with the intermediate values H = 3/2 and H = 2/3, which correspond approximately to situations in which the stream-to-sole distances are 1/4 and 3/4, respectively, of the total distance between sole and anode electrodes.

9.2.2.1 Finite Beam Thickness ($r > 0$), and $\bar{y} = y_c$ ($H = 1$)

When H = 1, the factor containing it in Eq. 9.10 vanishes, and the dispersion equation becomes

$$(\ell - b)(\ell^2 + r^2) + \ell = 0 \quad ; \qquad (9.14)$$

the beam thickness parameter, r, thus enters the dispersion equation in only one place. Equation 9.14 is a more general form of a cubic equation then Eq. 9.6; it simplifies only when b = 0 ("synchronism"), yielding then

$$\ell = 0 , \tag{9.15}$$

$$\ell = \pm j\sqrt{1 + r^2} \quad . \tag{9.16}$$

When $b \neq 0$, Eq. 9.14 is solved numerically; the real and imaginary components of the three roots are shown graphically in Figs. 9.2 and 9.3 for two different values of r.

Comparison of the above results with those for an infinitesimally thin "sheet" beam, ($r = 0$), shows that aside from the effect on the interaction parameter, D_i, the effect of increasing the beam thickness (and, consequently, increasing the velocity spread) is to further enhance the gain and decay rates—the ν's. This effect, of course, is most pronounced near $b = 0$. Farther from "synchronism," two of the three solutions approach the "drift tube" assymptotes discussed in Sec. 9.1. These assymptotic solutions indicate waves which grow/decay along the z-axis in proportion to the parameter r.

9.2.2.2 Finite Beam Thickness ($r > 0$), and $\bar{y} = y_d$ ($H = 0$)

When the electron stream is adjacent to, or grazes, the anode, $H = 0$ and the dispersion equation for forward-wave interaction, Eq. 9.10, becomes

$$(\ell - b)(\ell + r)^2 + \ell = 0 \quad . \tag{9.17}$$

Figure 9.4 shows numerical results for the condition $H = 0$, $r = 1$. Comparison with Fig. 9.1, for which $H = 0$, $r = 0$ applies, shows that the range of electron velocity (the parameter b) over which gain occurs is extended in the present case. Comparison with Fig. 9.3, for which $H = 1$, $r = 1$, shows that the gain for $H = 0$ is less than for $H = 1$.

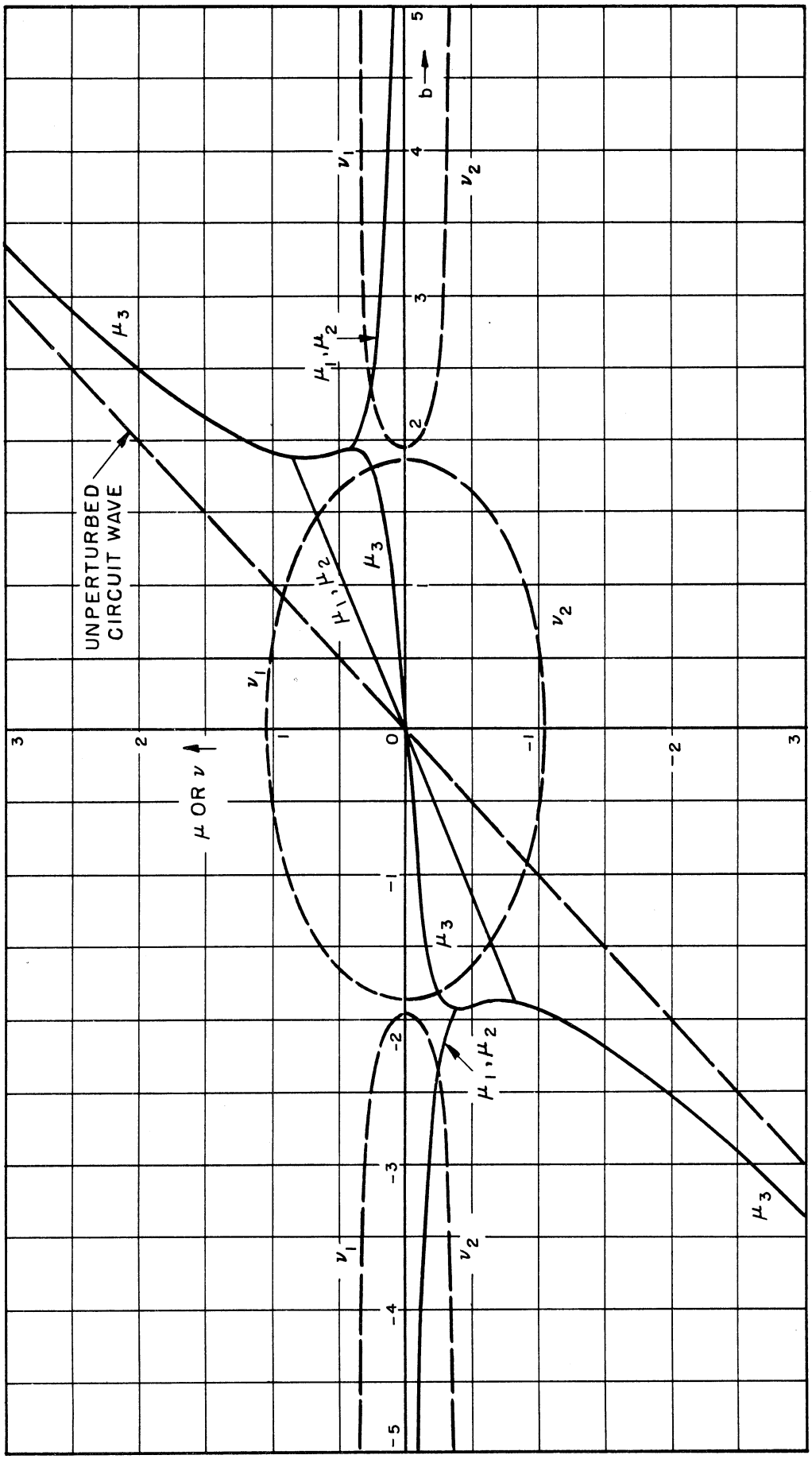

FIG. 9.2 SOLUTIONS OF THE QUASI-SYNCHRONOUS DISPERSION EQUATION: FORWARD-WAVE INTERACTION; $r^2 = 0.1$, $H = 1$. $\Gamma' = j\frac{\omega}{\omega_0}(1 + \mu - j\nu)$.

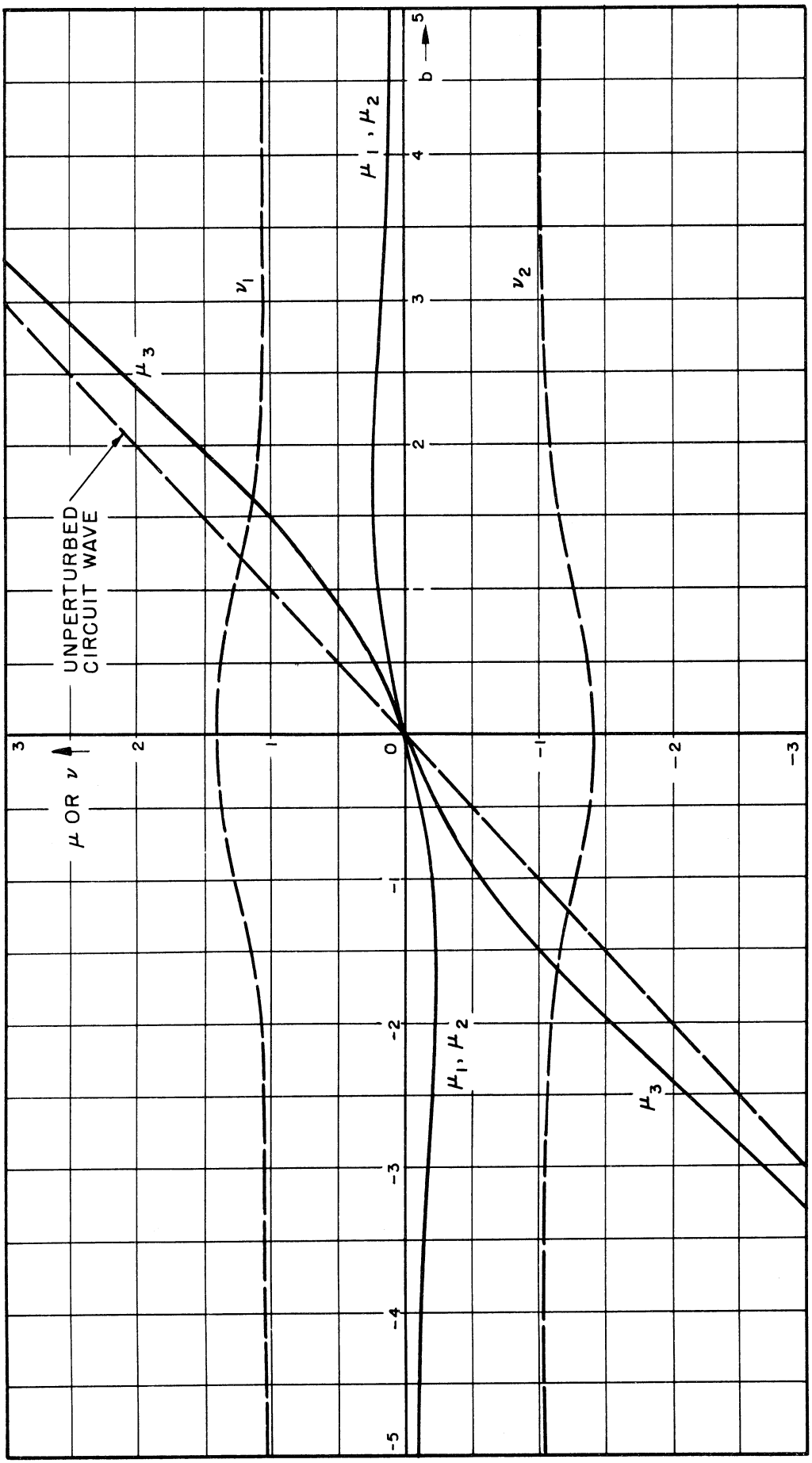

FIG. 9.3 SOLUTIONS OF THE QUASI-SYNCHRONOUS DISPERSION EQUATION: FORWARD-WAVE INTERACTION; $r^2 = 1.0$, $H = 1$. $\Gamma = j\frac{\omega}{u_0}(1 + \mu - j\nu)$.

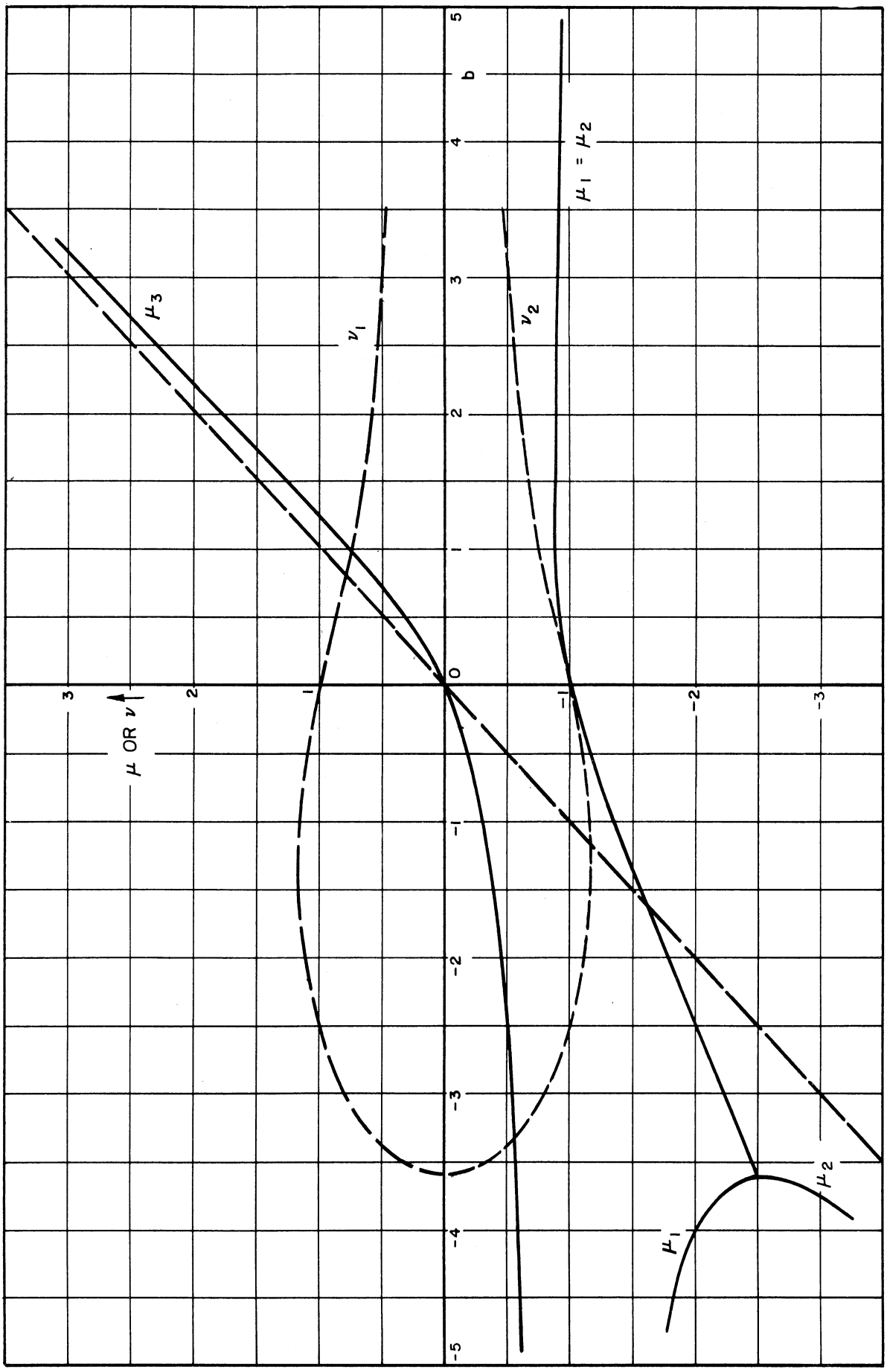

FIG. 9.4 SOLUTIONS OF THE QUASI-SYNCHRONOUS DISPERSION EQUATION, FORWARD-WAVE INTERACTION; $r^2 = 1.0$, $H = 0$. $\Gamma = j\frac{\omega}{u_0}(1 + \mu - j\nu)$.

9.2.2.3 Finite Beam Thickness ($r > 0$), and Intermediate Values of H.

Figure 9.5 shows numerical results for the condition $H = 3/2$, $r = 1$; this value of H corresponds to a stream location

$$y \approx y_s + \frac{1}{4}(y_d - y_s) \quad , \tag{9.18}$$

i.e., the stream-to-sole distance is one-quarter of the total width of the interaction space. The exact value of y for a particular value of H depends on Γ; it can be determined from Eq. 8.32. Figure 9.6 shows the results of numerical calculation of the roots of the dispersion equation for the conditions $H = 2/3$, $r = 1$. This value of H corresponds to the stream location

$$\bar{y} \approx y_s + \frac{3}{4}(y_d - y_s) \quad , \tag{9.19}$$

or a stream location symmetrical to the location of Fig. 9.5, with respect to the midplane, $y = y_c$, of the interaction space. The results shown in Figs. 9.5 and 9.6 show that the maximum gain rate, $\nu_{1\ max}$, does not occur at "synchronism" between the mean d-c electron stream velocity and the cold circuit phase velocity. A small value of b, i.e., small "under-drive" or "over-drive" of mean d-c electron velocity relative to the cold circuit is required. Furthermore, the maximum value of the gain rate, $\nu_{1\ max}$, as b is varied, appears to be in all instances less than under the condition $H = 1$ for the same value of r. Figure 9.7 shows the variation of the "maximum normalized gain rate," $\nu_{1\ max}$, as a function of stream location.

9.2.2.4 Summary of the Effect of Finite Beam Thickness ($r > 0$)

It may be concluded from the above calculations that the effect of beam thickness and velocity spread which accompanies it, expressed by the parameter r, is to enhance the gain rate of the increasing wave in addition

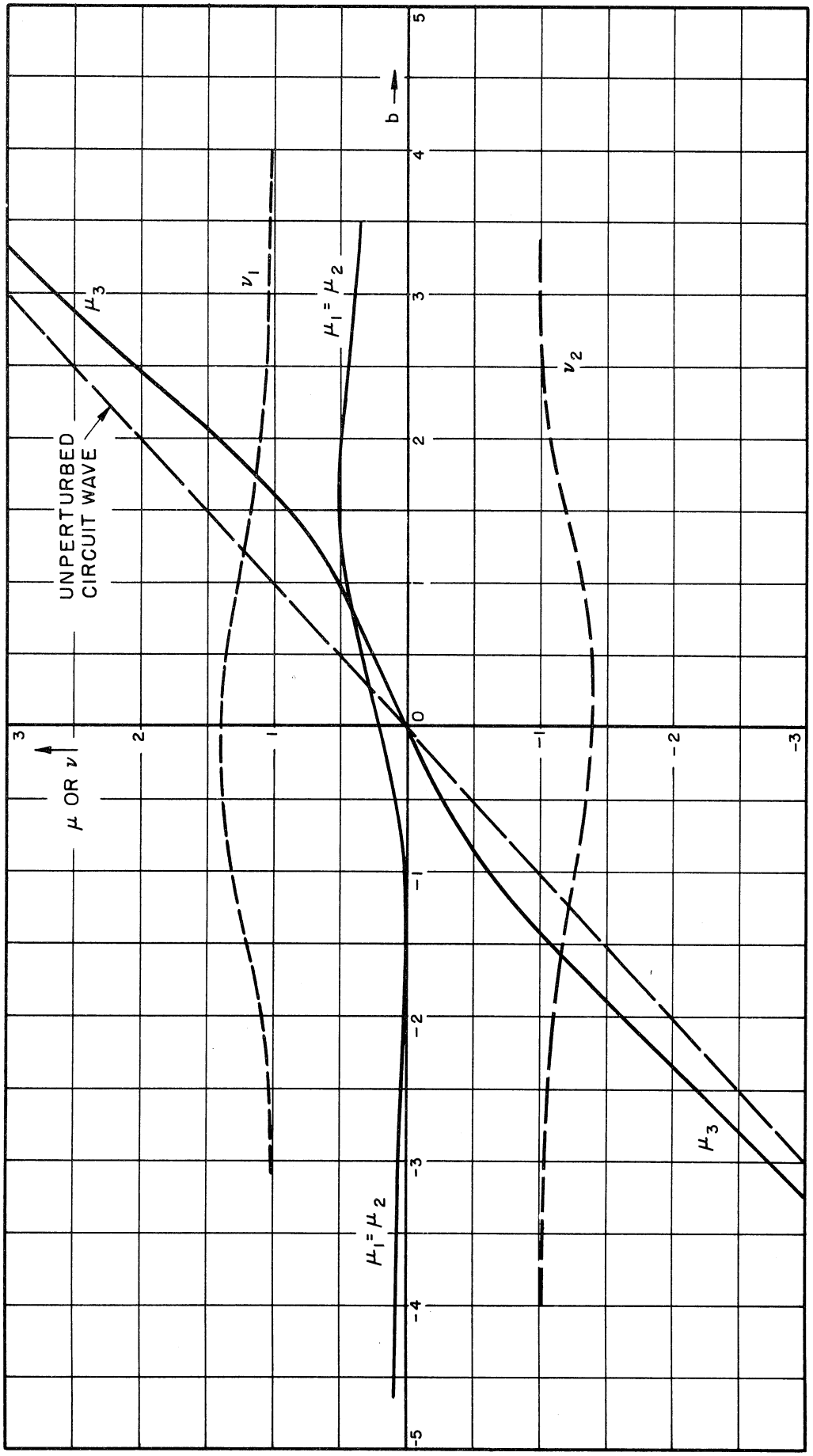

FIG. 9.5 SOLUTIONS OF THE QUASI-SYNCHRONOUS DISPERSION EQUATION: FORWARD-WAVE INTERACTION; $r^2 = 1.0$, $H = 3/2$. $\Gamma = j\frac{\omega}{u_0}(1 + \mu - j\nu)$.

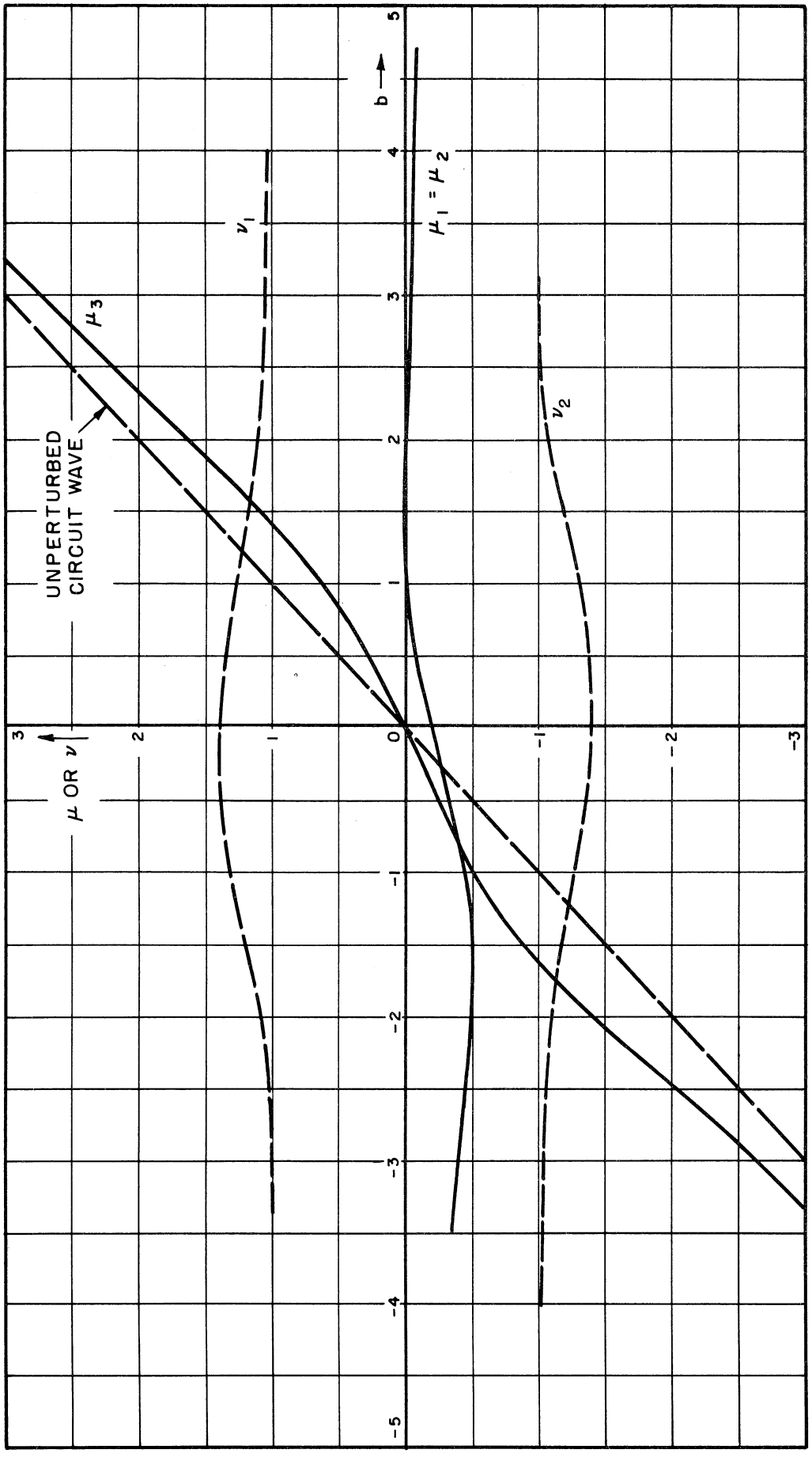

FIG. 9.6 SOLUTIONS OF THE QUASI-SYNCHRONOUS DISPERSION EQUATION: FORWARD-WAVE INTERACTION; $r^2 = 1.0$, $H = 2/3$. $\Gamma = j\frac{\omega}{u_0}(1 + \mu - j\nu)$.

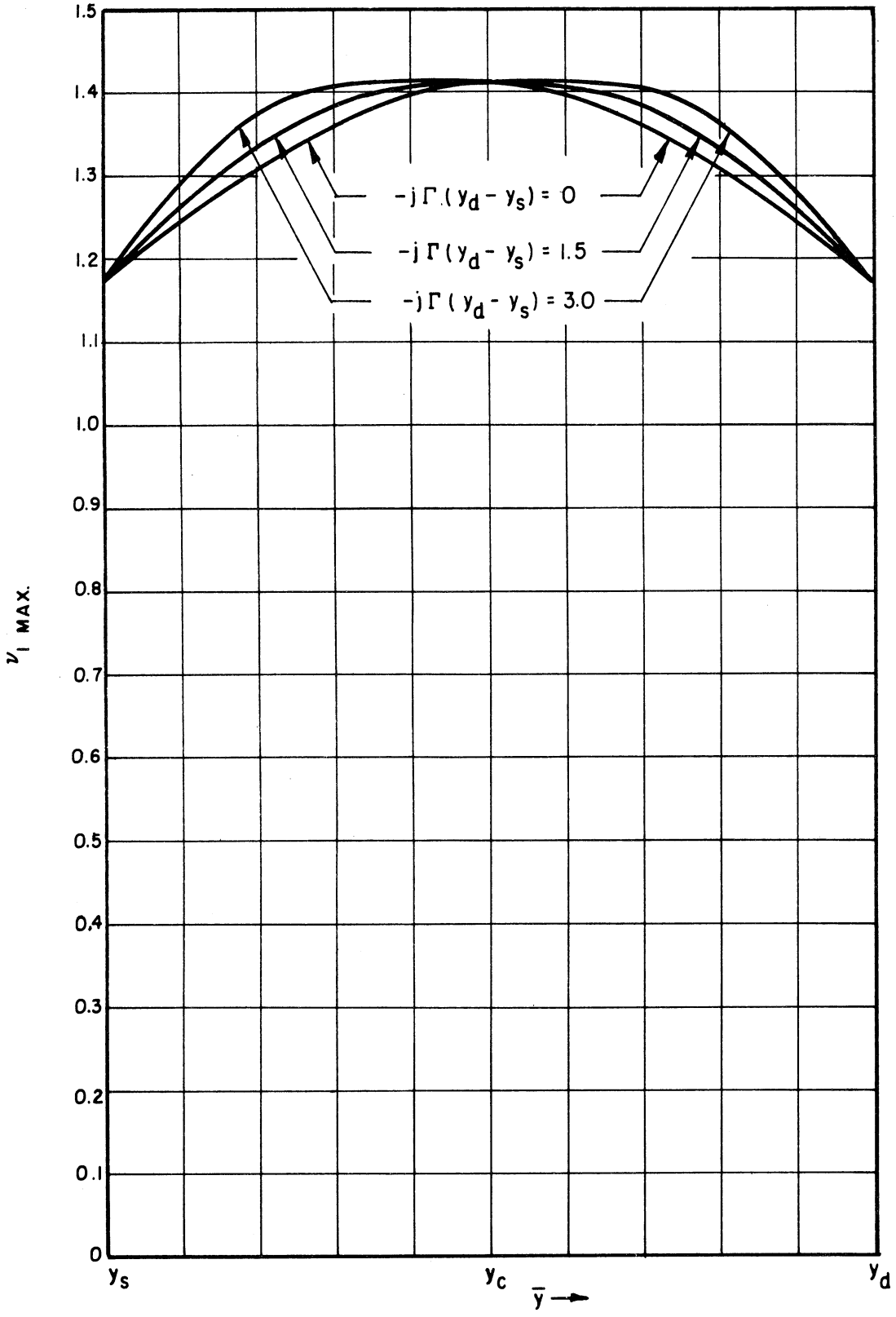

FIG. 9.7 VARIATION OF MAXIMUM GAIN RATE, $\nu_{1\ MAX.}$, WITH STREAM LOCATION; $r^2 = 1.0$.

to the effect on the interaction parameter, D_i. This phenomenon is closely related to the gain of drift-tube waves as discussed in Sec. 8.7. It is more complicated, however, because the gain/decay rate is enhanced even when the stream is adjacent to the anode; this does not occur in drift-tube wave theory (cf. Fig. 8.1).

9.3 Backward-wave Interaction

For interaction between the electron stream and a backward-wave space harmonic, the negative sign applies in Eq. 9.1; thus,

$$(\ell - b)\left[\ell^2 - 2r\frac{H-1}{H+1}\ell + r^2\right] - \ell = 0 \quad . \tag{9.20}$$

It should be noted that in backward-wave devices of the conventional, or traveling-wave tube, type, gain of the various waves is of secondary importance to the relative phase constants of the waves. Therefore, in the solutions of the dispersion equation, Eq. 9.20, attention must be given to the nature of the real component, μ, of the roots, ℓ, as well as to the imaginary component, ν. In any device, whether operating as a forward-wave or backward-wave tube, the real and imaginary components of ℓ must be considered in determining the extent to which the individual waves are excited at longitudinal discontinuities (cf. Chapter XIV).

9.3.1 Infinitesimal Beam Thickness—$r = 0$

When $r = 0$, the dispersion relation, Eq. 9.20, becomes

$$(\ell - b)(\ell^2) - \ell^2 = 0 \quad , \tag{9.21}$$

and the dependence on H is missing. One of the three roots is obviously

$$\ell = 0 \quad . \tag{9.22}$$

The other two are the roots of the quadratic equation

$$\ell^2 - b\ell - 1 = 0 \quad ; \tag{9.23}$$

they are

$$\ell = \frac{b}{2} \pm \sqrt{1 + \left(\frac{b}{2}\right)^2} \quad . \tag{9.24}$$

Thus, all three solutions for ℓ are purely real for all values of b; they are shown in Fig. 9.8. The three solutions therefore represent the following waves, the amplitudes of which are all invariant in the z-direction:

(1) One wave, $\ell_1 = \mu_1 > 0$, which is slightly slower than either the mean d-c electron stream velocity or the cold circuit phase velocity.

(2) One wave, $\ell_2 = \mu_2 < 0$, which is slightly faster than either the mean d-c electron stream velocity or the cold circuit phase velocity.

(3) One wave, $\ell_3 = \mu_3 = 0$, which has the same phase velocity as the mean d-c electron stream velocity. This wave is represented by the horizontal axis in Fig. 9.8.

Comparison of this result with that of Sec. 9.2.2.1 shows the radical difference in the waves that result from forward- and backward-wave interaction. These results for backward-wave interaction are identical with the results of Muller's sheet beam analysis of the M-type backward-wave device.

9.3.2 Finite Beam Thickness—r > 0

As in Sec. 9.2.2, accounting for finite r requires at the same time consideration of the variable H. The symmetry property noted in Eq. 9.13 is valid in the case of backward waves also. The special cases, H = 1 and H = 0 are discussed below. Solutions of the dispersion equation are also presented for intermediate values of H.

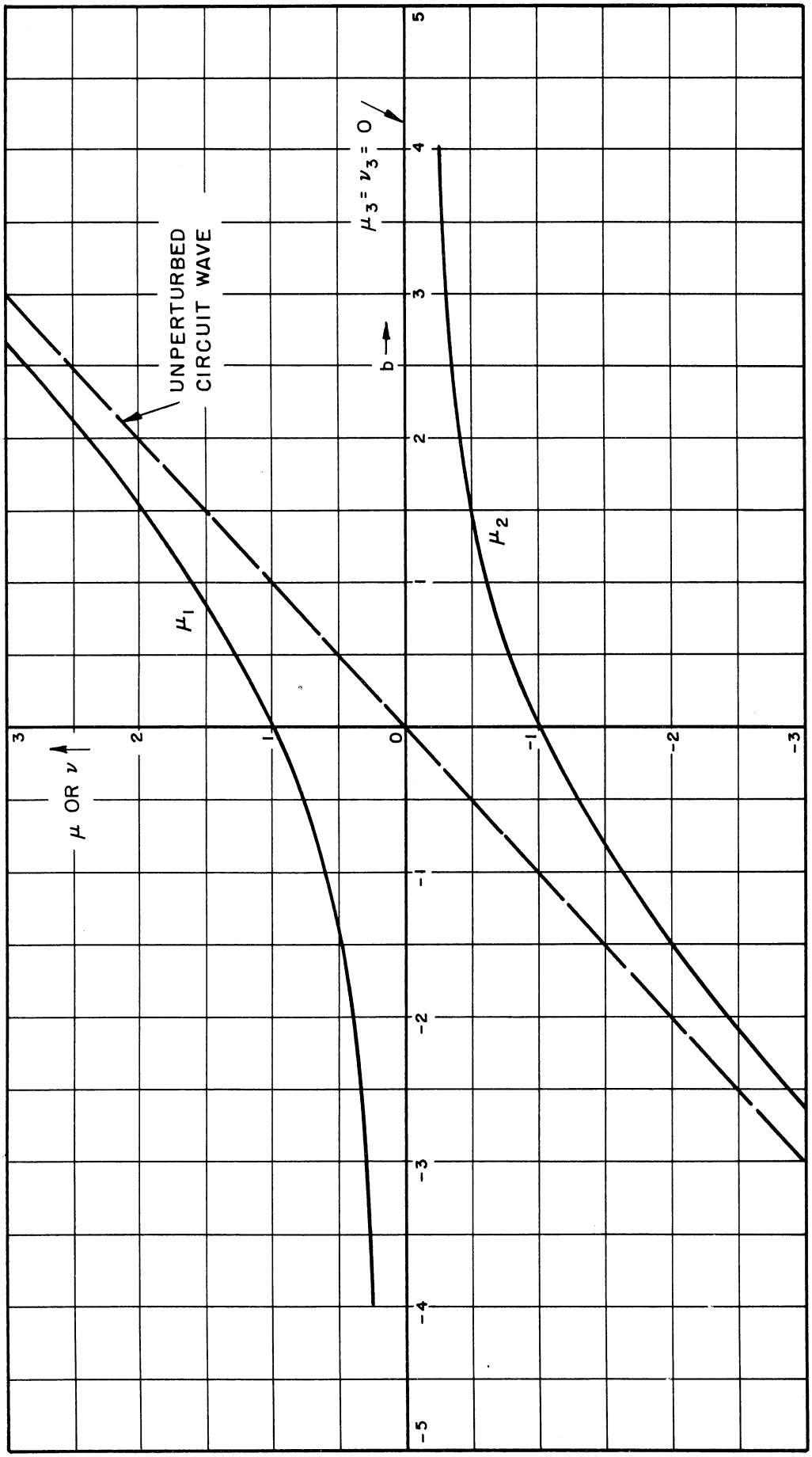

FIG. 9.8 SOLUTIONS OF THE QUASI-SYNCHRONOUS DISPERSION EQUATION: BACKWARD-WAVE INTERACTION; $r^2 = 0$. $\Gamma = j\frac{\omega}{u_0}(1 + \mu - j\nu)$.

9.3.2.1 Finite Beam Thickness and $\bar{y}$ = yc (H = 1)

When the stream is at the midplane of the interaction space, H = 1, and the dispersion equation becomes

$$(\ell - b)(\ell^2 + r^2) - \ell = 0 \quad . \tag{9.25}$$

When b = 0, it yields

$$\ell = 0 \tag{9.26}$$

and

$$\ell = \pm\sqrt{1 - r^2} \quad . \tag{9.27}$$

When b $\neq$ 0, the cubic equation is solved numerically. Figures 9.9, 9.10 and 9.11 are charts of the solutions for the three values of r^2 of 0.1, 1.0, and 2.0, respectively.

Comparison of Figs. 9.8-9.11 shows that the effect of increasing the beam thickness (exclusive of the effect on the interaction parameter) is to decrease the relative differences between the phase velocities of the waves and ultimately to give rise to waves which are characterized by gain/decay rather than by their phase constant differences. The effect of increasing the parameter r is in this case, as in general, to submerge the "circuit effect" so that only the drift-tube or smooth-anode situation remains.

9.3.2.2 Finite Beam Thickness and y = yd (H = 0)

When the stream grazes the anode plane, H = 0, and the dispersion relation, Eq. 9.20, becomes

$$(\ell - b)(\ell + r)^2 - \ell = 0 \quad . \tag{9.28}$$

When b = 0, the solutions are simply

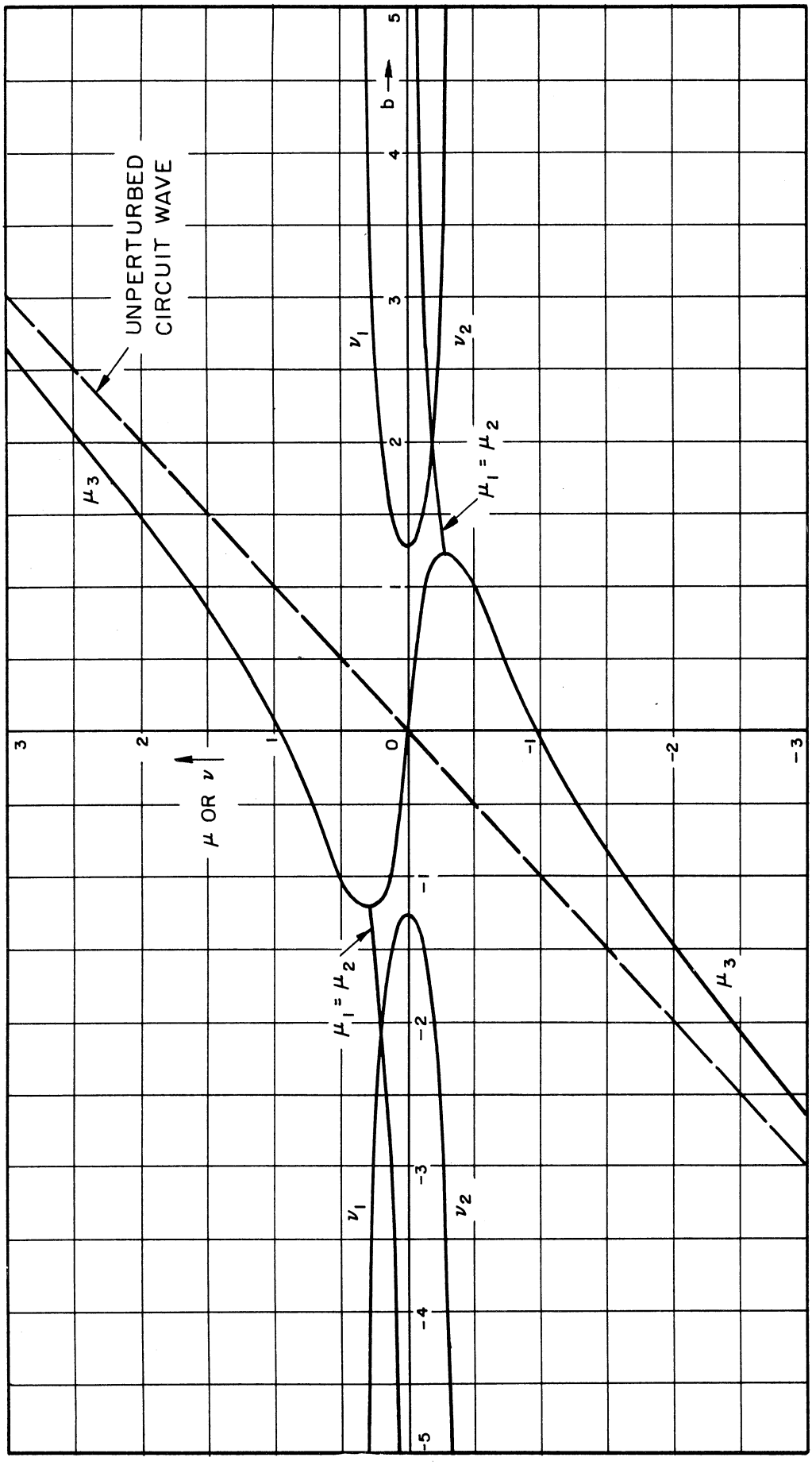

FIG. 9.9 SOLUTIONS OF THE QUASI-SYNCHRONOUS DISPERSION EQUATION: BACKWARD-WAVE INTERACTION; $r^2 = 0.1$, $H = 1$. $\Gamma = j\frac{\omega}{u_0}(1 + \mu - j\nu)$.

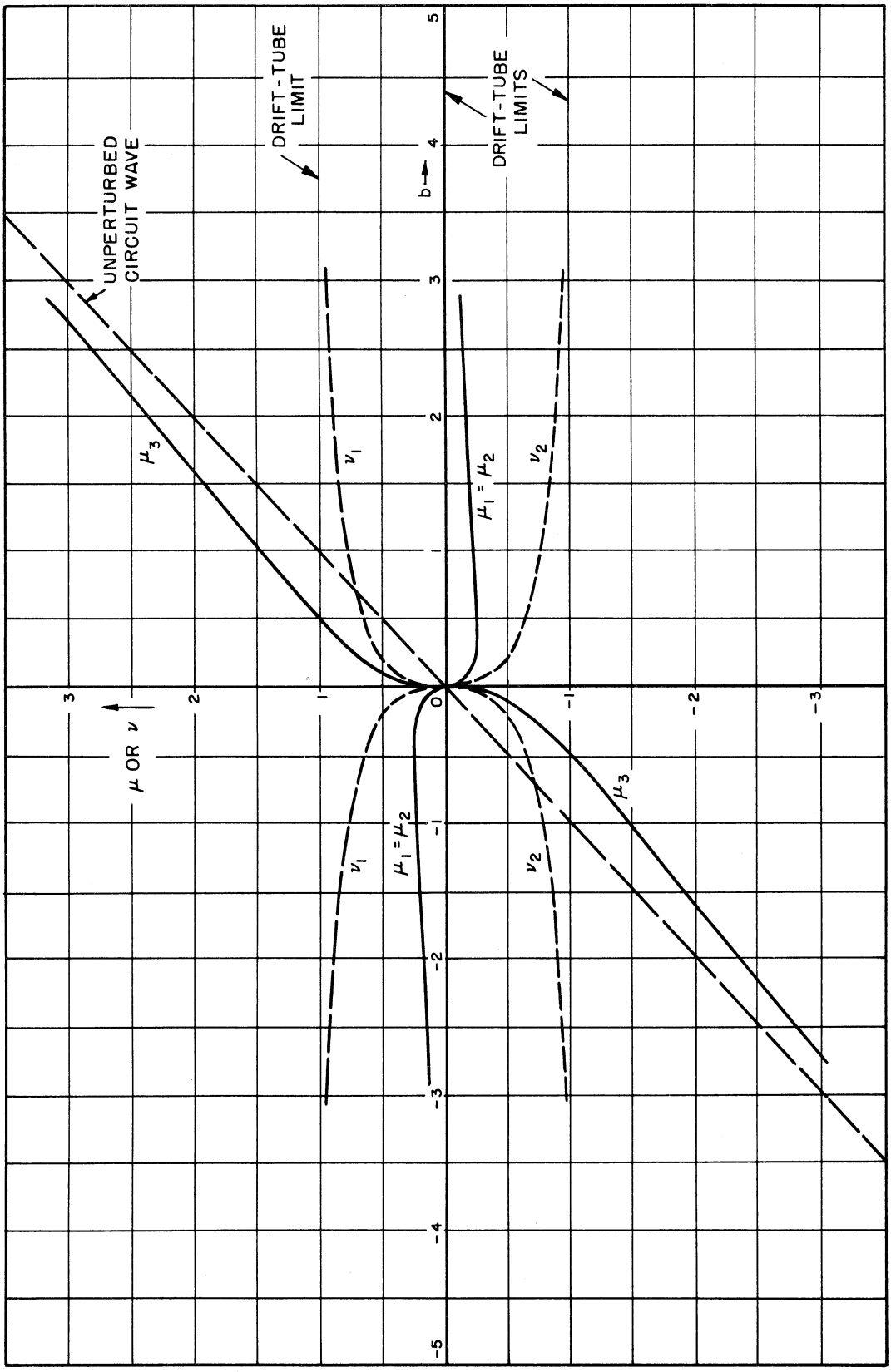

FIG. 9.10 SOLUTIONS OF THE QUASI-SYNCHRONOUS DISPERSION EQUATION: BACKWARD-WAVE INTERACTION; $r^2 = 1.0$, $H = 1$. $\Gamma = j\frac{\omega}{u_0}(1 + \mu - j\nu)$.

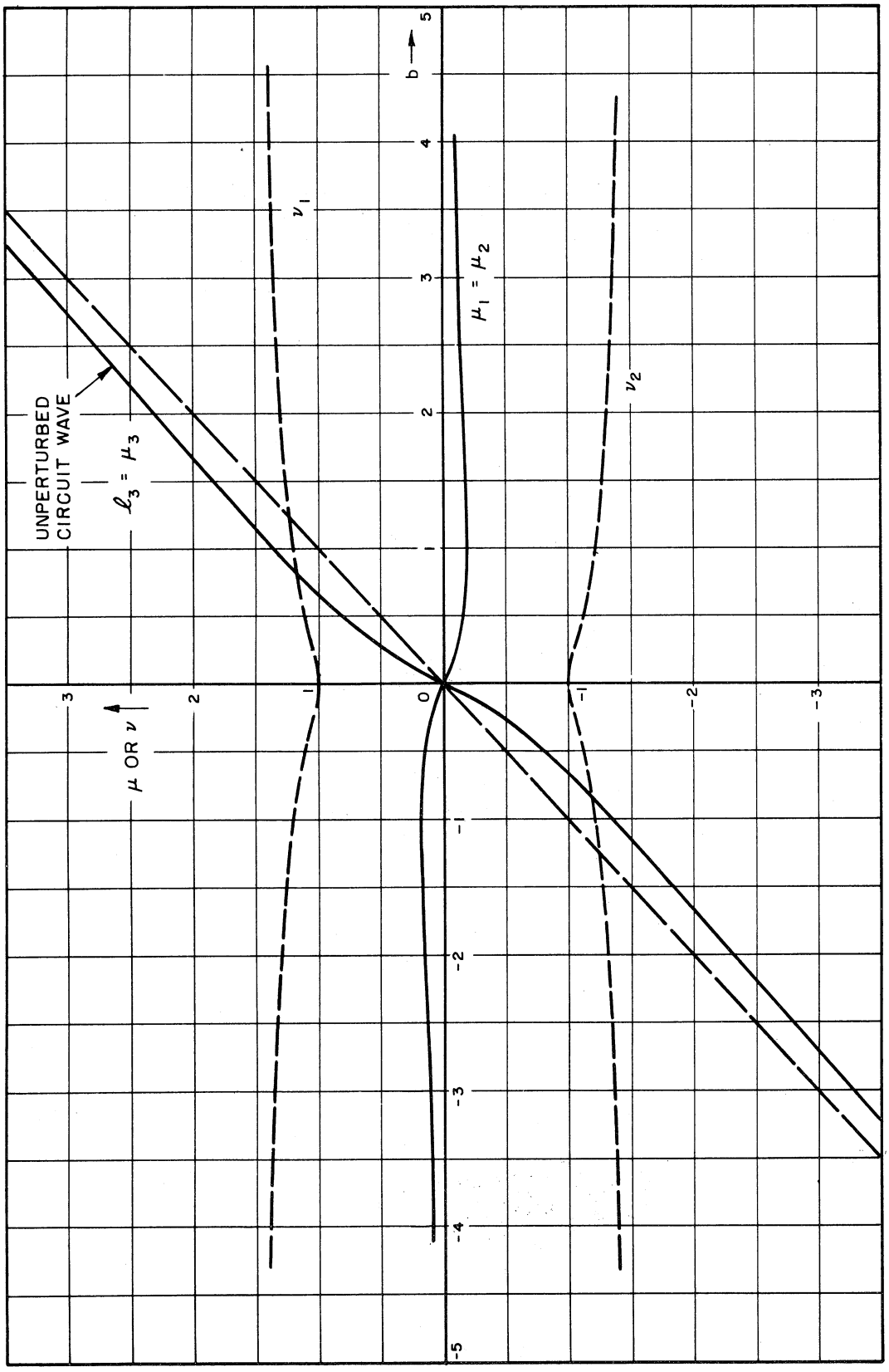

FIG. 9.11 SOLUTIONS OF THE QUASI-SYNCHRONOUS DISPERSION EQUATION: BACKWARD-WAVE INTERACTION; $r^2 = 2.0$, $H = 1$. $\Gamma = j\frac{\omega}{u_0}(1 + \mu - j\nu)$.

$$\ell = 0 \tag{9.29}$$

and

$$\ell = -r \pm 1 \ . \tag{9.30}$$

Figure 9.12 shows numerical results under this conditions for $r^2 = 1$ and a range of the velocity injection parameter, b. Although it is noted that there is gain/decay for $b < 0$ (a result not expected for drift-tube wave considerations, since the stream is adjacent to the anode), no simple explanation or interpretation can be given at this point to the results regarding the phase constants.

9.3.2.3 Finite Beam Thickness and Intermediate Values of H

The discussion of Sec. 9.2.2.3 regarding the values of H of 3/2 and 2/3 is applicable here; Figs. 9.13 and 9.14 chart the solutions of the backward-wave dispersion equations for these respective values of H. As in Sec. 9.3.2.2, these results are presented for future use without an immediate physical interpretation.

9.3.2.4 Summary of the Effect on Backward-wave Interaction of Finite Beam Thickness ($r > 0$)

It would appear from the above calculations that the effect of increasing the beam thickness-velocity spread parameter, r, is to reduce the differences between the phase constants of the waves and to introduce gain and decay. Thus, it would appear that the "circuit effect" is reduced and that the device would therefore be less effective as a backward-wave tube. Such a conclusion cannot be drawn, however, until the analysis is complete—in particular, until the input boundary conditions (see Chapter XIII) have been solved. Indeed, it is found that the effect of finite beam thickness is to increase the effectiveness of the interaction.

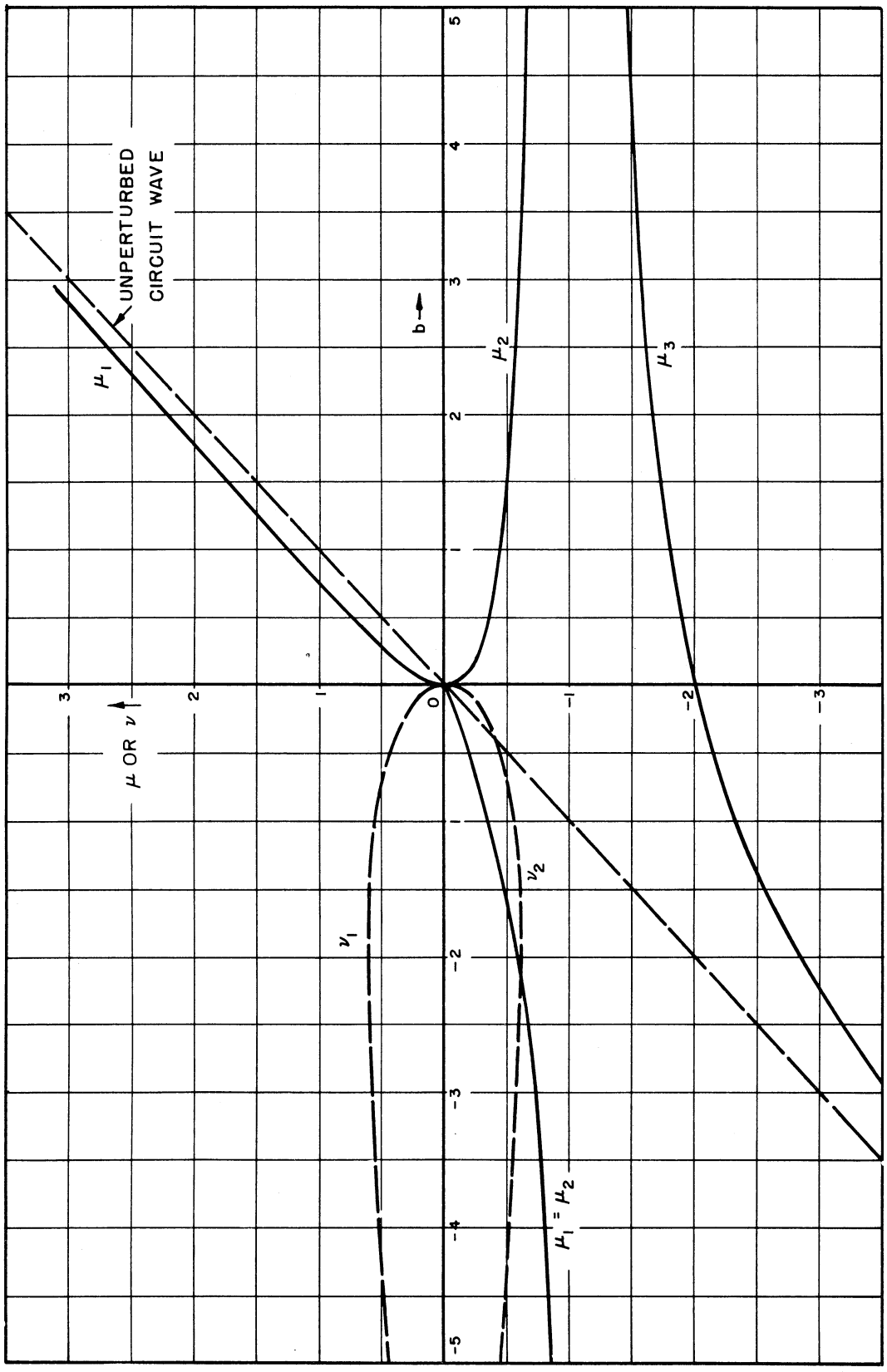

FIG. 9.12 SOLUTIONS OF THE QUASI-SYNCHRONOUS DISPERSION EQUATION: BACKWARD-WAVE INTERACTION; $r^2 = 1.0$, $H = 0$. $\Gamma = j\frac{\omega}{u_0}(1 + \mu - j\nu)$.

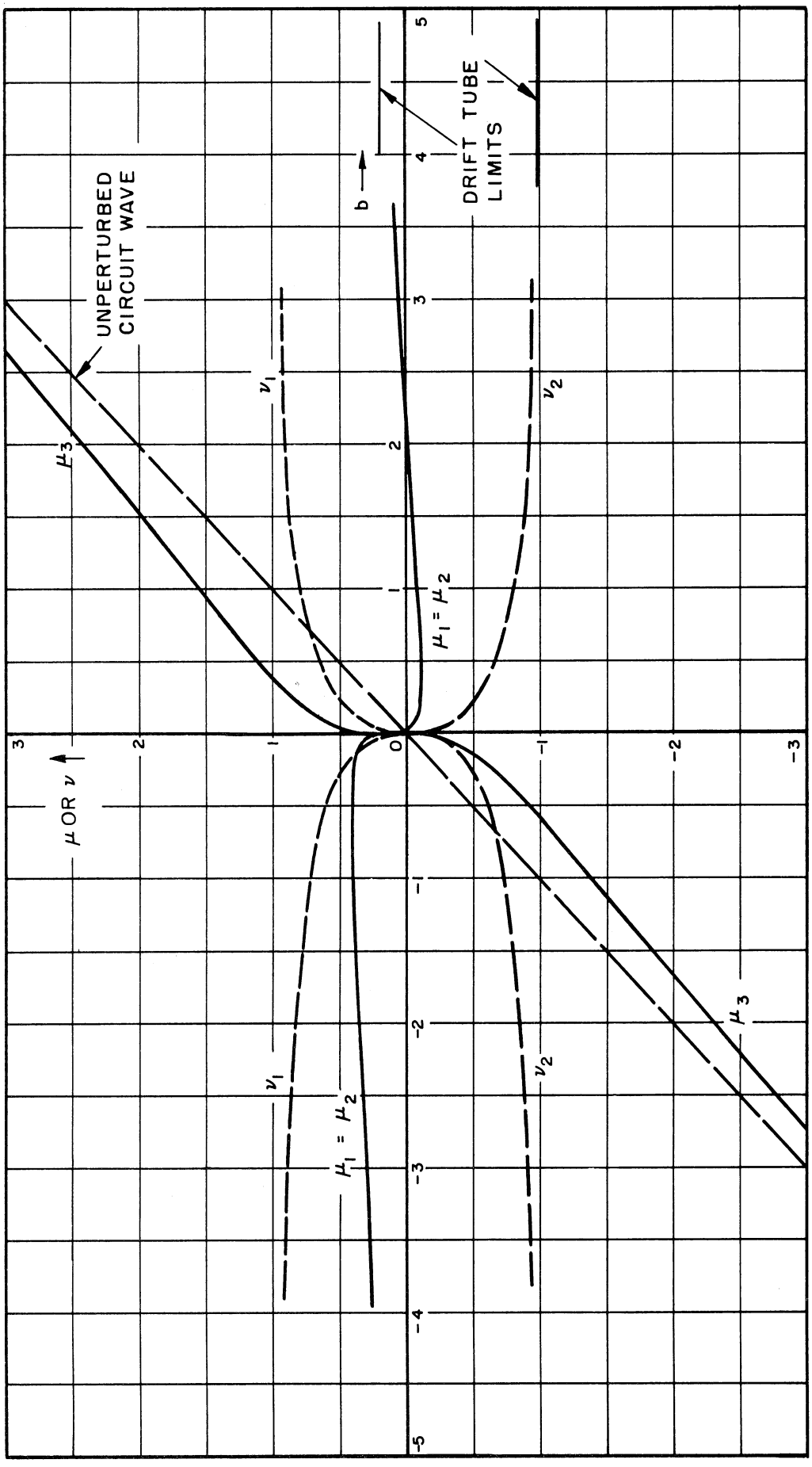

FIG. 9.13 SOLUTIONS OF THE QUASI-SYNCHRONOUS DISPERSION EQUATION: BACKWARD-WAVE INTERACTION; $r^2 = 1.0$, $H = 3/2$. $\Gamma = j\frac{\omega}{u_0}(1 + \mu - j\nu)$.

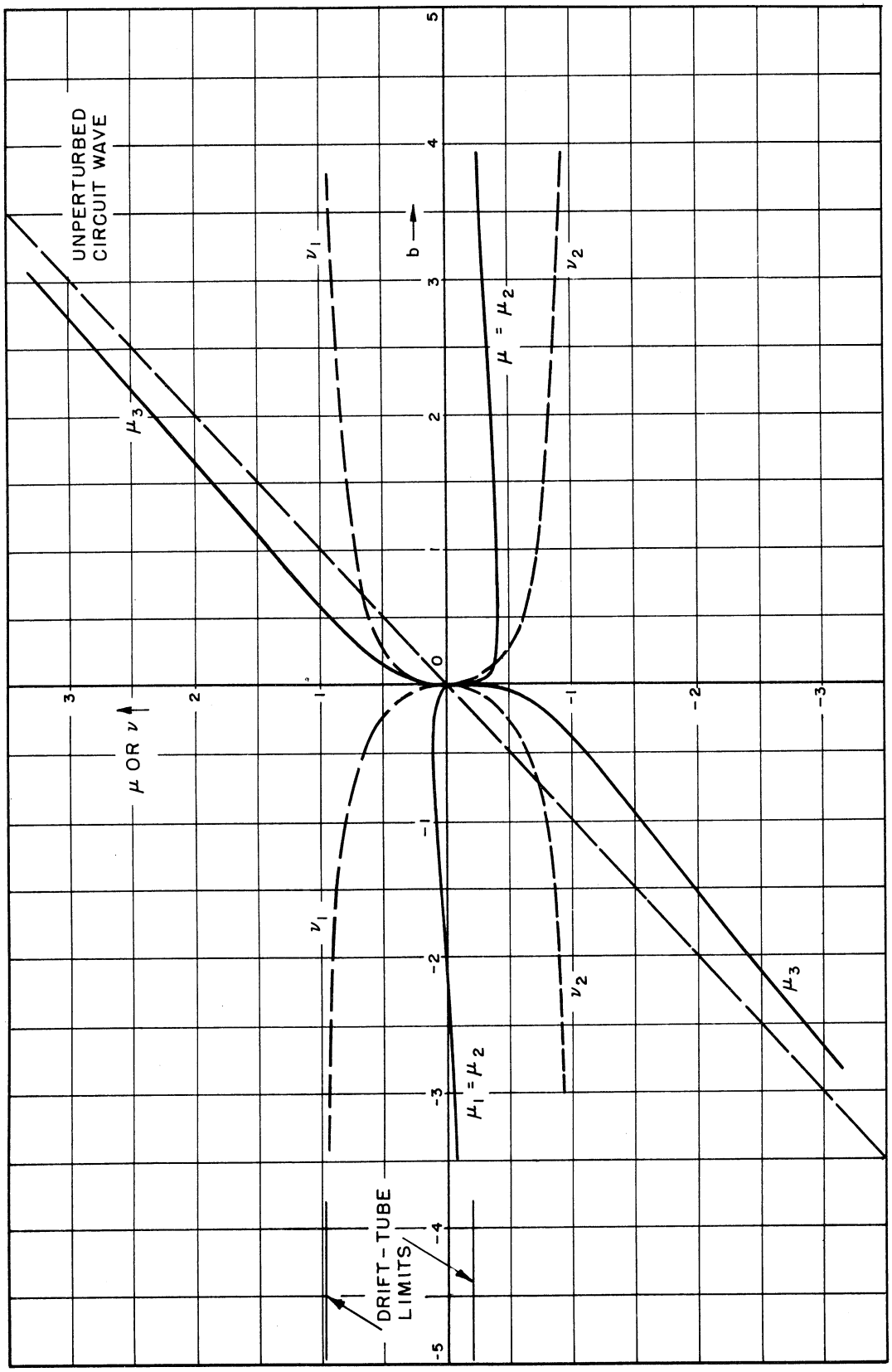

FIG. 9.14 SOLUTIONS OF THE QUASI-SYNCHRONOUS DISPERSION EQUATION: BACKWARD-WAVE INTERACTION; $r^2 = 1.0$, $H = 2/3$. $\Gamma = j\frac{\omega}{u_0}(1 + \mu - j\nu)$.

9.4 Properties of Quasi-synchronous Waves

The physical nature of the interaction can be more readily appreciated if the wave propagation information obtained in the previous sections is used to evaluate the behavior of the stream variables. Moreover, the more complete view of the interaction so obtained enables the analyst to define the limitations of the theory and also to generalize the results obtained under specific conditions. A knowledge of the stream behavior is also needed for handling the boundary-value problem for the longitudinal or z-dimension.

9.4.1 The Electric Potential and the Electric Field Within the Stream

In Sec. 8.8.1 it was shown that the electric potential function is accurately represented by the approximation

$$\phi \approx C \xi \tag{9.31}$$

within the stream for the quasi-synchronous wave whose propagation constant is Γ_n. C as given by Eq. 8.42 is of the order of magnitude ψ/ξ; therefore

$$\phi \text{ is of order } \psi \tag{9.32}$$

Since $\Gamma_n \approx \Gamma_o$, the z-component of electric field of the quasi-synchronous wave, within the stream, is also of the same order as that of the "cold" circuit wave:

$$E_{zn} = \Gamma_n \phi_n V_n \text{ is of order } \Gamma_n \psi V_n \tag{9.33}$$

The approximate y-component of electric field, obtained by differentiation of Eq. 9.31 with respect to y, is

$$E_{yn} = - V_n \frac{d\phi_n}{dy} \approx - V_n C \, j\Gamma_n \tag{9.34}$$

Therefore, the y-component of electric field within the stream for quasi-synchronous waves is of the order

$$E_{yn} \text{ is of order } \frac{\Gamma_n V_n \psi}{\xi_n} \quad . \tag{9.35}$$

Since $|\xi_n|$ is much less than unity, the y-component of electric field within the stream far exceeds the z-component:

$$|E_{yn}| \gg |E_{yn}| \quad . \tag{9.36}$$

The result Eq. 9.36 is somewhat surprising, since it is known that, in the absence of space charge, the two field components are approximately equal in magnitude except in the region near the sole electrode. The extremely high transverse field is indeed the result of the space-charge configuration. It was shown in Sec. 8.8.1 that the bulk space-charge-density perturbation is quite small in comparison with the effective charge produced by the distortion of the stream boundaries. The space-charge configuration which gives rise to the strong electric field in the y-direction may therefore be considered to consist of the surface charges at the upper and lower unperturbed stream boundaries—the Hahn equivalent of the rippled stream boundaries. This configuration is shown in Fig. 9.15; since $|\xi|$ is always small within the stream, the ripple of the two boundaries are always very nearly the same, as Eq. 9.42 shows. Since the stream is thin, practically all of the electric flux emanating from the surface charges of Fig. 9.15 is confined to the interior of the stream. This accounts for the high transverse electric field in the stream.

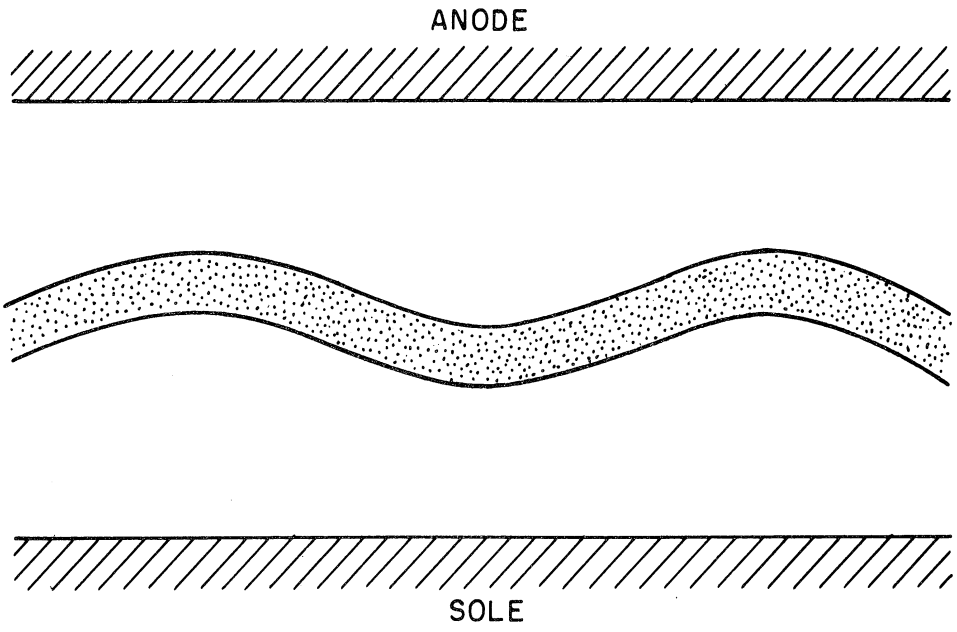

a. ACTUAL CONFIGURATION (EXAGGERATED)

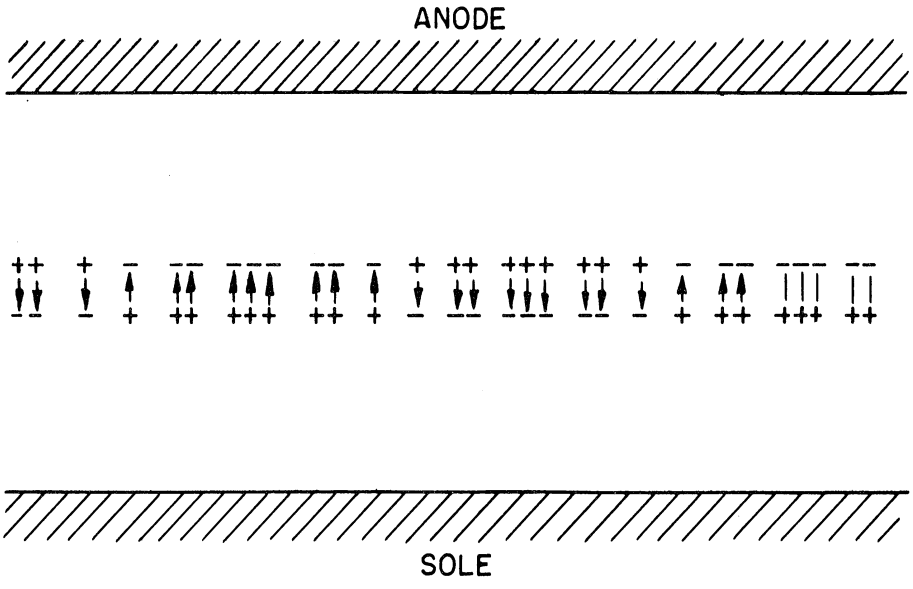

b. HAHN EQUIVALENT SURFACE CHARGES AND THEIR FIELDS.

FIG. 9.15 SPACE-CHARGE FIELD CONFIGURATION OF A QUASI-SYNCHRONOUS WAVE.

9.4.2 Electron Motion

Use of Eq. 9.31 for the potential in Eq. 3.24 for the z-component of electron velocity leads to

$$u_{zn} \approx \frac{-\eta V_n \Gamma_n C_n}{j\omega_c} \approx -\frac{E_{yn}}{B_{d-c}} \quad . \tag{9.37}$$

If Eq. 9.31 were used in a similar way to determine an approximate expression for the y-component of velocity, the result would be zero. A more precise expression for the potential function must be used since the y-component of velocity is a second-order quantity. Using the approximation

$$\phi \approx \left(C\,\xi + \frac{1}{2}\,\xi^3 \right) , \tag{9.38}$$

it is found that

$$u_{yn} \approx \frac{\eta V_n \Gamma_n C_n \xi_n}{\omega_c} \approx \frac{E_{zn}}{B_{d-c}} \quad . \tag{9.39}$$

The two equations above for the velocity components may be combined into the vector equation

$$\vec{u}_n \approx \frac{\vec{E}_n \times \vec{B}_{d-c}}{|B_{d-c}|^2} \quad , \tag{9.40}$$

which states that the electrons have perturbational velocities for quasi-synchronous waves which are normal to both the rf electric field and the d-c magnetic field (both of which appear to be nearly stationary to the electrons). The electrons therefore closely follow the rf equipotential contours; this is a principle which is not restricted to small-signal theory and which has been long recognized in magnetron analysis.

The components of the displacement of the electrons from their unperturbed orbits are calculated from Eqs. 3.28 and 3.29:

$$(\delta z)_n \approx \frac{\eta V_n \Gamma_n C_n}{\omega_c^2 \xi_n} \approx - \frac{E_{yn}}{j\omega_c \xi_n B_{d-c}} , \tag{9.41}$$

$$(\delta y)_n \approx -j \frac{\eta \Gamma_n V_n C_n}{\omega_c^2} \approx \frac{E_{zn}}{j\omega_c \xi_n B_{d-c}} . \tag{9.42}$$

It is noted that the y-component of electron motion (velocity as well as displacement) is much smaller than the z-component for quasi-synchronous waves.

9.4.3 Estimate of the Limit of the Small-Signal Theory for Quasi-synchronous Waves

If the potential of the r-f perturbation at the point in space where the unperturbed electron would be is represented by

$$v(y_o, z_o) \tag{9.43}$$

then the potential of the perturbation at the actual position of the electron is

$$v(y, z) = v(y_o, z_o) + \left.\frac{\partial v}{\partial z}\right|_{y_o, z_o} \delta z + \left.\frac{\partial v}{\partial y}\right|_{y_o, z_o} \delta y . \tag{9.44}$$

In the small signal linearizing process it is assumed that Eq. 9.43 is a sufficiently accurate expression of Eq. 9.44; its simplicity enables the analytic treatment of the linear perturbation theory. In order that this approximation be a valid one, both

$$\left|\frac{1}{v} \frac{\partial v}{\partial z} \delta z\right| \ll 1 \tag{9.45}$$

and

$$\left|\frac{1}{v} \frac{\partial v}{\partial y} \delta y\right| \ll 1 \tag{9.46}$$

must hold true. In the notation pertinent to the nth wave of the perturbations, these inequalities become

$$|\Gamma_n(\delta z)_n| \ll 1 \quad , \tag{9.47}$$

and

$$\left|\frac{1}{\phi_n}\frac{d\phi_n}{dy}(\delta y)_n\right| \ll 1 \quad . \tag{9.48}$$

At this point, the expressions of Sec. 9.4.2 for the displacement components can be used to advantage. Thus, using Eqs. 9.31 and 9.34 for the potential and its transverse derivative, and Eqs. 9.41 and 9.42 for the two components of displacement, assuming also that $|\ell|$ is of the order of unity, it is found that the two inequalities, Eqs. 9.47 and 9.48 yield the identical expression:

$$V\psi \ll \frac{\omega_c B d\text{-}c}{\Gamma^2} D_i^2 \approx 2\left(\frac{\omega_c}{\omega}\right)^2 V_{beam} D_i^2 \quad . \tag{9.49}$$

Thus, the small-signal limitation for quasi-synchronous waves is estimated to be that the rms magnitude of the "circuit potential" at the stream location, $V\psi$, must be much less than the equivalent d-c electron stream potential, V_{beam}, multiplied by a factor which is of the order of D_i^2. Typically, the beam voltage may be several hundreds of volts and the square of the interaction parameter may be of the order of 10^{-4}; thus small signal conditions appear to limit the rf voltage to the millivolt range. The assumption that $|\ell|$ is of the order of unity is not always justified for all of the quasi-synchronous waves, however. Thus, Fig. 9.8 shows that for b = 0, the waves labelled ℓ_1 and ℓ_2 are such that $|\ell| = 1$, but $\ell_3 = 0$.* The value of ξ equals zero within the stream for this third wave; Eq. 9.41 then indicates that the z-component of displacement becomes

*The actual root for b = 0 is not $\ell_3 = 0$, but ℓ_3 = a very small real quantity which can be calculated by taking into account the charges $t_{ripple,1}$ and $t_{\rho,1}$. Cf. the discussion following Eq. 8.55. This does not alter the present argument significantly.

infinite for this wave unless its amplitude is everywhere zero. The infinite peak becomes finite when the circuit losses (attenuation component of the cold circuit propagation constant) are taken into account, but the fact remains that the small-signal limit is quite severe for this wave. The actual small-signal limit for a device can only be determined when the relative excitations of all the waves are determined. For example, it is shown in Chapter XVI that the wave corresponding to ℓ_3 is only weakly excited; the signal levels of the other waves may reach relatively high amplitudes before the third wave becomes appreciably non-linear.

9.4.2 Summary of the Properties of the Field and Stream Quantities of Quasi-synchronous Waves

The approximate dependence on the transverse coordinate for the various field and stream quantities of quasi-synchronous waves is summarized in Table 9.1. The dependence on the z-coordinate and time is expressed by the factor $\exp(j\omega t - \Gamma_n z)$.

TABLE 9.1. THE APPROXIMATE DEPENDENCE ON TRANSVERSE COORDINATE OF FIELD AND STREAM QUANTITIES OF QUASI-SYNCHRONOUS WAVES

Quantity	Functional Dependence on y
ϕ	Linear
E_z	Linear
E_y	Constant
u_z	Constant
u_y	Linear
δz	Inverse of linear
δy	Linear

CHAPTER X

CYCLOTRON WAVES

10.1 Definition of the Term "Cyclotron Wave"

A "cyclotron wave" is one which propagates at such a phase velocity relative to the electron stream that the forces experienced by the particles of the stream vary at approximately the cyclotron frequency. Mathematically, this requires that, in reference to Eq. 3.17,

$$\Omega \equiv j\omega - u_{zo}\Gamma \approx \pm j\,\omega_c \quad , \tag{10.1}$$

which corresponds to the two regions in the neighborhood of the singularities

$$\xi = +1 \tag{10.2}$$

and

$$\xi = -1 \tag{10.3}$$

in the complex ξ-plane as shown in Fig. 4.2.

A construction in the ξ-plane, shown in Fig. 10.1, shows that the wave corresponding to the positive singularity, Eq. 10.2, has a higher phase velocity than the wave of the negative singularity, Eq. 10.3. Since

$$\xi = \frac{\omega}{\omega_c} + j\Gamma y \quad , \tag{10.4}$$

the vector $\vec{\xi}$ consists of two component vectors which correspond to the two terms on the right of Eq. 10.4. It is apparent from the figure that of the two vectors ξ_+ and ξ_-, which represent the two cyclotron waves, the vector ξ_+ has the shorter component $j\vec{\Gamma}y$. Thus,

$$|\Gamma_+| > |\Gamma_-| \quad . \tag{10.5}$$

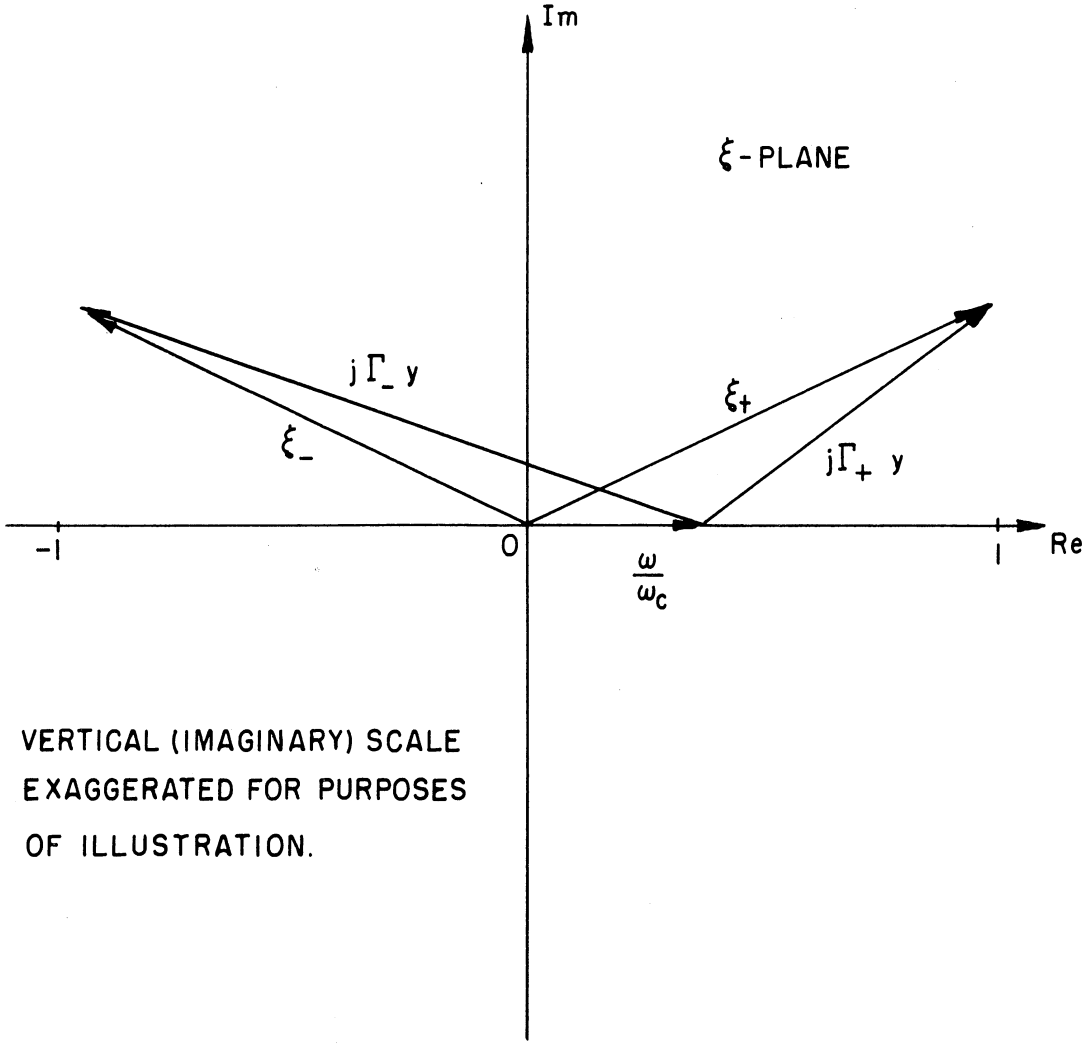

FIG. 10.1 CONSTRUCTION OF THE ξ-PLANE TO SHOW RELATIVE PHASE VELOCITIES OF THE TWO CYCLOTRON WAVES.

Since

$$I_m[\Gamma] = \frac{\omega}{V_{ph}} \quad , \tag{10.6}$$

it follows that the cyclotron wave of the singularity $\xi \approx +1$ has the greater phase velocity. This wave will therefore be called the "faster cyclotron wave" as a convenient means of distinguishing it from the other cyclotron wave, which is accordingly called the "slower cyclotron wave." It should be noted that both waves are considered "slow" waves in the electromagnetic sense of Sec. 3.4.

Expressions for the solutions of the differential equation for the transverse dependence of the potential function for cyclotron waves were obtained in Sec. 4.4. In this chapter, these expressions will be used to determine the dispersion relation for the cyclotron waves. The dispersion will be solved, and the waves thereby specified will be described.

10.2 The Potential Function and Its Transverse Gradient

The following finite series is used to approximate the infinite series representation of Eq. 4.25:

$$\phi = C\left(1 - \chi + \frac{1}{4}\chi^2\right) + D\left[\left(1 - \chi + \frac{1}{4}\chi^2\right) \ln \chi + \frac{1}{2}\chi - \frac{5}{8}\chi^2\right] \tag{10.7}$$

In this form, χ is a variable related to ξ by

$$\xi = 1 - \chi \tag{10.8}$$

for the faster ($\xi \approx +1$) wave; it is related to ξ by

$$\xi = -(1 - \chi) \tag{10.9}$$

for the slower ($\xi \approx -1$) wave. In subsequent analysis both signs will be included for compactness. The upper sign will refer to the faster wave; the lower sign, to the slower wave. Thus, the last two equations are written jointly as

$$\xi = \pm(1 - \chi) \quad . \tag{10.10}$$

The transverse potential gradient within the stream can be expressed in terms of derivatives with respect to y, ξ, or χ as follows:

$$\frac{d\phi}{dy} = j\Gamma\frac{d\phi}{d\xi} = \mp j\Gamma\frac{d\phi}{d\chi} \quad . \tag{10.11}$$

In terms of χ, the transverse potential derivative is

$$\frac{d\phi}{dy} = \mp j\Gamma\left\{C\left(-1+\frac{\chi}{2}\right) + D\left[\left(-1+\frac{\chi}{2}\right)\ln\chi + \frac{1}{\chi} - \frac{1}{2} - \chi\right]\right\} . \tag{10.12}$$

In the charge-free region between the stream and the sole, the potential is, as in Eq. 8.9,

$$\phi = E \sinh j\Gamma(y-y_s) , \qquad y_s \leq y \leq y_a \quad . \tag{10.13}$$

The transverse potential gradient in this region is

$$\frac{d\phi}{dy} = j\Gamma E \cosh j\Gamma(y-y_s) , \qquad y_s \leq y \leq y_a \quad . \tag{10.14}$$

Since there is assumed to be negligible induction of potential on the anode circuit by the stream modulated by the cyclotron waves (cf. Sec. 6.3), the r-f potential on the anode surface is taken to be zero. The potential expression for the charge-free region between the upper edge of the stream and the anode plane is therefore similar to that in the lower (sole) region; it is

$$\phi = P \sinh j\Gamma(y_d-y) \quad , \tag{10.15}$$

where P is a coefficient similar to C, D, and E. The transverse derivative of this potential function is

$$\frac{d\phi}{dy} = -j\Gamma P \cosh j\Gamma(y_d-y) \quad . \tag{10.16}$$

10.3 The Transverse Boundary Problem

The transverse boundary value problem consists in determining the relations between the four coefficients E, C, D, and P. Although the

corresponding smooth-anode case with quasi-synchronous waves could also have been expressed in terms of only four coefficients, the more complicated treatment of Sec. 8.7, which uses five coefficients (A-E), was used to demonstrate the connection with the interaction in the presence of a slow-wave circuit (Chapter IX).

10.3.1 The Transverse Boundary Equations

Requirement of continuity of the potential across the equivalent stream boundaries, $y = y_a$ and $y = y_b$, leads to the following two equations, respectively:

$$E \sinh j\Gamma(y_a - y_s) = C(1 - \chi_a) + D\left[(1 - \chi_a)\ln \chi_a + 2 - \frac{\chi_a}{2}\right] \quad (10.17)$$

and

$$P \sinh j\Gamma(y_d - y_b) = C(1 - \chi_b) + D\left[(1 - \chi_b)\ln \chi_b + 2 - \frac{\chi_b}{2}\right]. \quad (10.18)$$

As to the requirement concerning the discontinuity of the transverse potential gradient, it should be noted that the derivation of Sec. 8.5 applies to the entire range of the variable ξ as far as Eq. 8.19. In terms of the cyclotron wave variable, χ, Eq. 8.19 becomes

$$\left.\frac{d\phi}{dy}\right|_{y_b+} = \mp j\Gamma\left\{\left.\frac{d\phi}{d\chi}\right|_{\chi_b}\left[1 - \frac{1}{(1-\chi)^2}\right] \pm \frac{\phi}{(1-\chi)^3}\right\} \approx \mp j\Gamma\left[\frac{d\phi}{d\chi}(-2\chi) \pm \phi(1+3\chi)\right] . \quad (10.19)$$

On using the expressions of Sec. 10.2 for the potential and its transverse derivative, Eq. 10.19 becomes

$$\mp P \cosh j\Gamma(y_d - y_b) = C + D\left(\ln \chi_b + 2 - \frac{1}{2}\chi_b\right) , \quad (10.20)$$

since $|\chi| \ll 1$ is assumed. The corresponding discontinuity of transverse potential gradient requirement at the lower edge of the stream is

$$\pm E \cosh j\Gamma(y_a - y_s) = C + D\left(\ln \chi_a + 2 - \frac{1}{2}\chi_a\right) . \quad (10.21)$$

The set of four boundary equations, Eqs. 10.17, 10.18, 10.20, and

10.21, is capable of further simplification. Let

$$\theta_a \equiv j\Gamma(y_a - y_s) \tag{10.22}$$

and

$$\theta_b \equiv j\Gamma(y_d - y_b) \ , \tag{10.23}$$

the angles introduced in Eq. 8.33, serve as a short notation for the electrical distance between the stream and the electrode planes. Addition of Eqs. 10.17 and 10.21, with the use of this simple notation, results in

$$\pm E \exp(\pm\theta_a) = C(2-\chi_a) + D[(2-\chi_a)\ln \chi_a + 2] \ ; \tag{10.24}$$

subtraction results in

$$\pm E \exp(\mp\theta_a) = C(\chi_a) + D[(\chi_a \ln \chi_a + 2 - \chi_a] \ . \tag{10.25}$$

Similar operations on Eqs. 10.18 and 10.20 result in the pair of equations

$$\pm P \exp(\mp\theta_b) = C(2-\chi_b) + D[(2-\chi_b)\ln \chi_b + 2] \tag{10.26}$$

and

$$\pm P \exp(\pm\theta_b) = C(\chi_b) + D(\chi_b \ln \chi_b + 2 - \chi_b) \ . \tag{10.27}$$

The four equations, Eqs. 10.24-10.27, constitute the transverse boundary set of equations.

10.4 The Dispersion Equation for Cyclotron Waves and Its Solutions

As was the case in Sec. 8.7, the set of transverse boundary equations, the matrix equation

$$\begin{bmatrix} 2-\chi_a & (2-\chi_a)\ln \chi_a + 2 & \pm \exp(\pm\theta_a) & 0 \\ \chi_a & \chi_a \ln \chi_a + 2 - \chi_a & \pm \exp(\mp\theta_a) & 0 \\ 2-\chi_b & (2-\chi_b)\ln \chi_b + 2 & 0 & \pm \exp(\mp\theta_b) \\ \chi_b & \chi_b \ln \chi_b + 2 - \chi_b & 0 & \pm \exp(\pm\theta_b) \end{bmatrix} \times \begin{bmatrix} C \\ D \\ E \\ P \end{bmatrix} = \begin{bmatrix} 0 \\ 0 \\ 0 \\ 0 \end{bmatrix} \tag{10.28}$$

contains a complete description of the propagating medium—there is no "circuit" to require the introduction of an induction equation. Hence, the transverse boundary equations, Eq. 10.28, is also the dispersion equation: unless all four coefficients C, D, E, and P, are zero, the determinant of the 4-by-4 matrix of Eq. 10.28 must be zero.

The first approximation to the solution of the dispersion equation retains only the largest terms resulting from the expansion of the determinant when $|\chi|$ is much smaller than unity. The result of this operation is

$$\ln \frac{\chi_b}{\chi_a} = - \frac{2 \sinh [\pm(\theta_a+\theta_b]}{\exp [\pm(\theta_b-\theta_a)]} \quad . \tag{10.29}$$

The only streams to be considered for the present are those streams sufficiently thin so that the first approximation, given above, is valid. The present study will be further restricted to the special case

$$\overline{y} = \frac{y_s+y_d}{2} = y_c \ , \quad \text{or} \quad \theta_a = \theta_b \ , \tag{10.30}$$

and

$$y_s = 0 \quad . \tag{10.31}$$

The second condition requires the sole electrode to be at emitter (cathode)/d-c potential. Attention is limited to this particular instance in order to obtain a detailed result yielding a clear picture of this type of interaction. It would appear from Eq. 10.29 that other electrode-to-stream spacings would change the results to some numerical degree, but would not change the nature of the interaction significantly.

Under the restrictions of the above paragraph, the dispersion relation, Eq. 10.29, becomes

$$\ln \frac{\chi_b}{\chi_a} = - 2 \sinh (\pm 2\theta) \ , \tag{10.32}$$

where θ represents the common value of θ_a and θ_b. This value is, moreover, approximately

$$\theta \approx j\Gamma\bar{y} = \pm 1 - \frac{\omega}{\omega_c} , \qquad (10.33)$$

assuming that $|\bar{X}|$ is small enough to be negligible. Obviously, this is not the case when $\omega \approx \omega_c$, and such a situation cannot be considered under such an approximation. However, when $\omega \approx \omega_c$ and $|\xi| \approx 1$, Eq. 10.1 requires that $|\Gamma|$ be quite small. This range of Γ corresponds to fast waves which are excluded from consideration, anyway, in Sec. 3.4 because the electric potential of such fast waves is not accurately derivable from a scalar electric potential.

Another relation between X_a and X_b, in addition to Eq. 10.32, can be obtained from the definitions of ξ, X, and s_u, Eqs. 3.40, 4.16, and 8.35; this relation is

$$X_b = X_a \mp 2 s_u \theta . \qquad (10.34)$$

The solution of Eqs. 10.32 and 10.34, subject to the approximation of Eq. 10.33, is

$$X_a = \frac{2 s_u \left(1 \mp \frac{\omega}{\omega_c}\right)}{1 + \exp\left[-2 \sinh\left(1 \mp \frac{\omega}{\omega_c}\right)\right]} ; \qquad (10.35)$$

the value of X_b can then be gotten from Eq. 10.32. Figure 10.2 shows these faster cyclotron wave solutions for a range of the ratio ω/ω_c; in this figure is also shown the value of X at the midplane of the stream (which in this special case is also the midplane of the interaction space). For the slower cyclotron wave, the exponential term in the denominator of Eq. 10.35 may be neglected; there results

$$X_a = 2 s_u \left(1 + \frac{\omega}{\omega_c}\right) . \qquad (10.36)$$

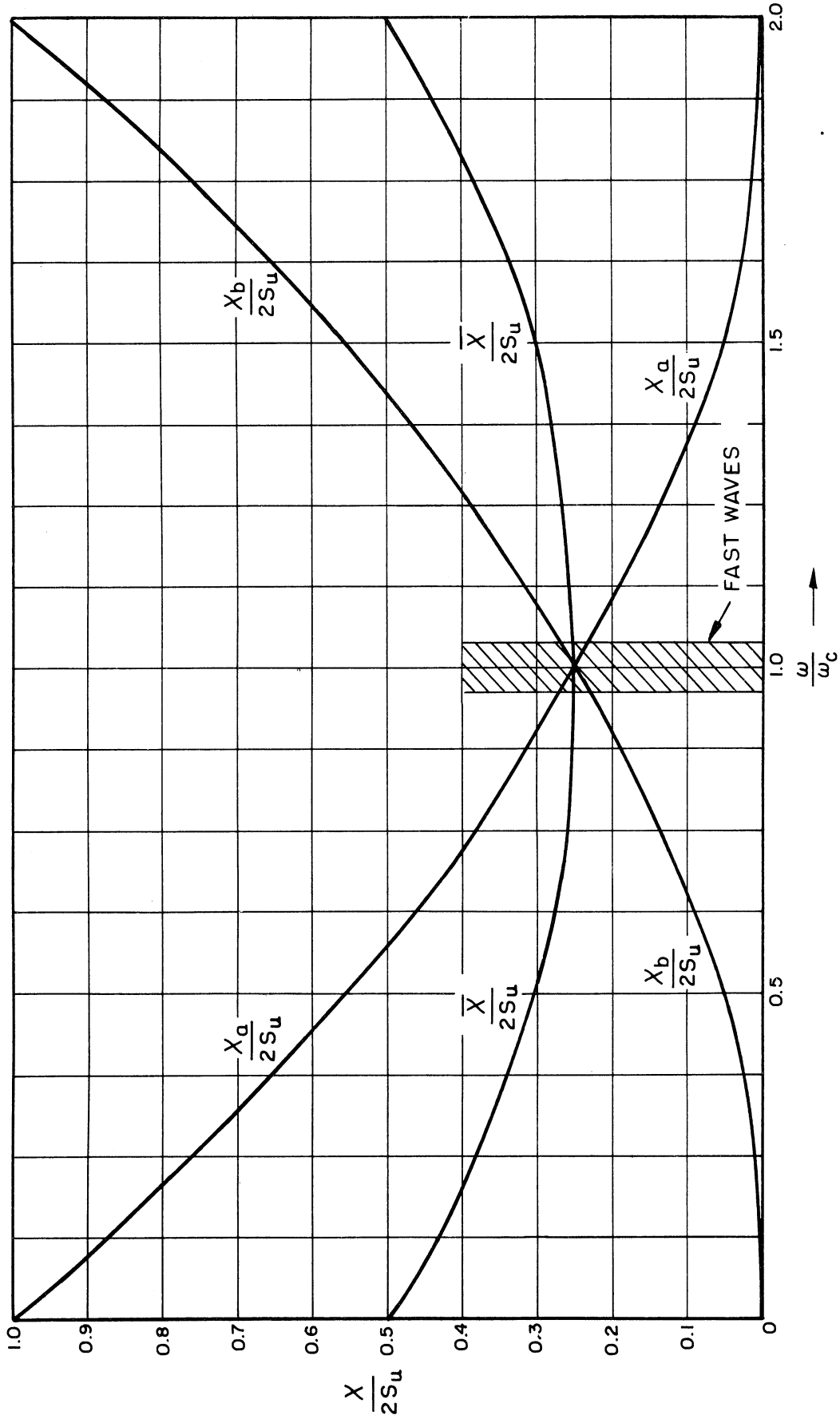

FIG. 10.2 SOLUTIONS OF THE CYCLOTRON DISPERSION EQUATION FOR THE FASTER CYCLOTRON WAVE.

Also, because the hyperbolic sine in Eq. 10.32 is a large quantity for the slower cyclotron wave,

$$\chi_b = \chi_a \exp\left[-2 \sinh\left(1 + \frac{\omega}{\omega_c}\right)\right] \ll \chi_a \quad . \tag{10.37}$$

The values of $\frac{\chi}{2S_u}$ for the slower cyclotron wave may be thought of as the extension of the curves of Fig. 10.2 into the region of negative values of ω/ω_c.

It is apparent in this special case that no part of the stream has a value of χ exactly equal to zero, corresponding to either singularity. One edge of the stream—the higher velocity edge when $\omega/\omega_c < 1$, for example—has a value of χ closer to the singularity than the other edge. Furthermore, there is neither gain nor loss present in either of the cyclotron waves in this case. It would seem that the behavior noted in this paragraph would apply to cases in which the stream-to-sole and stream-to-anode distances were different.

It should be noted that the results given above are limited to certain ranges of the ratio ω/ω_c or, rather, that certain small ranges of this ratio are excluded. One such range is the range near unity, which gives rise to the fast waves which are excluded from the theory. Assuming that

$$\frac{V_{ph}^{\ 2}}{c} = \frac{1}{10} \tag{10.38}$$

represents the limit of reasonable accuracy of the slow-wave treatment, the limits to the range of ω/ω_c can be found from

$$|\Gamma\bar{y}| = \frac{\omega}{V_{ph}} \frac{\omega_c \bar{y}}{\omega_c} = \frac{\omega}{\omega_c} \frac{c}{V_{ph}} \frac{\bar{u}_o}{c} = \sqrt{10}\, \frac{\omega}{\omega_c} \frac{\bar{u}_o}{c} \quad , \tag{10.39}$$

or

$$\frac{1}{1 + \sqrt{10}\, \frac{\bar{u}_o}{c}} < \frac{\omega}{\omega_c} < \frac{1}{1 - \sqrt{10}\, \frac{\bar{u}_o}{c}} \quad . \tag{10.40}$$

The other ranges of the ratio ω/ω_c which must be excluded from the present consideration are those for which the phase velocity of the wave as computed above would be close to the phase velocity of one of the space harmonics of the cold circuit, for large induction effects would then occur. The present theory, it will be recalled, assumed such induction effects to be absent. Of special interest in this regard is the value $\omega/\omega_c = 1/2$; in this case the faster cyclotron wave is such that

$$\Gamma_+ \approx -\Gamma_o \qquad [\omega/\omega_c = 1/2] \quad . \tag{10.41}$$

This wave carries energy in the opposite direction to that of the "interacting space harmonic," Γ_o; relatively large induction effects may be expected. Since appreciable induction takes place only for a small range Γ close to that of a cold circuit space harmonic, the ranges of ω/ω_c which correspond to this condition are very small. Figure 10.3 shows the range of ω/ω_c for which the cyclotron theory is valid in a typical case.

The range of stream thickness, expressed in the parameter s_u, for which the theory is valid, should also be delineated. Equation 10.33 omits the term $\bar{\chi}$; therefore the following limit must be imposed on the magnitude of $\bar{\chi}$:

$$|\bar{\chi}| \ll \left|1 - \frac{\omega}{\omega_c}\right| \qquad \text{[pos. singularity]} \tag{10.42}$$

From Eq. 10.40,

$$\left|1 - \frac{\omega}{\omega_c}\right| > \sqrt{10}\,\frac{\bar{u}_o}{c} \quad . \tag{10.43}$$

Hence, the stream thickness parameter must be such that (see Fig. 10.2)

$$|\bar{\chi}| < \frac{1}{2}\,s_u \ll \sqrt{10}\,\frac{\bar{u}_o}{c} \quad ; \tag{10.44}$$

this does not appear to be a serious restriction.

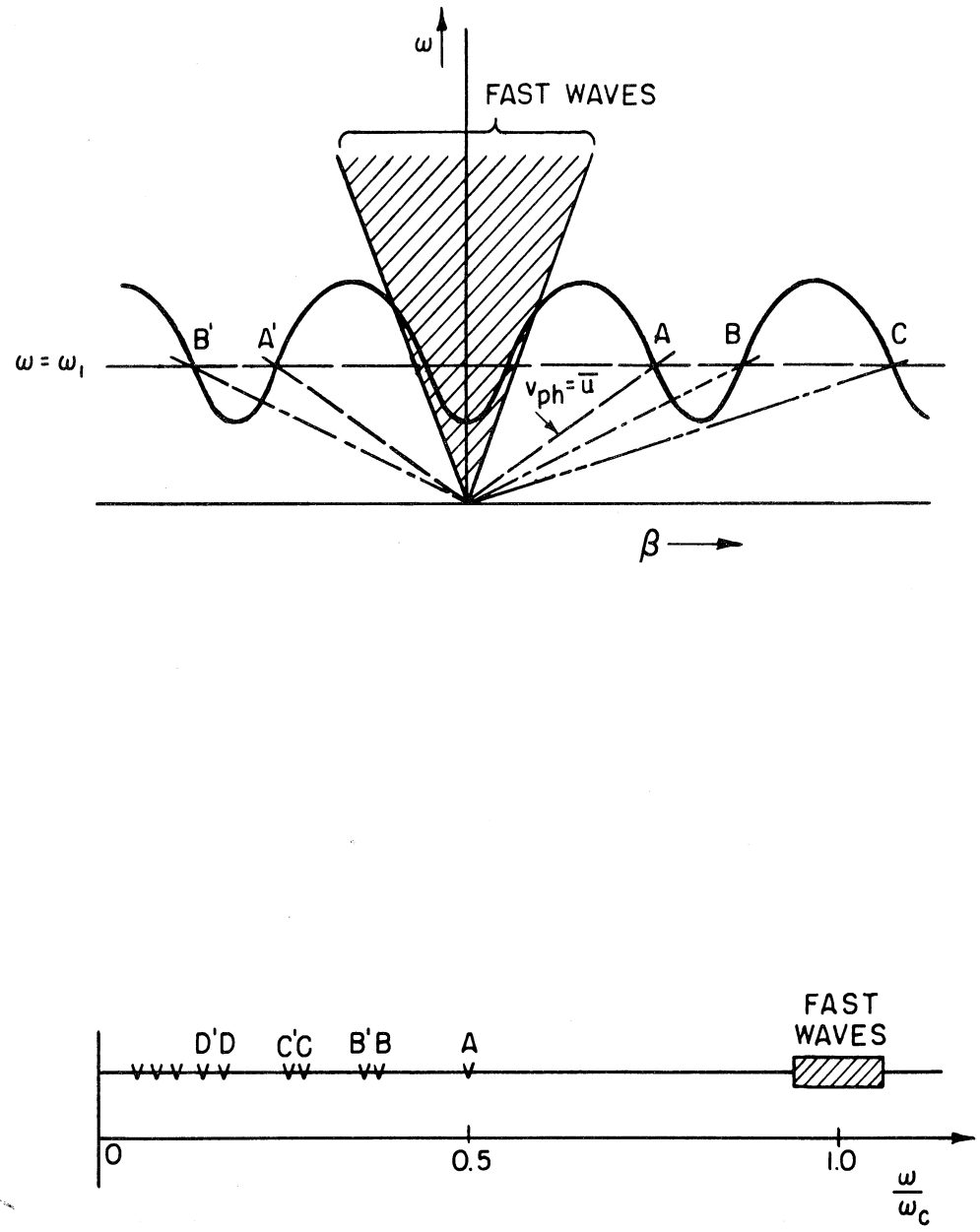

FIG. 10.3 RANGES OF THE RATIO ω/ω_c FOR WHICH THE APPROXIMATE THEORY IS VALID FOR A TYPICAL PERIODICALLY LOADED DELAY LINE.

10.5 The Nature of the Cyclotron Waves

The two wave solutions, one at each singularity, found in the analysis above do in fact justify the expectation of Sec. 4.2.3 regarding "plasma" waves. Moreover, it was found that the waves propagate with neither gain nor loss.

Figure 10.4 shows the phase constants of the two cyclotron waves in relation to the phase constants of the quasi-synchronous waves as the electron stream d-c velocity is varied. The charts of the quasi-synchronous wave solutions, such as Fig. 9.1, occupy a region at the origin of Fig. 10.4 which is so small that the detailed nature of the quasi-synchronous waves is not visible. Although it is apparent that at some electron velocities the cyclotron waves and the circuit waves may couple to each other, this situation is not of present interest. The present analysis is concerned only with electron velocities nearly equal to the cold circuit phase velocity; this condition corresponds to the region close to the vertical axis in Fig. 10.4.

Other properties of the cyclotron waves will become apparent as the stream variables are evaluated.

10.5.1 The Electric Potential Function and Electric Field

Assuming $|X|$ to be small in comparison with unity, the potential, Eq. 10.7, can be written approximately as

$$\phi \approx C + D \ln X \quad . \tag{10.45}$$

This means that the difference in potential between any two y-coordinates in the stream is

$$\phi(y_2) - \phi(y_1) \approx D \ln \frac{X_2}{X_1} \quad , \tag{10.46}$$

involving only one of the constants—D, but not C. The potential func-

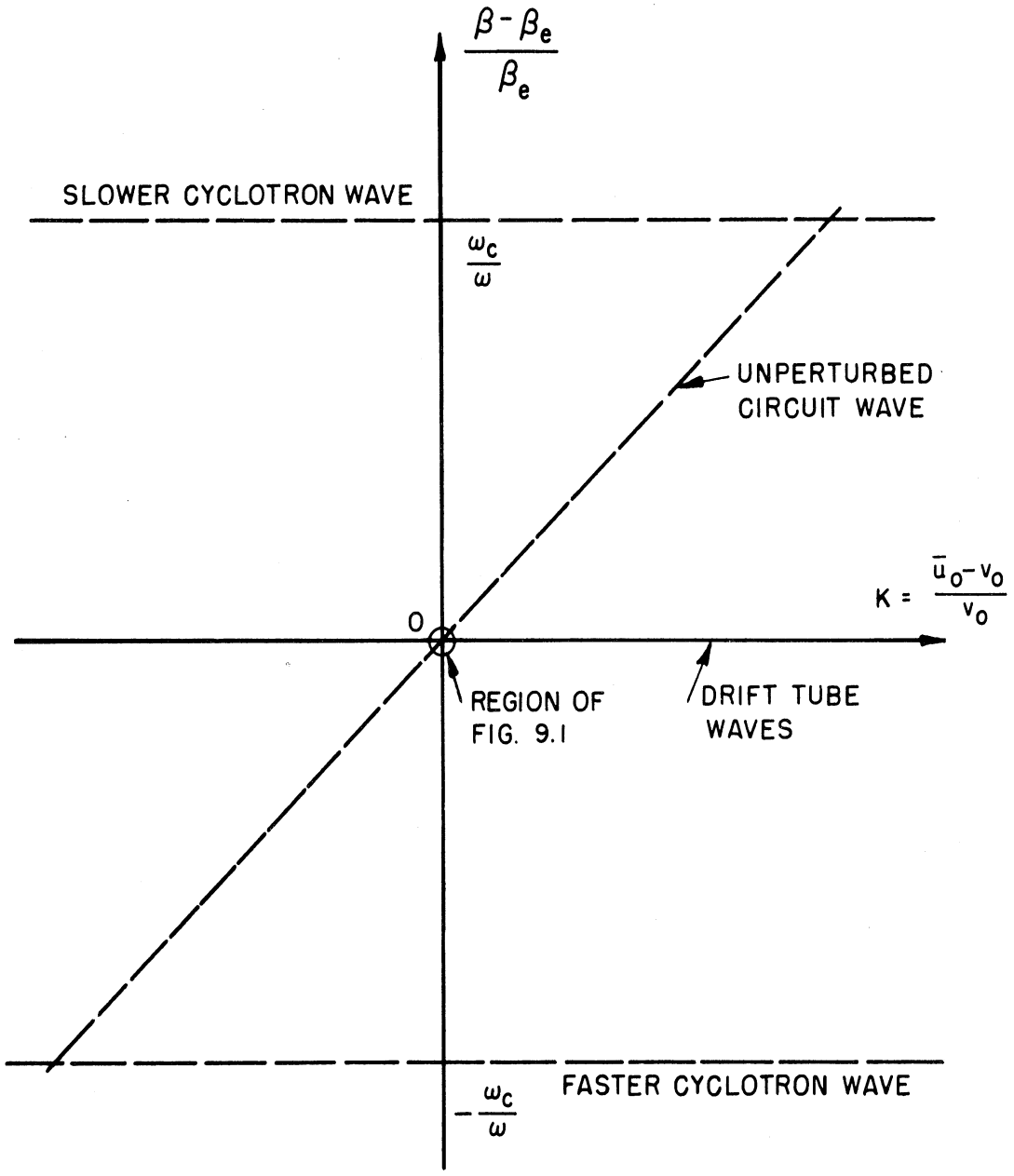

FIG. 10.4 CHART OF WAVE SOLUTIONS SHOWING QUASI-SYNCHRONOUS WAVES IN RELATION TO THE CYCLOTRON WAVES.

tion can therefore be represented graphically, as in Fig. 10.5, without first requiring the evaluation of the relative magnitudes of C and D. It is seen that the potential at the edge of the stream nearest the "singularity plane," i.e., the plane outside the stream where X is zero, is smaller than the potential at the other edge. In Fig. 10.5, this edge of lower potential is the upper edge, $y = y_b$.

The z-component of electric field is

$$E_z = \Gamma V\phi \quad ; \tag{10.47}$$

it is therefore proportional to the potential function. The y-component of electric field of the cyclotron wave is approximately

$$-E_y = V\frac{d\phi}{dy} \approx V\left(-C + \frac{D}{X}\right) \quad ; \tag{10.48}$$

the transverse variation of the y-field is shown in Fig. 10.6.

It will be noted that the electric fields outside the upper edge of the stream—the edge nearest the singularity plane—are quite small. This result should be compared with the plasma wave propagation in ion-neutralized beams such as used in klystrons or traveling-wave tubes. In this latter case, there is no field at all outside the stream; the departure from this condition in the present analysis may be attributed to the complex nature of the crossed-field dynamics of the electrons and also to the velocity gradient in the d-c electron stream.

10.5.2 The Longitudinal Components of Motion

The z-components of velocity and displacement of the electrons from their unperturbed coordinates, calculated from Eqs. 3.24 and 3.28, respectively, are

$$u_z = \frac{-\eta\Gamma V\phi}{\pm j\omega_c} = \pm\frac{j\Gamma V\phi}{B_{d\text{-}c}} = \pm\frac{j\Gamma\eta V}{\omega_c}(C + D\ln X) \quad , \tag{10.49}$$

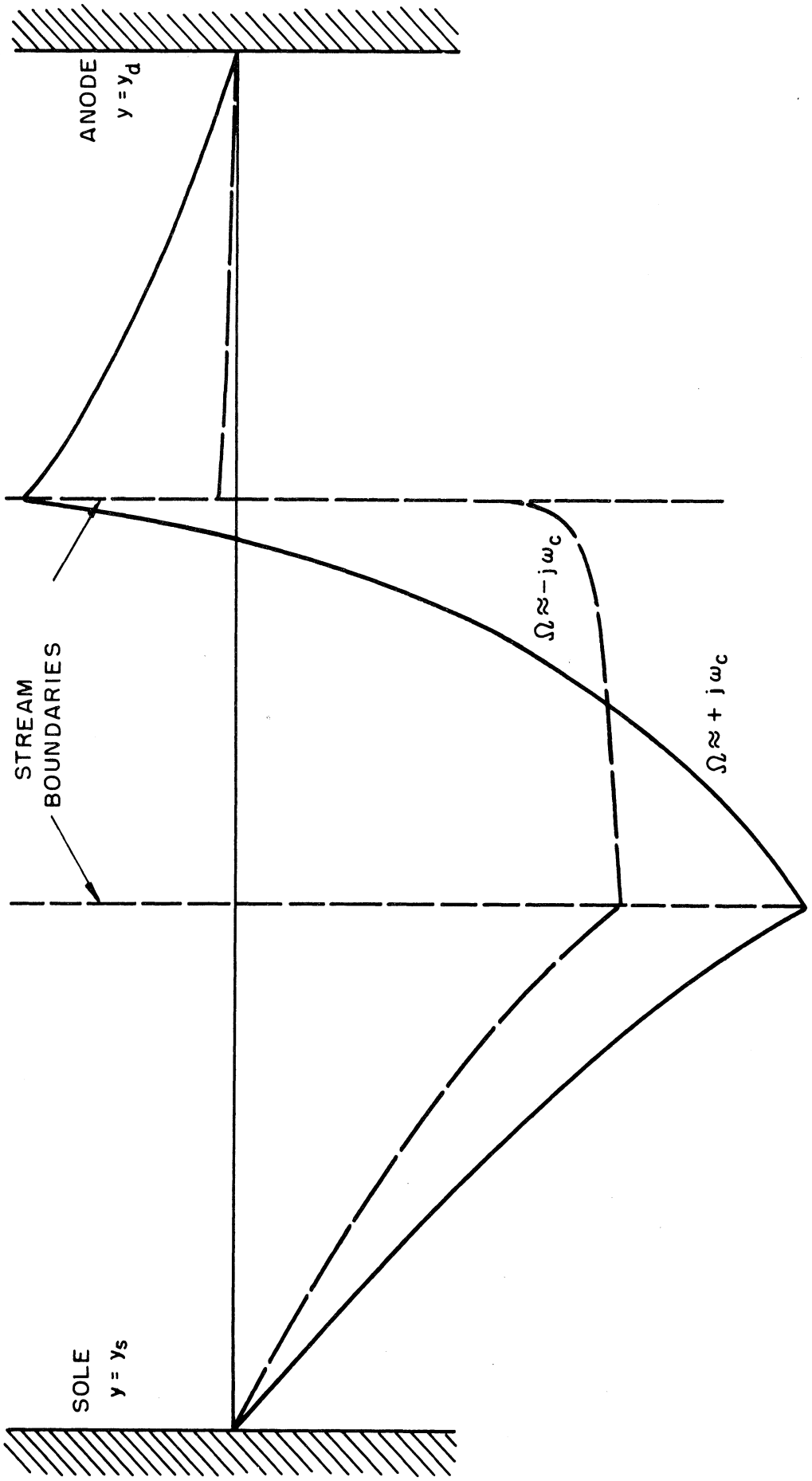

FIG. 10.5 POTENTIAL PROFILES OF CYCLOTRON WAVES, $\omega/\omega_c = 1/2$. (STREAM THICKNESS GREATLY EXAGGERATED.)

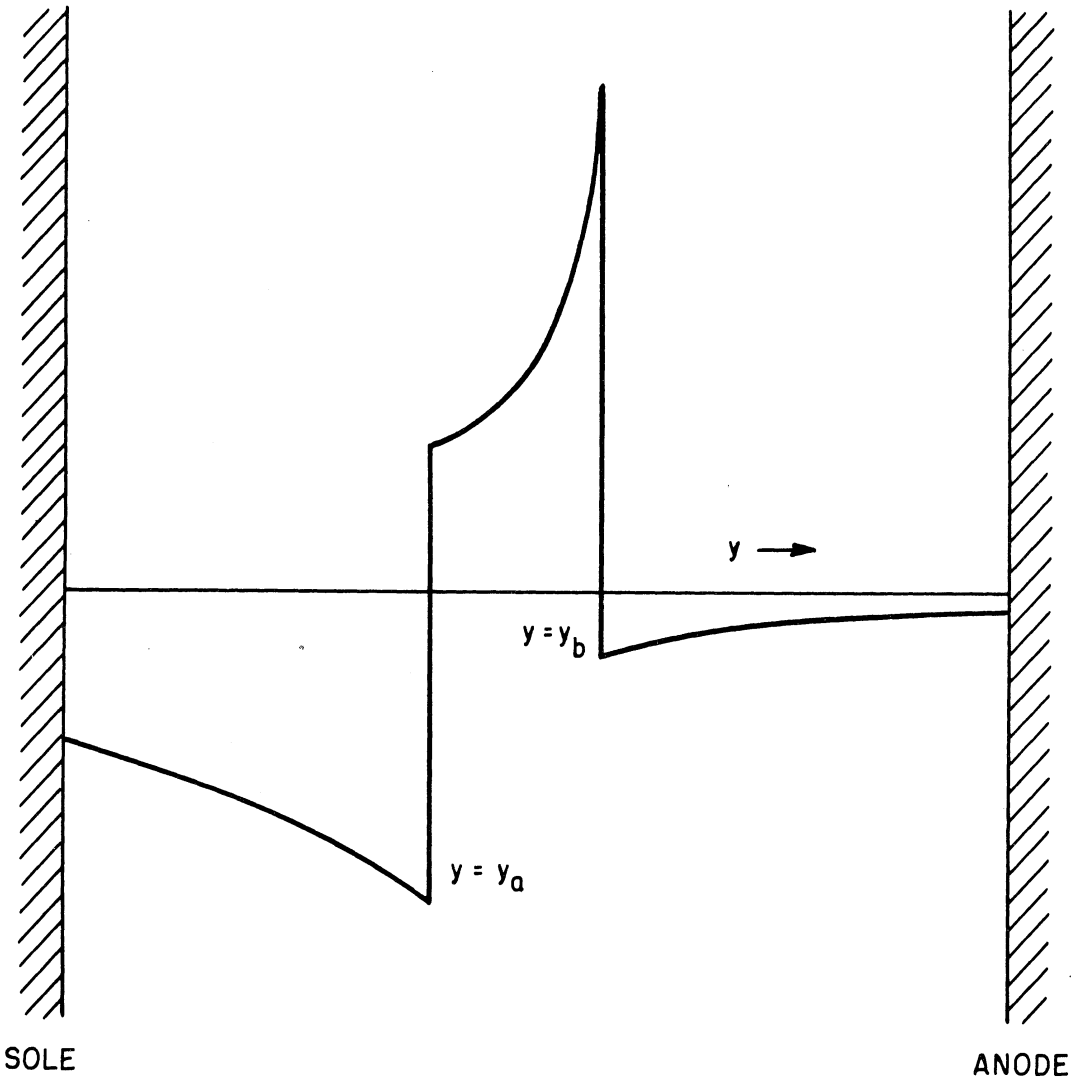

FIG. 10.6 VARIATION OF THE TRANSVERSE ELECTRIC FIELD OF A CYCLOTRON WAVE.

and

$$\delta z = \frac{\eta\Gamma V\phi}{c^2} = \frac{\eta\Gamma V}{c^2}(C + D \ln X) \quad , \tag{10.50}$$

in which the approximate expression, Eq. 10.47, is used for the potential. The approximation $\Omega \approx \pm j\omega_c$ is also used, in which it is seen that the complication of synchronism (large relative change of Ω across the beam cross section) does not appear. The two longitudinal components of motion, therefore, are proportional to the potential function; they thus have the same transverse variation as shown in Fig. 10.5. It is noted that there exists a plane in the stream at which there is no z-component of motion.

10.5.3 The Transverse Components of Motion

The use of the approximation $\Omega \approx \pm j\omega_c$, and Eqs. 10.47 and 10.48 in Eqs. 3.25 and 3.27 for the y-components of electron motion leads to

$$u_y = \frac{-\eta V\Gamma}{\omega_c}\left(\phi + \frac{d\phi}{dX}\right) = \frac{-V\Gamma}{B_{d\text{-}c}}\left(\phi + \frac{d\phi}{dX}\right) = \frac{-\eta\Gamma VD}{\omega_c}\left(\frac{1}{X} + \ln X\right) \quad . \tag{10.51}$$

and

$$y = \pm \frac{j\eta V\Gamma D}{\omega_c^2}\left(\frac{1}{X} + \ln X\right) \quad . \tag{10.52}$$

Both the velocity and the displacement have the same transverse variation, which is substantially the same as shown in Fig. 10.6. It is notes that the y-components of motion have simple poles at the singularity plane $X = 0$. Thus, the y-directed motion of the stream is the dominant motion; the reverse was found to hold for quasi-synchronous waves.

10.5.4 The Space-Charge Density

Again using the approximation, Eq. 10.47, evaluation of the space-charge density through Poisson's Law yields

$$\rho \approx - \frac{\epsilon_o V \Gamma^2 D}{\chi^2} \quad . \tag{10.53}$$

The space-charge density thus has a double pole at the singularity plane; it is therefore an important quantity for cyclotron wave propagation. The comparison with the ion-neutralized klystron beam is again suggested, for in that case also, the plasma waves are characterized by strong space-charge density modulation with little electronic motion. It is also noted that the cyclotron waves differ greatly from the quasi-synchronous waves, which have virtually no density modulation.

10.5.5 Summary of the Properties of the Field and Stream Quantities of Cyclotron Waves

The transverse variations of the fields and stream variables of cyclotron waves are summarized in Table 10.1. Only the dominating factors in the dependence on the y-coordinate are listed.

TABLE 10.1. THE APPROXIMATE DEPENDENCE ON TRANSVERSE COORDINATE OF FIELD AND STREAM QUANTITIES OF CYCLOTRON WAVES

Quantity	Approximate Functional Dependence on y
ϕ	Logarithmic
E_z	Logarithmic
E_y	Inverse of linear
u_z	Logarithmic
u_y	Inverse of linear
δz	Logarithmic
δy	Inverse of linear
ρ	Inverse square of linear

CHAPTER XI

NON-INTERACTING ELECTROMAGNETIC WAVES

11.1 General Description of Non-interacting Electromagnetic Waves

The class of "non-interacting electromagnetic waves" includes those waves for which neither quasi-synchronous nor cyclotron conditions hold. Such waves are expected to exist because of the properties of the cold circuit discussed below. The electron stream interaction with the fields of these waves is considered to be negligible in the present analysis. With this qualification, the waves are described as "non-interacting waves." The properties of such waves in the presence of the electron stream are therefore presumed to be determined by considerations other than the electron interaction with them. Although there is little interaction of interest with such waves, an accounting of them is required for the proper solution of the longitudinal boundary value problem.

11.2 Non-interacting Space Harmonics Accompanying the Quasi-synchronous Waves

In Chapter VI it was shown that when energy is transmitted in a given direction along a periodic structure, an infinite set of space harmonic waves is present in the interaction space. The one space harmonic of this set, called the "interaction space harmonic", has been carefully considered in Chapters VIII and IX, since the effect of this wave on the stream is considerable. Although the electron interaction with the other space harmonics is negligible, it is noted from the fixed geometric relation between the amplitudes of the space harmonics (Eq. 6.9) for the cold circuit, that these non-interacting space harmonics will be present everywhere on the

"hot" circuit in approximately the same amplitudes relative to the interaction harmonic. Thus, if there is a change in the amplitude of the interacting space harmonic with the stream present (gain, for instance), there must be corresponding change (gain) in the amplitudes of the non-interacting space harmonics in order that the relative strengths of the harmonic fields may be preserved. This means that although the electron stream does not influence the propagation constants of the non-interacting space harmonics by direct interaction with them, it does have an influence on them because of the effect on the interacting harmonic.

11.3 Other Non-interacting Space Harmonics

When energy is propagated on a structure with a group velocity directed opposite to that of the interaction space harmonic discussed above, the entire set of space harmonics associated with this reverse energy flow is a set of non-interaction harmonics. These non-interacting space harmonics include the harmonic which has a phase velocity which is the negative of that of the interaction harmonic. They are different from the harmonics of Sec. 11.2 in that their amplitudes are not related to the amplitude of any interacting harmonic; the reverse energy propagation is therefore unaffected by the electron stream. In devices in which both ends of the interactions space are well terminated, such reverse energy propagating is not excited appreciably. In the theory, therefore, such waves as described in this section are assumed to be nonexistent.

11.4 Cut-off, or "Evanescent" Modes

In Sec. 6.2 it was assumed that only one of the modes of the transmission structure is a propagating one. The other modes are therefore cut-off modes; energy associated with them does not propagate. These modes may produce local electric fields near discontinuities, however.

Hence, these cut-off modes may be required for the solution of longitudinal boundary value problems, just as they are required in the theory of waveguide discontinuities. In the present analysis it is assumed that, since the effect of the fields of these modes on the electron stream is negligible, then the electron stream does not perturb such fields appreciably. Thus, it is concluded that the cut-off mode fields at longitudinal discontinuities are essentially the same in the presence of the stream as on the cold circuit.

CHAPTER XII

"TRIVIAL" SOLUTIONS OF THE DISPERSION EQUATIONS— A "PHANTOM" SOLUTION

12.1 Trivial Solution of the Quasi-synchronous Dispersion Equation

In Chapter VIII a set of transverse boundary equations was derived which, in the case where the anode r-f potential is zero, is also equivalent to a dispersion equation. This set of equations, Eq. 8.22, in matrix form, is

$$[M] \times \begin{bmatrix} A \\ B \\ C \\ D \\ E \end{bmatrix} = \begin{bmatrix} 0 \\ 0 \\ 0 \\ 0 \\ 0 \end{bmatrix} \qquad (12.1)$$

The dispersion relation between Γ and ω was obtained by requiring that not all of the coefficients A-E be zero. If all coefficients are zero, then Eq. 12.1 is satisfied with any matrix [M] or, equivalently, with any value of Γ. This latter condition, the mathematically "trivial" solution, was mentioned briefly in Sec. 8.7.

The trivial nature of such a solution is readily seen by noting that when all coefficients vanish, the r-f potential, expressed by Eqs. 8.6, 8.9, and 8.10, is everywhere zero. Thus, there can be no electric field. Furthermore, by virtue of Poisson's Law, there can be no space-charge density in the region, either. Finally, Eqs. 3.24 and 3.25 show that, since the fields are zero, there can be no velocity perturbation of the

stream. However,—and this is the significance of the mathematically "trivial" solution—the displacement calculations in Eqs. 9.41 and 9.42 yield indeterminate results if ξ is zero. If it is assumed that C and D are infinitesimals of the same order as ξ, then the displacement components may be finite and may be arbitrary.

More specifically, if $y = y_1$ is some plane in the stream, then the requirement that $\xi = 0$ at this level can be expressed as

$$\Gamma = j\frac{\omega}{u_{zo}(y = y_1)} = j\frac{\omega}{\omega_c y_1}, \tag{12.2}$$

thus determining the propagation constant of the wave for the mathematically trivial solution. When Eq. 8.10 is used for the potential function in Eqs. 3.28 and 3.29, the displacement components under these conditions are found to be

$$\delta z = \frac{-\eta V\Gamma C}{j\omega_c \xi} = \begin{cases} \text{arbitrary}, & y = y_1 \\ 0, & y \neq y_1 \end{cases} \tag{12.3}$$

and

$$\delta y = \frac{j\eta V\Gamma D}{j\omega_c \xi} = \frac{\eta V\Gamma D}{\omega_c \xi} = \begin{cases} \text{arbitrary}, & y = y_1 \\ 0, & y \neq y_1 \end{cases}. \tag{12.4}$$

The trivial solution thus has a meaning only at a single plane in the stream; it is finite at this plane and zero everywhere else.

12.2 An Interpretation of the "Trivial" Quasi-synchronous Solution

An important property of the trivial solution found above can be seen in the calculation of the displacement of an individual electron from its unperturbed position. Using the small-signal approximation

$$z = u_{zo}(t - t_o), \tag{12.5}$$

where t_o is a constant for any one electron, it is found that the electron displacement is simply

$$\delta z = \mathrm{Re}[\sqrt{2}\,\delta z(y = y_1)\exp(j\omega t_o)] \,. \qquad (12.6)$$

The displacement is thus constant for any electron. This fact suggests that the trivial solution is equivalent to an integration constant, as described below.

Consider an electron entering, at time $t = t_o$, into an interaction region, $z \geq 0$, in which only one nontrivial wave is present. Suppose further that small-signal conditions hold. Then the electron displacement from its unperturbed position (z-component) is the integral

$$\delta z = \mathrm{Re}\sqrt{2}\int_{t=t_o}^{t=t} (u_z)_n \exp(j\omega t - \Gamma_n z)dt \,. \qquad (12.7)$$

Assuming that Ω_n is not zero, the integration leads to

$$\delta z = \mathrm{Re}\sqrt{2}\int_{t_o}^{t} (u_z)_n \exp(\Omega_n t)dt = \mathrm{Re}\sqrt{2}\frac{u_{zn}}{\Omega_n}[\exp \Omega_n t]_{t_o}^{t}, \qquad (12.8)$$

or

$$\delta z = \mathrm{Re}\sqrt{2}\left[\frac{u_{zn}}{\Omega_n}\exp \Omega_n t - \frac{u_{zn}}{\Omega_n}\exp \Omega_n t_o\right] \qquad (12.9)$$

Again using the small signal Eq. 12.5,

$$\delta z = \mathrm{Re}\sqrt{2}\frac{u_{zn}}{\Omega_n}\exp(j\omega t - \Gamma_n z) - \mathrm{Re}\sqrt{2}\frac{u_{zn}}{\Omega_n}\exp(j\omega t - j\frac{\omega}{u_o}z). \qquad (12.10)$$

Clearly, the first term is a wave having the same propagation constant as the nontrivial wave; it is the result obtained in Eq. 3.28. The second term of Eq. 12.10, however, represents the mathematically trivial solution; it arises from the lower limit of the integration and is therefore a constant of integration for an individual electron. The amplitude of the second term is in this case determined from the entrance (longitudinal) boundary requirement that the integral of Eq. 12.7 must be a continuous function of its upper limit (time). A similar situation

prevails when more than one nontrivial wave is present.

Another important property of the trivial solution is found when it is noted that there are no r-f electric fields or electron velocities associated with the wave, nor is there any r-f space-charge density present. The stream is therefore indistinguishable from the d-c Brillouin stream (except for possible ripple of one of its surfaces, in case the level y_1 coincides with one of the surfaces). Thus, although the positions of individual electrons are perturbed in this solution, there is still no observable perturbation of the stream as a whole.

12.3 The Ensemble of Synchronous Trivial Solutions—The "Phantom" Solution

It is difficult to deal with the individual solutions obtained in the above sections—partly because there is an infinite set of them, and partly because the singular nature of the transverse variations are difficult to reconcile with the small-signal limitations of the type expressed by Eq. 9.48.

Since the stratum $y = y_1$ in Eq. 12.2 can be any level in the stream, the totality of trivial solutions is equivalent to a single wave having a propagation "constant" which is a function of the transverse coordinate, viz.,

$$\Gamma = j\frac{\omega}{V_{\rho n}} = j\frac{\omega}{u_o} = j\frac{\omega}{\omega_c y}, \qquad (12.11)$$

such that all parts of the d-c stream are in exact synchronism with this wave. This wave is therefore called an "omni-synchronous" wave. The components of electron displacement are continuous functions of y generated by the Eqs. 12.3 and 12.4 when y_1 is allowed to vary continuously through the stream.

Some important restrictions must be placed on the nature of the

amplitudes δy and δz, however, in order to make the ensemble, or "omni-synchronous" wave, a self-consistent solution of the transverse boundary value problem. In order that there be no r-f electric fields within the stream, Poisson's Law shows that it is necessary that the r-f space-charge density be everywhere zero within the stream. This requirement can be stated as

$$\nabla \cdot \delta\vec{r} = 0 \tag{12.12}$$

or

$$\frac{\partial \delta y}{\delta y} + \frac{\partial \delta z}{\delta z} = 0 . \tag{12.13}$$

Thus, the displacement components, δy and δz, are not both arbitrary, as was the case with the individual trivial solutions of Sec. 12.1.

Furthermore, there must be no electric field external to the stream, otherwise charge would be induced in the anode and a "circuit" field would result. The circuit field would then be different from zero inside the stream. In order that there be no electric field outside the stream, there must be no ripple of the stream boundaries. This requirement may be stated as

$$\delta y = 0, \; y = y_a \text{ and } y = y_b , \tag{12.14}$$

and

$$\left| \frac{\partial \delta y}{\partial y} \right| < 1 . \tag{12.15}$$

The latter requirement assures that electron trajectories do not cross over from the interior of the stream to the exterior; it is assumed to be valid for all waves in this theory.

The omni-synchronous wave, with the restrictions imposed above, does not perturb the appearance of the stream. The only difference between

the ensemble of trivial solutions and the d-c Brillouin stream lies in the way in which the individual parts of the stream (electrons) are identified. In the omni-synchronous wave, the electrons are considered to be displaced from their "unperturbed" positions even though the entire stream appears otherwise unperturbed.

The principal value of the omni-synchronous wave is in the solution of the longitudinal boundary value problem, which is treated in Chapter XIII. Obviously, such a wave is needed to assure the continuity of the velocity integral, as exemplified by Eq. 12.7.

PART V

THE LONGITUDINAL BOUNDARY-VALUE PROBLEM

CHAPTER XIII

THE LONGITUDINAL BOUNDARY-VALUE PROBLEM

13.1 General Discussion of the Longitudinal Boundary-Value Problem

As defined in Chapter V, the longitudinal boundary-value problem is concerned with the relations which are satisfied by the variables of the interaction system at those planes, z = constant, which define the interface between the interaction space and some other region. Such another region might be the region "upstream" from the interaction region where the d-c Brillouin stream is formed, i.e., the "gun" region. Another such region might be the region in which the stream is intercepted by a collector electrode. Alternatively, the interface of interest might be that between two interaction regions having different characteristics.

In this dissertation, attention is directed toward the solution of the longitudinal boundary-value problem arising from the entry of the stream into the interaction region, since this problem is common to all microwave beam devices. It will be assumed that the exit conditions at the "downstream" end of the interaction space are so arranged that no backward-traveling waves in the sense of Sec. 11.3 are excited. This calls for the prevention of the "reflection" of either electromagnetic energy or the re-entry of electrons (such as by the mechanism of secondary emission) into the interaction space.

Attention will be further confined to those entering streams which may be considered to be unmodulated, i.e., those which are completely unperturbed until acted on by the forces of the fields in the interaction region. The restricted boundary-value problem thus defined is termed the

unmodulated input problem.

13.2 The Longitudinal Boundary Relations

The physical quantities which must be considered at the longitudinal boundaries may be conveniently classified as electromagnetic or kinetic variables.

13.2.1 Kinetic Variables

As noted in Sec. 3.5, the motion of the electron stream is completely described by the velocity and displacement components. The longitudinal boundary requirements concerning the electron motion are that both velocity and position (displacement) must be continuous functions of time for an individual electron, or small portion of the electron fluid. These requirements, of course, follow from the Newtonian mechanics. Expressed in perturbational terms, they become requirements that, for example,

$$\tilde{u}_z\ (z = z_{1-}) = \mathrm{Re} \sum_{n'} \sqrt{2}\, u_{zn'} \exp(j\omega t - \Gamma_{n'} z_1)$$

$$= \tilde{u}_z\ (z = z_{1+}) = \mathrm{Re} \sum_{n} \sqrt{2}\, u_{zn} \exp(j\omega t - \Gamma_n z_1)\ , \qquad (13.1)$$

where the planes $z = z_{1-}$ and $z = z_{1+}$ refer to the left and right sides of the plane $z = z_1$, where the quantities $u_{zn'}$ refer to the waves in the region on the left of the interface and where the quantities u_{zn} refer to the interaction region on the right of the interface. Equation 13.1 is specialized to the case of an unmodulated entering stream, placing the origin of the z-axis at the entry plane. There results

$$0 = \sum_{n} u_{zn}\ , \qquad (13.2)$$

in which the complex variable notation and the time variation are implied. It should be noted that the indicated summation must be taken over a complete set of waves capable of existing on the interaction system. The input relations for the other components of motion are found in a similar way; they are

$$0 = \sum_n u_{yn} , \tag{13.3}$$

$$0 = \sum_n (\delta z)_n , \tag{13.4}$$

and

$$0 = \sum_n (\delta y)_n , \tag{13.5}$$

The quantities entering these equations are complex rms magnitudes. These equations are therefore complex vector (phasor) equations which determine both the wave amplitudes and phases.

13.2.2 Electromagnetic Variables

The longitudinal boundary-value problem must also be considered from the standpoint of electromagnetic field theory. Thus, the electric field must be continuous everywhere except at the metallic or dielectric surfaces involved. This requirement can be expressed at the plane $z = z_1$ for the two cartesian components of electric field in the following perturbational form:

$$E_z\ (z = z_{1-}) = \mathrm{Re} \sum_{n'} \sqrt{2}\, \Gamma_{n'} V_{n'} \phi_{n'} \exp(j\omega t - \Gamma_{n'} z_1)$$

$$= E_z\ (z = z_{1+}) = \mathrm{Re} \sum_n \sqrt{2}\, \Gamma_n V_n \phi_n \exp(j\omega t - \Gamma_n z_1) \tag{13.6}$$

or

$$\sum_{n'} \Gamma_{n'} V_{n'} \phi_{n'} = \sum_n \Gamma_n V_n \phi_n ,$$

and
$$\sum_{n'} V_{n'} \frac{d\phi_{n'}}{dy} = \sum_{n} V_n \frac{d\phi_n}{dy} \quad . \tag{13.7}$$

Since the convection current density, $\rho\vec{u}$, must also be continuous, and since the linear perturbational form of the convection current density is

$$k_n = (\rho\vec{u})_n = \rho_o \vec{u}_n + \rho_n \vec{u}_{zo} =$$

$$= (\rho_o u_{zn} + \rho_n u_{zo})\hat{z} + \rho_o u_{yn} \hat{y} \quad , \tag{13.8}$$

it follows that the unmodulated-input requirement of continuity of convection current density can be stated as

$$0 = \rho_o \sum_{n} u_{zn} + u_{zo} \sum_{n} \rho_n \tag{13.9}$$

$$0 = \rho_o \sum_{n} u_{yn} \quad . \tag{13.10}$$

However, since it is required kinematically that the velocity perturbation be zero (Eqs. 13.2 and 13.3),

$$0 = \sum_{n} \rho_n \quad . \tag{13.11}$$

This is, effectively, a requirement that the space-charge density vary continuously within the stream. Discontinuities in space-charge density occur only at stream boundaries such as at emitters, collectors and boundaries between the stream and free space. Since convection current may be also considered to be a kinematic variable, and two kinematic quantities determine the stream, the above discussion concerning convection current and space-charge density must be regarded as superfluous—the electron velocity and displacement have already been considered.

Since there is no r-f space-charge density in the stream at the entry plane (and indeed for some distance farther into the interaction space), the stream has no effect on the electromagnetic input boundary-value problem. Thus, the input electromagnetic fields with the stream present are identical to the fields which form the solution to the electromagnetic problem in the absence of the stream. This field is illustrated in Fig. 13.1, which purports to show the r-f nature of a typical delay-line input region. This field, at the plane $z = 0$, is denoted by $E_{in}(y)$, with the result that the input field equations, Eqs. 13.6 and 13.7, become

$$E_{in,z}(y) = \sum_n V_n \Gamma_n \phi_n \tag{13.12}$$

and

$$E_{in,y}(y) = -\sum_n V_n \frac{d\phi_n}{dy} \quad . \tag{13.13}$$

It is assumed that the region to the left of the entry plane does not support a propagating electromagnetic mode. The input field is therefore a linear combination of space harmonics of the propagating mode of the interaction space and of cutoff modes of both regions. Although calculation of the cutoff, or "fringing," fields at the input discontinuity is necessary to the solution of the electromagnetic problem, the cutoff fields have negligible interaction with the stream and are therefore of little interest in the interaction analysis. The artifice of an "ideal gap" is introduced below in order to exclude the cutoff-wave fields from detailed consideration in the present analysis of the interaction.

13.3 The Two-dimensional Ideal Gap

The fields of the cutoff modes decay exponentially with distance from the entry region at rapid rates. It is therefore possible to construct planes, as in Fig. 13.2, on either side of the entry plane, which

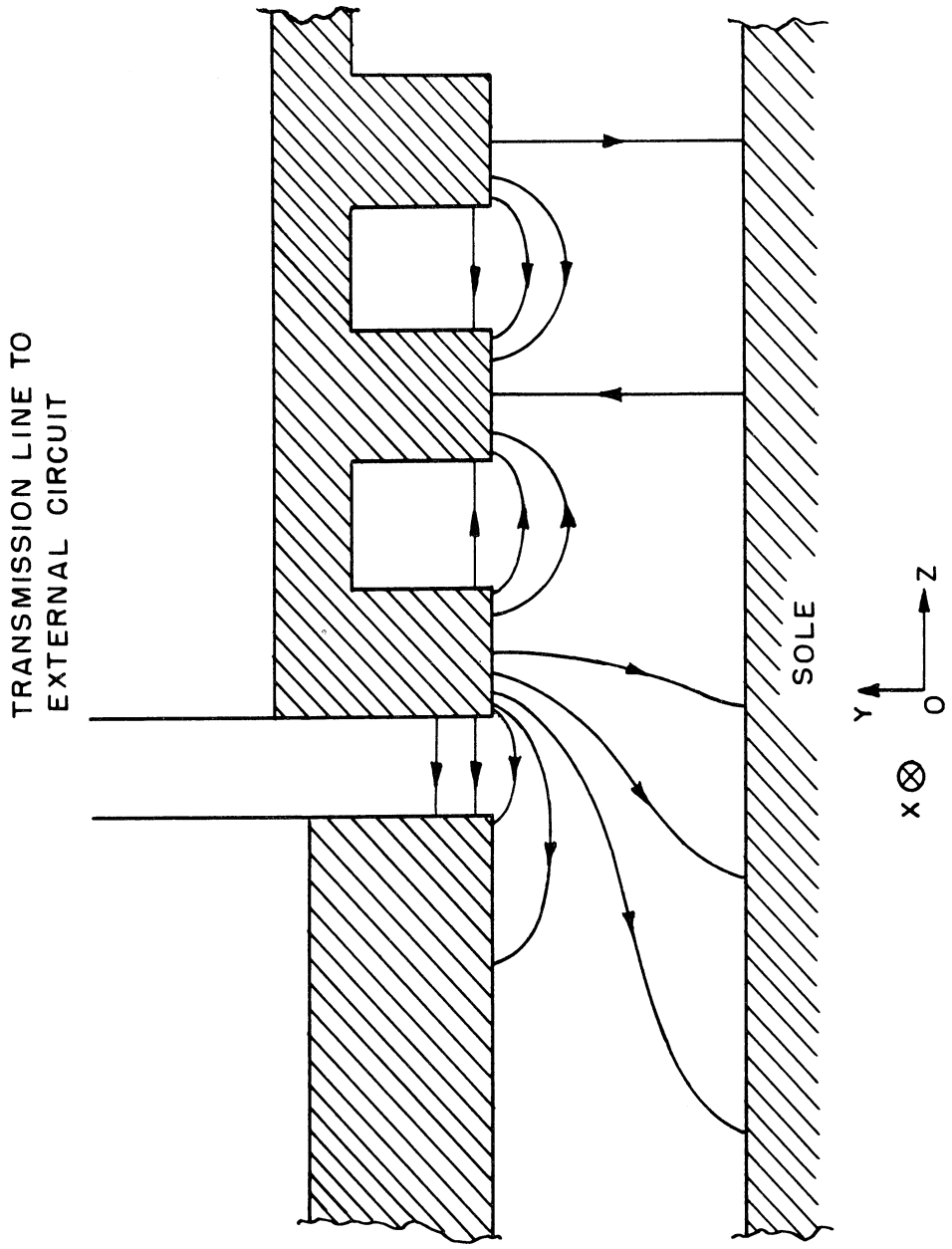

FIG. 13.1 ELECTRIC FIELD CONFIGURATION AT THE STREAM ENTRANCE TO THE INTERACTION SPACE.

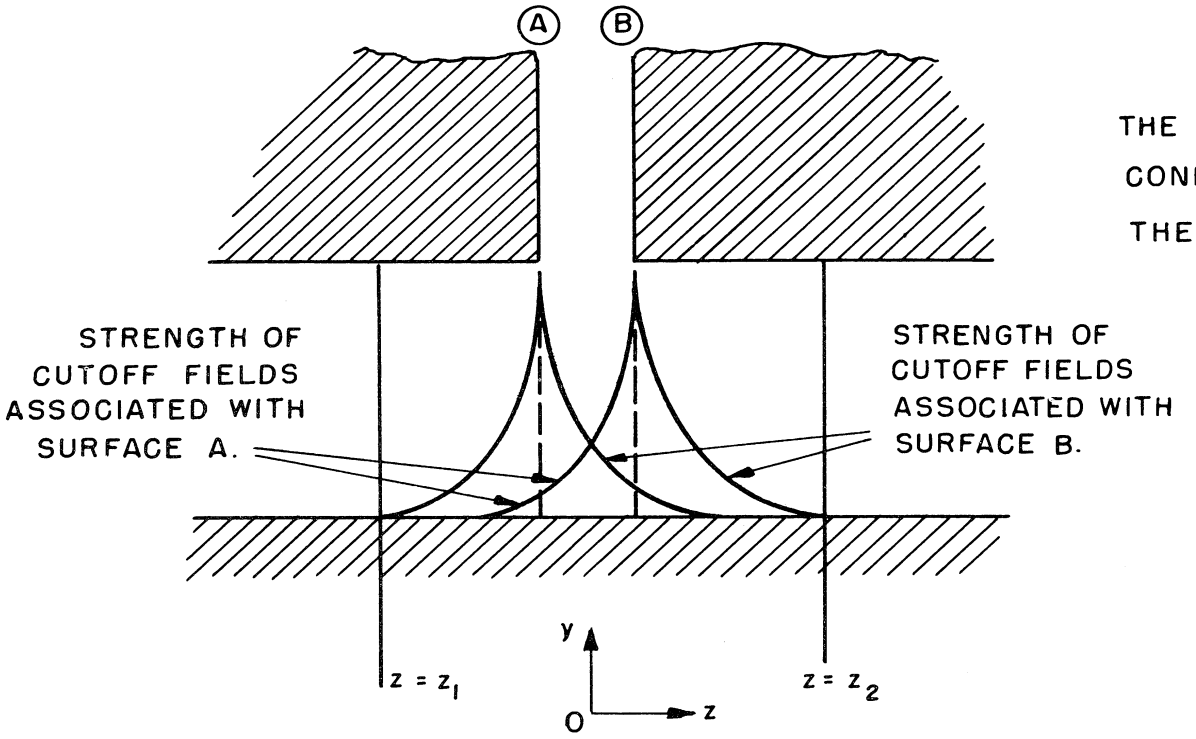

THE PLANES $z = z_1$ AND $z = z_2$ CONFINE VIRTUALLY ALL OF THE CUTOFF MODE ENERGY.

FIG. 13.2 REPRESENTATION OF THE INPUT REGION AS A "GAP" BETWEEN TWO PLANES.

confine most of the fields of the cutoff modes. The "input plane" for the interaction analysis is now taken to be the exit plane of the "gap" formed by the two planes constructed above. Since the cutoff fields are negligible at this plane, the electromagnetic problem can be formulated in terms of propagating modes only. Thus,

$$V_{in}\Gamma_o\psi = \sum_{n,\text{prop.}} V_n\Gamma_n\phi_n \ , \tag{13.14}$$

and

$$V_{in}\frac{d\psi}{dy} = \sum_{n,\text{prop.}} V_n\frac{d\phi_n}{dy} \tag{13.15}$$

where the summations are to be taken only over the propagating modes of the interaction region, and the terms on the left of the equations refer to the interacting space harmonic of the propagating mode in the absence of the stream. The cutoff modes are thus eliminated from the electromagnetic input problem.

The use of the ideal gap concept requires a reconsideration of the kinematic problem, however, since the kinetic variables at the exit of the gap are altered. In most devices of the traveling-wave type, the interaction region is many times longer than the input, or coupling, region. It is assumed here that the electrons of the stream make the transit through the gap in a time which is short in comparison with the period, $\frac{2\pi}{\omega}$, of the r-f perturbations. This assumption renders the gap an "ideal gap;" it permits the use of the concepts of impulse mechanics in describing the effect of the gap on the stream. Thus, the electrons pass through the gap so quickly that they suffer no displacement. The displacement Eqs. 13.4 and 13.5 therefore apply at the exit of the ideal gap, with the difference that only propagating modes need be considered in the summations:

$$0 = \sum_{n,\text{prop.}} (\delta z)_n \tag{13.16}$$

and

$$0 = \sum_{n,\text{prop.}} (\delta y)_n \tag{13.17}$$

The idealization of the gap indicates that the electrons undergo an impulsive change in velocity which can be calculated from the law of conservation of energy. Thus,

$$m \frac{\Delta|\vec{u}^2|}{2} = -e \Delta v \quad . \tag{13.18}$$

Use is made of the small-signal approximations

$$\vec{u} = (u_{zo} + \tilde{u}_z)\hat{z} + \tilde{u}_y \hat{y} \ , \qquad \begin{matrix} |\tilde{u}_z| << u_{zo} \\ |\tilde{u}_y| << u_{zo} \end{matrix} \tag{13.19}$$

for the electron velocity, resulting in

$$\Delta|\vec{u}^2| \approx 2 u_{zo} \tilde{u}_z \quad . \tag{13.20}$$

The change in electric potential of an electron making an ideally instantaneous transit through the gap, Δv, is calculated by noting that there is no potential at the entrance to the gap and that the potential at the exit of the gap is a sum over only propagating waves. Hence,

$$\Delta v = v_{exit} = \text{Re}\sqrt{2} \sum_{n,\text{prop.}} V_n \phi_n \exp(j\omega t) \ . \tag{13.21}$$

The impulse of momentum given the electrons of the stream as they pass through the ideal gap therefore results in the following velocity of the stream at the exit of the gap:

$$0 = \sum_{n,\text{prop.}} u_{yn} \tag{13.22}$$

$$u_{zo} \sum_{n,\text{prop.}} u_{zn} = -\eta \sum_{n,\text{prop.}} V_n \phi_n \quad . \tag{13.23}$$

It will later be shown that the velocity modulation thus produced by the gap fields is negligible in comparison with the subsequent modulation produced by the traveling-wave interaction. This is also true in conventional traveling-wave tubes, but is not true in klystrons, which do not have traveling-wave interaction.

13.4 Summary of the Longitudinal Boundary Requirements

Six longitudinal boundary requirements have been obtained—four kinematic requirements and two electromagnetic requirements. These are assembled below:

$$\sum_n (\delta z)_n = 0 \tag{13.16}$$

$$\sum_n (\delta y)_n = 0 \tag{13.17}$$

$$\sum_n u_{zn} = \frac{-\eta}{u_{zo}} \sum_n V_n \phi_n \tag{13.23}$$

$$\sum_n u_{yn} = 0 \tag{13.22}$$

$$\sum_n V_n \Gamma_n \phi_n = V_{in} \Gamma_n \psi \tag{13.14}$$

$$\sum_n V_n \frac{d\phi_n}{dy} = V_{in} \frac{d\psi}{dy} \tag{13.15}$$

13.5 Discussion of the Longitudinal Boundary Requirements

It is noted that four kinematic boundary requirements have been obtained. This results from the fact that the differential equations of

motion are of second order and that two dimensions are involved. The requirements are here stated in terms of the two components of velocity and displacement. Alternatively, velocity and convection-current components could be used.

It is remarked here that there is a subtle distinction between the two-dimensional theory of the present analysis and the one-dimensional theory of the conventional traveling-wave tube. In the one-dimensional case, the convection current, charge density and electron displacement are all interdependent; for example,

$$\sum_n (k_z)_n = 0 \iff \sum_n \rho_n = 0 \iff \sum_n (\delta z)_n = 0 \qquad (13.24)$$

The stream is therefore defined in terms of the electron velocity and one of the three variables of Eq. 13.16. In two-dimensional analysis, however, this is not so. In particular, specification of electron velocity and charge density does not uniquely describe the stream, since only three quantities are then known. The continuity equation, Eq. 3.34, can be written

$$\rho_n = -\rho_o\left[\frac{\partial \delta z}{\partial z} + \frac{\partial \delta y}{\partial y} - \frac{\omega_c \Gamma\, \delta y}{\Omega}\right] , \qquad (13.25)$$

which implies that the electron displacements are not uniquely specified by a knowledge of the charge density. The converse is true, however.

Since Eqs. 13.14 and 13.15 apply over the entire cross-section of the interaction space, and Eqs. 13.16, 13.17, 13.22, and 13.23 apply over the cross-section of the electron stream, it appears necessary to have an infinite set of wave solutions to satisfy the detailed transverse variation of the quantities of those equations. The transverse variations are generally small, however, so that an approximate solution is feasible.

This approximate solution is presented in Chapter XIV.

Since there are six requirements to be satisfied at each point in the input plane (the exit of the ideal gap), six propagating waves in the interaction space will in general be required for a solution of the input problem at that one point alone. It is noted here that the quasi-synchronous waves alone are insufficient for this purpose. Equations 9.37 and 9.39 show that if the quasi-synchronous waves were to satisfy the velocity requirements of Eqs. 13.22 and 13.23, then the fields at the exit of the entrance gap would necessarily be zero, contradicting Eqs. 13.14 and 13.15. The introduction of cyclotron waves as described in Chapter X removes this contradiction, since the cyclotron waves do not have the same relations between fields and velocities as do the quasi-synchronous waves.

CHAPTER XIV

AN APPROXIMATE SOLUTION TO THE INPUT PROBLEM

14.1 The General Nature of the Approximations

The set of input longitudinal boundary equations, when applied on the entire transverse entrance plane, requires an infinite set of propagating waves for a solution. In this chapter, an approximate solution of the set of input conditions is described in which only the quasi-synchronous, the cyclotron, and the "omni-synchronous" waves are required.

The input region is considered to be an ideal gap as discussed in Sec. 13.3. Use is made of the simple, yet accurate approximate description of the transverse variation of the physical variables of the quasi-synchronous waves as discussed in Sec. 9.4 and summarized in Table 9.1. The transverse variation of the quantities of the cyclotron waves, summarized in Table 10.1, are also represented by linear approximations. Although this approximation is not as good everywhere in the transverse plane as in the case of the quasi-synchronous waves, it is nevertheless a reasonably good one in the sense of "least squares," as demonstrated below.

14.2 Input Requirements Regrading the Electric Field

Equation 13.14, which indicates that the z-component of the electric field at the exit of the ideal gap is the same with the stream present as it is without the stream, is expressed as

$$\sum_{q\text{-}s} V_n \Gamma_n \phi_n + \sum_{c} V_n \Gamma_n \phi_n = V_{in} \Gamma_o \psi_o \qquad (14.1)$$

where the subscript q-s indicates the group of three quasi-synchronous waves and the subscript c indicates the pair of nontrivial cyclotron-wave solutions. The "omni-synchronous" wave has no electric field. Equation 13.15, which is a similar expression for the y-component of electric field, becomes

$$\sum_{q\text{-}s} V_n \frac{d\phi_n}{dy} + \sum_{c} V_n \frac{d\phi_n}{dy} = V_{in} \frac{d\psi_o}{dy} \quad , \qquad (14.2)$$

or, by virtue of the definition of χ (Sec. 4.4)

$$\sum_{q\text{-}s} V_n \frac{d\phi_n}{dy} + \sum_{c} V_n (\mp j\Gamma) \frac{d\phi}{d\chi} = V_{in} \frac{d\psi_o}{dy} \quad , \qquad (14.3)$$

within the stream.

14.3 Input Requirements Regarding the Electron Velocity

The transverse component of electron velocity will be considered first. In the present notation, Eq. 13.22 becomes

$$\sum_{q\text{-}s} u_{yn} + \sum_{c} u_{yn} = 0 \quad . \qquad (14.4)$$

The quasi-synchronous transverse velocities are discussed in Sec. 9.4.2; to a good degree of approximation for thin streams,

$$u_{yn} = \frac{E_{zn}}{B_{dc}} = \frac{V_n \Gamma_n \phi_n}{B_{dc}} \quad . \qquad (14.5)$$

In the case of the cyclotron waves, the y-component of velocity is related to the potential by Eq. 10.51:

$$u_y = -\frac{V\Gamma}{B_{dc}}\left(\phi + \frac{d\phi}{dX}\right) . \qquad (14.6)$$

Consequently, Eq. 14.4 takes the form

$$\sum_{q\text{-}s} V\Gamma\phi + \sum_{c} (-V\Gamma)\left(\phi + \frac{d\phi}{dX}\right) = 0 . \qquad (14.7)$$

The longitudinal component of electron velocity will next be considered. Equation 13.23 takes the form

$$\sum_{q\text{-}s} u_{zn} + \sum_{c} u_{zn} = -\frac{\eta}{u_{zo}}\left[\sum_{q\text{-}s} V\phi + \sum_{c} V\phi\right] . \qquad (14.8)$$

From Sec. 9.4.2, the quasi-synchronous expression for the z-component of electron velocity is

$$u_{zn} = -\frac{E_{yn}}{B_{dc}} = \frac{V_n \frac{d\phi_n}{dy}}{B_{dc}} . \qquad (14.9)$$

This is much larger than the term on the right side of Eq. 14.8, which is the alteration of the stream velocity produced by the action of the fields of the input gap. The effect of the input gap on the electron velocity in this equation will therefore be neglected in comparison with the terms of Eq. 14.9. Effectively, the effect of the input gap is neglected in comparison with the subsequent events in the interaction space which take place over a much longer period of time.

Then, using the expression of Eq. 10.49 for the longitudinal velocity component of the cyclotron waves, viz.,

$$u_z = \pm j\frac{\Gamma V \phi}{B_{dc}} , \qquad (14.10)$$

the input requirement regarding the longitudinal velocity becomes

$$\sum_{q\text{-}s} V_n \frac{d\phi_n}{dy} + \sum_{c} (\pm j\Gamma)\, V\, \phi = 0 \quad . \tag{14.11}$$

Attention is drawn to the fact that the "omni-synchronous" wave does not have electron velocity components, and is therefore ignored in the formulation of the velocity relations.

14.4 Manipulation of the Input Velocity and Field Equations

The input requirements regarding the electric-field components and the electron-velocity components are Eqs. 14.1, 14.3, 14.7, and 14.11. The set can be put into a more useful form through some simple operations, resulting in a pair involving only the quasi-synchronous waves.

14.4.1 Input Equations for the Cyclotron Waves

Subtraction of Eq. 14.7 from Eq. 14.1 results in

$$\sum_{c} V\Gamma \left(2\phi + \frac{d\phi}{dX}\right) = V_{in}\Gamma_o\psi_o \quad . \tag{14.12}$$

Subtraction of Eq. 14.11 from Eq. 14.3 yields

$$\sum_{c} V(\pm j\Gamma)\left(2\phi + \frac{d\phi}{dX}\right) = V_{in} \frac{d\psi_o}{dy} \quad . \tag{14.13}$$

Eqs. 14.12 and 14.13 thus form a set of simultaneous equations in which the amplitudes of the two cyclotron waves are the unknowns.

An approximate solution for this pair of equations is obtained by noting that (cf. Eqs. 6.24 and 8.52)

$$\frac{d\psi_o}{dy} = j\Gamma_o[\coth j\Gamma_o(y - y_E)]\psi_o \approx -j\Gamma_o\psi_o V_{in} \quad , \tag{14.14}$$

and also that for cyclotron waves (Sec. 10.5.1)

$$\left|\frac{d\phi}{dX}\right| >> |\phi| . \qquad (14.15)$$

Using these approximations, the solution of Eqs. 14.12 and 14.13 is found to be

$$j\Gamma_+ V_+ \frac{d\phi_+}{dX} \approx j\Gamma_o\psi_o V_{in} \qquad (14.16)$$

and

$$V_- \approx 0 . \qquad (14.17)$$

Because the potential function varies with y, however, Eq. 14.16 cannot be satisfied everywhere in the cross-section of the stream. It is seen that the transverse gradient of the potential function, shown in Fig. 10.5, corresponding to the faster cyclotron wave is relatively constant, varying the most near the upper edge of the stream. It is fortunate that the slower cyclotron wave is not excited (Eq. 14.17) since there is a much more radical variation of its potential function across the stream. By assuming that Eq. 14.16 is fulfilled at the center of the stream, the error in "match", or the fulfillment of Eq. 14.16 everywhere within the stream, is made small. The actual degree of "mismatch" is discussed in Sec. 14.6.

14.4.2 The Input Equations for the Quasi-synchronous Waves

When the results of the calculations of the cyclotron-wave amplitudes are used with the original set of four input equations of Sec. 14.4, the following equations involving only the quasi-synchronous waves results:

$$\sum_{q\text{-}s} V_n \frac{d\phi_n}{dy} = 0 \qquad (14.18)$$

$$\sum_{q\text{-}s} V_n \Gamma_n \phi_n = V_{in} \Gamma_o \psi_o . \qquad (14.19)$$

Since all quasi-synchronous waves have propagation constants very nearly

the same as the unperturbed interaction space harmonic, the latter equation can be written

$$\sum_{q\text{-}s} V_n \phi_n = V_{in}\psi_o \quad . \tag{14.20}$$

Since the cyclotron longitudinal fields outside the stream are quite small, Eq. 14.20 applies outside the stream as well as within it. In particular, it applies at the anode, where the only longitudinal fields are those of the quasi-synchronous wave. Hence,

$$\sum_{q\text{-}s} V_n \phi_n(y = y_d) = \sum_{q\text{-}s} V_n = V_{in}\psi_o(y_d) = V_{in} \quad . \tag{14.21}$$

Equations 14.18, 14.20, and 14.21 form a set of three equations in the amplitudes of the three quasi-synchronous waves as unknowns. Since the potential functions of the quasi-synchronous waves are approximately linear functions of the transverse coordinates (Eq. 9.31), the set of equations is approximately satisfied by the three waves as long as ψ_o does not vary too greatly within the stream. This set of equations can therefore be written

$$\begin{aligned} \sum_{q\text{-}s} V_n &= V_{in} \\ \sum_{q\text{-}s} V_n \overline{\phi_n} &= V_{in}\overline{\psi_o} \\ \sum_{q\text{-}s} V_n \frac{\overline{d\phi_n}}{dy} &= 0 \quad , \end{aligned} \tag{14.22}$$

where the bars denote that the quantities are to be evaluated at the midplane of the stream.

The set of equations, Eq. 14.22, 14.16, and 14.17 form an approximate solution of the input problem which, strictly speaking, is limited by the cyclotron-wave theory to a stream which is thin and which is located at the midplane of the interaction space. The generalizations made in Eq. 14.15, however, appear to apply to cyclotron waves in general. Thus, although the amplitude of the cyclotron wave may not be accurately given by Eqs. 14.16 and 14.17, it is believed that the solutions of Eq. 14.22 are rather accurate in the more general stream configuration.

14.5 Input Requirements Concerning the Electron Displacement

Up to this point, the electron displacement requirements have been carefully avoided. In this section they are considered, and it is shown that introduction of the "omni-synchronous" wave accounts for the displacement requirements. To show this, it is first noted that the y-components of displacement are significant only for the quasi-synchronous waves. Equation 9.42 shows that the y-displacement is proportional to the transverse potential gradient. But Eq. 14.18 shows that the sum of the potential gradients of the three quasi-synchronous waves is zero at the input. Hence, there is no ripple of the stream as described by the quasi-synchronous waves at the input. Furthermore, the space-charge density of the quasi-synchronous waves is, to the first order, zero (Eq. 8.54). The longitudinal component of electron displacement, however, does not match when only the quasi-synchronous and cyclotron waves are considered; the sum of displacements is approximately

$$\sum_{q\text{-}s} (\delta z)_n = \sum_{q\text{-}s} \frac{V_n \frac{d\phi_n}{dy}}{\Omega_n B_{d\text{-}c}} , \qquad (14.23)$$

which is a large quantity which varies appreciably with y.

The "omni-synchronous" wave has the properties described above for the y-displacement and charge density of the quasi-synchronous waves. Furthermore, the z-displacement of the "omni-synchronous" wave assures the satisfaction of the displacements without disturbing the other variables (velocity and fields) if the displacement of this wave is made equal to the negative of Eq. 14.23. When this is done,

$$\sum_{q\text{-}s} (\delta z)_n + (\delta z)_{o\text{-}s} = 0, \quad \text{all } y_a < y < y_b \ , \qquad (14.24)$$

and the input requirements are all satisfied.

14.6 Analysis of the Error, or "Mismatch" Involved in the Approximate Solution

In the handling of the input problem above, it was seen that a perfect "match" of all the physical quantities of the input problem is possible only at one level in the stream if only six waves are used. Therefore, there will be a difference, or "mismatch" between the prescribed entrance values and the sum of the values of the propagating waves at other levels in the stream. The amount of mismatch depends on the accuracy of the approximations which were made concerning the transverse variation of the physical quantities associated with each wave.

14.6.1 Mismatch in the Longitudinal Component of Electric Field

Consideration of Eq. 14.1 shows that in the approximate solution several errors have been incurred concerning the longitudinal electric field:

(1) The linear approximation for the potential function, ϕ, for the quasi-synchronous waves leads to a slight error. The error is small because the terms neglected in the potential function representation (see

Eq. 8.10) are all of the order of ξ^3 or less. The quantity ξ is of order of magnitude of the interaction parameter, D_i, or of the velocity spread parameter, s_u, whichever is the larger. The error involved here is that of the neglect of ξ^3 in comparison with ξ, and is therefore of the order of D_i^2 or s_u^2.

(2) The linear approximation for the potential function for the cyclotron waves at first appears to be more serious a source of error than with the quasi-synchronous waves. Equations 14.15 and 14.19 show, however, that the cyclotron waves are not excited to such a degree that they contribute much to the longitudinal electric field. The neglect of the cyclotron-wave potential in comparison with the gradient in Eq. 14.15 is justified by the following order-of-magnitude relation:

$$|\phi| \sim s_u \left|\frac{d\phi}{dX}\right| \quad . \tag{14.25}$$

Use of this relation with Eq. 14.16 shows that the longitudinal component of the cyclotron wave neglected in Eq. 14.19 is of the order of magnitude

$$V_+\Gamma_+\phi_+ \sim s_u V_{in}\Gamma_o\psi_o \quad . \tag{14.26}$$

(3) The linear approximation for the space-charge-free potential, ψ_o, is also a source of error. This error is rather small because the largest neglected term of the Taylor expansion of the function about the midplane of the stream is of the order

$$\frac{1}{2}\overline{\psi_o''}\left(\frac{\Delta y}{2}\right)^2 \sim \frac{1}{2}\left(\frac{\omega}{\omega_c}s_u\right)^2\overline{\psi_o} \quad . \tag{14.27}$$

(4) The approximation $\Gamma_n \approx \Gamma_o$ has also been made regarding the quasi-synchronous waves in Eq. 14.20. This is made more for convenience than necessity, but is eminently justified.

Item (2) above, concerning the cyclotron waves, appears to be the poorest approximation, since the error dependence on s_u (assumed to be a small fraction) is of the first degree.

14.6.2 Mismatch of the Transverse Electric Field

The discussion regarding the sources of errors in items (1), (3), and (4) in the above section are applicable here also. Equation 10.48 shows that the y-component of electric field varies more rapidly with the transverse coordinate than the z-component, Eq. 10.45. The first order approximation used for the transverse field variation in the input problem therefore leads to greater error than was the case with the longitudinal field approximation. Assuming that the only important source of "mismatch" is that of the cyclotron-wave approximation, the mismatch of the transverse electric field has the appearance shown in Fig. 14.1. Equation 14.16 shows that the mismatch of the y-component of electric field is of the same order of magnitude as the y-component of electric field of the cold circuit.

There are two factors which mitigate this apparently serious inconsistency of the approximate solution:

(1) Although the mismatch is large in comparison with the transverse field of the cold circuit, it is quite small in comparison with the transverse fields of the quasi-synchronous waves individually, as shown in Sec. 9.4.1. The fields of the individual waves themselves are the measure of the fields which exist after appreciable interaction has taken place. Considered in this light, the mismatch does not appear to be serious.

(2) If the discrepancy, or mismatch, of one of the physical quantities of the system—in this instance, transverse electric field—is represented by $\epsilon_i(y)$, a function of the transverse coordinate, then a mean-

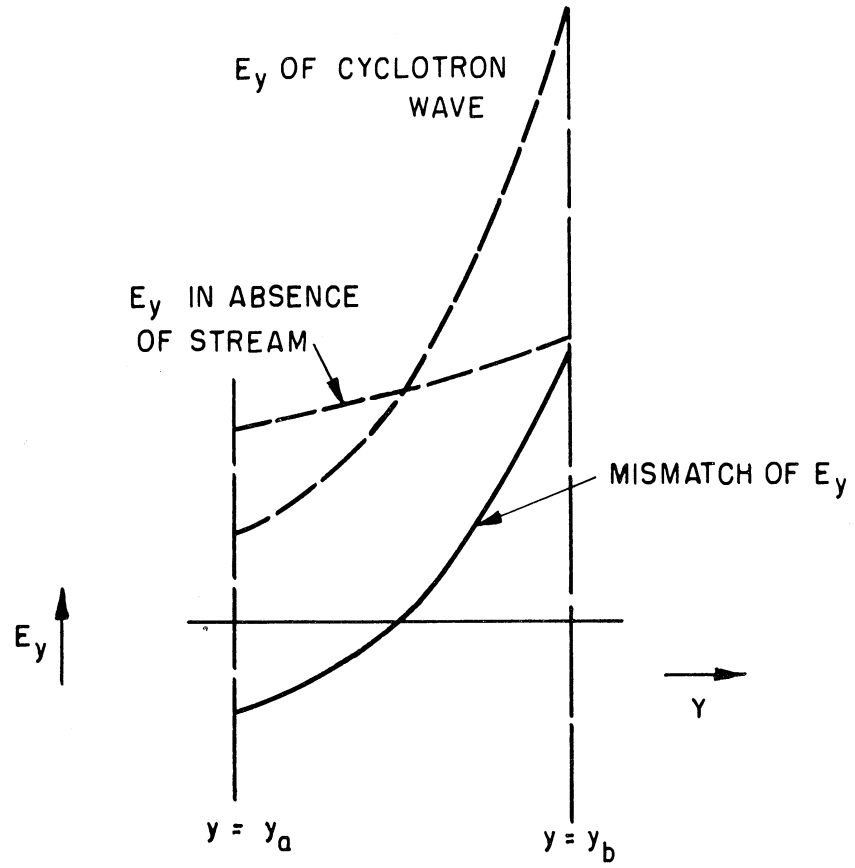

FIG. 14.1 SKETCH OF THE MISMATCH OF THE TRANSVERSE ELECTRIC FIELD IN THE APPROXIMATE SOLUTION.

square discrepancy, $\overline{\epsilon_i^2}$, can be defined as

$$\overline{\epsilon_i^2} = \frac{\int_{y_s}^{y_d} \epsilon_i^2 \, dy}{y_d - y_s} \quad . \tag{14.28}$$

Since the discrepancies are in general large only for a small range of y near the upper edge of the stream (because of the nature of the cyclotron waves), it follows that the mean-square discrepancies are rather small even though the discrepancy may be relatively large near the upper edge of the stream.

The mean-square value as a figure of merit for a solution of the input boundary value problem has justification here because of the nature of the infinite set of cutoff waves which, in the general electromagnetic boundary-value problem, are excited in sufficient amplitude to maintain the continuity of fields required. These cutoff waves have trigonometric variation on the interval of the transverse plane between the anode and the sole. A well-known property of such a series of trigonometric functions is that a finite Fourier series of such functions represents a given function on the interval best in the sense of "least squares," i.e., with a minimum mean-square discrepancy. It is this property of the cutoff waves which suggests that the mean-square discrepancy be used as a natural measure of the error involved in the approximate solution.

14.6.3 Mismatch of the Longitudinal Component of Velocity

The failure of Eq. 14.11 to be satisfied exactly at all levels in the stream, thereby causing the mismatch between the approximate solution and the actual solution provided by nature, arises from the following two sources:

(1) the approximate representation of the transverse electric fields of the quasi-synchronous waves as independent of y, and

(2) the linear approximation to the potential of the cyclotron waves. The first of these errors is small because the first order approximation is quite good for quasi-synchronous waves. While the second of these errors varies more over the cross-section of the stream, the overall error is small because the velocity caused by the cyclotron wave fields is much smaller than those caused by the fields of the quasi-synchronous waves.

14.6.4 Mismatch of the Transverse Component of Velocity

Consideration of Eq. 14.7 shows that mismatch between the approximate solution and the input requirements arises from

(1) the linear approximation for the potential function of the quasi-synchronous waves,

(2) the linear approximation for the potential function of the cyclotron waves, and

(3) the approximation as independent of y of the transverse gradient of the potential function of the cyclotron waves.

Each of these approximations has been discussed above. Because there is very little transverse motion in the quasi-synchronous waves, and because of the inequality Eq. 14.15, item (3) is the major source of error. This error is still small, however, in comparison with the longitudinal component of the velocity of the quasi-synchronous waves.

14.6.5 Mismatch of the Electron Displacements

Because of the property of the "omni-synchronous wave" given by Eq. 14.24, there is a complete match between the approximate solution and the input requirement as far as the longitudinal displacement component is concerned.

The transverse displacements of the "omni-synchronous" wave and the

group of three quasi-synchronous waves are both zero at the edges of the stream at the input and are both related to the respective longitudinal displacement components by the continuity relation for the common situation of zero first-order space-charge density. Therefore, since there is no mismatch in the longitudinal component of displacement, there is also no mismatch in the transverse component.

14.6.6 Summary of the Analysis of the Error of the Approximate Solution

The above discussion of the discrepancy between the approximate solution of the input boundary value problem and the conditions which must obtain if an unmodulated stream enters the interaction space shows that the approximate solution of the input problem is in error by only the degree incurred in solving the transverse boundary value problem. Both have assumed, for instance, that the velocity spread, or thickness, of the stream is only a few percent of the mean d-c stream velocity; both are in error to the degree that the square of this quantity is not negligible in comparison with the first power of the quantity itself. Nature, of course, does not admit of any "approximate solutions." It is suggested that the cutoff waves in an actual instance account for the discrepancies in the longitudinal boundary value problem.

One of the primary motivations for making a detailed analysis of the match of an approximate solution is the determination of whether a sufficiently complete set of waves on the interaction system has been found and utilized. This seems to be the case, for no important lack of match has been noted.

14.7 An Explicit Form of the Quasi-synchronous Input Conditions

The set of equations, Eq. 14.22, can be replaced for the purpose of

calculation of the wave amplitudes by equations which make use of the wave natures determined in Chapter IX. Thus, the potential function, as obtained from Eqs. 8.42 and 8.45, is

$$\phi \equiv C\xi = \frac{\xi\,\xi_b}{\xi_b^2 + \xi_a^2\,H} \cdot \frac{1}{\cosh j\Gamma_o\,(y_d - y_b)} \quad . \qquad (14.29)$$

Expression of ξ in terms of the normalized incremental propagation constant, ℓ, and in terms of the normalized velocity spread (beam thickness) parameter, r, (cf Eqs. 8.64 and 8.68) leads to

$$\bar{\phi} \equiv \phi\,(y = \bar{y}) = \frac{\ell(\ell + r)}{(\ell + r)^2 + H(\ell - r)^2} \; \frac{1}{\cosh j\Gamma_o(y_d - y_b)} \quad . \qquad (14.30)$$

Using the dispersion relation for quasi-synchronous waves, Eq. 9.1, the potential can also be expressed as

$$\bar{\phi} = \frac{\pm\,(\ell + r)(\ell - b)}{2\cosh j\Gamma_o(y_d - y_b)} \quad . \qquad (14.31)$$

Similarly, it is found that the transverse potential gradient is proportional to

$$\frac{d\phi}{dy} \propto \frac{\ell + r}{(\ell + r)^2 + H(\ell - r)^2} \qquad (14.32)$$

or, using the dispersion relation,

$$\frac{d\phi}{dy} \propto \frac{(\ell + r)(\ell - b)}{\ell} \quad . \qquad (14.33)$$

Using the above expressions for the potential function and its derivative, the input equations for the quasi-synchronous waves can be written either as

$$\sum V_n = V_{in}$$

$$\sum \frac{V_n (\ell_n + r)\, \ell_n}{(\ell_n + r)^2 + H(\ell_n - r)^2} = V_{in} \bar{\psi} \cosh j\Gamma_o(y_d - y_b) \qquad (14.34)$$

$$\sum \frac{V_n (\ell_n + r)}{(\ell_n + r)^2 + H(\ell_n - r)^2} = 0$$

or as

$$\sum V_n = V_{in}$$

$$\sum V_n (\ell_n + r)(\ell_n - b) = \pm (1 + H) \bar{\psi} \cosh j\Gamma_o(y_d - y_b) V_{in} \qquad (14.35)$$

$$\sum V_n \frac{(\ell_n + r)(\ell_n - b)}{\ell_n} = 0 \ .$$

The geometrical factor on the right side of the second equation of Eq. 14.35 is identically equal to unity for all stream locations relative to the electrode planes. This second equation therefore can be written

$$\sum V_n (\ell_n + r)(\ell_n - b) = \pm V_{in} \ . \qquad (14.36)$$

When the first equation of Eq. 14.35 is combined with Eq. 14.36, the set Eq. 14.35 takes on the simple form

$$\sum V_n = V_{in}$$

$$\sum V_n [(\ell_n + r)(\ell_n - b) \pm 1] = 0 \qquad (14.37)$$

$$\sum V_n \frac{(\ell_n + r)(\ell_n - b)}{\ell_n} = 0 \ .$$

Similar operations on the set Eq. 14.34 lead to the set

$$\sum V_n = V_{in}$$

$$\sum V_n \frac{(\ell_n - r) - \ell_n \frac{(1 - H)}{(1 + H)}}{(\ell_n + r)^2 + H(\ell_n - r)^2} = 0 \qquad (14.38)$$

$$\sum V_n \frac{(\ell_n + r)}{(\ell_n + r)^2 + H(\ell_n - r)^2} = 0 \ .$$

In these equations, the summation is understood to refer to the three quasi-synchronous waves only.

Equations 14.37 and 14.38 are in forms which can be readily solved when the stream and circuit parameters are specified, thus determining the incremental propagation constants (the ℓ_n's) as in Chapter IX. Some solutions of these equations for the determination of the wave amplitudes are presented in the succeeding chapters.

PART VI

RESULTS AND CONCLUSIONS

CHAPTER XV

FORWARD-WAVE INTERACTION

15.1 The Quasi-synchronous Input Conditions for Forward-wave Interaction

In the case of forward-wave interaction, the upper sign of the second equation of Eq. 14.37 applies; hence

$$\sum V_n = V_{in}$$

$$\sum V_n [(\ell_n + r)(\ell_n - b) + 1] = 0 \qquad (15.1)$$

$$\sum V \frac{(\ell_n + r)(\ell_n - b)}{\ell_n} = 0 \ .$$

The special cases considered in this chapter are those for which the dispersion relation was solved in Chapter IX.

15.2 The Special Case of a Stream at the Midplane of the Interaction Space—H = 1

The relative location of the stream and electrode planes of this special case is the only instance for which the cyclotron wave calculation is valid. For other configurations the approximate solution to the input problem is not strictly correct; it would appear, however, that the cyclotron wave calculations have little bearing on the conditions governing the quasi-synchronous waves as long as the cyclotron waves have the general properties ascribed to them in Chapter XIV.

When H = 1, the set Eq. 14.38 becomes

$$\sum V_n = V_{in}$$

$$\sum V_n \frac{(\ell_n - r)}{\ell_n^2 + r^2} = 0 \qquad (15.2)$$

$$\sum V_n \frac{\ell_n + r}{\ell_n^2 + r^2} = 0 \ .$$

Both sets Eqs. 15.1 and 15.2 are suitable for detailed calculation. Attention will first be given to the special case of a d-c stream having the same mean velocity as the phase velocity of the interaction space harmonic of the cold circuit, i. e., b = 0. This condition is expected to result in strong interaction and also renders the equations much simpler.

15.2.1 Further Specialization to the Case of Mean D-c Stream Velocity Equal to the Phase Velocity of the Unperturbed Circuit—H = 1 and b = 0

When H = 1 and b = 0, the roots of the dispersion equation are, from Eqs. 9.15 and 9.16,

$$\ell_1 = -\ell_2 = -j\sqrt{1 + r^2} \ , \qquad (15.3)$$

$$\ell_3 = 0 \ . \qquad (15.4)$$

Because both b and ℓ_3 are zero, the third equation of Eq. 15.1 is indeterminate. In this case the set Eq. 15.2 is used (which is the reason for carrying it along). Substitution of the values from Eqs. 15.3 and 15.4 into the set Eq. 15.2 leads to

$$V_1 + V_2 + V_3 = V_{in}$$

$$V_1(-j\sqrt{1 + r^2} - r) + V_2(j\sqrt{1 + r^2} - r) + V_3(-\frac{1}{r}) = 0 \qquad (15.5)$$

$$V_1(-j\sqrt{1 + r^2} + r) + V_2(j\sqrt{1 + r^2} + r) + V_3(\frac{1}{r}) = 0 \ .$$

where V_1 is the rms magnitude of the growing wave,

V_2 is the rms magnitude of the declining wave, and

V_3 is the rms magnitude of the wave, of unchanging amplitude, having the same phase velocity as the mean d-c stream velocity and the phase velocity of the unperturbed circuit.

The solution of Eq. 15.5 is

$$V_1 = \frac{1}{2}\frac{1}{1 + r^2} \tag{15.6}$$

$$V_2 = \frac{1}{2}\frac{1}{1 + r^2} \tag{15.7}$$

$$V_3 = \frac{r^2}{1 + r^2} \quad . \tag{15.8}$$

15.2.1.1 Gain of the Forward-wave Amplifier in the Special Case H = 1, b = 0

The total r-f potential at the anode plane is the sum of the potentials of the three quasi-synchronous waves; it therefore has the expression of Eq. 3.19 with N = 3 and $\phi_n = 1$. In view of Eqs. 8.4, 8.5, and 8.64, the total r-f potential can be written

$$v_{TOT,r\text{-}f} = \mathrm{Re}\sqrt{2}\, V_{TOT}(z) \exp j\omega t$$

$$V_{TOT}(z) = \exp(-\Gamma_o z)\left\{V_1 e^{-\Gamma_o \ell_1 D_i z} + V_2 e^{-\Gamma_o \ell_2 D_i z} + V_3 e^{-\Gamma_o \ell_3 D_i z}\right\} \tag{15.9}$$

or, using Eqs. 15.6-15.8,

$$V_T = V_{in}\frac{e^{-\theta_o}}{1 + r^2}\left[\cosh\sqrt{1 + r^2}\, D_i\theta_o + r^2\right] \quad , \tag{15.10}$$

where $\theta_o = 2\pi N = |\Gamma_o L|$ is the electrical radian length of the cold circuit, measured in terms of the propagation constant (wave-length) of the interaction space harmonic.

Equation 15.10 indicates that the amplitude of the total circuit

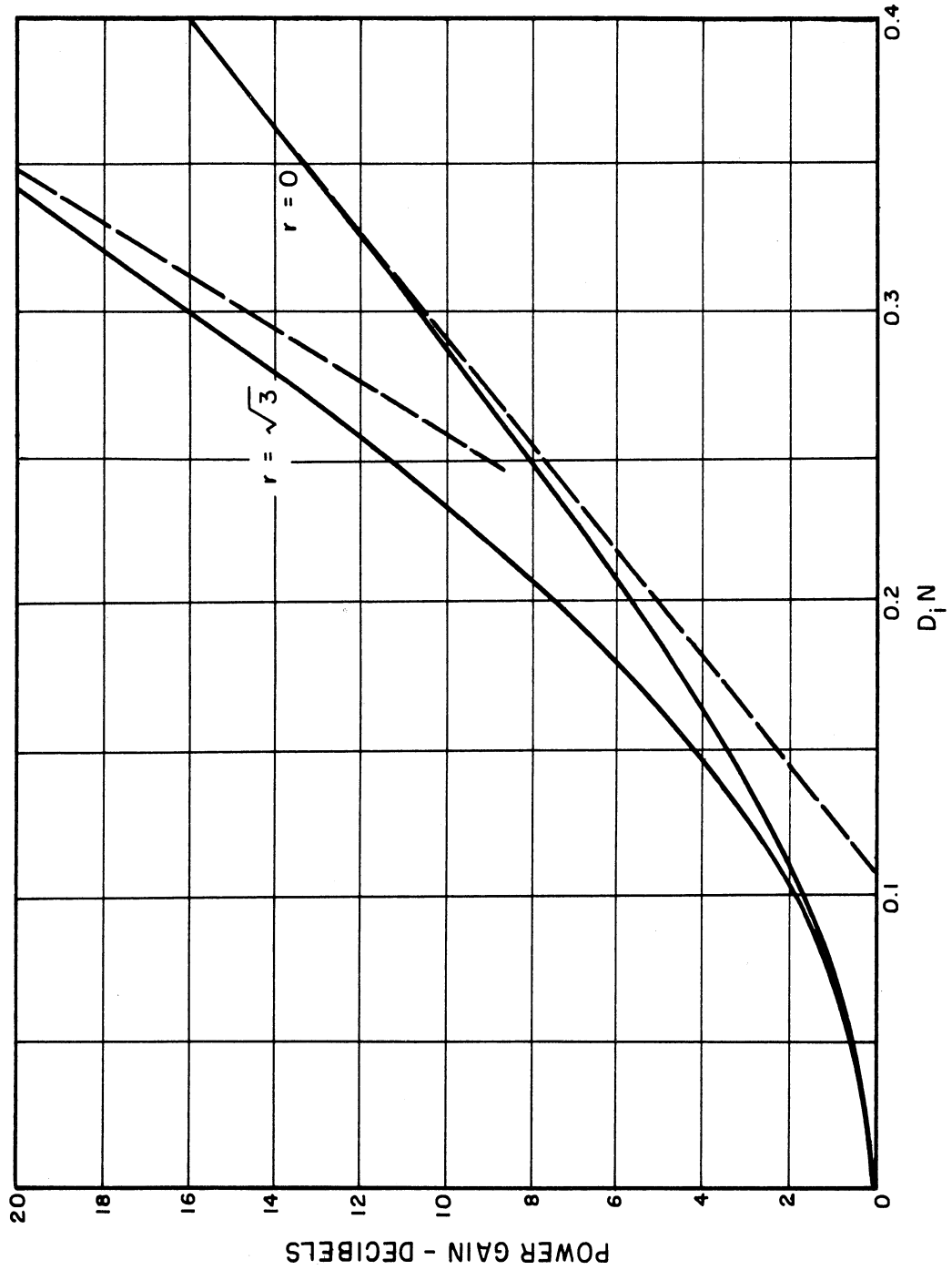

FIG. 15.1 POWER GAIN VS DISTANCE ALONG THE INTERACTION SPACE IN A FORWARD-WAVE AMPLIFIER - SPECIAL CASE H = 1, b = 0

potential increases with distance along the interaction space in a forward-wave device. There is accordingly power gain present in the amount

$$\text{Power Gain} = \frac{[r^2 + \cosh(\sqrt{1 + r^2}\, D_i \theta_o)]^2}{r^2 + 1} \quad . \qquad (15.11)$$

Figure 15.1 shows the manner in which the power gain varies with the length of the interaction space and also shows the dependence of the power gain on the beam thickness parameter, r. In the straight portions of these curves the gaining wave is the predominant one. In these portions the gain is approximately

$$\text{Power Gain (db)} \approx -6.02 - 20 \log(1 + r^2) + 54.5 \sqrt{1 + r^2}\, D_i N \quad . (15.12)$$

It is noted that, aside from the effect on the interaction parameter, D_i, the stream thickness has a further effect on the gain of the forward-wave amplifier. Specifically, increasing the velocity-spread, or beam-thickness, parameter actually increases the gain more than is accounted for in the interaction parameter alone.

CHAPTER XVI

BACKWARD-WAVE INTERACTION

16.1 The Quasi-synchronous Input Conditions for Backward-wave Interaction

In the case of backward-wave interaction, the lower sign of the second equation of the set Eq. 14.37 is applicable; thus

$$\sum V_n = V_{in}$$

$$\sum V_n [(\ell_n + r)(\ell_n - b) - 1] = 0 \qquad (16.1)$$

$$\sum V_n \frac{(\ell_n + r)(\ell_n - b)}{\ell_n} = 0 \ .$$

Much of the discussion of Chapter XV regarding these equations is applicable here also. Special cases will be considered in which the stream has certain locations with respect to the anode and the sole.

16.2 The Special Case in Which the Stream Is at the Midplane of the Interaction Space—H = 1

When H = 1, the set Eq. 14.38 becomes

$$\sum V_n = V_{in}$$

$$\sum V_n \frac{\ell_n - r}{\ell_n^2 + r^2} = 0 \qquad (16.2)$$

$$\sum V_n \frac{\ell_n + r}{\ell_n^2 + r^2} = 0 \ .$$

Attention will first be given to the special case in which the mean d-c

stream velocity is equal to the phase velocity of the unperturbed interaction space harmonic, i.e., the case b = 0.

16.2.1 Further Specialization to the Case of Mean d-c Stream Velocity Equal to the Phase Velocity of the Unperturbed Circuit—H = 1 and b = 0

When H = 1 and b = 0, the solutions of the quasi-synchronous dispersion equation for backward-wave interaction are given by Eqs. 9.26 and 9.27; they are written in the following form:

$$\ell_1 = -\ell_2 = \sqrt{1 - r^2} \tag{16.6}$$

$$\ell_3 = 0 \ . \tag{16.7}$$

As discussed in Sec. 15.2.1, the set Eq. 16.1 is indeterminate in this special case; Eq. 16.2 must be used. Combination of this set with Eqs. 16.6 and 16.7 leads to the set of equations

$$\begin{aligned} V_1 + V_2 + V_3 &= V_{in} \\ V_1(\sqrt{1 - r^2} - r) + V_2(-\sqrt{1 - r^2} - r) + V_3(\tfrac{1}{r}) &= 0 \\ V_1(\sqrt{1 - r^2} - r) + V_2(-\sqrt{1 - r^2} + r) + V_3(-\tfrac{1}{r}) &= 0 \ . \end{aligned} \tag{16.8}$$

where V_1 is the rms magnitude of the slow quasi-synchronous wave,

V_2 is the rms magnitude of the fast wave, and

V_3 is the rms magnitude of the wave which is synchronous with the electrons having the mean d-c stream velocity.

The solution of Eq. 16.8 is

$$V_1 = \frac{1}{2}\frac{1}{1 - r^2} \tag{16.9}$$

$$V_2 = \frac{1}{2}\frac{1}{1 - r^2} \tag{16.10}$$

$$V_3 = \frac{-r^2}{1 - r^2} \ . \tag{16.11}$$

16.2.1.1 The Total Circuit Potential of the Backward-wave Device in the Special Case H = 1, b = 0—Start-oscillation Conditions

As discussed in Sec. 15.2.1.1, the total potential at the anode plane can be represented as a function of distance along the interaction space in the form

$$V_{TOT}(z) = \exp(-\Gamma_o z)\left\{V_1 e^{-\Gamma_o \ell_1 D_i z} + V_2 e^{-\Gamma_o \ell_2 D_i z} + V_3 e^{-\Gamma_o \ell_3 D_i z}\right\} . \tag{16.12}$$

When the values of the ℓ's and the wave amplitudes as given by Eqs. 16.9, 16.10, and 16.11 are applied to Eq. 16.12, the resulting behavior of the total wave potential is found to be

$$V_{TOT} = V_{in} \frac{e^{-\theta_o}}{1 - r^2} \left[\cos(\sqrt{1 - r^2}\, D_i \theta_o) - r^2\right] , \tag{16.13}$$

$$r < 1 , \tag{16.14}$$

or the more convenient form

$$V_{TOT} = V_{in} \frac{e^{-\theta_o}}{1 - r^2} \left[\cosh(\sqrt{r^2 - 1}\, D_i \theta_o) - r^2\right] \tag{16.15}$$

$$r > 1 . \tag{16.16}$$

The two forms, Eqs. 16.13 and 16.15, are mathematically equivalent but have different physical interpretations. The two ranges of the beam thickness parameter, r, are therefore treated separately below.

16.2.1.1.1 Beam Thickness Parameter Less than Unity—r < 1

When r < 1, the dispersion relation (Sec. 9.3.2.1) shows that all three quasi-synchronous waves are of unchanging amplitude but have different phase velocities. The total potential, which has the form given in Eq. 16.13, therefore takes on the aspect of the interference of these three waves. Figure 16.1 shows the behavior of the total potential in

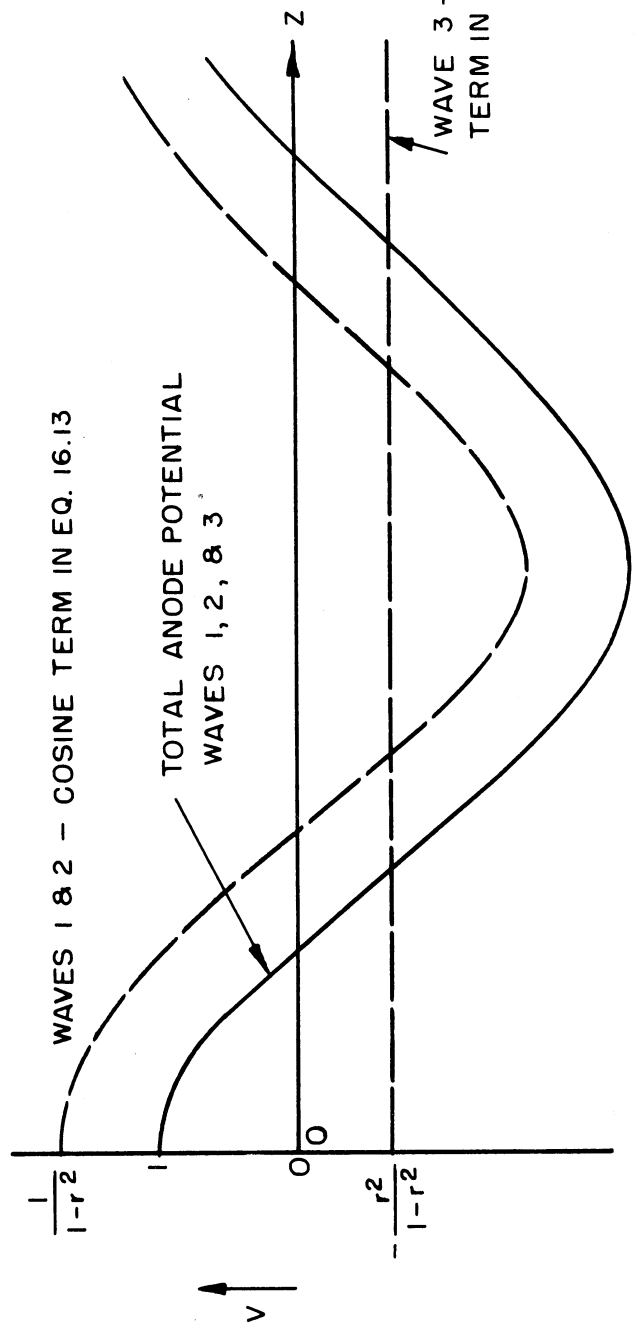

FIG. 16.1 VARIATION ALONG THE Z-AXIS OF THE TOTAL ANODE POTENTIAL IN THE BACKWARD–WAVE TUBE– SPECIAL CASE $H=1$, $b=0$, $r<1$

this case. Because the interaction is with a backward-wave space harmonic, the energy flow is in the direction opposite to the electron flow. The backward-wave device in practice must therefore be excited at the downstream end of the interaction region; energy is removed to a useful load at the input of the stream. This aspect of the backward-wave device is also shown in Fig. 16.1. When the device is used in this manner, it is apparent that gain is obtained, since the potential at the downstream end of the interaction space is less than that at the stream entrance. In particular, when the potential becomes zero, or of the order of thermal noise levels, no external potential source is needed; spontaneous oscillations can then occur. In the special case considered here, the total potential becomes zero when

$$\cos \sqrt{1 - r^2}\, D_i\theta_o = r \quad . \tag{16.17}$$

There are an infinite number of values of the product of interaction parameter and circuit length such that

$$D_i\theta_o = \frac{\text{arc cos } r^2}{\sqrt{1 - r^2}} \; ; \tag{16.18}$$

usually oscillations on an actual device occur at the smallest of them. Figure 16.2 shows this start-oscillation value as a function of the stream thickness parameter, r.

16.2.1.1.2 Beam Thickness Parameter Greater than Unity—r > 1

When r > 1, the interaction in this special case takes on a different nature from the previous section, since all of the quasi-synchronous waves have the same phase velocity and only one of them has a constant amplitude along the z-direction. One of the remaining two waves increases in amplitude with distance along the z-axis; the other decreases at the same rate.

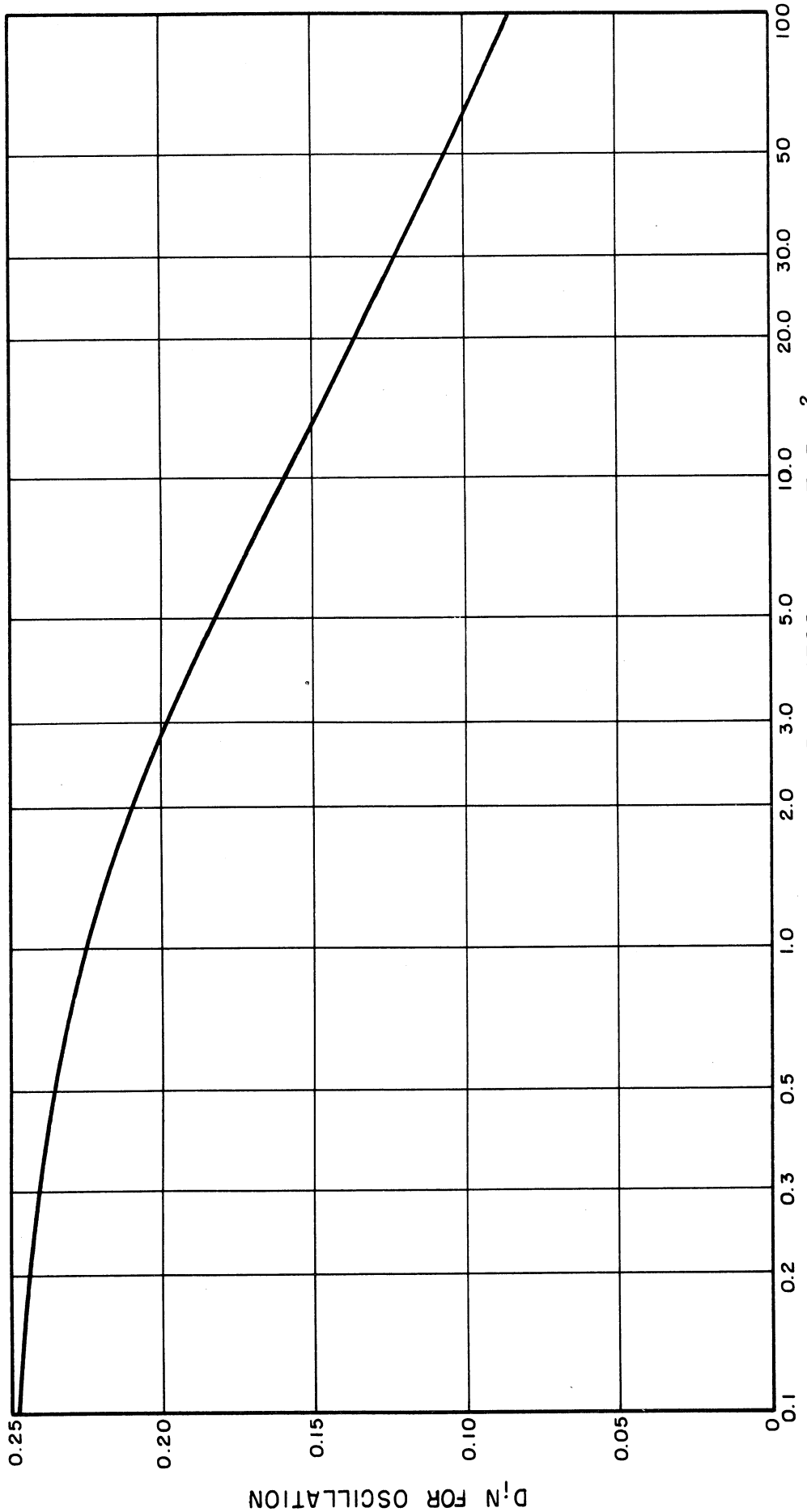

FIG. 16.2 START-OSCILLATION CONDITION FOR THE BACKWARD-WAVE OSCILLATOR – SPECIAL CASE H = 1.

Equation 16.15 for the variation of the total anode potential shows this gain phenomenon in the hyperbolic function.

Figure 16.3 shows the nature of the variation of the total potential along the longitudinal axis of the interaction space. It is evident that a cancellation can occur in this instance, also. This is not a simple harmonic interference, however; the cancellation is brought about by the gain of the combination of the two changing waves to sufficient amplitude to equal the amplitude of the unchanging wave. The condition necessary for complete cancellation of potential, or the start of oscillation, is

$$\cosh \sqrt{r^2 - 1}\, D_i\theta_o = r^2 \quad . \tag{16.19}$$

In this case there is only one solution, viz.,

$$D_i\theta_o = \frac{\text{arc cosh } r^2}{\sqrt{r^2 - 1}} \quad . \tag{16.20}$$

The start-oscillation condition as a function of the stream thickness parameter, r, is also shown in Fig. 16.2. The entire range of r is thus covered.

16.2.2 Start-oscillation Conditions for the Backward-wave Oscillator in the Special Case H = 1

The fact that the special case b = 0 leads to the initiation of oscillation, as shown in Sec. 16.2.1, is an accidental result. In general the total potential does not completely vanish anywhere in the interaction space and it is necessary to use a trial-and-error procedure to find the value (or values) of b for which the cancellation is complete. In the special case H = 1, the required value of b is

$$b_{osc.} = 0 \quad ; \tag{16.21}$$

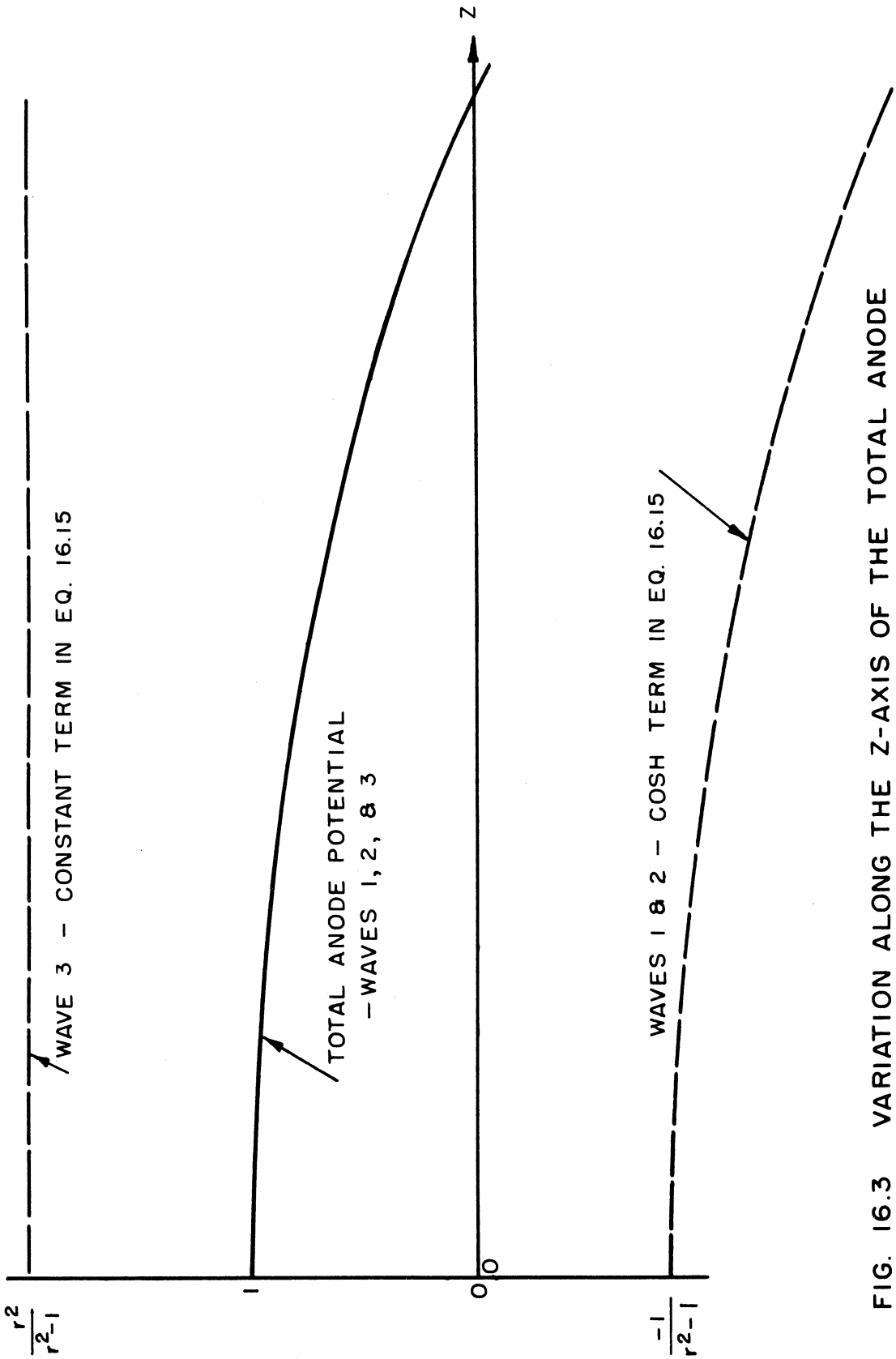

FIG. 16.3 VARIATION ALONG THE Z-AXIS OF THE TOTAL ANODE POTENTIAL IN THE BACKWARD-WAVE TUBE - SPECIAL CASE H = 1, b = 0, r > 1.

this should be regarded as one of the criteria for start-oscillation. It determines the necessary d-c stream velocity for oscillation at the frequency, ω. Conversely, it determines the frequency of oscillation (low level) for a particular stream velocity and a particular circuit if the other conditions for oscillation are satisfied.

The required values of interaction parameter and circuit length are as given by Fig. 16.2. In addition, the presentation of Fig. 16.4 shows how, with all other parameters held constant, the length of circuit required for oscillation depends on the stream thickness parameter, r. Also shown is the sheet-beam result of Muller. It is apparent that the length of circuit needed for oscillation with a given stream (i.e., a given stream thickness parameter) may be much less in the present theory than in Muller's theory. Using Eqs. 8.59, 8.60, and 8.68, together with the characteristics of the d-c Brillouin beam, the following expression for the stream thickness (velocity spread) parameter is obtained:

$$r^2 = \frac{s_u^2}{D_i} = \frac{I_{beam}}{2\,\epsilon_o^2\,\omega_c\,\omega\,K\,h\,V_{beam}G^2} \quad . \qquad (16.22)$$

The square of the stream thickness parameter, r^2, is thus seen to be proportional to the beam current. Consequently, the construction in Fig. 16.4 shows that the beam current required for the initiation of oscillations may be considerably less than that predicted by the simple sheet beam theory. This result is in qualitative agreement with experimental results on existing devices which, however, do not use streams having Brillouin characteristics.

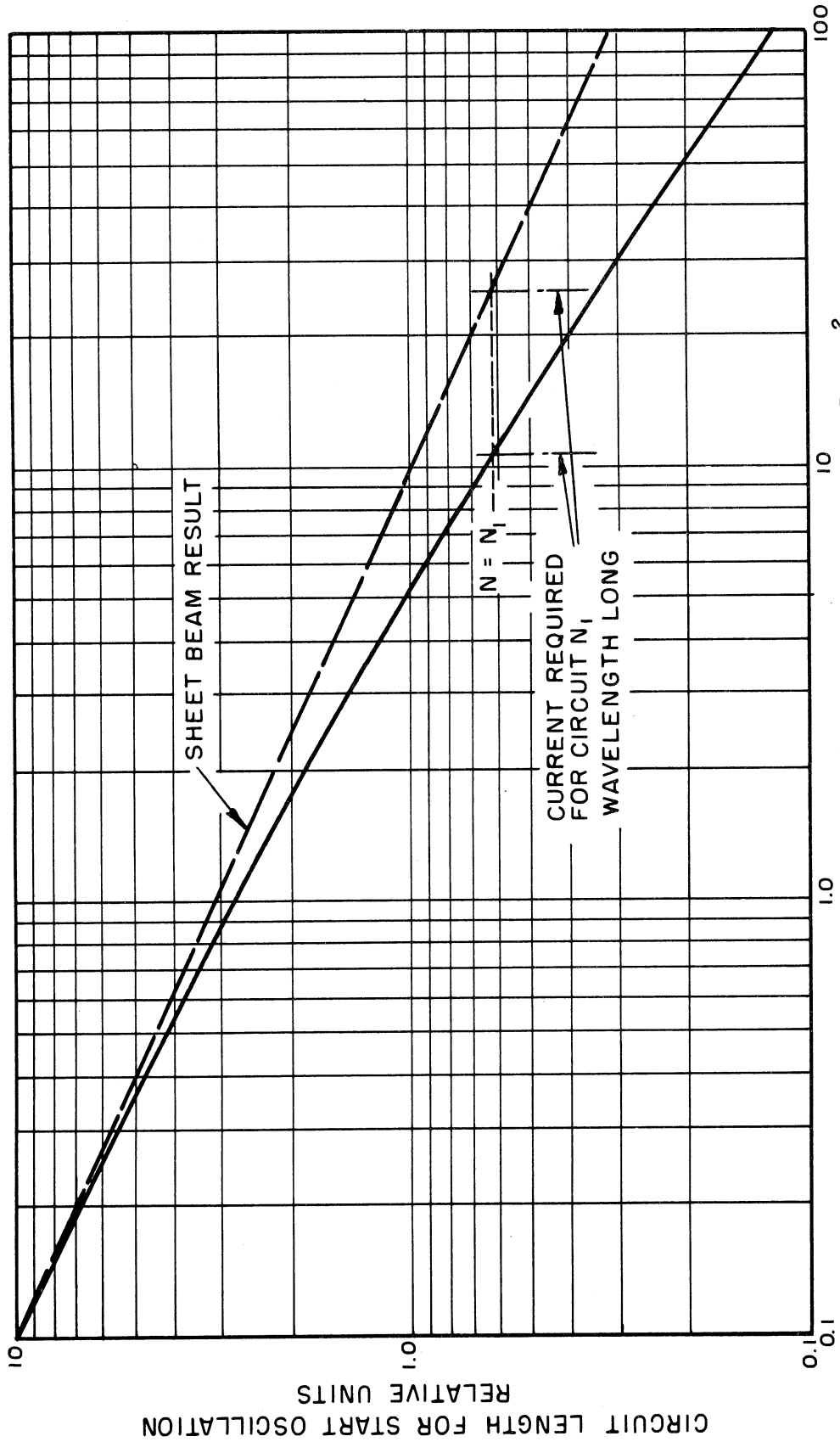

FIG. 16.4 LENGTH OF CIRCUIT REQUIRED FOR OSCILLATION AS A FUNCTION OF STREAM THICKNESS PARAMETER, r — SPECIAL CASE H = 1.

CHAPTER XVII

CONCLUSIONS—RECOMMENDATIONS FOR FUTURE RESEARCH

17.1 Conclusions

Linear perturbation theory has been applied to the electron-wave interaction in crossed fields and the waves capable of existing have been determined. The longitudinal boundary value problem has been studied for the case of an unmodulated entering stream. An approximate, first-order solution of this boundary value problem has been found. Results of calculations based on this solution have been obtained and are presented in Part VI: Chapter XV shows forward-wave amplifier gain characteristics; Chapter XVI shows start-oscillation criteria for the backward-wave crossed-field oscillator. "Space-charge effects"—more specifically the d-c velocity gradient and finite thickness of the stream—show an increase of forward-wave gain and a decrease of beam current required for backward-wave oscillation, in comparison with the sheet-beam results.

The restrictions on the theory outlined in Chapter II should be recalled. In particular, the results obtained in this dissertation are valid only for the high-density Brillouin stream. Strictly speaking, the test of this theory must await the time when a beam-type of magnetron device can be built to have a Brillouin stream and can be operated at small-signal levels. The fact that the modification of the present theory over the sheet-beam theory is in better agreement with existing observations suggests, however, that the detailed nature of the d-c stream may not be an especially important factor in the interaction.

17.2 Recommendations for Further Research

17.2.1 Extension of Calculations

The calculations presented in Chapters XV and XVI are concerned only with the special case in which the stream is located equidistant from sole and anode planes. It would be of interest to consider also cases in which the stream is closer to the anode, to see if the stream thickness effects result in the same degree of enhancement of the rate of interaction that occurs in the special case presented here. The curves of Fig. 9.7 are of interest in this respect, inasmuch as they predict increased gain over the sheet-beam result, even when the stream grazes the anode. Figure 8.1, on the other hand, is a denial of gain in a smooth-anode tube in such an instance. Thus, an interesting question remains to be answered.

17.2.2 Extension of the Theory to Account for Other Phenomena

The theory presented here ignores the possibility of interaction between the circuit and more than one space harmonic of the circuits at any one time. With relatively little increase in complexity, the theory presented here could be adapted to such a situation. Two important situations could thereby be examined:

(1) Interaction near the cutoff frequency of the propagating mode. Near the cutoff frequency, operation with both a forward-wave and a backward-wave harmonic is possible.

(2) Interaction with one harmonic in quasi-synchronous fashion and, simultaneously, with another harmonic in cyclotron fashion. This would lead to an analysis of the "rising-sun" effect.

Analysis of re-entrant streams is desirable in the light of recent

technological developments. This would appear to be a formidable problem, however.

17.2.3 Application to Large-Signal Calculations

Using the small-signal results of the present theory as a starting-point, it is desirable, and may be feasible, to calculate the large-signal performance of crossed-field devices in much the same manner as has been done with the traveling-wave tube.

APPENDICES

APPENDIX I

ELECTRIC POTENTIAL RELATIONS IN BRILLOUIN FLOW

The equations which define the velocity and charge distribution in Brillouin flow, Eqs. 3.2-3.4, also determine the potential distribution. If the electrons all originate from a common potential with the same velocity (e.g., a unipotential cathode with negligible emission velocity), then the Law of Conservation of Energy dictates that

$$V = \left|\frac{m}{e}\right| \frac{|\vec{u}_o|^2}{2} = \left|\frac{m}{e}\right| \frac{u_{zo}^2}{2} . \qquad \text{(A1.1)}$$

Use of the velocity relation, Eq. 3.3, with the above equation leads to

$$V(y) = \frac{\omega_c^2 y^2}{2\eta} . \qquad \text{(A1.2)}$$

Evaluation of the Laplacian of this potential function,

$$\nabla^2 V = \frac{\omega_c^2}{\eta} = \frac{-\rho_o}{\epsilon_o} , \qquad \text{(A1.3)}$$

shows the consistency of the solution, since the charge density obtained from the above equation is in agreement with Eq. 3.2.

The potential in the stream is thus a quadratic function; Fig. A1.1 shows this function extending to the origin of the Y coordinates (the virtual cathode). The extension of the function does not, of course, imply the existence of electrons in the extended region. The stream is confined by the planes $y=y_a$ and $y=y_b$.

Since there is no charge outside the stream, the actual potential in those regions must be either constant or a linear function of y. Further, the potential gradient must be continuous at the stream boundaries. There-

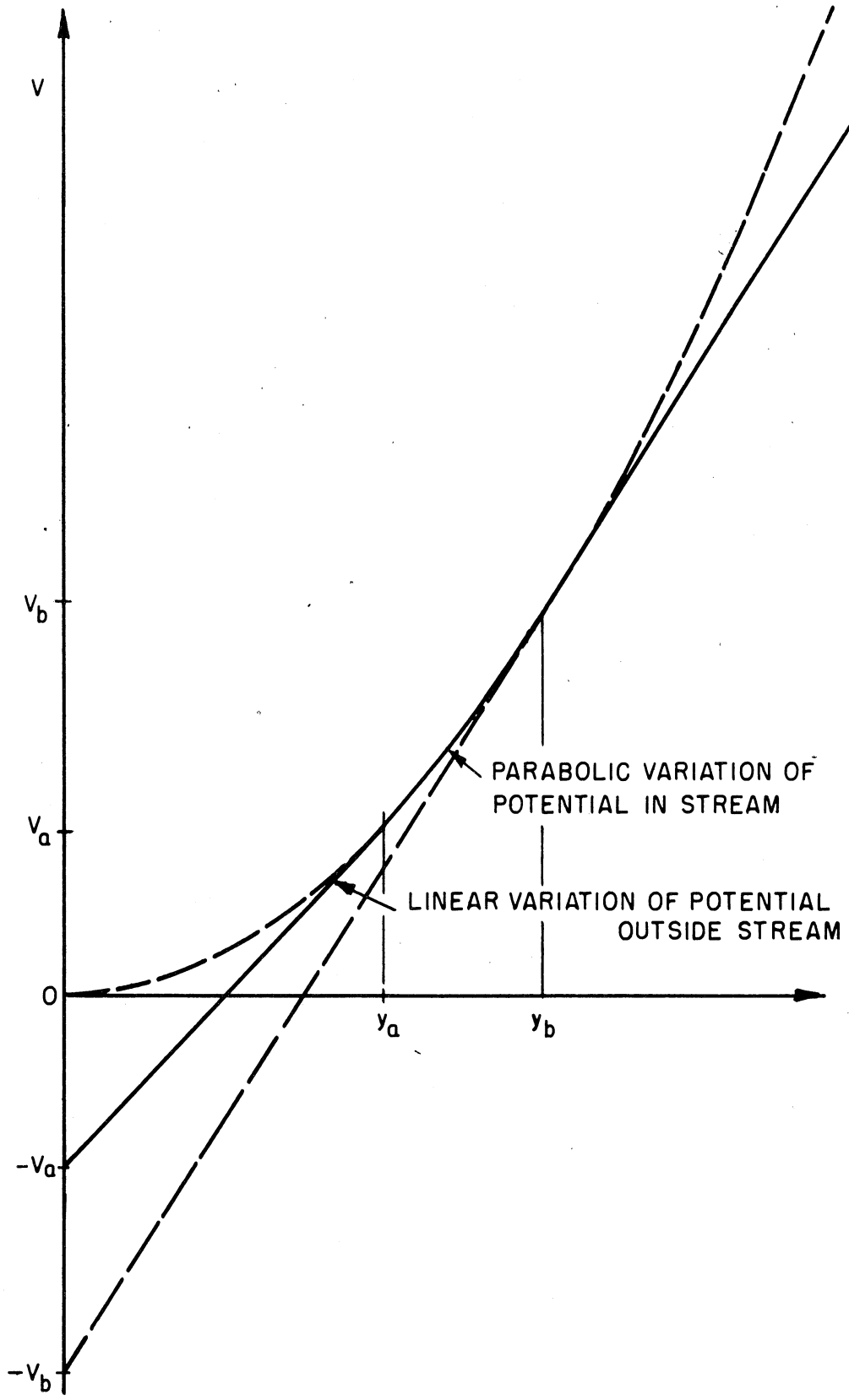

FIG. A1.1 POTENTIAL PROFILE OF BRILLOUIN STREAM AND ADJACENT SPACE.

fore, the potential in the charge-free regions is represented by the straight lines tangent to the parabola at the stream boundaries, as shown in Fig. A1.1.

It is obvious that the potentials in the interaction region can be established by placing the planar sole and anode electrodes at any values of y in the regions beneath the stream and above the stream, respectively, provided that the electrodes have the potentials corresponding to their respective y coordinates. Thus, for example, the sole electrode could be placed at the lower edge of the stream itself if its potential were V_a relative to the emitter.

The more general case of arbitrary positions of the sole of anode can be conveniently handled by noting the geometric properties of the parabola and its tangent. Thus, the potential axis intercept of the tangent is the exact negative of the potential (ordinate) at the point of tangency:

$$V(y = 0) = - V_a = \frac{- \omega_c^2 y_a^2}{2\eta} \qquad (A1.4)$$

From this it is seen that the slope of the tangent is simply

$$\frac{dV}{dy} = \frac{\Delta V}{\Delta y} = \frac{2V_a}{y_a} = \frac{\omega_c^2 y_a}{\eta} \ , \qquad (A1.5)$$

which could, of course, also be obtained by differentiation of the potential function. The sole potential, therefore, is related to the sole coordinate, y_s, by the linear relation

$$V_s(y_s) = \frac{- \omega_c^2 y_a^2}{2\eta} + \frac{\omega_c^2 y_a y_s}{\eta} \ , \qquad (A1.6)$$

which is equivalent to Eq. 3.6 of the text.

The proper potential for the anode plane is obtained in precisely the same way.

APPENDIX II

CALCULATION OF THE COEFFICIENTS a_k OF THE POTENTIAL FUNCTION REPRESENTATIONS FOR CYCLOTRON WAVES

The detailed evaluation of the recursion relation, Eq. 4.18 of the test, for different values of the summation index, k, is presented here.

It will be recalled that all a_k for negative values of k are zero, since the expansion is in the form of a Taylor series. Thus, when k is -2 or a more negative integer, the recursion relation is completely trivial. When k = -1, the recursion equation contains only one term different from zero, viz., the term containing the coefficient $a_{k+1} = a_o$. For k = 0, the recursion equation contains two terms, and so on.

Specifically, when k = -1 the recursion relation becomes

$$0 \cdot a_o = 0 \quad , \tag{A2.1}$$

which yields the result that a_o is arbitrary:

$$a_o = C' \tag{A2.2}$$

When k = 0, the recursion relation becomes

$$2\, a_1 + 2\, a_o = 0 \quad , \tag{A2.3}$$

and

$$a_1 = -a_o = -C' \tag{A2.4}$$

The recurrence relations for successive integer values of k, and the resulting relation of a_{k+1} to the arbitrary coefficient, a_o, are presented below.

$$k = 1: \quad 8\,a_2 + 0\,a_1 - 2\,a_0 = 0 \quad , \tag{A2.5}$$

$$a_2 = +\,.250000\,a_0$$

$$k = 2: \quad 18\,a_3 - 12\,a_2 - 2\,a_1 + 5\,a_0 = 0 \quad , \tag{A2.6}$$

$$a_3 = -\,.222222\,a_0$$

$$k = 3: \quad 32\,a_4 - 34\,a_3 + 6\,a_2 + 5\,a_1 - 4\,a_0 = 0 \quad , \tag{A2.7}$$

$$a_4 = -\,.001735\,a_0$$

$$k = 4: \quad 50\,a_5 - 66\,a_4 + 22\,a_3 + 3\,a_2 - 4\,a_1 + a_0 = 0 \quad , \tag{A2.8}$$

$$a_5 = -\,.019572\,a_0$$

$$k = 5: \quad 72\,a_6 - 108\,a_5 + 46\,a_4 - 1\,a_3 - 4\,a_2 + a_1 = 0 \quad , \tag{A2.9}$$

$$a_6 = -\,.003468\,a_0$$

$$k = 6: \quad 98\,a_7 - 160\,a_6 + 78\,a_5 - 7\,a_4 - 4\,a_3 + a_2 = 0 \quad , \tag{A2.10}$$

$$a_7 = +\,.001877\,a_0$$

$$k = 7: \quad 128\,a_8 - 222\,a_7 + 118\,a_6 - 15\,a_5 - 4\,a_4 + a_3 = 0 \quad , \tag{A2.11}$$

$$a_8 = -\,.000663\,a_0$$

etc.

APPENDIX III

CALCULATION OF THE COEFFICIENTS b_k OF THE POTENTIAL FUNCTION REPRESENTATIONS FOR CYCLOTRON WAVES

When the second solution of the differential equation is written as in Eq. 4.23 of the text, the recursion relation for the b_k can be found from consideration of a special case of the more general situation below.

Let S_1 be a solution of the differential equation

$$g(\chi) \frac{d^2\xi}{d\chi^2} + h(\chi) \frac{d\xi}{d\chi} + j(\chi)\, d\xi = 0 \qquad \text{(A3.1)}$$

in which g, h, and j are functions of the independent variable, χ. Then it will be shown that

$$\xi_2 = S_1(\chi)\, f(\chi) + S_2(\chi) \qquad \text{(A3.2)}$$

is a solution of the differential equation provided that

$$g\, S_1\, f'' + 2\, g\, S_1'\, f' + h\, S_1\, f' + g\, S_2'' + h\, S_2' + j\, S_2 = 0 \ , \qquad \text{(A3.3)}$$

where f is an arbitrary function of χ and primes denote differentiation with respect to χ.

The proof of the above contention is established by performing the indicated differentiations:

$$\frac{d\xi}{d\chi} = S_1' f + S_1 f' + S_2' \qquad \text{(A3.4)}$$

and

$$\frac{d^2\xi}{d\chi^2} = S_1'' f + 2\, S_1' f' + S_1 f'' + S_2'' \qquad \text{(A3.5)}$$

and substituting the results in the differential equation. Thus,

$$\begin{aligned} &g\,S_1''\,f + 2\,g\,S_2'\,f' + g\,S_2 f'' + g\,S_2'' \\ &h\,S_1'\,f + h\,S_2\,f' + h\,S_2' \\ &j\,S_1\,f + j\,S_2 = 0\,. \end{aligned} \qquad \text{(A3.6)}$$

The sum of the terms in the column on the left add to zero regardless of the function f, since S_1 satisfies the differential equation. The remaining sum satisfies the condition Eq. A3.3, thus completing the procf.

In the present application, f is taken to be the logarithmic function

$$f = \ln 2\sqrt{\chi}\,. \qquad \text{(A3.7)}$$

Hence,

$$f' = \frac{1}{2\chi}\,, \qquad \text{(A3.8)}$$

and

$$f'' = -\frac{1}{2\chi^2}\,. \qquad \text{(A3.9)}$$

Furthermore,

$$g = 2\chi - 5\chi^2 + 4\chi^3 + \chi^4 \qquad \text{(A3.10)}$$

$$h = 2 - 2\chi \qquad \text{(A3.11)}$$

and

$$j = 2 - 2\chi + 5\chi^2 - 4\chi^3 + \chi^4\,. \qquad \text{(A3.12)}$$

With the above specialization and with the Taylor series

$$S_2 = \sum_{k=0}^{\infty} b_k \chi^k \quad , \tag{A3.13}$$

calculation of the terms appearing in Eq. A3.3 proceeds as follows:

$$\begin{aligned} j\, S_2 &= \sum_{k=0}^{\infty} [2b_k \chi^k - 2b_k \chi^{k+1} + 5b_k \chi^{k+2} - 4b_k \chi^{k+3} + b_k \chi^{k+4}] \\ &= \sum_{k=0}^{\infty} [2b_k - 2b_{k-1} + 5b_{k-2} - 4b_{k-3} + b_{k-4}]\chi^k \end{aligned} \tag{A3.14}$$

$$\begin{aligned} h\, S_2' &= \sum_{k=0}^{\infty} (2 - 2\chi)\,(k\, b_k \chi^{k-1}) \\ &= \sum_{k=0}^{\infty} [2(k+1)b_{k+1} - 2k\, b_k]\chi^k \end{aligned} \tag{A3.15}$$

$$\begin{aligned} g\, S_2'' &= \sum_{k=0}^{\infty} [2\chi - 5\chi^2 + 4\chi^3 - \chi^4]\,[k(k-1)b_k \chi^{k-2}] \\ &= \sum_{k=0}^{\infty} [2(k+1)k\, b_{k+1} - 5k(k-1)b_k + 4(k-1)(k-2)b_{k-1} - (k-2)(k-3)b_{k-2}]\chi^k \end{aligned} \tag{A3.16}$$

$$\begin{aligned} h\, S_1 f' &= \sum_{k=0}^{\infty} [2 - 2\chi]\,[a_k \chi^k]\,[1/2\chi] \\ &= \sum_{k=0}^{\infty} [a_{k+1} - a_k]\chi^k \end{aligned} \tag{A3.17}$$

$$\begin{aligned} 2g\, S_1' f' &= 2\sum_{k=0}^{\infty} [2\chi - 5\chi^2 + 4\chi^3 - \chi^4]\,[k a_k \chi^{k-1}]\,[1/2\chi] \\ &= \sum_{k=0}^{\infty} [2(k+1)a_{k+1} - 5k a_k + 4(k-1)a_{k-1} - (k-2)a_{k-2}]\chi^k \end{aligned} \tag{A3.18}$$

$$\begin{aligned} g\, S_1 f'' &= \sum_{k=0}^{\infty} [2\chi - 5\chi^2 + 4\chi^3 - \chi^4]\,[a_k \chi^k]\,[-1/2\chi^2] \\ &= -\sum_{k=0}^{\infty} [a_{k+1} - 5/2\, a_k + 2a_{k-1} - 1/2\, a_{k-2}]\chi^k \quad . \end{aligned} \tag{A3.19}$$

Upon substitution of the above equations into Eq. A3.3, the following recursion relation is obtained:

$$
\begin{aligned}
& 2b_k - 2b_{k-1} + 5b_{k-2} - 4b_{k-3} + b_{k-4} \\
& + 2(k+1)b_{k+1} - 2kb_k \\
& + 2k(k+1)b_{k+1} - 5k(k-1)b_k + 4(k-1)(k-2)b_{k-1} - (k-2)(k-3)b_{k-2} \\
& + a_{k+1} - a_k \\
& + 2(k+1)a_{k+1} - 5k a_k + 4(k-1) a_{k-1} - (k-2) a_{k-2} \\
& - a_{k+1} + \frac{5}{2} a_k - 2 a_{k-1} + \frac{1}{2} a_{k-2} = 0 .
\end{aligned}
\tag{A3.20}
$$

This is equivalent to

$$
\begin{aligned}
& 2(k+1)a_{k+1} - \left(5k - \frac{3}{2}\right)a_k + [4(k-1) - 2]a_{k-1} - \left(k - \frac{5}{2}\right)a_{k-2} \\
& + 2(k+1)^2 b_{k+1} - (5k+2)(k-1)b_k + [4(k-1)(k-2) - 2]b_{k-1} \\
& - [(k-2)(k-3) - 5]b_{k-2} - 4b_{k-3} + b_{k-4} = 0.
\end{aligned}
\tag{A3.21}
$$

The a_k are those determined in Appendix II.

Only a few of the b_k will be presented here; the process is a tedious one, and only a few terms will be needed. If many of the coefficients were required, a simpler form of the differential equation (e.g., Eq. 4.7) could be employed to obtain a simpler recursion relation, thereby reducing the amount of labor required to calculate the coefficients.

First, it is observed that the term involving b_0 is simply a constant. Nothing is gained by including such a term, since the first solution also contains a constant. The coefficients b_k, when k is zero or a negative integer, are hence all zero.

When k = 0, the recursion relation, Eq. A3.21 becomes simply

$$2a_1 + \frac{3}{2} a_0 + 2b_1 = 0 \quad , \tag{A3.22}$$

which indicates that, using Appendix II for a_0 and a_1,

$$b_1 = \frac{1}{4} a_0 \quad . \tag{A3.23}$$

When k = 1, the following is obtained:

$$\begin{aligned} 4a_2 - \frac{7}{2} a_1 - a_0 + 8b_2 &= 0 \quad , \\ b_2 &= -\frac{5}{16} a_0 \quad . \end{aligned} \tag{A3.24}$$

When k = 2,

$$\begin{aligned} 6a_3 - \frac{17}{2} a_2 + 2a_1 + \frac{1}{2} a_0 + 18b_3 - 12b_2 - 2b_1 &= 0 \quad , \\ b_3 &= \frac{17}{18 \cdot 24} a_0 \quad . \end{aligned} \tag{A3.25}$$

REFERENCES

1. J. G. Fisk, H. D. Hagstrum, and P. L. Hartman, "The magnetron as a generator of centimeter waves," Bell Syst. Tech. Jour., vol. 25, pp. 167-348; April, 1946.

2. G. B. Collins, ed., "Microwave Magnetrons," (M.I.T. Radiation Lab. Series, Vol. 6), McGraw-Hill; 1948.

3. J. A. Boyd, "The Mitron—an interdigital voltage-tunable magnetron," Proc. I.R.E., vol. 43, pp. 332-338; March, 1955.

4. P. Guénard, O. Doehler, B. Epsztein, and R. Warnecke, "Nouveaux tubes oscillateurs a large bande d'accord electronique pour hyperfrequences," Acad. des Sci., Comptes Rendus, vol. 235, pp. 236-238; July 21, 1952.

5. R. Warnecke, P. Guénard, O. Doehler, and B. Epsztein, "The 'M'-type Carcinotron tube," Proc. I.R.E., vol. 43, pp. 413-424; April, 1955.

6. R. Warnecke, W. Kleen, A. Lerbs, O. Doehler, and H. Huber, "The magnetron type traveling-wave amplifier tube," Proc. I.R.E., vol. 38, pp. 486-495; May, 1950.

7. D. R. Hartree, CVD Reports, Mag. 36; 1944.

8. Tibbs and Wright, CVD Reports, Mag. 41; 1945.

9. O. Bunemann, "A small amplitude theory for magnetrons," CVD Reports, Mag. 37; 1944.

10. J. R. Pierce, "Theory of the Beam-type traveling-wave tube," Proc. I.R.E., vol. 35, p. 111; Feb., 1947.

11. J. R. Pierce, "Traveling-wave tubes," Van Nostrand, 1950.

12. R. Kompfner, "Traveling-wave tube—centimetre wave amplifier," Wireless Engineer, vol. 24, p. 255; Sept., 1947.

13. H. W. Welch, Jr., "Effects of space charge on frequency characteristics of magnetrons," Proc. I.R.E., p. 1434; Dec., 1950.

14. H. W. Welch, Jr., "Prediction of traveling-wave magnetron frequency pushing and voltage tuning," Proc. I.R.E., vol. 41, p. 1631; Nov., 1953.

15. J. F. Hull, Private communication re: calculation of the shape of the magnetron "gauss line."

16. O. Doehler, "On the Properties of Tubes in a Constant Magnetic Field—Part I, Characteristics and Trajectories of the Electrons in the Magnetron," Ann. de Radioelec., vol. 3, pp. 29; Jan., 1948.

17. O. Doehler, "On the Properties of Tubes in a Constant Magnetic Field—Part II, The Oscillations of Resonance," ibid., p. 169; July, 1948.

18. O. Doehler, "On the Properties of Tubes in a Constant Magnetic Field—Part III, The Traveling-Wave Tube in a Magnetic Field," ibid., p. 328, Oct., 1948.

19. O. Doehler, J. Brossart, and G. Mourier, "On the Properties of Tubes in a Constant Magnetic Field—Part IV, Extension of the Linear Theory, the Effects of Non-Linearities and the Efficiency," ibid., vol. 5, p. 293, Oct., 1950.

20. M. Muller, "Traveling-wave amplifiers and backward-wave oscillators," Proc. I.R.E., vol 42, p. 1651; Nov., 1954.

21. R. C. Fletcher, "A broad-band interdigital circuit for use in traveling-wave-type amplifiers," Proc. I.R.E., vol. 40, p. 951, Aug., 1952.

22. W. W. Harman, Fundamentals of Electron Motion, Chapter 9; McGraw-Hill, 1953.

23. R. Kompfner, and N. T. Williams, "Backward-wave tubes," Proc. I.R.E., vol. 41, p. 1602; Nov., 1953.

24. H. R. Johnson, "Backward-wave Oscillators," Proc. I.R.E., vol. 43, p. 684; June, 1955.

25. G. C. MacFarlane, and H. G. Hay, "Wave propagation in a slipping stream of electrons: small amplitude theory," Proc. Phys. Soc. London, vol. B63, p. 409; , 1950.

26. R. W. Gould, "A field analysis of the M-type backwave wave oscillator," California Institute of Technology Electron Tube and Microwave Laboratory Tech. Report No. 3; Sept., 1955.

27. R. W. Gould, "Space charge effects in beam-type magnetrons," Jour. Appl. Phys., vol. 28, p. 599; May, 1957.

28. A. W. Hull, "The effect of a uniform magnetic field on the motion of electrons between coaxial cylinders," Phys. Rev., vol. 18, p. 31; 1921.

29. L. P. Page, and N. I. Adams, Jr., "Space charge in plane magnetron," Phys. Rev., vol. 69, p. 492; 1946.

30. R. Q. Twiss, "On the steady state and noise properties of linear and cylinderical magnetrons," Ph.D. Thesis, Massachusetts Institute of Technology, 1950.

31. W. W. Peterson, "The trajection—an experimental d-c magnetron," Ph.D. dissertation, University of Michigan, 1954.

32. D. L. Reverdin, "Electron optical exploration of space charge in a cutoff magnetron," J. Appl. Phys., vol. 22, p. 257; 1951.

33. R. Svenson, "An experimental investigation of the electron orbits in a magnetron," Proc. I.R.E., vol. 39, p. 838; 1951.

34. L. Brillouin, "Trajectories in a single-anode magnetron," Elec. Commun., p. 460; 1946.

35. J. A. Stratton, Electromagnetic Theory, McGraw-Hill; 1941.

36. R. R. Warnecke, and P. Guenard, Les Tubes Electroniques à Commandé par Modulation de Vitesse, Gauthier-Villars; 1951; pp. 25-27.

37. E. G Linder, "Effect of high energy electron random motion upon the shape of the magnetron cutoff curve," Jour. Appl. Phys., vol. 9, p. 331; 1938.

38. G. Hok, "Space charge equilibrium in a magnetron—a statistical approach," Jour. Appl. Phys., vol. 23, p. 983; Sept., 1952.

39. H. W. Reddick, Differential Equations, Wiley, 1943.

40. A. Cohen, An Elementary Treatise on Differential Equations, Heath, 1933; Chapter 9.

41. E. A. Guillemin, The Mathematics of Circuit Analysis, Wiley, 1949; p. 276 ff.

42. L. Tonks, and I. Langmuir, "Oscillations in ionized gases," Phys. Rev., vol. 33, p. 195; Feb., 1929.

43. G. R. Brewer, "The Propagation of Electromagnetic Waves in a Magnetron-tupe Space Charge," Ph.D. dissertation, University of Michigan, 1950.

44. G. Hok, "Theoretical study of the initiation of oscillations in electron streams through crossed fields," University of Michigan Electron Tube Laboratory Tech. Report No. 16; Nov., 1953.

45. E. Jahnke, and F. Emde, Tables of Functions with Formulas and Curves; Dover, 1945.

46. E. T. Whittaker, A Course in Modern Analysis, pp. 294-298; Cambridge, 1902.

47. D. Gabor, "Advanced Electron Dynamics and Optics," Notes from Post-graduate Course in Electronics and Communications, MIT, Summer Term, 1951.

48. W. C. Hahn, "Small signal theory of velocity-modulated electron streams," Gen. Elec. Rev., vol. 6, p. 258; June, 1939.

49. L. M. Field, "Some slow-wave structures for travelling-wave tubes," Proc. I.R.E., vol. 37, p. 34; Jan., 1949.

50. L. Brillouin, Wave Propagation in Periodic Structures, McGraw-Hill; 1946.

51. J. C. Slater, Microwave Electronics, D. Van Nostrand; 1950.

52. H. Batten, W. W. Peterson, S. Ruthberg, and H. W. Welch, "Analysis of dynamic characteristics of the magnetron space charge—preliminary results," University of Michigan Electron Tube Laboratory Tech. Report No. 5, pp. 65-73; Jan., 1951.

53. L. J. Chu, and J. D. Jackson, "Field theory of traveling-wave tubes," Proc. I.R.E., vol. 36, p. 853; July, 1948.

54. C. K. Birdsall, and J. R. Whinnery, "Waves in an Electron Stream with a general admittance wall," Jour. Appl. Phys., vol. 24, p. 315; 1953.

DISTRIBUTION LIST

No. Copies	Agency
3	Project Engineer, Microwave Tube Branch, Evans Signal Laboratory, Belmar, New Jersey
1	Mail and Records, Evans Signal Laboratory, Belmar, New Jersey
1	Technical Documents Center, Evans Signal Laboratory, Belmar, New Jersey
1	Director of Research, Hexagon, Fort Monmouth, New Jersey
1	Electronics Research Laboratory, Stanford University, Stanford, California, Attention: Applied Electronics Laboratory, Document Library
1	The Director, U. S. Naval Research Laboratory, Code 2021, Washington 25, D. C.
1	Commander, Air Force Cambridge Research Center, CROOTR-2E, L. G. Hanscom Field, Bedford, Massachusetts
1	Commander, Rome Air Development Center, Electronic Development Division, RCSSTL-1, Griffis Air Force Base, New York
1	Chief Signal Officer, Department of the Army, Washington 25, D. C., Attention: SIGRD
1	Advisory Group on Electron Tubes, 346 Broadway, New York 13, New York
5	Armed Services Technical Information Agency, Document Service Center, Knott Building, Dayton 2, Ohio
2	Commander, Wright Air Development Center, WCOSI-3, Wright-Patterson Air Force Base, Ohio
1	Commanding Officer, U. S. Army Signal Electronics Research Unit, Mountain View, California
1	Chief of Ordnance, Washington 25, D. C., Attention: ORDTX-AR
1	Commanding General, Redstone Arsenal, Huntsville, Alabama, Attention: Technical Library
1	Commanding Officer, Watertown Arsenal, Watertown, Massachusetts, Attention: OMRO
1	Commanding Officer, Frankford Arsenal, Philadelphia 37, Pennsylvania, Attention: ORDBA-FEL

No. Copies	Agency
1	Chief, Bureau of Ships, Department of the Navy, Washington 25, D. C. Attention: Code 816A
1	Commander, Wright Air Development Center, WCRETT-3, Wright-Patterson Air Force Base, Ohio
1	Chief, Ordnance Corps, Department of the Army, Diamond Ordnance Fuze Laboratories, Connecticut Avenue and Van Ness Street, N.W., Washington 25, D. C., Attention: T. T. Liimatainen
1	Commanding General, U. S. Army Electronic Proving Ground, Fort Huachuca, Arizona, Attention: EWD (Technical Library)
1	Commanding General, Aberdeen Proving Ground, Aberdeen, Maryland, Attention: Development and Proof Service, Fire Control Division, Capt. Alter
1	Chief, Radar Development Branch, Radar Division, Surveillance Dept., USASEL, Evans Area, Belmar, New Jersey
1	General Electric Company, 1 River Road, Schenectady 5, New York, Attention: Dr. E. D. MacArthur
1	Raytheon Manufacturing Company, Foundry Avenue, Waltham 54, Massachusetts, Attention: W. T. Welsh
1	Varian Associates, 611 Hansen Way, Palo Alto, California, Attention: Mrs. Helen Dean, Technical Library
1	Litton Industries, East Brittan Avenue, San Carlos, California, Attention: Dr. N. Moore
1	Sylvania Electric Products, Inc., 100 Sylvan Road, Woburn, Massachusetts, Attention: Mr. M. Pease
1	Director, National Bureau of Standards, Boulder, Colorado, Attention: Radio Library
1	Director, Countermeasures Division, Evans Signal Laboratory, Belmar, New Jersey
1	Director, Evans Signal Laboratory, Belmar, New Jersey, Attention: Mrs. Betty Kennett, Report Distribution Unit, Electron Devices Division
11	Director, Evans Signal Laboratory, Belmar, New Jersey, Attention: Mr. Gerald Pokorney, Microwave Tubes Branch, Electron Devices Division
1	Sylvania Electric Products, Inc., Microwave Tube Laboratory, Mountain View, California, Attention: Dr. D. Goodman
1	Sylvania Electric Products, Inc., Physics Laboratories, Bayside 60, Long Island, New York, Attention: Dr. R. G. E. Hutter

No. Copies	Agency
1	Prof. Jules S. Needle, Electrical Engineering Department, Northwestern University, Evanston, Illinois
1	Bendix Aviation Laboratories, Northwestern Highway and 10 1/2 Mile Road, Detroit 35, Michigan, Attention: Dr. J. H. Bryant
1	General Electric Microwave Laboratory, Palo Alto, California, Attention: Dr. E. Nalos
1	California Institute of Technology, Pasadena, California, Attention: Dr. R. Gould, Electrical Engineering Department
1	Commanding Officer, U. S. Signal Support Agency, Fort Monmouth, New Jersey, Attention: SIGRM/ES-ASA
1	Electronics Research Laboratories, Stanford University, Stanford, California, Attention: Dr. M. Hare and Mr. Dould
1	Engineering Research Institute, Project Files, 132A Cooley Building North Campus, The University of Michigan, Ann Arbor, Michigan